Dental Pulp Progenitor-Derived Neuronal- and Oligodendrocyte-Like Cells for Spinal Cord Repair

This thesis is being submitted to Cardiff University in partial fulfilment of the requirements for the degree of

Doctor of Philosophy

August 2013

Fraser Young BSc (Hons)

Tissue Engineering and Reparative Dentistry

School of Dentistry

Cardiff University

Declaration

This work has not been submitted in substance for any other degree or award at this or any other university or place of learning, nor is being submitted concurrently in candidature for any degree or other award.

Signed …… (candidate) Date
……

STATEMENT 1

This thesis is being submitted in partial fulfilment of the requirements for the degree of PhD

Signed ……(candidate) Date ……

STATEMENT 2

This thesis is the result of my own independent work/investigation, except where otherwise stated. Other sources are acknowledged by explicit references. The views expressed are my own.

Signed …… (candidate) Date ……

STATEMENT 3

I hereby give consent for my thesis, if accepted, to be available for photocopying and for inter-library loan, and for the title and summary to be made available to outside organisations.

Signed ……(candidate) Date ……

STATEMENT 4: PREVIOUSLY APPROVED BAR ON ACCESS

I hereby give consent for my thesis, if accepted, to be available for photocopying and for inter-library loans **after expiry of a bar on access previously approved by the Academic Standards & Quality Committee.**

Signed ……(candidate) Date ……

Table of Contents

Acknowledgments

My first and foremost thanks must go to my supervisory team of Professors: Bing Song, Alastair Sloan and Rachel Waddington. Your readily available support & advice over the last 3 years has helped guide the project and enabled me to develop as a scientist, and for that I will always be indebted.

This work would not have been possible without the assistance of the Dental School technical staff. Particular thanks must go to the JBIOS technicians who work tirelessly in supporting the needs of our research group.

A number of people have provided access to equipment and expertise that form fundamental aspects of this thesis. My sincerest thanks go to: Prof. Paul Kemp & Seva Telezhkin for assistance with patch clamp studies, Prof. Frank Sengpiel & Asta Vasalauskaite for allowing me to acquire two-photon images of samples, and to Prof. Ketan Patel from the University of Reading for providing GFP mice from his colony, without which the final chapter of this thesis would not have been possible.

The pilot *in vivo* study required assistance from other members of the lab. I extend my gratitude towards my "surgical team" of experts, Niels, Bangfu and Qian, for the days spent in theatre and help with the least pleasant of tasks – daily manual bladder evacuations.

The many friends I have made at the Dental School ensured that I never became too disheartened when things did not quite work out as hoped. Never a dull moment was had during all the hours spent in tissue culture with John, Jodie, Amr, Rachel and Yati around. A big thanks to Matt and Niels for helping to keep me entertained during the regular entire mornings spent doing repetitive washing steps.

My family have been thoroughly supportive for everything I have done in my life and the last 3 years have been no exception, thanks for being there. My final thanks are extended to Rachel who has experienced everything alongside me. Your love and support have been absolutely instrumental in getting me to this stage.

Abstract

Spinal cord regeneration following injury represents a major clinical challenge. Over recent years, stem cells have demonstrated promise for promoting spinal repair in the lab and in early stage clinical trials through functional replacement of neuronal and glial cells and through secondary trophic mechanisms to promote endogenous regeneration. Research has primarily focused on the use of embryonic tissue-derived stem cells of potentially limited therapeutic application due to related ethical concerns. The dental pulp harbours a source of easily accessible progenitor cells that have demonstrated early promise in improving functional outcome of experimental models of spinal cord injury via growth factor release. This thesis explores the potential of dental pulp progenitor cells (DPPCs) to promote spinal repair through direct cellular replacement. Progenitor cells isolated from murine incisors were found to express early stage neural and glial markers. Specific protocols were developed demonstrating the ability of DPPCs to differentiate *in vitro* into neuronal-like and oligodendrocyte-like cells with appropriate morphology and expression of mature markers. Electrophysiological testing revealed that DPPC-derived neuronal-like cells were of an immature non-functional phenotype. Undifferentiated DPPCs injected into an *ex vivo* spinal cord slice model showed signs of proliferation, migration and spontaneous differentiation within spinal tissue. DPPCs pre-differentiated into oligodendrocyte-like cells failed to survive transplantation but neuronally pre-differentiated cells survived, showing signs of integration into endogenous neuronal pathways. In a small scale pilot study, neuronally pre-differentiated DPPCs were transplanted into a clinically relevant *in vivo* model of spinal cord injury. DPPCs maintained expression of neuronal markers four weeks after grafting into the injured spinal cord. Axonal projections towards grafted cells and synaptic protein expression suggested possible integration into neuronal pathways, albeit without an associated statistical functional improvement. The results presented in this thesis provide a strong case for the potential of DPPCs to facilitate functional recovery through direct cell replacement mechanisms.

List of Abbreviations

αMEM	-	α-modification minimum essential medium
BBB	-	Basso, Beattie and Bresnahan locomotor scale
BDNF	-	Brain-derived neurotrophic factor
bFGF	-	Basic fibroblast growth factor
BLBP	-	Brain lipid binding protein
BMSC	-	Bone marrow stromal cell
BSA	-	Bovine serum albumin fraction V
CFE	-	Colony forming efficiency
CNPase	-	2',3'-cyclic-nucleotide 3'-phosphodiesterase
CNS	-	Central nervous system
DMEM	-	Dulbecco’s modified eagles medium
DMSO	-	Dimethyl sulphoxide
DPPC	-	Dental pulp progenitor cell
EGF	-	Epidermal growth factor
ESC	-	Embryonic stem cell
FBS	-	Foetal bovine serum
GalC	-	Galactocerebroside
GDNF	-	Glial cell line-derived neurotrophic factor
GFAP	-	Glial fibrillary acidic protein
GFP	-	Green fluorescent protein
GLAST	-	Glutamate aspartate transporter
GRP	-	Glial restricted precursor
HEPES	-	N-2-hydroxyethylpiperazine-N′-2-ethanesulfonic acid

ICC	-	Immunocytochemistry
IGF-1	-	Insulin-like growth factor-1
LANGFR	-	Low-affinity nerve growth factor receptor
Map2	-	Microtubule-associated protein 2
MBP	-	Myelin basic protein
MOSP	-	Myelin/oligodendrocyte specific protein
MSC	-	Mesenchymal stem cell
Myt1l	-	Myelin transcription factor 1-like
NCAM	-	Neural cell adhesion molecule
NEAA	-	Non-essential amino acids
NF	-	Neurofilament
NF-l	-	Neurofilament, light chain
NGF	-	Nerve growth factor
Ngn2	-	Neurogenin-2
NSC	-	Neural stem cell
NT-3	-	Neurotrophin-3
NT-4	-	Neurotrophin-4
OPC	-	Oligodendrocyte precursor cell
PBS	-	Phosphate buffered saline
PCR	-	Polymerase chain reaction
PD	-	Population doubling
PDGF-a	-	Platelet-derived growth factor-a
PDGFR-α	-	Platelet-derived growth factor receptor-α
PFA	-	Paraformaldehyde
PLP	-	Proteolipid protein
PNS	-	Peripheral nervous system

qPCR	-	Quantitative polymerase chain reaction
rt-PCR	-	Reverse transcriptase polymerase chain reaction
SCA1	-	Stem cell antigen 1
SCI	-	Spinal cord injury
SD	-	Standard deviation
SEM	-	Standard error of the mean
SHED	-	Stem cells from human exfoliated deciduous teeth
TGFβ-1	-	Transforming growth factor β-1
VEGF-A	-	Vascular endothelial growth factor-A

Chapter 1: General introduction

1.1 Introduction

Over recent years, substantial progress has been made in the field of stem cell research. Stem cells, and more lineage-restricted progenitor cells, possess increased self-renewal capabilities and the ability to differentiate into multiple cell types, depending upon their tissue of origin. A wide range of therapeutic applications have been proposed for stem cells including the treatment of diabetes mellitus, cancer and heart damage.

Spinal cord injury (SCI) represents one such clinical challenge as no natural repair or regeneration is seen following injury and victims are left severely debilitated with motor and sensory deficits (Thumbikat *et al*., 2009). Substantial evidence suggests that stem cells are able to promote a degree of recovery from such damage (Kim and de Vellis, 2009). There are two proposed mechanisms as to how transplanted stem cells are able to exert this effect. The first is through the release of soluble factors that minimise the extent of damage, recruit endogenous cells and promote natural repair and regeneration. Others suggest that grafted cells can differentiate into neuronal and glial cell types to directly replace those lost following injury. Clinical trials have commenced investigating stem cells isolated from embryonic (Keirstead *et al*., 2005), neural (Gupta *et al*., 2012) and bone marrow (Park *et al*., 2012) tissues as treatments for SCI. However, the use of embryonic or neural stem cells derived from foetal tissue remains a highly controversial ethical issue that will unlikely ever be satisfactorily resolved, and the isolation of bone marrow stem cells involves invasive and painful surgical procedures. As such, alternative sources from which stem/progenitor cells can be

painlessly isolated, without the destruction of embryonic tissue, are actively sought.

The dental pulp harbours progenitor cells that can be easily accessed as part of routine orthodontic treatment, and cryogenically preserved to create a pool of patient-matched cells that are readily-available for future use (Woods *et al*., 2009). Early animal studies have demonstrated promise for the ability of dental pulp progenitor cells (DPPCs) to improve functional outcome following damage to the spinal cord (de Almeida *et al*., 2011; Sakai *et al*., 2012). These effects appear to be mostly protective and mediated through growth factor release. It is, as yet, unclear whether DPPCs are capable of differentiation into neuronal and glial cell types in the injured spinal cord. Against this background, the overall aim of this thesis is to assess the potential of DPPCs to functionally replace neurons and oligodendrocytes lost following SCI.

1.2 The peripheral and central nervous systems

In order to understand neuronal damage, and the lack of subsequent regeneration, the basic fundamentals of central nervous system (CNS) functionality and the contributions made by each specialised cell type must be discussed. The CNS, comprising of the brain and spinal cord, acts as the control centre of the human body. It receives and processes sensory information from the peripheral nervous system (PNS) and returns electrical signals, coordinating bodily functions. Resident cells of the PNS and CNS broadly fall under one of two categories: neuronal or glial cells.

1.2.1 Cell types

1.2.1.1 Neurons

Neurons are responsible for the transmission of electrical signals between the CNS and all tissues via highly a highly connected neuronal network. Neuronal cells are often identified by the presence of structural proteins such as βIII-tubulin, microtubule associated protein 2 (Map2) (Cáceres *et al*., 1986) and subtypes of neurofilament (NF) (Lee and Cleveland, 1996). There are many classes of neuron, differing in morphology, electrophysiological properties, neurotransmitter signalling molecules and precise functions. Typically multipolar, neuronal cells often possess dense networks of dendrites, surrounding a small cell body, which act to receive chemical signals from other interconnected neurons. Neurons may then relay these signals via axonal projections which extend over long distances to other cells.

The key property of neuronal cells that enables them to function in this manner is an electrically excitable membrane that allows the generation of action potentials (Figure 1.1). Our knowledge of the ionic basis of events underlying action potentials is based on a series of electrical recordings taken from the giant axons of squid by Hodgkin and Huxley (1952). Although it is now known that there is a huge diversity in action potential dynamics, depending upon neuronal type and even the location on the cell at which a recording is taken from (reviewed by Bean, 2007), the basic principles of Hodgkin and Huxley's model still hold true. At rest, neuronal membranes are held at a low potential, with high intracellular levels of K^+ and low Na^+, and contain many voltage-gated ion channels. Depolarisation of the cell membrane, following an appropriate chemical stimulation, results in the opening of voltage-activated channels and influx of Na^+ ions into the cell. This change in membrane potential results in further depolarisation and activation of more Na^+ channels. After a sustained opening period, Na^+ channels inactivate and the efflux of K^+ ions through voltage-activated channels begins to predominate, reducing the membrane potential towards resting levels (Figure 1.1 A). During repolarisation, efflux of K^+ often results in a small period of hyperpolarisation, where the membrane potential is at a lower voltage than at rest. Passive leakage of potassium down its electrochemical gradient slowly brings the membrane voltage back to resting levels. Whilst sodium channels remain inactive, further action potentials cannot be evoked, this is known as the refractory period and allows the unidirectional propagation of action potentials. Action potentials travel as a wave along the length of axons, whereby the excitation of one region results

in the depolarisation, and subsequent excitation, of adjacent regions. This process continues until the action potential reaches an axon terminal/cell body. Action potentials cannot be evoked in recently excited regions of membrane that are refractory and so the electrical signals travel in one direction only (Figure 1.1 B). Upon reaching an axon terminus, membrane depolarisation results in the activation of voltage-sensitive Ca^{2+} channels allowing the influx of Ca^{2+} ions (reviewed by Rusakov, 2006). Increased intracellular calcium initiates the process of neurotransmitter release, whereby vesicles bind to the membrane and release their neurotransmitter contents into the synaptic cleft. The neurotransmitters then bind with complimentary receptors on the membrane of connected target cells to exert their specific effects.

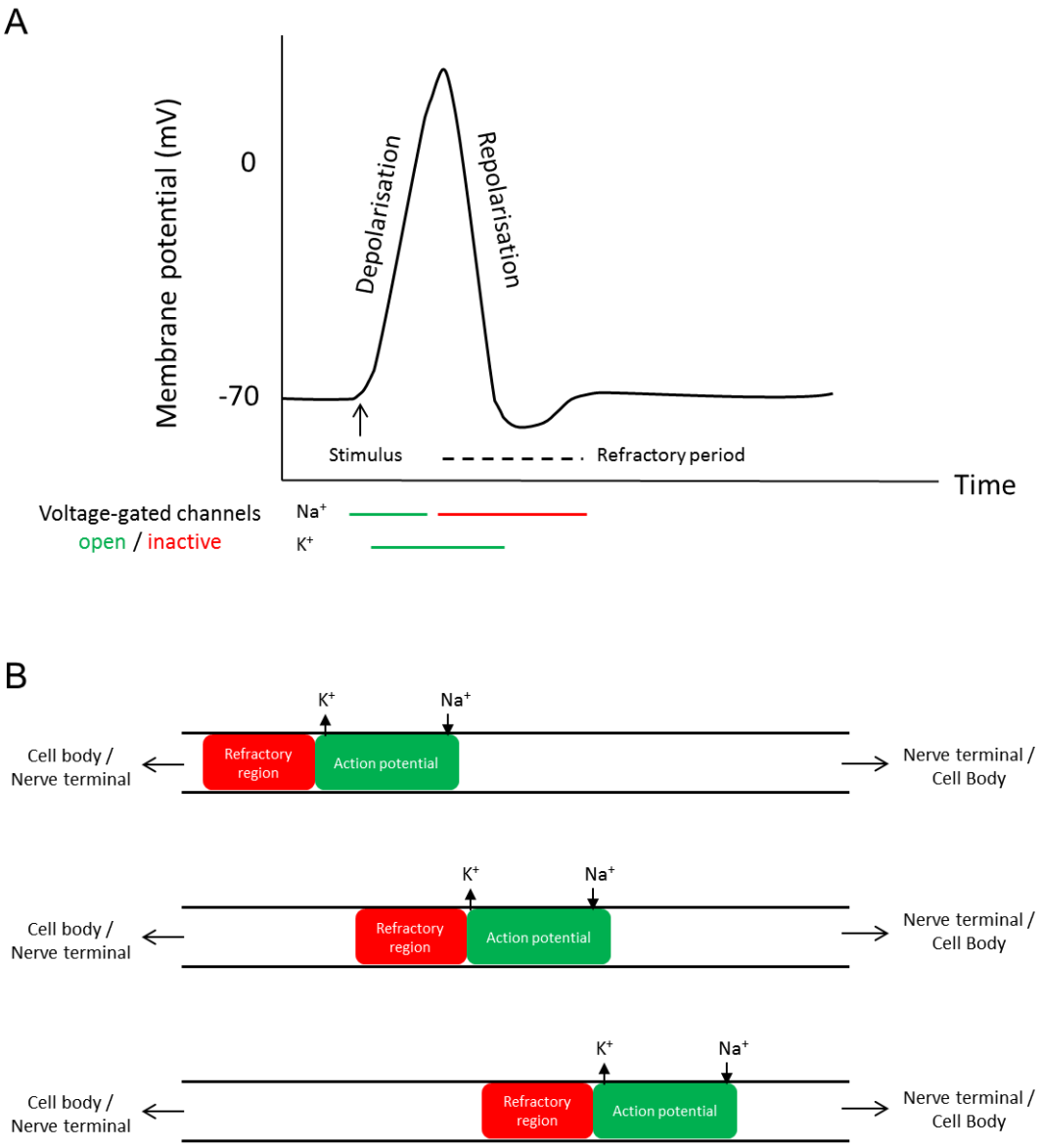

Figure 1.1 – Generation and propagation of neuronal action potentials

A) Neuronal action potentials are generated following an appropriate stimulus to depolarise the membrane resulting in the opening of voltage-activated Na^+ and K^+ channels. Initially Na^+ currents predominate, resulting in further membrane depolarisation until sodium channels become inactivated. The cell membrane then repolarises through the efflux of K^+ ions. During the refractory period, while sodium channels remain inactive, the membrane is unable to be further excited to generate another action potential. B) Action potentials are propagated unidirectionally along the lengths of axons either from cell bodies towards nerve terminals, or in reverse. Depolarisation of the axonal membrane, during an action potential, results in depolarisation and excitation of adjacent sections. Recently excited membrane regions remain refractory and so the action potential is unable to travel back in the direction from where it came.

1.2.1.2 Glial cells

Neuronal cells are able to function in this specialised signalling role thanks to a diverse cast of supporting cells – the glia. Each type of glial cell plays a specific well-defined role.

Microglia are the resident immune cells of the brain and spinal cord, and can be identified by expression of cell surface markers such as CD11b, CD45 and IBA-1 (Sedgwick *et al*., 1991; Hirasawa *et al*., 2005). Their function is analogous to that of macrophages within other body tissues, scavenging and phagocytosing cellular debris and invading pathogens (reviewed by Napoli and Neumann, 2009).

Astrocytes provide homeostatic support to neuronal cells and are often identified by the expression of glial fibrillary acidic protein (GFAP) and S100b calcium-binding protein (Nolte *et al*., 2001; Ogata and Kosaka, 2002). Astrocytes assist in maintaining a favourable environment for neuronal survival and function via numerous mechanisms including: the release of growth factors (Dreyfus *et al*., 1999), production of matrix proteins to provide structural support (Liesi *et al*., 1983), K^+ buffering to maintain ionic balance (Holthoff and Witte, 2000), formation and maintenance of the blood-brain barrier (Sobue *et al*., 1999) and provision of metabolic support (Wender *et al*., 2000).

Oligodendrocytes are highly branched cells that act to facilitate the conduction of action potentials in the CNS by attaching to axons and

insulating them with layers of myelin. This allows electrical signals to travel at speed over great distances without decreasing in strength via saltatory propagation (Figure 1.2). Due to the electrical insulating properties of myelin, action potentials are able to effectively “leap” from one region of unmyelinated axon (known as a Node of Ranvier) to the next (Figure 1.2 B), increasing speeds of conduction up to 10-fold (Purves *et al*., 2001). One oligodendrocyte cell can attach to and myelinate multiple axons within its vicinity (Lubetzki *et al*., 1993). Mature oligodendrocytes are typically identified by the expression of myelin-associated proteins such as myelin basic protein (MBP), myelin/oligodendrocyte specific protein (MOSP) or galactocerebroside (GalC) (reviewed by Buchet and Baron Van-Evercooren, 2009).

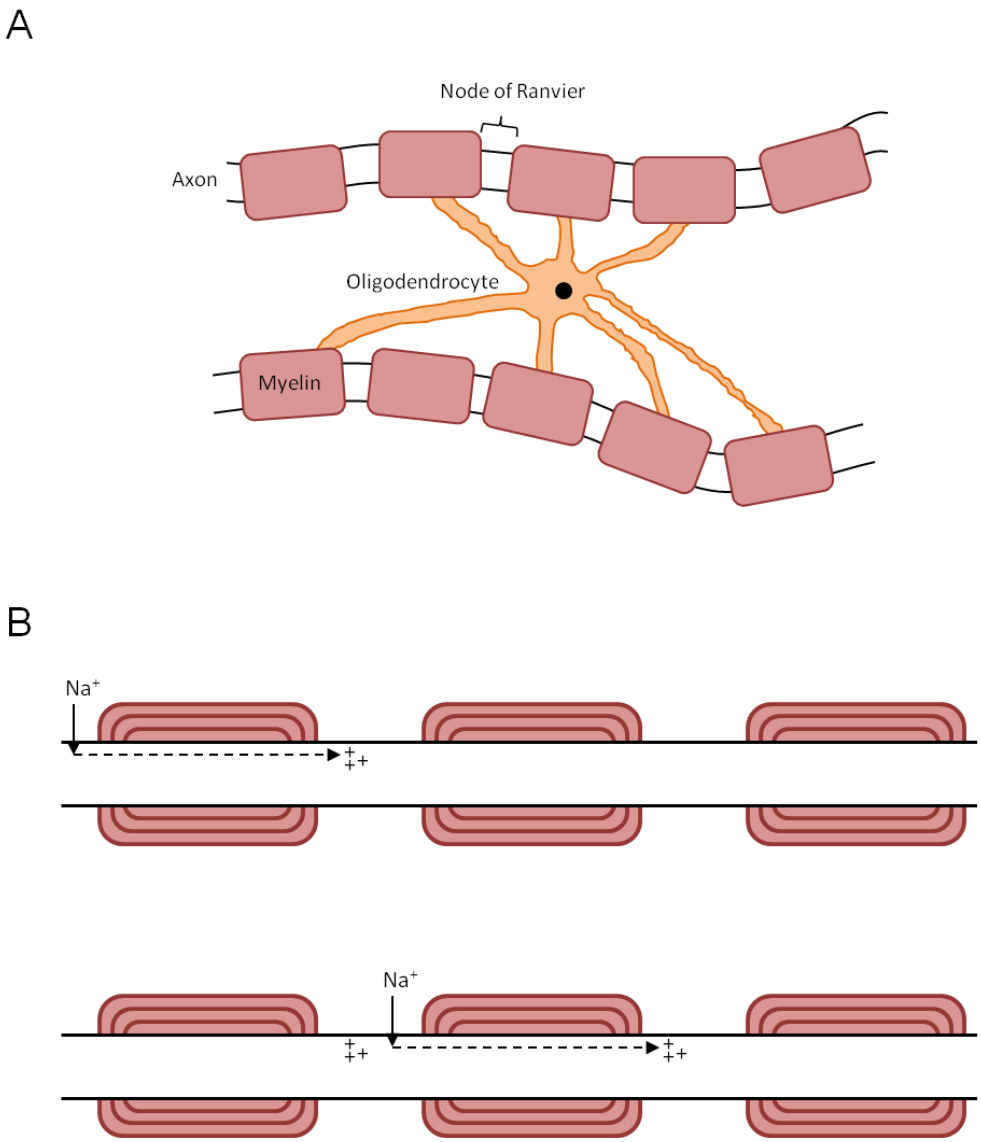

Figure 1.2 – Facilitation of neuronal signalling by oligodendrocytes

The propagation of action potentials over long distances at speed is aided by the actions of oligodendrocyte cells. A) Oligodendrocytes extend a network of processes which attach to nearby neuronal axons. The oligodendrocytes ensheath axons with multiple layers of myelin, providing electrical insulation. Action potentials "skip" between Nodes of Ranvier (regions of unmyelinated axon) by the process of saltatory conduction (B). Following excitation, opening of voltage-gated Na^+ channels results in a region of localised depolarisation. Due to the insulation provided by myelin, the charge cannot leak out in immediately adjacent regions of membrane and, instead, travels further along the axon to the next Node of Ranvier. This localised depolarisation results in the activation of voltage-gated Na^+ channels to trigger an action potential which, in turn, depolarises the membrane at the subsequent Node of Ranvier and so on down the length of the axon. In this manner, action potentials can travel along myelinated axons up to 10 times faster than unmyelinated equivalents (Purves *et al*., 2001).

Schwann cells are the myelinating cell of the PNS. In contrast to oligodendrocytes, each Schwann cell is typically associated with, and myelinates, only a single axon. As a result they demonstrate much less complex branching and are more bipolar in morphology (Corfas *et al*., 2004). S100 calcium-binding proteins are the most commonly used marker to identify Schwann cells (Gonzalez-Martinez *et al*., 2003), although, as with oligodendrocytes, they also express myelin-associated proteins including MBP.

Myelin sheets consist primarily of lipids with structural stability provided by cross-linking proteins. Although slight differences in the lipid compositions of CNS and PNS myelin are evident, it is in the protein fraction where significant variations are observed. Proteolipid protein (PLP) is the main structural protein found in CNS myelin, constituting 30 – 50% of the total protein content. Very little PLP is found in PNS myelin, where its crosslinking function is compensated for by P_0 glycoprotein to provide stabilisation of lipid layers (Quarles *et al*., 2005). Similarly MBP accounts for approximately 30% of the protein content of CNS myelin, but only 5 – 18% of PNS myelin. Despite the differences in myelin composition within the central and peripheral nervous systems, the functionality is largely unaffected.

1.2.2 Neurotrophic and growth factors

A number of growth factor molecules help to maintain nervous system functionality by supporting cell survival. Members of the neurotrophin family: nerve growth factor (NGF), neurotrophin-3 (NT-3) and brain-derived

neurotrophic factor (BDNF) help to differentially maintain survival of neuronal subtypes under normal physiological conditions (reviewed by Skaper, 2012). Other growth factors, such as basic fibroblast growth factor (bFGF) and platelet-derived growth factor-a (PDGF-a) act as potent mitogens for early stage neuronal and oligodendrocyte cells. (Engel and Wolswijk, 1996; Gritti *et al*., 1996). Transforming growth factor β-1 (TGFβ-1) and the closely-related glial cell line-derived neurotrophic factor (GDNF) may afford protection to neuronal cells against excitotoxicity as a result of elevated glutamate levels (Ho *et al*., 2000). Insulin-like growth factor-1 (IGF-1) has been demonstrated to possess anti-apoptotic properties for oligodendrocytes (Ness and Wood, 2002) and can encourage their maturation (Hsieh *et al*., 2004).

1.3 Spinal cord injury

Spinal cord injury (SCI) is a major cause of paralysis worldwide. Often fatal, due to paralysis of the intercostal and other muscles essential for maintenance of breathing, there is an estimated global incidence rate of 15 – 40 non-lethal cases per million people per year (Lee *et al*., 2013). The causes of injury are wide and varied, although, perhaps unsurprisingly, motor vehicle accidents, trips/falls, sports injuries and violence all feature prominently (Figure 1.3).

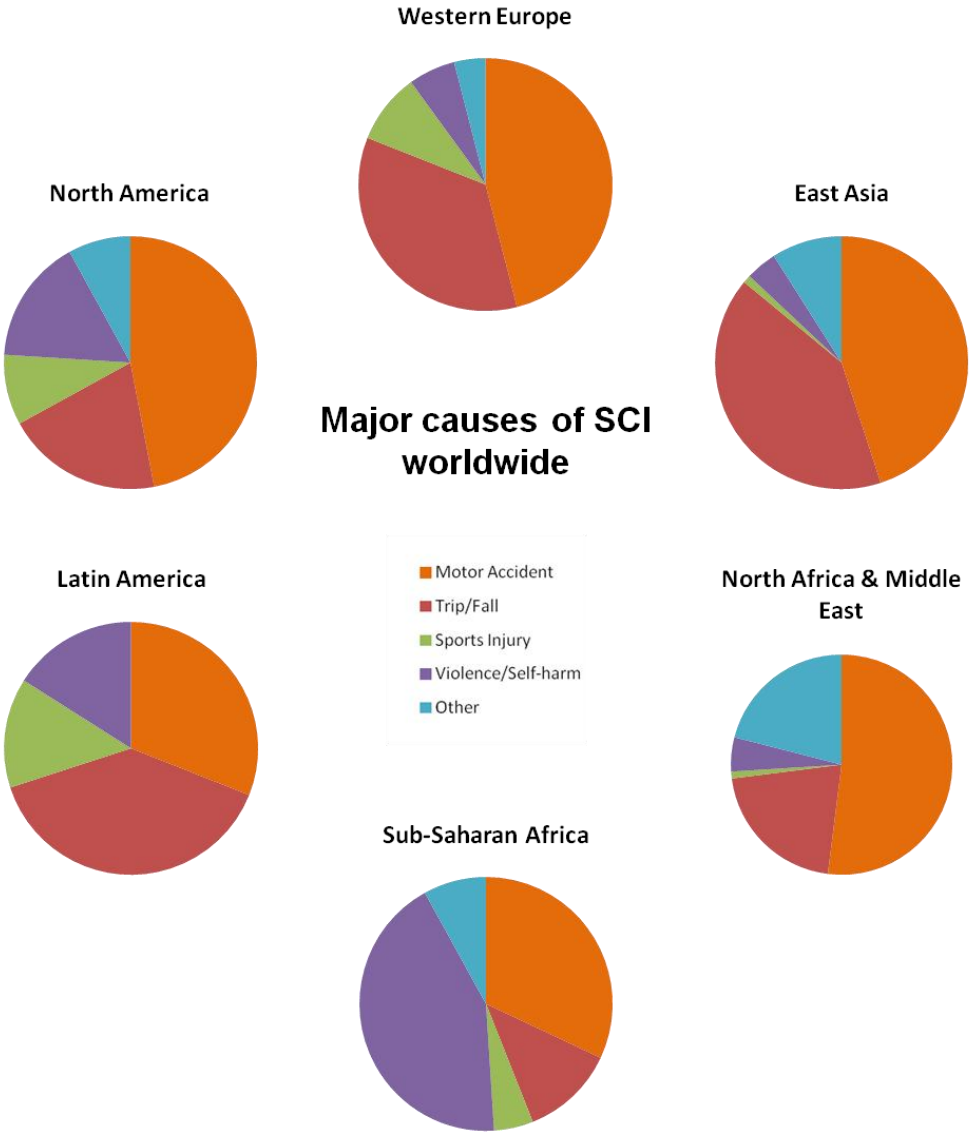

Figure 1.3 – Major causes of SCI resulting in paralysis
Worldwide, motor vehicle accidents and falls are among the major causes of paralysis (statistics taken from Lee *et al*., 2013).

There are four main types of damage that can be inflicted upon the cord. Contusion injuries are the most commonly observed and occur as the result of a sudden impact bruising the cord. Increased pressure placed upon the spinal cord, by a developing tumour for example, may cause a compression injury. Laceration injuries occur where fragments of shattered bones sever the neural tissue. Finally, the spinal cord is susceptible to concussion injuries, where the effects may only be temporary and recovery is usually seen within 24 – 48 hours (Zwimpfer and Bernstein, 1990). Most SCIs usually involve a combination of the above mechanisms (Sekhon and Fehlings, 2001).

In addition to the physical consequences of SCI, which vary in severity depending upon the location and type of injury, significant psychological and social burdens are inflicted on both patients and their families. In the most severe of non-fatal cases, there is a complete loss of all motor and sensory functions, as well as reflexes, at spinal levels below the site of injury (Thumbikat *et al*., 2009). An injury affecting only one side of the spinal cord may result in unilateral paralysis. It is estimated that lifetime care costs for a 25 year old who suffers a complete injury in the upper cervical region, resulting in quadriplegia, may be as high as $3million and so there is also a considerable financial impact (Priebe *et al*., 2007).

1.3.1 Pathophysiology

The pathophysiology of SCI can be divided into two separate phases. The primary phase involves the physical insult to the spinal cord itself disrupting blood vessels, axons and cell membranes. The secondary phase includes multiple events that subsequently occur at the cellular level.

The initial damage compromises the blood-brain barrier integrity allowing the infiltration of leukocytes and other inflammatory cells into the neural tissue (Fleming *et al*., 2006). The resulting inflammatory response triggers activation of microglia and astrocytes which, in turn, release further pro-inflammatory factors attracting more white blood cells and exacerbating the inflammation (Babcock *et al*., 2003). The release of proteolytic and oxidative enzymes by activated microglia enlarges the injury area and contributes to neurological dysfunction (Fleming *et al*., 2006).

The neurological deficits that occur as a result of SCI are primarily attributed directly to cellular loss, and the resultant disruption of neuronal signalling. Various factors induce cellular death additional to the initial physical trauma. Activated microglia express Fas ligand to induce glial and neuronal apoptosis (Casha *et al*., 2001). Disruption of the vascular supply results in extensive haemorrhaging at the injury site (Tator and Koyanagi, 1997) and the subsequent ischaemia can contribute to cell death via mitochondrial dysfunction (Sullivan *et al*., 2007). Loss of ionic homeostasis leads to the accumulation of neurotransmitters, including glutamate, which can induce neuronal cell death via excitotoxic mechanisms (Yanase *et al*., 1995;

Wrathall *et al*., 1996). Oxidative radicals are released in the immediate aftermath of SCI and are responsible for membrane peroxidation and DNA and protein damage. Activated leukocytes and macrophages release superoxide as part of the inflammatory response, and ischaemia-reperfusion events increase free radical generation, contributing to cell death (reviewed by Genovese and Cuzzocrea, 2006).

The degradation of normal axonal signalling pathways is also heavily involved in functional impairment. Wallerian degeneration, a process whereby the section of a severed axon distal to the cell body progressively disintegrates, is observed extensively following injury (Guth *et al*., 1999). Also of key importance is the delayed chronic demyelination that presents as a result of oligodendrocyte death (Totoui and Keirstead, 2005).

1.3.2 Repair and regeneration following SCI

The CNS lacks capacity for endogenous repair, unlike the PNS where a degree of natural regeneration is observed to restore functionality (reviewed by Navarro, 2009). Overcoming the numerous factors that prevent CNS regeneration is a key goal for research into treatments for various conditions including SCI, stroke and Parkinsons disease.

Astrocytes are heavily involved in the pathological events inhibiting CNS regeneration. Over a number of days following injury, astrocytes proliferate at the site of injury and bind tightly together through numerous interwoven extracellular processes to form the glial scar (Wilhelmsson *et al.,* 2006; Sun *et al*., 2010). This is primarily a protective mechanism as the scar is largely

impenetrable, providing a physical barrier to prevent the infiltration of inflammatory leukocytes and to restrict damaging factors to the injury site. However, access of endogenous oligodendrocyte precursor cells (OPCs) to demyelinated axons is also blocked, preventing remyelination. Additionally, the scar is inhibitive to axonal regrowth and regeneration due to the expression of inhibitory molecules including chondroitin sulphate proteoglycans and cytotactin/tenascins (McKeon *et al*., 1991). Furthermore, axonal growth inhibitory molecules – myelin-associated glycoprotein and NoGo – may be released as by-products from the breakdown of myelin (reviewed by Sandvig *et al*., 2004). As a consequence, the injured spinal cord presents an extremely hostile environment to cell growth.

1.3.3 Roles of neurotrophic and growth factors

A recent study has suggested that, following a spinal cord injury, only minor changes in the mRNA expression profile of neurotrophin and growth factors are observed. Excepting increases in expression of IGF-1 and TGFβ-1 and downregulation of PDGF-a, the endogenous growth factor profile remains largely unchanged (Hawryluk *et al*., 2012a). Modulating the injured spinal cord environment by administering exogenous neurotrophins and/or growth factors can help to create more supportive conditions for regrowth and regeneration. Such strategies have proven effective in promoting locomotor recovery in a number of experimental models of SCI (Bregman *et al*., 1997; McTigue *et al*., 1998; Rabchevsky *et al*., 2000; Koda *et al*., 2002; Widenfalk *et al*., 2003; Iannotti *et al*., 2004; Zhang *et al*., 2013). The precise mechanisms resulting in functional recovery are varied and help to highlight

the significance of each growth factor in the regenerative process. BDNF and NT-3 can each promote axonal regrowth (Bregman *et al*., 1997; McTigue *et al*., 1998), with BDNF also observed to inhibit oligodendrocyte apoptosis resulting in increased axonal remyelination (Koda *et al*., 2002). Administration of GDNF has been associated with increased neuronal survival and decreased cavity size (Iannotti *et al*., 2004). Similarly, bFGF may help protect against apoptosis of neuronal cells (Rabchevsky *et al*., 2000; Zhang *et al*., 2013). Administration of vascular endothelial growth factor-A (VEGF-A) results in improved locomotor function through an alternative mechanism associated with the maintenance/repair of spinal cord blood vessel architecture (Widenfalk *et al*., 2003). The reported lack of upregulation of neurotrophic and growth factor expression (Hawryluk *et al*., 2012a) will certainly contribute to the limited regenerative ability of the injured spinal cord.

1.3.4 Current clinical treatment

Using treatments currently available, it is impossible to completely reverse the effects of spinal cord injury. Instead, short-term emphasis is placed on minimising the extent of further damage after the initial injury, and longer term rehabilitation and symptom management through physiotherapy. An immediate focus is placed on immobilising and stabilising the injury site to prevent any further damage caused by the movement of shattered vertebrae, as well as maintaining blood pressure and clear airways (Bernhard *et al*., 2005). The steroidal anti-inflammatory Methylprednisolone is commonly administered in the weeks following SCI and may prove useful in reducing

secondary inflammatory damage. However, its actual beneficial value still remains a matter of some controversy (Sayer *et al*., 2006; Suberviola *et al*., 2008). Decompression surgery, the removal of various tissues or bone fragments that may exert pressure on the cord, can be carefully performed with benefit in some patients (Papadopoulos *et al*., 2002). Physiotherapy can assist with physical rehabilitation, allowing patients to maximise their capabilities (Jacobs and Nash, 2004).

1.3.5 Clinical treatments in development

A number of emerging treatments that may help to improve recovery after SCI are currently in early stage clinical trials. A number of these developing therapeutics focus on neuroprotection strategies to reduce the extent of damage in the early stages of SCI. Following systemic hypothermia treatment, where the vascular system is cooled to 33°C to reduce secondary inflammation, increased numbers of patients show improved physical recovery, in comparison to control subjects, without adverse effects (Levi *et al*., 2010). Riluzole, a Na^+ channel blocker known to reduce excitotoxic cell death and already approved for the treatment of amyotrophic lateral sclerosis, is currently undergoing phase I trials for SCI (Fehlings *et al*., 2012). Minocycline acts against a number of the secondary mechanisms of injury by inhibiting microglia activation, stabilising mitochondrial activity and neutralising oxidative radicals. Improved motor recovery over one year of minocycline treatment was observed in a randomised placebo-controlled phase II clinical trial (Casha *et al*., 2012).

Alternative approaches act to reverse the inhibition of endogenous CNS regeneration by myelin-breakdown products. Monoclonal antibodies against NoGo protein are currently in phase II clinical trials (Zörner and Schwab, 2010). The inhibition of Rho signalling, normally activated by myelin-breakdown products resulting in axonal growth cone collapse, using Cethrin, has proven effective in early-stage clinical trials of injuries at the cervical level (Fehlings *et al*., 2011).

Due to the complexity of the pathological events following spinal cord injury, it is improbable that one single treatment will act as a “magic bullet” to promote complete recovery. Rather, a combination of therapies will likely prove more effective by targeting multiple mechanisms to reduce damage and promote recovery. A great focus of research emphasis over recent years has been placed on cell replacement strategies using stem cells which can promote recovery through multiple mechanisms (Figure 1.4). The ideal treatment would help to recover normal neural function by replacing lost neuronal and glial cells, promoting the remyelination of demyelinated axons and assisting the formation of neural connections to bridge the lesion site, thereby, allowing efficient signal transduction.

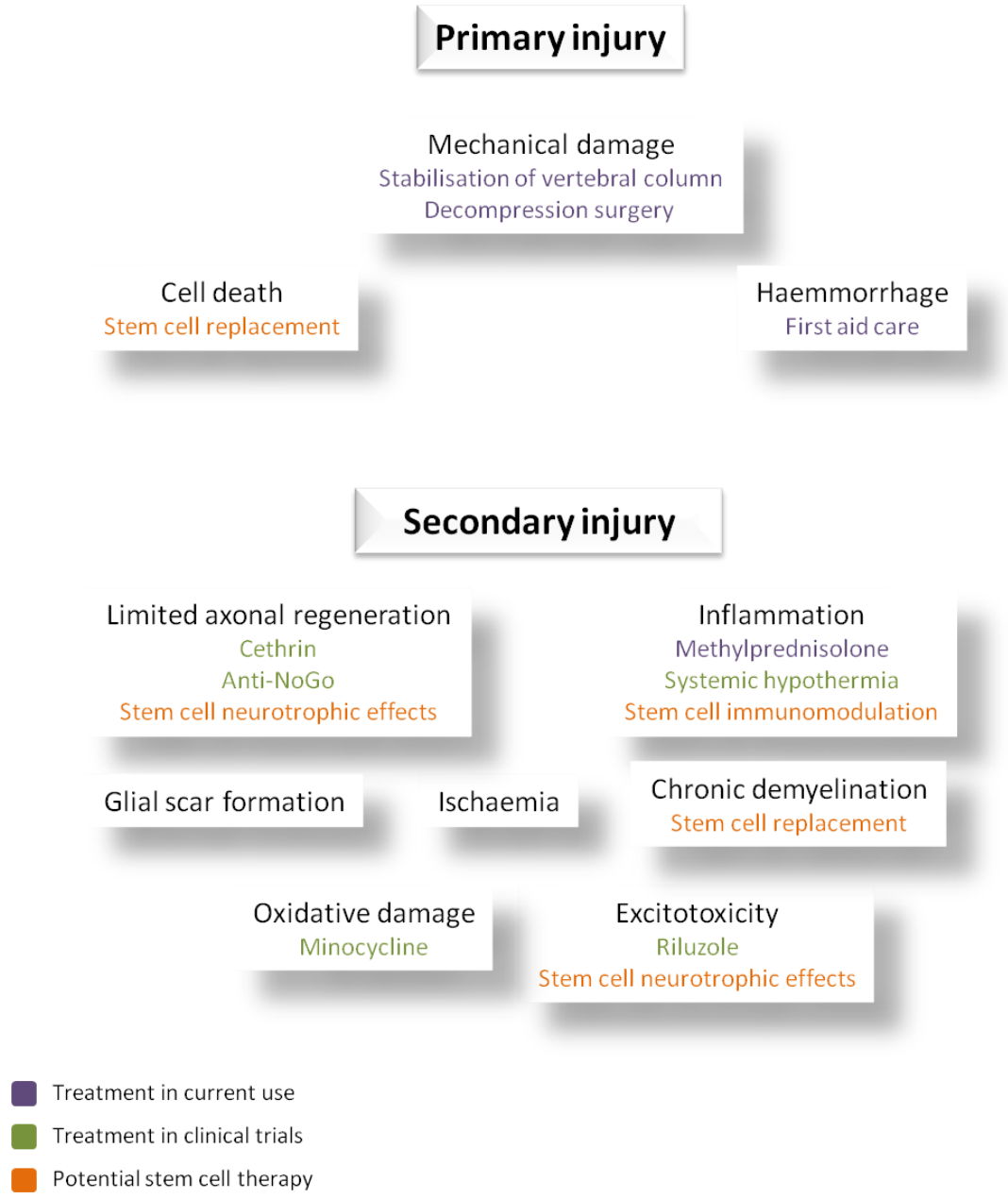

Figure 1.4 – Targets for therapeutic intervention in SCI

The complex multifaceted nature of spinal cord injury provides a range of potential targets for therapeutic intervention to reduce damage and promote repair. Stem cell transplantation strategies could prove particularly effective due to their potential to act through multiple mechanisms.

1.4 Stem cells

Stem cells, undifferentiated cells with enhanced renewal capacity and the potential to differentiate into multiple lineages, offer great promise for the treatment of a multitude of medical conditions. Stem cells can be generally classified under one of two categories depending upon their tissue of origin: embryonic stem cells (ESCs) derived from a developing embryo and adult stem cells which may be found in a number of tissues within fully developed organisms. For the treatment of spinal cord injury, research has focused primarily on ESCs, neural stem cells (NSCs) and, more recently, mesenchymal stem cells (MSCs).

1.4.1 Embryonic stem cells

Embryonic stem cells are isolated from the inner cell mass of a developing embryo during blastomere formation. These cells possess unlimited self-renewal capabilities and can be maintained in culture indefinitely (Suda *et al*., 1987). ESCs are described as pluripotent cells due to their potential to differentiate into cell types from all three primary germ layers: the endoderm, ectoderm and mesoderm (Thomson *et al*., 1998). Included among the many specific cell types that ESCs have been demonstrated to differentiate into *in vitro* are neural cell types including astrocytes, neurons and oligodendrocytes (Reubinoff *et al*., 2001)

1.4.2 Stem cells of the CNS

A diverse range of multipotent stem cells give rise to the glial and neuronal cells of the CNS in regionally and temporally specified patterns via a series of intermediate lineage-restricted precursors,. The NSCs commonly investigated *in vitro* are multipotent and can be isolated from embryonic tissue or from a number of regions of the adult CNS including: the subventricular zone (Doetsch *et al*., 1999), cortex (Arsenijevic *et al*., 2001), hippocampus (Kukekov *et al*., 1999) and the spinal cord (Weiss *et al*., 1996). NSCs are typically characterised by the expression of nestin, an intermediate filament protein (Lendahl *et al*., 1990). Under appropriate culture conditions, with the addition of bFGF and epidermal growth factor (EGF), NSCs proliferate as floating bodies of cells known as neurospheres (Wachs *et al*., 2003). NSCs within neurospheres maintain multipotency and demonstrate the ability to differentiate into astrocytes, neurons and oligodendrocytes (Arsenijevich *et al*., 2001).

Over recent years there has been a shift in the perception of what constitutes the true neural stem cell *in vivo.* Traditionally, neuroepithelial cells residing in neurogenic regions of the embryonic CNS, such as the subventricular zone, were believed to give rise directly to neuronal and glial cells (Figure 1.5). Increasing evidence, however, now points to the common precursor being more glial in nature (reviewed by Malatesta and Götz, 2013). Radial glia arise from dividing neuroepithelial cells and are typically identified by the expression of brain lipid binding protein (BLBP) and glutamate aspartate transporter (GLAST) (Anthony *et al*., 2004). Radial glia possess the ability to

divide asymmetrically: self-renewing while also giving rise to daughter post-mitotic neurons or intermediate precursor cells (Noctor *et al*., 2004) (Figure 1.5). Evidence suggests that radial glial cells give rise to the vast majority of neurons in the adult CNS (Anthony *et al*., 2004; Merckle *et al*., 2004). However, the line between neuroepithelial and radial glial cells remains blurred and, as such, the term NSC is often used interchangeably to apply to either phenotype.

Bipotential cell types with the ability to differentiate into oligodendrocytes and astrocytes, via intermediate precursors, are known as glial restricted precursors (GRPs) (Gregori *et al*., 2002). These arise from both neuroepithelial stem cells and radial glia, and are identified by expression of A2B5 antigen (Rao and Mayer-Proschel, 1997; Kessaris *et al*., 2008).

A further restriction in differentiation potential results in the derivation of oligodendrocyte precursor cells (OPCs). These are found throughout the developing CNS and diminish in number post-natally. It is believed that populations of OPCs arise from radial glial cells via GRPs (Merkle *et al*., 2004; Fogarty *et al*., 2005) although regionally specified oligodendrocytes of the spinal cord have been observed to derive from a shared motorneuron progenitor (Lu *et al*., 2002; Zhou and Anderson, 2002).

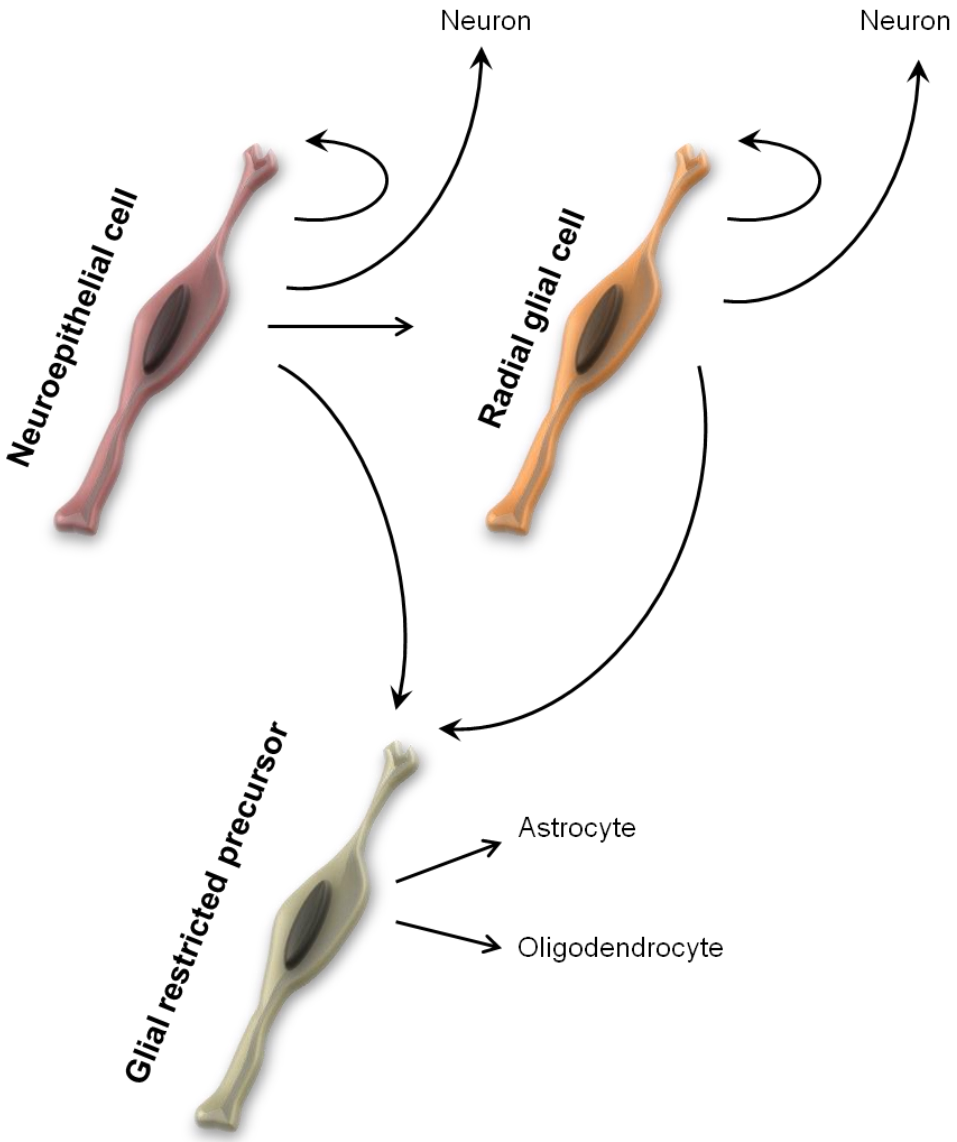

Figure 1.5 – Stem cells of the central nervous system

The concept of a neural stem cell is fluid and constantly evolving. Candidates for NSCs include neuroepithelial cells and radial glial cells, which can both give rise to daughter neuronal cells via asymmetric cell division. Glial cells typically derive from glial restricted precursor cells, themselves differentiated from radial glia and/or neuroepithelial cells.

1.4.3 Mesenchymal stem cells

MSCs represent a source of adult stem cells that can be isolated from a number of different tissues. MSCs are identified by the expression of cell surface antigens, such as CD73, CD90 and C105, together with the absence of markers for cells of haematopoetic origin, such as CD11b, CD33 and CD45 (Dominici *et al*., 2006). MSCs are typically multipotent and possess the ability to differentiate into osteoblasts, chondrocytes and adipocytes. Human MSCs have been isolated from a diverse range of sources including: bone marrow (Pittenger *et al*., 1999), known as bone marrow stromal cells (BMSCs), adipose tissue (Zuk *et al*., 2002) and umbilical cord blood (Kern *et al*., 2006).

MSCs possess an advantage over ESCs and NSCs in that their isolation does not require the destruction of brain or foetal tissue. However, MSCs may be considered less versatile due to their more restricted differentiation potential. Nevertheless, limited evidence demonstrates the *in vitro* differentiation of neuronal-like (Tropel *et al*., 2006; Anghileri *et al*., 2009) and glial-like (Kennea *et al*., 2009; Radtke *et al*., 2009; Park *et al*., 2010a) phenotypes from MSCs.

1.4.4 Stem cell therapeutics for SCI

Because the loss and/or death of cells is a significant contributing factor to the complications observed following a spinal cord injury, replacement of these cells proves an appealing therapeutic strategy. If transplanted stem cells can survive and integrate into the neural environment then recovery

may be observed (Kim and de Vellis, 2009). A number of different stem cell populations have been investigated in animal models and have demonstrated promise, justifying stem cell transplantation as a potential treatment for SCI.

1.4.4.1 Embryonic stem cell transplantation

A degree of functional recovery following the transplantation of undifferentiated ESCs into rodent models of SCI has been established by a number of studies. Murine ESCs transplanted into the spinal cords of rats 9 days after the induction of a weight drop injury can still be identified 33 days post-transplantation, demonstrating their ability to survive within the sub-acute injury environment. Markers for differentiated oligodendrocytes, astrocytes and neurons can be detected within the transplanted cell population. Improved hindlimb motor function in the transplant group is observed when compared to controls, suggesting this recovery is mediated through the spontaneous differentiation of neural cell types (McDonald *et al*., 1999).

Improved recovery following ESC transplantation, however, may not be solely mediated through direct cell replacement. Transplantation of mouse ESCs two hours following contusion injury in a mouse SCI model results in a quicker and more extensive recovery of motor function in comparison to control treated groups. Reduced levels of macrophages and neutrophils are found at the transplantation site (Bottai *et al*., 2010). As such, embryonic stem cell transplantation therapies may also help to minimise damage and

functional loss by inhibiting the inflammatory response, if applied within an acute timeframe.

1.4.4.2 Transplantation of ESC-derived neural precursors

Two cell types, in particular are thought to be essential for the restoration of normal neuronal function following a spinal cord injury. Functionally active neurons are required to reform the disrupted neural connections and oligodendrocytes are needed to myelinate demyelinated and/or newly formed axons, thereby, facilitating electrical conduction of nerve impulses. With the transplantation of undifferentiated stem cells, cell fate is entirely determined by the environment of the injured spinal cord, which is naturally inhibitive to neuronal growth and regeneration. Undesirable cell types which may hinder repair, particularly astrocytes, are often the predominant phenotype identified within grafted ESC populations (Sykova and Jendelova, 2005). One strategy to circumvent this is to pre-differentiate cells prior to transplantation, thereby restricting the potential for undesirable differentiation and improving functional outcome (Marques *et al*., 2010). The ability of ESCs to differentiate *in vitro* into precursors for oligodendrocytes and motorneurons, therefore, demonstrates promise for recovery and regeneration following SCI (Zhang *et al*., 2001; Nistor *et al*., 2005).

Using a 42 day differentiation protocol it is possible to derive a highly purified population of OPCs from human ESCs. These cells survive within spinal cord white matter and differentiate into mature oligodendrocytes. Furthermore, transplantation of these precursors is associated with elevated levels of

multilayered myelination in a mouse model of demyelination (Nistor *et al*., 2005). Following transplantation of human ESC-derived OPCs into a sub-acute model of rat SCI, increased remyelination of demyelinated axons was observed. Animals in the transplant groups showed improved hindlimb functional recovery, as assessed by behavioural and kinetic analyses. In a chronic SCI model however, although transplanted cells could still be identified within the spinal cord, there was no associated change in myelination levels or locomotion recovery. Interestingly, only around 55% of oligodendrocyte-remyelinated axons were physically associated with transplanted cells, suggesting that native oligodendrocytes may have been recruited to the site of injury (Keirstead *et al*., 2005). ESC-derived OPCs express multiple neurotrophic factors including BDNF and transforming growth factor β-2 which could be responsible for the recruitment of endogenous cells (Faulkner and Keirstead, 2005). ESC-derived OPCs have also demonstrated neuroprotective functions. Increased white and grey matter sparing is observed at OPC transplantation sites suggesting a possible inhibitory effect on factors influencing cell death following injury (Sharp *et al*., 2010). Similarly, sensory signalling pathways are preserved when OPCs are transplanted 2 hours following the induction of a contusion injury in rats (All *et al*., 2012).

Motorneuron progenitor cells derived from human ESCs and injected into the developing chick embryo survive, adopt appropriate mature morphology, projecting long range axons. Similarly, in the adult rat spinal cord, a large outgrowth of cholinergic axons can be identified (Lee *et al*., 2007). Following

a viral-induced spinal cord injury, ESC-derived motorneuron progenitor cells extend axons forming physiologically active neuromuscular junctions and are associated with an increased recovery of hindlimb grip strength (Deshpande *et al*., 2006).

The transplantation of ESC-derived oligodendrocyte and motorneuron precursor cells simultaneously may work synergistically to provide an even more effective therapeutic strategy. Following complete spinal transection, a greater extent of motor function recovery has been observed in dual transplant groups compared with transplantation of either progenitor individually (Erceg *et al*., 2010).

1.4.4.3 Transplantation of CNS stem cells

The most obvious stem cell candidates for transplantation into the injured spinal cord would be those that are resident within the CNS itself and give rise to mature neuronal and glial cells. Human foetal NSCs expanded *in vitro* as neurospheres, survive and express markers for mature neurons and oligodendrocytes following transplantation into the injured murine thoracic spinal cord. This is associated with improved locomotion recovery and, furthermore, the formation of synapses between host neurons and transplanted cells can be identified, indicating possible functional integration into neuronal signalling pathways (Cummings *et al*., 2005). Similarly, in a primate contusion injury model, mature neurons, astrocytes and oligodendrocytes can be identified as having differentiated from a population of transplanted foetal human NSCs. Animals in the transplant group

demonstrated increased spontaneous electrical activity and grip strength (Iwanami *et al*., 2005).

In addition to apparent direct cellular replacement, NSCs have also been demonstrated to promote functional recovery through neurotrophic effects. NSCs produce and secrete a range of neurotrophic factors that can promote endogenous axonal regrowth and sprouting into spinal cord lesions (Lu *et al*., 2003; Amemori *et al*., 2013). In fact, recovery may be a combination of both cellular replacement and neurotrophic effects working simultaneously. NSCs transplanted 9 days after induction of a rat SCI differentiate mainly into astrocytes and oligodendrocytes. Increased host oligodendrocyte survival can be observed together with axonal remyelination by transplanted cells (Parr *et al*., 2008)

As with embryonic stem cells, the transplantation of restricted lineage precursor cells may provide a more effective therapeutic strategy by preventing the differentiation of unwanted cell types. GRPs can be isolated from the embryonic spinal cord through fluorescence activated sorting based on expression of A2B5. These cells survive following transplantation into the injured spinal cord, migrating out from sites of injection and maturing into astrocytes and oligodendrocytes (Han *et al*., 2004). Transplantation of GRPs in combination with a similarly isolated population of neuronal-restricted progenitors into the rat spinal cord has resulted in improved locomotor activity and recovery of bladder control reflexes (Mitsui *et al*., 2005).

1.4.4.4 Transplantation of cells derived from other tissues

In addition to embryonic and CNS-derived stem cells, cells isolated from adult tissues have also demonstrated promise in experimental SCI models. BMSCs represent one such adult stem cell. Although expression of neuronal and astrocytic markers by BMSCs has been associated with functional recovery following transplantation into the spinal cord (Chiba *et al*., 2009), the regenerative effects are most likely mediated through growth factor production. BMSCs show the ability to express a range of neurotrophic factors *in vitro* (Hawryluk *et al*., 2012b) and can promote spinal cord recovery when not transplanted directly into the cord itself. Recovery has been observed following the administration of BMSCs systemically through tail vein injection (Quertainmont *et al*., 2012). Alternatively, BMSCs pre-differentiated into neuronal-like cells (Nagdhi *et al*., 2009) or Schwann cells (Someya *et al*., 2008; Kamada *et al*., 2011; Novikova *et al*., 2011) have also been shown to promote sparing of spinal cord tissue and been associated with improved functional recovery following SCI.

As an alternative to stem/progenitor cells, the transplantation of post-mitotic somatic cells can promote recovery after SCI. Increased remyelination can be observed after the transplantation of Schwann cells either alone, or in combination with olfactory ensheathing cells, a similar glial cell type found specifically in the olfactory bulb (Takami *et al*., 2002). The ability of olfactory ensheathing cells to promote this type of recovery remains a matter of debate due to a number of conflicting studies (Ramón-Cueto *et al*., 2000; Takami *et al*., 2002; Pearse *et al*., 2007).

1.4.4.5 Alternative mechanisms and approaches for stem cell therapy

A number of studies have investigated methods for enhancing stem cell-mediated functional recovery. Promising approaches include: augmentation of growth factor production, improving transplanted cell survival through the use of extracellular scaffolds or transplanting a combination of different cell types.

Genetically engineering stem cells to overexpress neurotrophic factors may provide a method for enhancing the regenerative effects mediated through growth factor release. This approach has demonstrated promise with NSCs (Lu *et al*., 2003), GRPs (Cao *et al*., 2005) and BMSCs (Lu *et al*., 2005).

Transplanted scaffolds or hydrogels can provide a means of bridging the cavity that arises following SCI. The injury site is inhospitable to neuronal growth but the provision of a suitable substrate by itself may be sufficient to aid and guide the growth and regeneration of cells and/or axons within this environment (Stokols and Tuszynski., 2006; Tysseling *et al*., 2010). Alternatively, they can be seeded with stem cells, improving transplanted cell survival and attracting axonal outgrowth (Hatami *et al*., 2009; Gros *et al*., 2010; Liu *et al*., 2013).

A synergistic effect may be achieved when transplanting more than one cell type simultaneously by targeting repair through complimentary mechanisms. Co-transplantation with Schwann cells (Olson *et al*., 2009), olfactory ensheathing cells (Luo *et al*., 2013) or BMSCs (Parr *et al*., 2008) can improve grafted NSC survival and functional outcomes.

A further alternative approach could involve the recruitment of endogenous progenitor cells to repair the damaged tissue. .Progenitors within the spinal cord are naturally recruited to differentiate and proliferate following injury (Barnabe-Heider *et al*., 2010). However, the proliferating population consists primarily of astrocyte and ependymal precursors as opposed to the more desirable oligodendrocytes and neuronal cells which could help in the recovery of neuronal function. For the greatest efficacy, any treatment to attract endogenous precursors would need to utilise a mechanism that facilitates navigation past the glial scar which would block the access of cells to the injury site.

1.4.4.6 Clinical trials

At this moment in time it remains unclear which source of stem/progenitor cells represents the most effective for use in SCI treatment. Despite the promise shown by stem cells of various origins in animal models, only a handful of treatments have progressed sufficiently to be entered into early stage clinical trials for human SCI.

The most high profile trial in recent years was run by California-based Geron pharmaceuticals investigating the use of human ESC-derived OPCs (as described by Keirstead *et al*., 2005 and Nistor *et al*., 2005). This trial was the focus of much media attention as it was the first approval for the clinical use of human ESCs. After only a year, the trial was abruptly discontinued. Despite the official line that this decision was taken on financial grounds,

whispers of safety concerns abound suggesting that even lineage-restricted ESCs may not be the best candidate for SCI stem cell therapy.

Elsewhere, no adverse effects have been reported following the transplantation of autologous BMSCs (Pal *et al*., 2009), which may even be associated with an improved quality of life for some patients (Park *et al*., 2012). The use of adipose tissue-derived MSCs has similarly demonstrated short-term safety (Ra *et al*., 2011). Human NSCs derived from 8-9 week gestational foetuses have already demonstrated promise in phase I trials for treatment of the myelin-associated disorder Pelizaeus-Merzbacher disease (Gupta *et al*., 2012) and are currently being tested for SCI.

Such early clinical trials are primarily focused on assessing safety and tolerance of transplanted cells. It is a few more years yet before any improvements, as a result of cell therapy for human SCI, can be confirmed.

1.4.4.7 Issues

The therapeutic use of stem cells remains a controversial topic, particularly with those isolated from embryonic tissues, and faces intense opposition. Isolating ESCs and NSCs involves the destruction of foetal and/or brain tissue, potentially placing limits upon their applications despite the recent advancements into clinical trials. Cells with similar properties derived from more easily accessible sources can provide a means of circumventing such ethical concerns. However, the isolation of BMSCs, the leading candidate in this field, is an extremely invasive procedure. This study aims to assess the

potential of progenitor cells residing in the dental pulp for use in SCI treatment.

1.5 The dental pulp

The dental pulp harbours the living components found within the core of the tooth. The pulp is comprised primarily of connective tissue but also contains an extensive blood capillary system and is highly innervated. A diverse range of cell types are found within the pulp including fibroblasts, odontoblasts and immune cells.

1.5.1 Function

The dental pulp has a number of physiological roles including: immune defence responses to oral pathogen invasion (reviewed by Goldberg *et al*., 2009), sensory functions (Holland, 1994; El Karim *et al*., 2011) and the production of dentine through the actions of odontoblast cells (Arana-Chavez and Massa, 2004). Dentine, an organic mineralised matrix similar in composition to bone, provides mechanical support for the brittle tooth enamel and physical protection from oral pathogen invasion. During tooth development, primary dentine, of a regular tubular structure, is secreted by odontoblasts to form a solid mass encasing the pulpal cavity. After the completion of root development, production is switched to secondary dentine, of a similar structure but at a much slower rate, through life. In response to mild pulpal injury, such as early caries, surviving odontoblasts at the pulp-dentine interface produce reactionary dentine. More severe damage, however, results in the death of odontoblasts and new odontoblast-

like cells are recruited to the injury site to produce atubular reparative dentine, protecting the vital pulp tissue (reviewed by Smith *et al*., 1995). The source of these new cells are thought to be dental pulp progenitor cells (DPPCs) which respond to extracellular signals and exogenous growth factors by migrating to the site of injury and differentiating into new dentine-forming odontoblasts (Tecles *et al*., 2005).

1.5.2 Progenitor cells

Cells with progenitor characteristics isolated from the dental pulp were first described by Gronthos *et al*. (2000). The authors isolated clonogenic populations of cells with fibroblast-like morphology from the dental pulp of human impacted molars. These cells possessed a stem cell marker profile similar to BMSCs with higher proliferative and colony-forming properties. The isolated DPPCs demonstrated the ability to produce mineralised dentine-like tissue both *in vitro* and *in vivo*. A similar population of cells, with even higher proliferation properties, were subsequently isolated from deciduous teeth and named stem cells from human exfoliated deciduous teeth (SHEDs) (Miura *et al*., 2003). Since these early reports, numerous investigations have been undertaken characterising the functions, properties, and potential uses of DPPCs and SHEDs in tissue engineering.

DPPCs represent a highly heterogeneous population of cells. Large differences are observed in the proliferation and mineralisation potential of single cell-derived clones, suggesting the existence of multiple progenitor populations within the pulp (Gronthos *et al*., 2002). One such population is

thought to be associated with perivascular region where rapid cellular proliferation is seen in response to odontoblastic injury (Shi and Gronthos, 2003; Tecles *et al*., 2005). Activation of notch signalling following pulp-capping suggests that further populations reside in the cell-rich region close to the odontoblast layer and within the pulpal stroma (Lovschall *et al*., 2005).

1.5.2.1 Properties

DPPCs are generally classified as mesenchymal stem cells due to their expression of markers such as CD44, CD73, CD90, CD105, stem cell antigen 1 (SCA1) and stro-1 (Patel *et al*., 2009; Govindasamy *et al*., 2010; Guimaraes *et al*., 2011). *In vitro,* DPPCs can be readily induced to differentiate into the classic MSC lineage cell types of osteoblasts/odontoblasts, chondrocytes and adipocytes using established protocols (Gronthos *et al*., 2002; Balic *et al*., 2010; Govindasamy *et al*., 2010).

The differentiation potential of DPPCs may not be strictly limited to mesenchymal cell types, however. Expression of pluripotency markers, such as nanog, Oct-4, SOX2 and SSEA4 can be found in cultured cells (Guimaraes *et al*., 2011; Osathanon *et al*., 2011; Karaöz *et al*., 2011). Additionally, DPPCs already express markers associated with more mature phenotypes, such as muscle (α-smooth muscle actin and myosin II (Patel *et al*., 2009)) and neurons (βIII-tubulin and Map2 (Karaöz *et al*., 2011)). A number of studies have demonstrated the potential for endothelial (Iohara *et al*., 2008 and 2013) myogenic (Kerkis *et al*., 2008; Nakatsuka *et al*., 2010),

hepatocytic (Ishkitiev *et al*., 2012) and melanocytic (Stevens *et al*., 2008; Paino *et al*., 2010) differentiation. Due to this potential versatility, a varied range of therapeutic applications have been proposed for DPPCs (Figure 1.6).

1.5.2.2 Advantages of DPPCs

The dental pulp has a distinct advantage over other adult sources of MSC-like cells in that it can be accessed through entirely non-invasive procedures. Healthy adult teeth, particularly impacted molars, are often extracted during orthodontic treatment, while deciduous teeth are naturally shed in childhood. Rather than simply discarding the teeth, pulpal tissue can be excavated and cryogenically preserved. DPPCs or SHEDs can subsequently be isolated from such tissue, following thawing, with no detrimental effects in viability, proliferation or differentiation (Woods *et al*., 2009; Ma *et al*., 2012). This has led to the founding of tissue banks which serve as stores of patient-matched progenitor cell samples ready to be accessed if and when required in the future.

A number of studies have demonstrated potent immunomodulatory properties of DPPCs. Immunogenic reactions to DPPCs may be suppressed by the inhibited activation and induced apoptosis of T-cells (Pierdomenico *et al*., 2005; Demircan *et al*., 2011; Zhao *et al*., 2012). This suggests that in addition to patient-matched autologous applications, DPPCs may be tolerated as an allogeneic cell transplant without the need for immunosuppression (Kerkis *et al*., 2008).

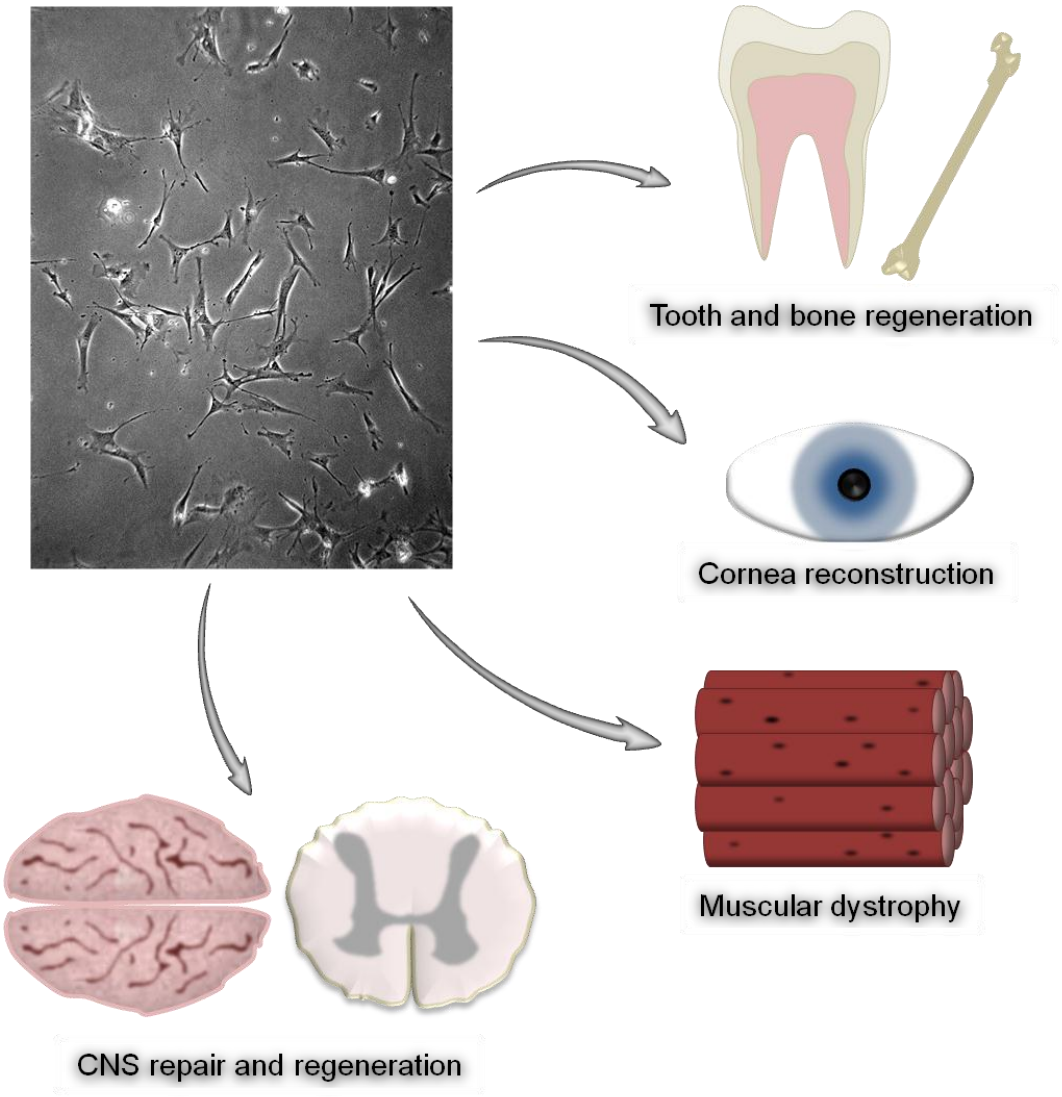

Figure 1.6 – Proposed therapeutic applications of DPPCs

Dental pulp progenitor cells demonstrate promise for the repair and regeneration for varied tissue types including neural, muscular, corneal and mineralised tissue.

1.5.2.3 DPPCs and the CNS

DPPCs possess a number of characteristics that suggest they may provide a suitable and effective alternative to embryonic or neural stem cells for cell replacement therapies in the CNS. A number of markers commonly used to identify the stem and progenitor cells of the CNS are expressed by DPPCs. Nestin (Gronthos *et al*., 2002; Király *et al*., 2009; Patel *et al*., 2009), musashi (Karbanová *et al*., 2011), SOX2 (Karaöz *et al*., 2011) and A2B5 (Sakai *et al*., 2012) have all been found to be expressed by cultured DPPCs indicating that they might have an inherent capacity to differentiate into neuronal and glial cell types. In fact, undifferentiated DPPCs often demonstrate low basal expression levels of more mature neuronal markers, such as Map2, NF and βIII-tubulin (Osathanon *et al*., 2011; Sakai *et al*., 2012). Similarly, expression of the astrocytic marker GFAP (Gronthos *et al*., 2002; Sakai *et al*., 2012) and oligodendrocyte-associated 2',3'-cyclic-nucleotide 3'-phosphodiesterase (CNPase) (Sakai *et al*., 2012) has also been reported.

1.5.2.3.1 Neuronal differentiation

Various protocols have been devised for the *in vitro* differentiation of neuronal-like cells from DPPCs (reviewed by Young *et al*., 2013). The most commonly adopted method involves the generation of floating neurosphere-like bodies by culturing in media containing bFGF and EGF on low-attachment culture surfaces (Table 1.1). When cells are dissociated from neurospheres and allowed to attach to coated plastics, they adopt appropriate neuronal morphology and express the early stage neuronal markers Map2 and βIII-tubulin (Sasaki *et al*., 2008). A further maturation

step, with the addition of neurotrophic factors to culture media, may result in a more complex morphology and the expression of later stage markers such as NF or neuromodulin (Iohara *et al*., 2006; Govindasamy *et al*., 2010).

Patch clamp recordings, to assess electrophysiological functionality of neuronal-like cells, have been reported for two further differentiation protocols (Arthur *et al*., 2008; Király *et al*., 2009) (Table 1.2). Arthur *et al*. devised two separate differentiation protocols resulting in the differentiation of βIII-tubulin, NF and neural cell adhesion molecule (NCAM)-positive sensory and motor neuron-like cells. Cells differentiated using this protocol display voltage-gated Na^+ currents consistent in properties with neuronal cells. The protocol developed by Király *et al*. involves stimulation of cAMP and protein kinase C signalling to induce expression of neurogenin-2 (Ngn2), NF and neuron-specific enolase. In addition to Na^+ currents, cells differentiated using this protocol also possess voltage-activated K^+ currents. However, no action potentials or spontaneous activity are demonstrated by these cells (Aanismaa *et al*., 2012). The generation of an action potential by neuronally-differentiated DPPCs has yet to be observed. This is a key requirement for proving that DPPCs truly can differentiate into functionally active neurons, providing evidence of their potential to promote CNS repair through direct cellular replacement.

Table 1.1 - *In vitro* protocols for the differentiation of neuronal-like cells from DPPCs involving the formation of neurosphere-like bodies (from Young *et al.,* 2013)

Reference	Cell source	Base medium	Supplements	Growth Factors	Coating	Duration	Outcome
(Takeyasu *et al.*, 2006)	Heterogeneous rat DPSC	DMEM/F12	N2 Plus 1.55mg/ml glucose 0.5mM L-glutamine 1.69mg/ml $NaHCO_3$	20ng/ml bFGF 20ng/ml EGF	Low-binding culture plates	2 weeks	Formation of neurosphere-like bodies Nestin expression downregulated and upregulated GFAP
(Sasaki *et al.*, 2008)	Heterogeneous rat DPSC	DMEM/F12	B27	20ng/ml bFGF 20ng/ml EGF	Superhydrophobic plates	3-4 days	Formation of neurosphere-like bodies Nestin expression localised along sphere edges, S100 expression in the centre Dissociated cells adopt neuronal-like morphology with βIII-tubulin and Map2 expression
(Iohara *et al.*, 2006)	Porcine side population DPSC	Neurobasal	B27 2mM L-glutamine	bFGF EGF		15 days	Formation of neurosphere-like bodies
		Neurobasal	10µg/ml N2 2mM L-glutamine	20ng/ml bFGF 40ng/ml EGF	1µg/ml laminin 1µg/ml fibronectin	24 hours	
		Neurobasal	10µg/ml N2 2mM L-glutamine	20ng/ml NT-3	1µg/ml laminin 1µg/ml fibronectin	28 days	Neuronal-like morphology NF, βIII-tubulin and GFAP expression
(Govindasamy *et al.*, 2010)	Heterogeneous human DPSC	Neurobasal	B27 2mM L-glutamine	bFGF EGF		15 days	Formation of neurosphere-like bodies
		Neurobasal	10µg/ml N2 2mM L-glutamine	20ng/ml bFGF 40ng/ml EGF	1µg/ml laminin 1µg/ml fibronectin	24 hours	
		Neurobasal	10µg/ml N2 2mM L-glutamine	20ng/ml NT-3	1µg/ml laminin 1µg/ml fibronectin	28 days	Neuronal-like morphology NF, βIII-tubulin and GFAP expression
(Osathanon *et al.*, 2011)	Heterogeneous human DPSC	Neurobasal	B27 2mM L-glutamine	20ng/ml bFGF 20ng/ml EGF		7 days	Formation of neurosphere-like bodies Expression of neuromodulin, βIII-tubulin and NF

Table 1.2 - *In vitro* protocols for the differentiation of neuronal-like cells from DPPCs resulting in functional electrophysiologcal recordings (from Young *et al.,* 2013)

Reference	Cell source	Base medium	Supplements	Growth Factors	Coating	Duration	Outcome
(Arthur *et al*., 2008)	Heterogeneous human DPSC	Neurobasal A	B27	40ng/ml bFGF 20ng/ml EGF	Polyornithine/laminin	3 weeks	Sensory-neuron-like morphology NF, βIII-tubulin and NCAM expression Fast-inactivating Na^+ currents
(Arthur *et al*., 2008)	Heterogeneous human DPSC	Neurobasal A	B27	40ng/ml bFGF	Polyornithine/laminin	7 days	
		DMEM/F12	Insulin-transferrin-sodium-selenite	40ng/ml bFGF	Polyornithine/laminin	7 days	
		DMEM/F12	Insulin-transferrin-sodium-selenite 50μM retinoic acid	40ng/ml bFGF	Polyornithine/laminin	7 days	Motor neuron-like morphology NF, βIII-tubulin and NCAM expression Fast-inactivating Na^+ currents
(Király *et al*., 2009 and 2011; Aanismaa *et al*., 2012)	Heterogeneous human DPSC	DMEM/F12	2.5% FBS		Poly-l-lysine	24 hours	
		DMEM/F12	2.5% FBS 10μM 5-azacytidine	10ng/ml bFGF	Poly-l-lysine	2 days	Cells become rounded
		DMEM/F12	250μM IBMX 50μM forskolin 200nM TPA 1mM dbcAMP 1% insulin-transferrin-sodium-selenite	10ng/ml bFGF 10ng/ml NGF 30ng/ml NT-3	Poly-l-lysine	3 days	Cells extend processes Strong NF expression Nestin and vimentin downregulated
		DMEM/F12	1mM dbcAMP	30ng/ml NT-3	Poly-l-lysine	3-7 days	Neuronal-like morphology, GFAP and Ngn2 expression Nestin and vimentin upregulated, NF downregulated Voltage-activated Na^+ and K^+ currents

1.5.2.3.2 Production of neurotrophic and growth factors in vitro

In vitro, DPPCs can produce and release a wide range of neurotrophic factors including BDNF, NGF, NT-3 and GDNF (Nosrat *et al*., 2001 and 2004; Soria *et al*., 2010; Nesti *et al*., 2011). Furthermore, DPPCs express VEGF-A (Iohara *et al*., 2008) and have comparable mRNA expression levels to BMSCs for other growth factors including IGF-1, bFGF, TGFβ-1 and PDGF (Shi *et al*., 2001).

Through the release of such soluble growth factors DPPCs have been demonstrated to promote the growth and survival of primary cultured neurons. Co-cultured DPPCs support trigeminal ganglion neuron survival, without a requirement for exogenous growth factors (Nosrat *et al*., 2001). Similarly, increased survival of primary cultured dopaminergic neurons is observed in DPPC co-cultures, which also offer a degree of protection from specific neurotoxins (Nosrat *et al*., 2004; Nesti *et al*., 2011). The neuronal differentiation of NSCs on three dimensional poly(ethyl acrylate-co-hydroxyethyl acrylate) scaffolds is enhanced when pre-seeded with DPPCs (Soria *et al*., 2010). DPPC-conditioned medium, alone, is sufficient to exert such neurotrophic effects, promoting survival, proliferation and neurite outgrowth of neuroblastoma cell lines (Sugiyama *et al*., 2011; Ishikaza *et al*., 2013), confirming actions through the release of soluble factors.

1.5.2.3.3 DPPCs and the uninjured nervous system

Such *in vitro* observations suggest the potential of DPPCs to promote neuronal survival and recruit endogenous NSCs *in vivo*. Similar neurotrophic effects have been observed following DPPC transplantation into the developing and/or healthy peripheral and central nervous systems.

Regenerating endogenous axons can be identified growing through pulp explants enclosed within chitosan mesh tubes 32 weeks following grafting into the transected rat sciatic nerve (Matsushita *et al*., 2012). A similar innervation, accompanied with vascularisation, is observed following the grafting of pulpal tissue intraocularly (Nosrat *et al*., 2001). An increase in proliferation of endogenous neural cells is observed following DPPC transplantation into murine hippocampus. Increased expression of nestin and βIII-tubulin suggests that the implanted DPPCs are inducing endogenous progenitor cells to differentiate. Elevated production of NGF, VEGF and BDNF is the proposed mechanism for this NSC recruitment (Huang *et al*., 2008). During avian embryogenesis, transplantated DPPCs are seen to attract axonal growth cones, disrupting normal neural development (Arthur *et al*., 2009).

1.5.2.3.4 DPPCs and **in vivo** *models of stroke*

Most of our knowledge regarding the transplantation of DPPCs into the injured CNS is obtained from *in vivo* models of stroke. DPPCs injected into the cerebrospinal fluid of newborn rats localise in regions adjacent to cold-induced lesions (Király *et al*., 2011) as well as neurogenic regions (the subventricular, subgranular and subcallosal zones). In a model of cerebral

ischaemia DPPCs are similarly identified settling within NSC niches (Fang *et al*., 2013). The localisation of transplanted DPPCs in regions of active neurogenesis suggests their potential for contributing to the regeneration of neural tissue.

Reduced functional deficits have been observed following the transplantation of DPPCs (Yang *et al*., 2009; Sugiyama *et al*., 2011; Fang *et al*., 2013; Ishikaza *et al*., 2013) or SHEDs (Yamagata *et al*., 2013) into rodent models of cerebral ischaemia. The transplantation of dental pulp-derived progenitor cells reduces tissue loss by increasing survival of endogenous neuronal cells (Yang *et al*., 2009; Yamagata *et al*., 2013) and promoting revascularisation (Sugiyama *et al*., 2011; Ishikaza *et al*., 2013). Although, limited expression of neuronal, astrocytic and oligodendrocytic markers has been identified among transplanted cells in one study (Fang *et al*., 2013), overwhelming evidence suggests the protective/regenerative effects are mediated through trophic actions. Comparable outcomes are seen following the injection of SHED-conditioned medium, alone, suggesting a paracrine mechanism (Yamagata *et al*., 2013). *In situ* expression of VEGF, BDNF, NGF and GDNF has been identified by transplanted cells and is likely responsible for these effects (Sugiyama *et al*., 2011; Ishikaza *et al*., 2013). Although models of stroke at first glance may appear to be removed from a spinal cord injury, pathological events at the cellular level and the obstructions to regeneration are similar and as such these results may be transferrable to SCI.

1.5.2.3.5 DPPCs and in vivo *models of SCI*

Less information is available regarding the transplantation of DPPCs into the injured spinal cord. Dental pulp tissue explants grafted into the rat lumbar spinal cord, immediately following a hemisection injury, express GDNF and more than double the survival rate of endogenous motor neurons (Nosrat *et al*., 2001). Improved functional outcome has been observed following DPPC transplantation into the injured spinal cord in two separate studies.

The transplantation of DPPCs directly into the injury epicentre at either 7 or 28 days after generation of a compressive SCI in mice is associated with improved recovery of hindlimb function (de Almeida *et al*., 2011). Increased expression of BDNF, NGF, NT-3 and NT-4 is observed, accompanied with greater preservation of white matter tissue. Expression of GFAP and S100 by transplanted cells suggests astrocytic/Schwann cell differentiation.

In a rat model, involving complete transection of the spinal cord, transplantation of DPPCs or SHEDs immediately following injury results in improved hindlimb functional outcome (Sakai *et al*., 2012). Given the timing of cellular transplantation it would appear the effects were likely mediated through neuroprotective actions attenuating secondary mechanisms of injury. Increased axonal sparing, preservation of myelin and decreased apoptosis of of resident neuronal and glial cells support this theory. Approximately 90% of transplanted cells were reported to express oligodendrocytic markers while the remaining 10% could not be identified. The differentiation of neuronal cells following DPPC transplantation into the injured spinal cord has yet to be reported.

1.6 Aims and outlines

Dental pulp progenitor cells have been demonstrated to promote functional improvements following spinal cord injury primarily through paracrine neuroprotective mechanisms. The overall objective of this study is to investigate the ability of DPPCs to promote spinal regeneration and repair through the direct replacement of neuronal and glial cells. This specific research question will be answered by dividing the work into three major aspects, beginning with the isolation of purified DPPC cultures with enhanced neural potential, determining their ability to differentiate into neuronal and glial cell types and, finally, the translation of these findings into spinal cord tissue.

The specific aims of this thesis are summarised as follows:

1) The isolation and characterisation of progenitor cells from murine dental pulp and assessment of neural potential based upon expression of Nestin and neurotrophic/growth factors

2) Development of protocols demonstrating the ability of DPPCs to differentiate *in vitro* into:
    a. Functionally active neurons
    b. Oligodendrocytes

3) Using these protocols to investigate the transplantation of pre-differentiated DPPCs into *ex vivo* and *in vivo* spinal cord tissue.

Chapter 2: Materials and Methods

2.1 Materials

2.1.1 Animals

All procedures were approved by the Cardiff University Biological Standards Office and performed in accordance with UK Home Office guidelines under the Animals (Scientific Procedures) Act 1986 (Project licence no: 30/2816, Personal licence no: 30/9506).

21-28 day old C57/Bl6 mice were used for tissue harvest and obtained from the University Animal House colonies at the JBIOS Heath Hospital site. Mice were sacrificed by CO_2 asphyxiation in accordance with Schedule 1 of the Animals (Scientific Procedures) Act 1986.

2.1.2 Tissue culture

To maintain sterility, all tissue culture procedures were performed in a Microflow Peroxide Class II advanced biological safety cabinet (Bioquell, UK). Unless otherwise specified, cells were cultured on Cell+ treated culture plastics (Sarstedt, Germany) and maintained at 37°C and 5% CO_2 in a tissue culture incubator (Binder, Germany).

2.1.3 Cellular imaging

2.1.3.1 Phase contrast imaging

Phase contrast images of cells in culture were captured using an Eclipse TS100 inverted phase contrast light microscope (Nikon, Japan) with a camera attachment (Canon, Japan).

2.1.3.2 Fluorescent imaging

Fixed and fluorescent antibody-stained cells were viewed and images acquired using an AX7 microscope (Olympus, Japan) connected to a DXM-1000 camera with ACT-1 imaging software (both Nikon, Japan).

2.1.3.3 Image processing

Acquired images were processed and overlapping images merged using freely available ImageJ software.

2.2 Methods

2.2.1 Tissue Culture

2.2.1.1 Dental pulp progenitor cell culture

Murine dental pulp cells (isolated as described in Chapter 3) were cultured in α-modification Minimum Essential Medium (αMEM) containing 2mM glutamine, ribonucleosides and deoxyribonucleosides (Life Technologies, UK). The medium was supplemented with 1% (v/v) penicillin/streptomycin, 20% (v/v) heat-inactivated foetal bovine serum (FBS) (Life Technologies, UK) and 100μM l-ascorbic acid 2-phosphate (Sigma-Aldrich, UK). Medium was changed every 2-3 days until cells reached 80-90% confluence.

2.2.1.2 Passaging DPPC Cultures

Upon reaching confluence, culture medium was removed by aspiration and the cells washed with phosphate buffered saline (PBS) (Sigma-Aldrich, UK). Cells were dissociated by adding Accutase (Sigma-Aldrich, UK) and returned

to the incubator for 10 minutes until they became rounded and detached. Culture medium was then added to neutralise the Accutase. The resultant solutions of medium plus cells were transferred to 15ml falcon tubes and centrifuged at 400G for 5 minutes. After discarding the supernatant, pellets were resuspended in medium and cell counts performed using a haemocytometer with trypan blue exclusion adopted to assess cell viability. Cells were reseeded on new culture plastics at a density of 4000 viable cells/cm^2 for continuous culture, or as per experimental requirements.

2.2.1.3 Cryopreservation and re-establishment of DPPCs

To maintain a stock of readily available cells, DPPCs were cryopreserved at regular intervals during culture. Following passaging, a minimum of 1 x 10^6 cells were resuspended at 1 x 10^6 cells/ml in heat inactivated FBS + 20% (w/v) dimethyl sulphoxide (DMSO) (Fisher Scientific, UK) and transferred to 2ml cryovials (Greiner Bio-one, Germany). Cryovials were slowly cooled to -80°C in propan-2-ol filled Mr Frostys (Nalgene, USA). After being stored for 24hours at -80°C, cryopreserved cells were transferred to liquid nitrogen storage.

As required, DPPCs were re-established from frozen stock by thawing in a 37°C water bath with gentle agitation. Thawed cell suspensions were transferred to 15ml conical tubes containing culture medium and centrifuged at 400G for 5 minutes. Following centrifugation, traces of DMSO were removed by discarding the supernatant and resuspending the cell pellets in culture medium for a further 5 minute centrifugation. Cell counts with trypan

blue exclusion were performed and the cells reseeded in culture plastics at 4000 cells/cm^2.

2.2.1.4 Embryonic neural stem cell culture

Neural stem cells isolated from the cortex of E14.5 C57Bl/6 mice by post-doctoral researcher colleagues were maintained in Dulbecco's Modified Eagles Medium (DMEM)/Ham's F12 (1:1) containing L-glutamine and HEPES buffer and 1% (v/v) penicillin/streptomycin (Life Technologies, UK). This was supplemented with 1x Non-Essential Amino Acids (NEAA (Sigma-Aldrich, UK)), 20ng/ml basic fibroblast growth factor (bFGF), 20ng/ml epidermal growth factor (EGF) (both Peprotech, UK) and 1x N2 supplement (Life Technologies, UK).

2.2.1.5 Subculturing NSC cultures

NSCs were cultured as floating neurospheres at 37°C with 5% CO_2 and half medium changes performed every 2 days. As neurospheres expanded and increased in size, the centre of the spheres began to turn dark as cells became deprived of nutrients. Before reaching this stage, spheres were subcultured. The medium and floating spheres were aspirated and centrifuged at 100G for 5 minutes. 1ml of Accutase was used to dissociate the pellet and left to incubate at room temperature for 10 minutes, dissociating spheres to a single cell suspension. The actions of Accutase were then stopped by the addition of culture medium. Following a further centrifugation at 100G for 5 minutes, the supernatant was discarded and the cells resuspended in medium. Cell counts were performed and the cells

resuspended at a density of 100,000 cells/ml for continuous culture or seeded on poly-l-lysine/laminin coated plates for experiments.

2.2.2 Characterisation Techniques

For characterisation of marker expression reverse-transcription polymerase chain reaction (rt-PCR), quantitative polymerase chain reaction (qPCR) and immunocytochemistry (ICC) methods were used.

2.2.2.1 Extraction of total RNA from cells

Approximately 5 x 10^5 cells were used per RNA extraction. Total RNA was extracted using an RNeasy Mini Kit with on-column DNase digestion (QIAGEN, UK) according to manufacturer's directions. All procedures were performed using certified RNase and DNase-free pipette tips (Fisher Scientific, UK). Briefly, cells were washed with PBS then lysed in Buffer RLT, to which 1% (v/v) β-mercaptoethanol (Sigma-Aldrich, UK) had been added. Lysates were then transferred to QIAshredder™ spin columns and homogenised by 2 minutes centrifucation at 13,600G. An equal volume of 70% (v/v) ethanol (Sigma-Aldrich, UK) was added to the filtrates and the samples then transferred to RNeasy™ spin columns. A further centrifugation for 20 seconds at 10,000G resulted in the binding of RNA to the spin column membranes. Following a wash-through, by the addition of 350µl Buffer RW1 to spin columns and 20 seconds centrifugation at 10,000G, genomic DNA contamination was eliminated by adding 80µl RNase-free DNase (QIAGEN, UK) to the membrane and incubating at room temperature for 15 minutes. A further wash-through with Buffer RW1 was then performed before two 20

second 10,000G centrifugation washes with 500µl Buffer RPE. Spin column membranes were then dried out by centrifuging at 13,600G for one minute and, finally, RNA was eluted by adding 30-50µl of nuclease-free water (Promega, UK) to the spin column and centrifuging for one minute at 10,000G. The total yield of RNA per extraction was measured using a Nanovue spectrophotometer (GE Healthcare, UK) to measure the absorbance at 260nm. A260/A280 ratios of 1.9-2.1 indicated extraction of good quality RNA. RNA samples were stored at -80°C until required for reverse transcription.

2.2.2.2 Extraction of total RNA from tissues

RNA samples extracted from murine spleen and corpus callosum tissue were used as positive controls for PCR experiments. These tissues were carefully dissected from adult C57Bl/6 mice and immediately frozen in sterile 1.5ml microcentrifuge tubes on dry ice, to prevent RNA degradation. Frozen tissues were then lysed by adding 700µl Buffer RLT + 1% β-mercaptoethanol and repeatedly triturating with progressively smaller pipette tips and sterile needles until the lysed tissues could pass through 25 gauge needles. Tissue lysates were then transferred to QIAshredder™ spin columns and RNA purified as described previously (section 2.2.2.1).

2.2.2.3 Reverse transcription

Reverse transcription reactions were performed using sterile autoclaved tubes and tips. 500/1000ng of extracted total RNA was mixed with 1µl of random primer (Promega, UK) and then made up to 15µl total volume with

nuclease-free water before heating at 70°C for 5 minutes in a thermocycler (VWR, UK). 10µl of reaction mastermix (1x MMLV buffer, 0.5mM dNTPs, 24units RNasin RNase inhibitor and 200units MMLV reverse transcriptase in nuclease-free water (all Promega, UK)) was added to the RNA/primer mix and incubated at 37°C for one hour. Following the reverse transcription reaction cDNA was used immediately for end point (section 2.2.2.4) or quantitative (section 2.2.2.5) PCR reactions or stored at -20°C. Matching RT-ve controls were produced for each reverse transcription reaction by substituting total RNA with nuclease-free water.

2.2.2.4 End-point polymerase chain reaction

1µl of cDNA was used per PCR reaction. Reaction mixtures were composed of cDNA, 1x reaction buffer, 200µM dNTPs, 0.5µM each of the appropriate forward and reverse primers, 1mM $MgCl_2$ and 1.25 units taq DNA polymerase and made up to 25µl total volume with nuclease-free water (all Promega, UK). 30-40 cycles of a 1 minute denaturation step at 95°C, followed by 1 minutes annealing at 60°C and 1.5 minutes elongation at 72°C were performed. A matching PCR-ve control was produced for each product of interest by substituting cDNA with 1µl nuclease-free water.

2.2.2.5 Agarose gel electrophoresis and PCR product visualisation

PCR products were visualised following electrophoresing in 1.4% (w/v) agarose/TAE gel. 1.4g of agarose powder was added to 100ml of TAE buffer (40mM Tris base, 20mM acetic acid and 1mM EDTA (all Fisher Scientific, UK) and heated in a microwave until fully dissolved. 5µl of ethidium bromide

(Promega, UK) was added to the mixture which was then poured into a gel cast and left in a fume hood until set. Up to 10µl of each PCR product was added into separate wells on the gel submerged in an electrophoresis tank filled with TAE buffer. After electrophoresing at 90V for 45 minutes, DNA was visualised under U.V. light and images acquired.

2.2.2.6 Real-time quantitative PCR

Following reverse transcription of 500ng or 1000ng RNA, the resultant cDNA was diluted with nuclease-free water 1:5 or 1:10, respectively. 5µl of diluted cDNA was added to wells of Bright White 96-well PCR plates (PrimerDesign, UK). To each well, a 15µl reaction/primer mix (10µl Precision MasterMix with ROX and SYBRgreen (PrimerDesign, UK), 300nM each of the appropriate forward and reverse primers and made up to 15µl with nuclease-free water) was added. Each reaction was performed in triplicate. Plates were sealed with a clear optical adhesive seal (PrimerDesign, UK) and centrifuged at 3000G for 5 minutes to ensure adequate mixing of reaction components. Plates were loaded into the ABI Prism 7000 qPCR machine (Advanced Biosystems, UK) and the following cycling conditions used: an initial denaturation step of 95°C for 10 minutes followed by 40 cycles of 15 seconds denaturation (95°C) and 1 minute annealing/elongation at 60°C. Dissociation curves starting from 60°C were recorded to check for specificity of the reactions and products were electrophoresed on 1.4% agarose gels (section 2.2.2.5) in order to confirm product size. Dissociation curves and confirmed sizes for each product are displayed in Appendices I and II, respectively. The threshold for Ct values was set at a stage where all

reactions were in the linear amplification stage using ABI Prism 7000 SDS software. Ct values were exported to Microsoft Excel and relative changes in expression calculated using the $2^{-\Delta\Delta CT}$ method (Livak and Schmittgen, 2001). Statistical analyses were performed using Graphpad Prism Software.

2.2.2.7 rt-PCR and qPCR primers

Unless previously published (denoted by *), primers were designed using Primer-BLAST software (NCBI, USA). Individual primers were designed to span exon-exon junctions and products to span at least one genomic intron wherever possible. Primer pairs were selected that matched only the desired product on the organism genome. Primer sequences are found in individual experimental chapters, with the exception of those used for the detection of neurotrophic and growth factor expression which are displayed below in Table 2.1.

Table 2.1 – Neurotrophic and growth factor primer sequences

Product	Accession no.	Primer Sequences (5' → 3)	Product Size (bp)	Tm (°C)
BDNF*	NM_007540.4	f: TGGCAGTGCAGGAGGAATTTCTGA r: GCAGAAGGCCTAAGCAACTTGACA	148	60
bFGF*	NM_008006.2	f: TTCAAGGATCCCAAGCGGCTCTA r: TGTGGGTCGCTCTTCTCCC	101	60
GDNF*	NM_010275.2	f: AGAATTCCAGAGGGAAAGGTCGCA r: TCCTCCTTGGTTTCGTAGCCCAAA	115	60
IGF-1*	NM_010512.4	f: TGGCACTCTGCTTGCTCACCTTTA r: TTGGTCCACACACGAACTGAAGAG	102	60
NGF*	NM_013609.2	f: ACTTCCAGGCCCATGGTACAATCT r: TTGATGTCCGTGGCTGTGGTCTTA	148	60
NT-3*	NM_001164034.1	f: ACTACGGCAACAGAGACGCTACAA r: ATAGCGTTTCCTCCGTGGTGATGT	145	60
PDGF-a*	NM_008808.3	f: ATTCCCGCAGTTTGCAAGACCA r: CCAGATCAAGAAGTTGGCCGATGT	87	60
TGFβ-1*	NM_011577.1	f: GTGGCCAGATCCTGTCCAAACTAA r: CATTAGCACGCGGGTGACTTCTTT	191	60
VEGF-A*	NM_001025250.3	f: TATTGCCGTCCAATTGAGACCCTG r: GCACACAGGACGGCTTGAAGATATAC	85	60

* Primer sequence described by Hawryluk *et al*., 2012b.

2.2.2.8 Immunocytochemistry staining

Following removal of medium, cells were washed with PBS for 3 minutes before being fixed with 4% (w/v) paraformaldehyde (PFA) for 20 minutes at room temperature. A further 3 minute wash with PBS was performed and the cells then permeabilised with 0.1% (v/v in PBS) Triton X-100 for 10 minutes at room temperature. After a 3 minute PBS wash, 2% (w/v) bovine serum albumin fraction V (BSA) (Fisher Scientific, UK) in PBS was applied for 30 minutes in order to block non-specific binding. This was removed and replaced with appropriate primary antibody(s) (Tables 2.2 and 2.3) diluted in 2% BSA and incubated overnight in a dark humid chamber at 4°C. The following day, 3 PBS washes lasting 5 minutes were performed. Slides were then incubated in 2% BSA with complementary fluorophore-conjugated secondary antibodies (Table 2.4.) in the dark at room temperature for 1 hour. Four further 5 minute washes with PBS were performed before the cells were mounted onto glass cover slips using mounting media supplemented with DAPI stain (VectorLabs, UK). Slides were stored at 4°C in the dark, to prevent bleaching, until required for imaging (section 2.1.3.2).

2.2.2.9 Tables of antibodies

The following antibodies were used for immunocytochemistry and/or immunohistochemistry staining.

Table 2.2 – Primary antibodies used

Antibody	Manufacturer	Cat. No.	Host Species	Isotype	Dilution
A2B5	Millipore	MAB312R	Mouse	IgM	1:500
β-actin	Cell Signalling	8H10D10	Mouse	IgG2b	1:600
βIII-tubulin	Cell Signalling	D71G9	Rabbit	IgG	1:200
GFAP	Millipore	041062	Rabbit	IgG	1:500
Map2	Millipore	AB5622	Rabbit	Polyclonal	1:250
MBP	Millipore	05-675	Mouse	IgG1	1:200
MOSP	Millipore	MAB328	Mouse	IgM	1:1000
Musashi	Life Technologies	710237	Rabbit	Polyclonal	1:500
Nestin	Santa Cruz	SC-33677	Mouse	IgG1	1:100
NF-l	Abcam	ab78159	Mouse	IgG2b	1:100
Olig1	Millipore	AB15620	Rabbit	Polyclonal	1:1000
Olig2	Millipore	AB9610	Rabbit	Polyclonal	1:500
S-100	Abcam	A4066	Mouse	IgG2a	1:100
SOX10	Abcam	ab27655	Rabbit	Polyclonal	1:1000
Synaptophysin	Abcam	AB8049	Mouse	IgG1	1:15

Table 2.3 – Isotype control antibodies used

Antibody	Manufacturer	Cat. No.	Concentration
Normal mouse IgG	Santa Cruz	sc-2025	Assay dependent
Normal mouse IgM	Santa Cruz	sc-3881	Assay dependent
Normal rabbit IgG	Santa Cruz	sc-2027	Assay dependent

Table 2.4– Secondary antibodies used

Antibody	Manufacturer	Cat. No.	Host Species	Fluorophore	Dilution
Anti-mouse IgG (H+L)	Life Technologies	A11001	Goat	Alexa Fluor 488	1:500
Anti-mouse IgM (µ chain)	Life Technologies	A21042	Goat	Alexa Fluor 488	1:500
Anti-mouse IgG (H+L)	Life Technologies	A11005	Goat	Alexa Fluor 594	1:500
Anti-rabbit IgG (H+L)	Life Technologies	A11012	Goat	Alexa Fluor 594	1:500

Chapter 3: Isolation and characterisation of murine dental pulp progenitor cells with neural potential

3.1 Introduction

The dental pulp and the CNS share similar developmental origins, deriving from the embryonic ectoderm layer. Following neurulation, migrating cranial neural crest cells give rise to the cellular components of the dental pulp (Chai *et al*., 2000) while the neural tube develops into the brain and spinal cord. Due to these developmental similarities, the dental pulp could represent a source of cells with enhanced potential for neural repair.

DPPCs possess a number of desirable characteristics that may be used to provide an indication of their potential for neural repair, through direct cell replacement or trophic effects. The expression of nestin, an early marker of neuronal lineage cells, is well established for both rat (Sasaki *et al*., 2008) and human (Gronthos *et al*., 2002) DPPCs, and could provide a potential marker for identifying cells with the ability for neuronal and glial differentiation. DPPCs have demonstrated potent *in vitro* neurotrophic effects in co-culture studies (Nosrat *et al*., 2001, 2004; Nesti *et al.,* 2011) or through the use of DPPC-conditioned media (Sugiyama *et al*., 2011; Ishikaza *et al*., 2013). Expression of transcripts for neurotrophic and growth factors could be used to identify DPPC cultures with a similar potential to promote CNS repair through the release of paracrine soluble factors.

Many techniques have been described for the derivation and culture of DPPCs, with the methods adopted depending largely upon the intended purpose of the study. Following extirpation from the tooth, a cellular suspension is often produced from the pulp by treatment with digestive

enzymes such as a collagenase/dispase mixture (Gronthos *et al*., 2000, 2002) or trypsin (Balic and Mina 2005). Alternatives to this approach include mechanical vortexing to release cells from the root of the tooth (Yang *et al*., 2009) or explant cultures (Spath *et al*., 2010; Lizier *et al*., 2012).

Largely, no purification method is used, resulting in mixed cultures where progenitor cells make up only a small fraction. For most purposes, it is beneficial to selectively isolate purified populations of progenitor cells. The simplest method is to clonally isolate single cell-derived populations (Gronthos *et al*., 2002), although time is required for expansion to provide suitable cell numbers for experimental procedures. Alternatively, a number of specific sorting techniques are available, and have been successfully used to isolate enriched cultures of mixed cells. Neural crest-derived progenitor cells can be specifically selected using antibodies to low-affinity nerve growth factor receptor (LANGFR/P75) in magnetic activated cell sorting (Waddington *et al*., 2009). Similarly, Stro-1 immunoreactive mesenchymal progenitor cells can be selectively sorted either magnetically (Yu *et al*., 2010) or fluorescently (Yang *et al*., 2007). Side population progenitor cells have been selected from porcine pulp using fluorescent-activated cell sorting techniques to purify cells with the ability to exclude Hoescht 33342 DNA dye, due to expression of breast cancer resistance protein (Iohara *et al*., 2008; Sugiyama *et al*., 2011; Ishikaza *et al*., 2013). As yet, however, there is no suitable protocol reported for the specific isolation of DPPCs with enhanced neural potential, as indicated by nestin expression and the ability to produce neurotrophic factors.

In this study, following collagenase/dispase digestion to a cellular suspension, the preferential adherence to fibronectin selection method was used to select for progenitor cells from the dental pulp of mouse incisors. This technique provides a simple method of isolating cells of more immature phenotypes, without the same requirement for specialist equipment as traditional fluorescence/magnetic sorting techniques. As cells differentiate, functionality of β1 integrin decreases. The limited amount of time allowed for attachment to fibronectin-coated surfaces results in adherence of only the most primitive cell types, separating them from transit amplifying and other terminally differentiated cell types which remain suspended in the culture medium (Jones and Watt, 1993; Dowthwaite *et al*., 2004). This method has already proven successful for the specific isolation of progenitor cells from oral tissues including the oral mucosa lamina propria (Davies *et al*., 2010) and the dental pulp (Waddington *et al*., 2009). Following isolation using this method, murine dental pulp cells were expanded as either clonal or heterogeneous populations. Each cell culture was then screened for neural potential by investigating the expression of nestin and transcripts for a selection of soluble neurotrophic and growth factors.

3.2 Objectives

- To isolate and expand clonal and heterogeneous populations of murine dental pulp cells

- To confirm progenitor status of cell cultures by determining the expression of mesenchymal markers

- To identify cultures with enhanced potential for neuronal and glial differentiation based on nestin expression

- To examine the expression of a range of neurotrophic and growth factors, identifying those DPPC cultures with the potential for promoting CNS repair through trophic mechanisms.

3.3 Materials and methods

3.3.1 Dental pulp extraction from murine incisors and cell isolation

The outer coats of CO_2-asphyxiated mice were sterilised by immersing in 70% (v/v) ethanol prior to dissection. Lateral incisions were made in each cheek using sterile surgical scissors to make for easier access to teeth. The soft tissue surrounding both the upper and lower incisors was carefully detached using a sterile scalpel and individual teeth extracted with a pair of sterile forceps. Once removed, teeth were kept hydrated by immersing in culture medium until ready for pulp removal. Under a dissecting microscope, a longitudinal incision was carefully made along the length of each incisor, exposing the pulpal cavity, and the pulp gently excavated.

Harvested pulp was minced in media on a sterile glass slide before being transferred to a 4mg/ml solution of collagenase/dispase (Roche Diagnostics, Germany) for enzymatic digestion at 37°C for 1 hour with regular agitation. Following digestion, a single-cell suspension was obtained by passing through a 70µm-pore mesh cell strainer (BD Biosciences, USA). The cell suspension was then spun at 400G in a centrifuge and the supernatant discarded. A cell count was performed using a haemocytometer before seeding cells for the fibronectin adhesion assay.

3.3.2 Fibronectin adhesion assay

6-well culture plates were coated with 10µg/ml fibronectin from human plasma (Sigma Aldrich, UK), diluted in PBS, overnight at 4°C. The following day, fibronectin solution was aspirated and the wells washed with PBS before seeding with cells. Cells were seeded at a density of 4000/cm^2 (40,000 per well) in DPPC medium (section 2.2.1.1). Plates were placed in the tissue culture incubator for 20 minutes to allow for the adhesion of cells with high integrin functionality, before the medium containing unattached, non-adherent, cells was transferred to separate wells and the initial wells filled with fresh DPPC medium. Following the fibronectin selection assay, cells were incubated at 37°C with 5% CO_2 and expanded for up to 12 days with medium changes performed every 2-3 days.

3.3.3 Colony forming efficiency (CFE)

24 hours after fibronectin selection, the total number of attached and spread-out cells was manually counted for each individual well by viewing under a microscope (section 2.1.3.1). The plates were then observed every other day and the number of colonies derived from a single cell, defined as a cluster of at least 32 cells, counted per well. Colony forming efficiencies were calculated by expressing the number of colonies counted in one well, on a given day, as a percentage of the total cell count of the same well 24 hours after fibronectin adhesion:

$$\mathrm{CFE} = \frac{\text{number of colonies} > 32 \text{ cells}}{\text{initial cell count at 24 hours}} \times 100$$

3.3.4 Isolation of single cell-derived clones and heterogeneous populations

At the end of the 12-day period a number of colonies were selected for isolation and expansion as single cell-derived clones from each well, based on cell number and a visual assessment of health. Medium was removed from wells before performing a PBS wash. Clonal rings, made by removing the ends of 1ml pipette tips and autoclaving, were used to isolate individual colonies by attaching to the base of the well with High Vacuum Grease (Dow Corning, UK) to form a water-tight seal. The cells within each colony were detached from the culture plate by addition of Accutase, pre-warmed to 37°C, for 10 minutes to the clonal ring. The subsequent detached cells were seeded into individual wells of 96-well plates, one clone per well, for expansion culture (section 3.3.6).

A number of isolated cells were expanded as heterogeneous populations by pooling together all colonies from one or more wells. To produce these mixed cultures, no clones were selected from the wells and the colonies allowed to expand and merge until the entire well reached 80-90% confluence. At this stage the cells were passaged and expanded as normal (section 3.3.6).

3.3.5 Nomenclature for isolated dental pulp cells

To identify each isolated clone/heterogeneous population the following nomenclature system was devised. The cultures were named starting with the date of isolation, followed by their fibronectin adhesion status (A = fibronectin-adherent, NA = fibronectin non-adherent), followed by the well

number from which they were isolated, and finishing with a clonal letter identification (if applicable). Thus, 19_8A2A represents a clonal population isolated on the 19th August that is fibronectin-adherent, was selected from well 2 and designated as clone A. Similarly, 9_7NA1 identifies a mixed population of cells isolated on the 9th July that was non-adherent and expanded from well 1.

3.3.6 Dental pulp cell expansion culture and population doublings

FDental pulp cells were expanded in culture, with a medium change every 2-3 days, until nearing confluence. At ~80% confluence, cells were passaged and counted as described previously (sections 2.2.1.1 and 2.2.1.2). Cells were reseeded at a density of 4000 viable cells/cm^2 on plastic dishes of increasing surface area and expanded until sufficient numbers were available for use in further experiments. Fibronectin-coated culture surfaces were not used beyond passage 0. The level of population doublings (PD) during expansion culture was monitored and calculated using the following formula:

$$\mathrm{PD} = \frac{\log10(\text{cell count}) - \log10(\text{no.of cells reseeded})}{\log10(2)}$$

3.3.7 Identification of progenitor cells

In order to confirm the cells as progenitor cells they were screened for the expression of a panel of stem cell markers including CD90, CD45, nestin and SCA1 (for primers see Tables 3.1 and 3.2). Total RNA was extracted from each clone/heterogeneous culture at the earliest possible opportunity, once sufficient cell numbers were reached, and used for rt-PCR and qPCR characterisation methods (sections 2.2.2.1 – 2.2.2.7). This same RNA was used to screen for the expression of transcripts for TGFβ-1, IGF-1, PDGF-a, bFGF, VEGF-A, NT-3, NGF, BDNF and GDNF (for primers see Table 2.1). Positive control samples were provided by RNA extracted from cultured NSCs (sections 2.2.1.4 and 2.2.1.5), as well as spleen and corpus callosum tissue (section 2.2.2.2).

Expression of nestin was confirmed at the protein level using immunocytochemistry (section 2.2.2.8). Following passaging, pulp cells were seeded at 4,000/cm^2 on 8-chamber culture slides (BD Biosciences, USA). After 24 hours these were fixed and stained immunocytochemically with antibodies against nestin and an appropriate isotype control (Tables 2.2 – 2.4). To quantify the number of nestin-expressing cells in heterogeneous cultures, low magnification images were acquired (section 2.1.3.2) and the number of Alexa-fluor-488-positive cells expressed as a percentage of DAPI-labelled cells. Counts were performed for at least ten separate visual fields per population and a mean percentage calculated ± standard deviation.

3.3.8 Tables of Primers

Table 3.1 – Primer sequences for identification of progenitor cells

Product	Accession no.	Primer Sequences (5' → 3)	Product Size (bp)	Tm (°C)
CD90	NM_009382.3	f: GCCTGACAGCCTGCCTGGTGAACCAAA r: TGCCGCCACACTTGACCAGCTTGTCTCT	330	60
CD45	NM_001111316.1	f: CCCATCAAAGATGCCCGAAAGCCCCACA r: CCGTCGAAGTTTGAGGAGCAGGTGAGGGT	507	60
Nestin	NM_016701.3	f: AACAGAGATTGGAAGGCCGCTGGCAGGAC r: GGGTTCTGGCCTTAAGGAATTCCTGTGTC	420	60
SCA1	NM_010738.2	f: ACCTGCCCCTACCCTGATGGAGTCTGT r: TGTGTGCCTCCAGGGTCATGAGCAGCA	522	60
GAPDH	NM_008084.2	f: AGACGGCCGCATCTTCTTGTGCAGTGC r: ACATACTCAGCACCGGCCTCACCCCAT	326	60

Table 3.2 – Primer sequences for qPCR

Product	Accession no.	Primer Sequences (5' → 3)	Product Size (bp)	Tm (°C)
Nestin	NM_016701.3	f: CCAAAGAGGTGTCCGATCATC r: CTCCCTTCTTCTTCATCAGCATCT	147	60
β-actin	NM_007393.3	f: TCTTTGCAGCTCCTTCGTTGCCG r: GTCCTTCTGACCCATTCCCACCA	200	60

3.4 Results

3.4.1 Colony formation following dental pulp cell isolation

Dental pulp cells were successfully isolated and cultured from murine incisors. The fibronectin preferential adhesion assay resulted in the separation of isolated cells into two distinct populations: those that successfully attached to fibronectin-coated plates within 20 minutes, termed the adherent population, and those that did not, termed the non-adherent cells. 24 hours following selection, both fibronectin-adherent and fibronectin-non-adherent wells were sparsely populated with small fibroblastic-like cells (Figure 3.1 A). Over the first 12 days of primary culture, a number of these fibroblastic-like cells in both fibronectin-adherent and non-adherent wells were found to rapidly clonally expand and form discrete individual colonies (Figure 3.1 B and C). At day 12 no difference was observed between the ability of adherent and non-adherent cells to form colonies as demonstrated by colony forming efficiencies of 0.0049 ± 0.0011 and 0.0050 ± 0.0003, respectively (Figure 3.1 E).

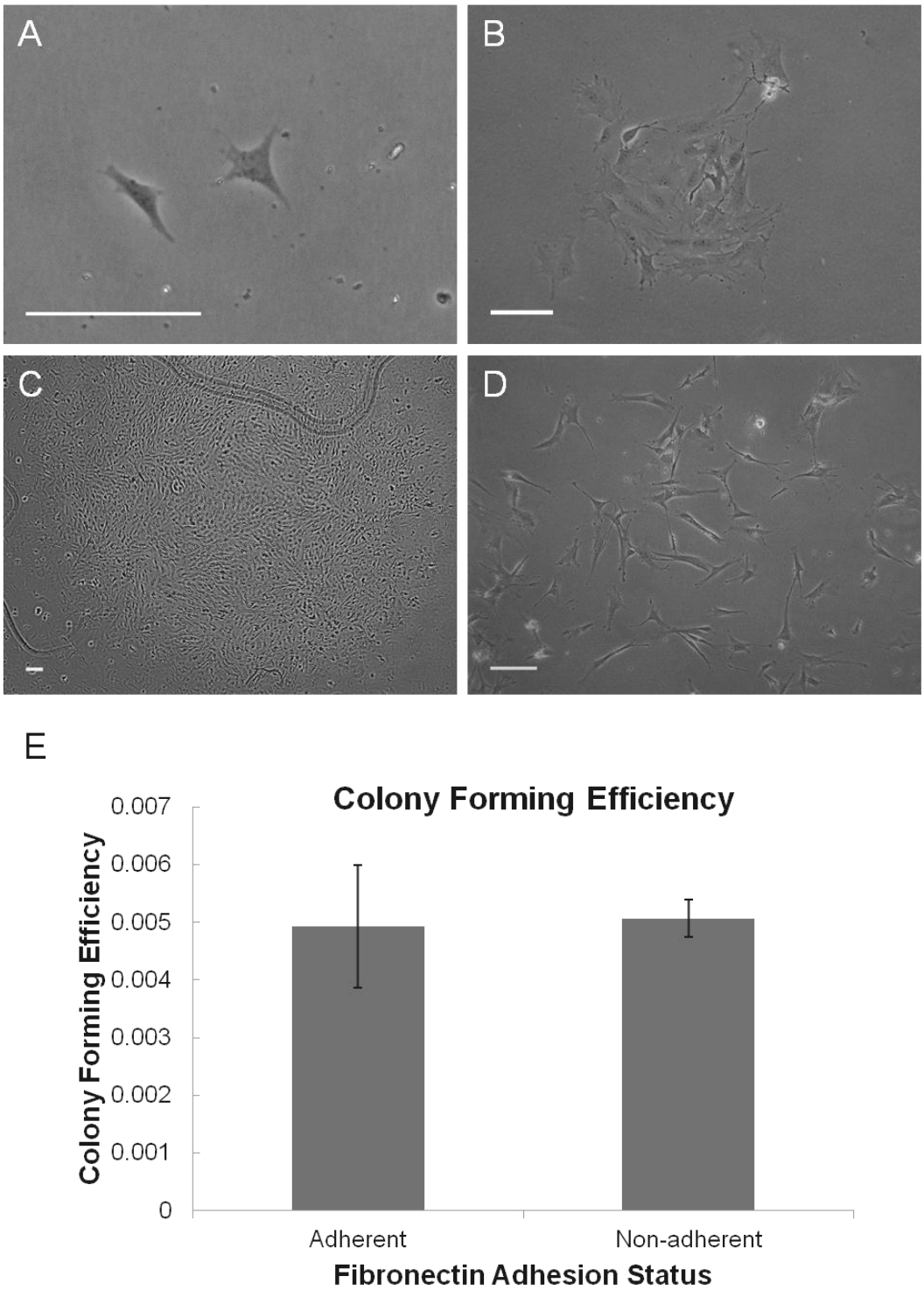

Figure 3.1 – Colony formation by primary cultured dental pulp cells.

Dental pulp cells proliferate rapidly over 12 days of primary culture and form distinct colonies. A) Individual cells growing on fibronectin 24 hours after isolation. B) A small clonally-derived cluster of cells after 3 days culture. C) A large colony before clonal isolation on day 12. D) During expansion culture single-cell derived clones adopt bipolar fibroblastic-like morphology typical of dental pulp cells (bars = 100µm). E) No difference in colony forming efficiency was observed between fibronectin-adherent and fibronectin-non-adherent cells at day 12 (n=7±SEM).

3.4.2 Expansion of clonal and heterogeneous populations

After 12 days individual colonies were selected for expansion as single cell-derived clones or allowed to merge together forming a heterogeneous population. Throughout expansion culture dental pulp cells remained typically bipolar and fibroblastic-like in morphology (Figure 3.1 D) with heterogeneity observed in mixed populations.

Single cell-derived clones demonstrated rapid initial proliferation, as measured by cumulative population doublings, in comparison to heterogeneous populations (Figure 3.2). Initial proliferation rates for heterogeneous populations of pulp cells remained lower than clonal rates for a sustained period. However, over longer-term culture, a sharp increase in proliferation was observed between 80-100 days. The rate of clonal expansion remained more stable throughout in comparison to mixed populations, although differences in the rates of doubling between clones were evident. Several clones (7_10BA1B, 7_10BA2C and 10_11BNA3A) were seen to expand for at least 40 population doublings without senescing (Figure 3.2 B).

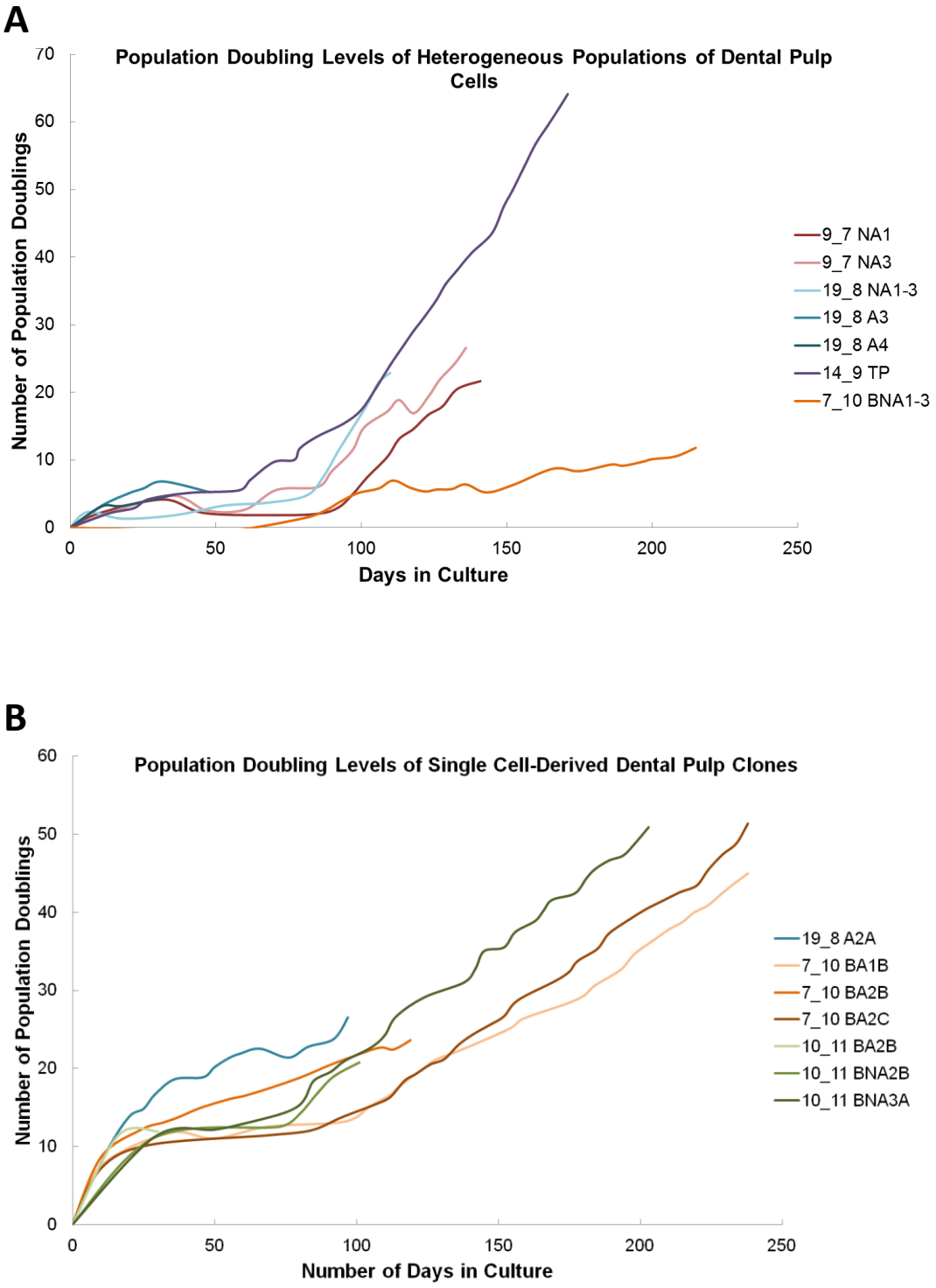

Figure 3.2 – Population doublings of dental pulp cells during expansion culture
Cumulative population doublings of both heterogeneous (A) and clonal (B) populations were recorded during expansion culture. A) In mixed populations a pronounced lag phase was seen over the first 80-90 days, after which the rate of population doubling sharply increases. B) A number of single cell-derived clones of dental pulp cells proliferate steadily for up to 240 days of culture reaching 50+ population doublings. Clonal differences in the rate of doubling were apparent

3.4.3 Characterisation of murine dental pulp cells

Total RNA was extracted from each clone or mixed population at as early a stage as was practicable (between 15 and 25 population doublings (PDs)). Rt-PCR was used to screen for mRNA expression of markers associated with mesenchymal (CD90 and SCA1), haematopoetic (CD45) and neural (nestin) progenitor cells (Figure 3.3). SCA1 was found to ubiquitously expressed, regardless of fibronectin adhesion properties or clonal/heterogeneous status. No expression of CD45 was detected in any culture. Expression of CD90 and nestin was found to vary between populations, being expressed either separately or together. No pattern of CD90/nestin expression was observed with respect to the fibronectin adhesion or clonal/heterogeneous properties of the cultures.

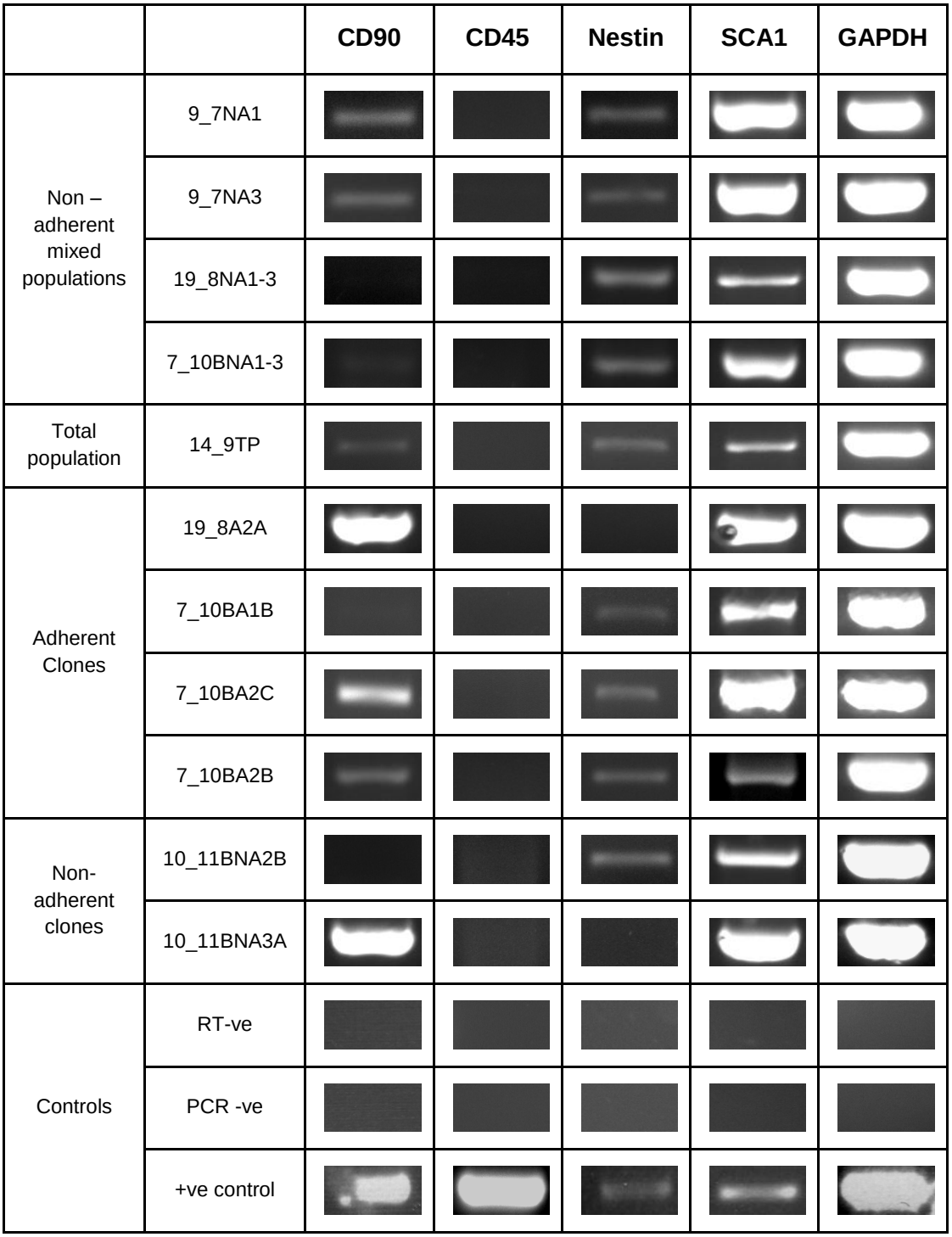

Figure 3.3 – mRNA expression of progenitor cell markers

Rt-PCR was used to detect the expression of CD90, CD45, Nestin,SCA1 and GAPDH in isolated dental pulp cells. SCA1 expression was identified in all isolates whereas CD90 and Nestin expression was found to be more variable. CD45 expression was not detected in any population. RNA extracted from NSCs was used as a positive control for CD90, Nestin, SCA1 and GAPDH whereas a CD45 positive control was provided by murine spleen tissue.

3.4.4 Nestin expression

As nestin is a key marker identifying early stage neural cells, its expression by murine dental pulp cells was explored in further detail using immunocytochemistry and qPCR.

The percentage nestin expression was calculated for three heterogeneous populations, 9_7NA1, 19_8NA1-3 and 14_9TP (15 – 20 PDs). Percentage expression was found to be 83.61% ± 7.37, 86.48% ± 5.84 and 79.04% ± 11.29, respectively (Figure 3.4).

Four clones, 19_8A2A, 7_10BA1B, 7_10BA2C and 10_11BNA3A (20 – 25 PDs), were immunostained for nestin expression (Figure 3.5). In contrast to rt-PCR results (Figure 3.3), positive staining of all four clones was observed with weaker staining of clones 19_8A2A and 10_11BNA3A. qPCR was used to quantify mRNA expression in each of these clones relative to β-actin (Figure 3.6). 19_8A2A (0.21% ± 0.05) and 10_11BNA3A (0.017% ± 0.005%) express significantly reduced ($p<0.01$) levels of nestin mRNA compared to both 7_10BA1B (5.56% ± 2.26) and 7_10BA2C (4.35% ± 0.076).

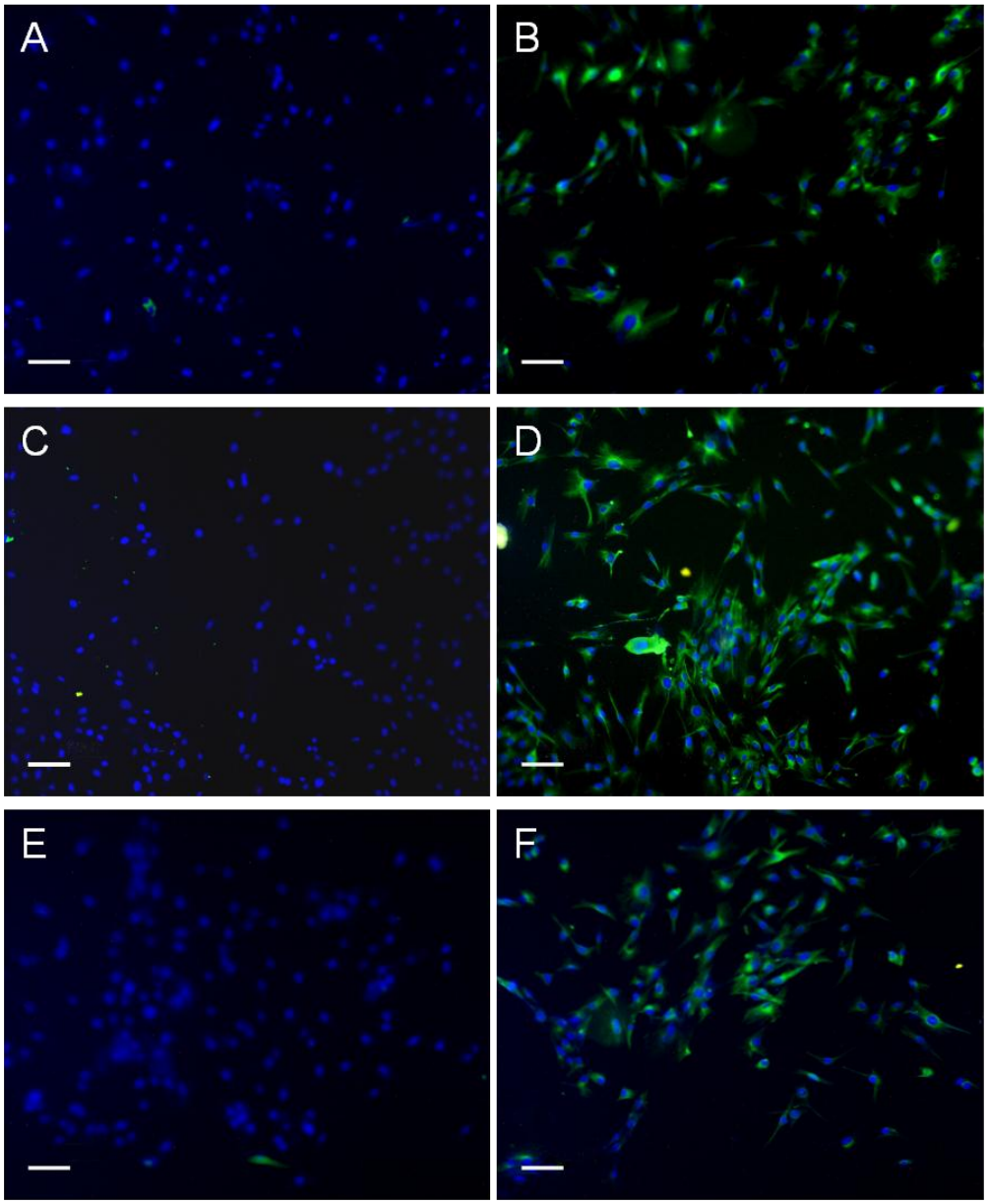

G

Cell Population	Nestin expression ± SD
9_7 NA1	83.61% ± 7.37
19_8 NA1-3	86.48 %± 5.84
14_9 TP	79.04% ± 11.29

Figure 3.4 – Immunocytochemistry of nestin in mixed populations

Three heterogeneous cultures were stained for nestin expression: 9_7NA1 (A & B), 19_8NA1-3 (C & D) and 14_9TP (E & F). Alexa-fluor 488 counterstained cells (B, D & F) were counted and expressed as a percentage ± SD of DAPI-stained nuclei (G). Respective mouse IgG isotype controls for each population are also displayed (A, C & E) (scale bars = 100µm).

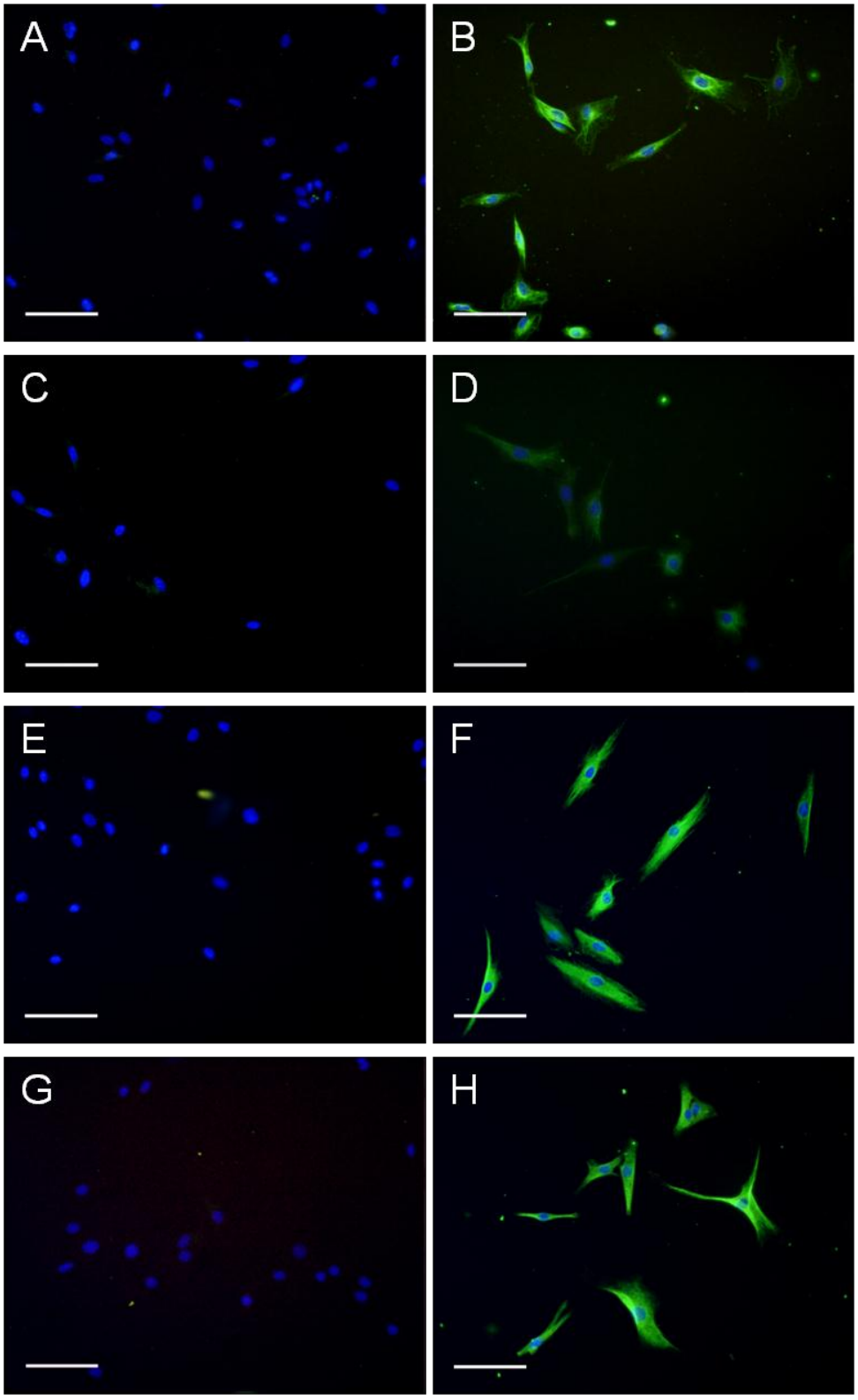

Figure 3.5 – Immunocytochemistry of nestin in single cell-derived clones
Four clonal cultures were stained for nestin expression: 19_8A2A (A & B), 10_11BNA3A (C & D), 7_10BA1B (E & F) and 7_10BA2C (G & H). Cultures were stained with anti-nestin (B, D, F & H) and normal mouse IgG antibodies (A, C, E & G) as an isotype control. Anti-mouse IgG alexa fluor 488 secondary antibody was used (scale bars = 100µm).

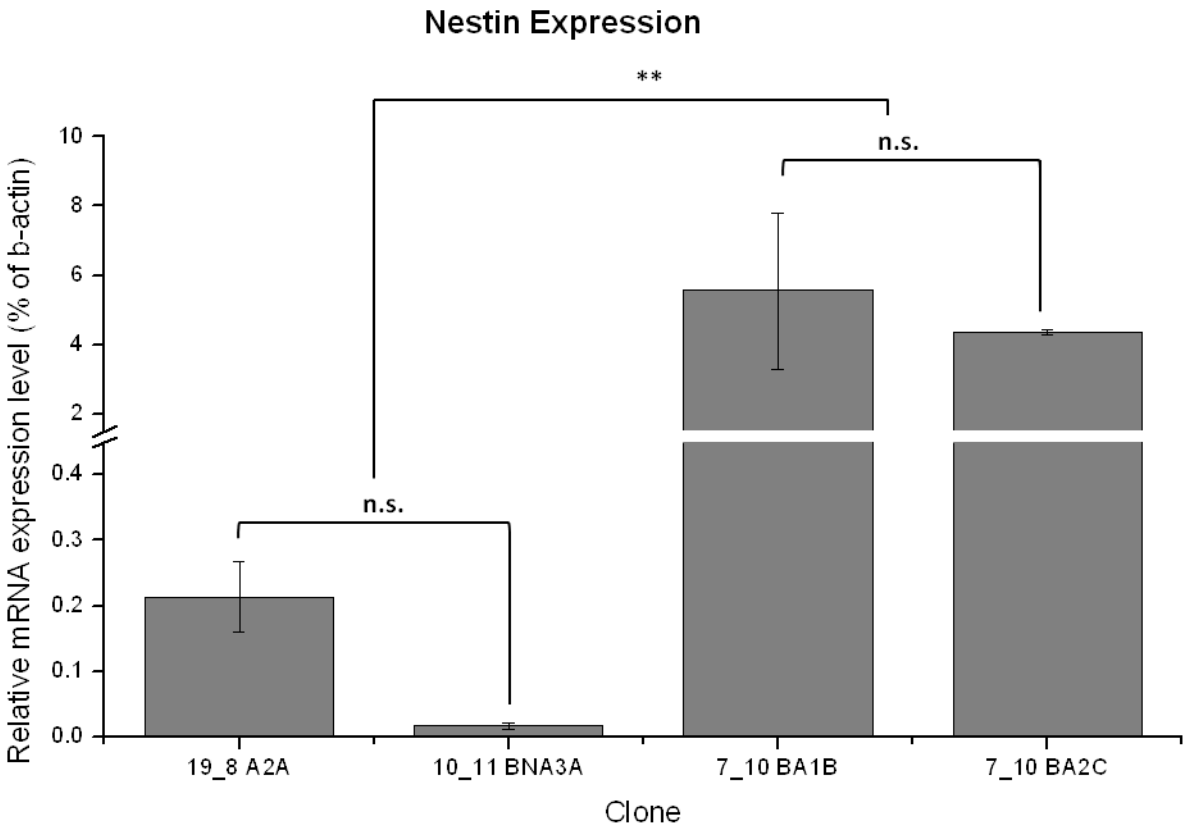

Figure 3.6 – Quantification of clonal nestin mRNA expression

Isolated dental pulp cells were divided into weakly nestin-positive clones (19_8A2A and 10_11BNA3A) and strongly nestin-positive clones (7_10BA1B and 7_10BA2C). Nestin expression was calculated as a relative percentage of β-actin ± SD, ** = $p<0.01$. One way ANOVA with Tukeys post-test.

3.4.5 Neurotrophic and growth factor expression

Total RNA extracted from murine dental pulp clones/heterogeneous cultures was also screened for the presence of RNA transcripts for a range of growth factors associated with promoting neuronal survival and repair: TGFβ-1, IGF-1, PDGF-a, bFGF, VEGF-A, NT-3, NGF, BDNF and GDNF (Figures 3.6 and 3.7). All cultures were found to express TGFβ-1, VEGF-A, NGF, BDNF and GDNF. Clonal differences were observed in the expression of IGF-1, PDGF-a and bFGF, whereas NT-3 was not found to be expressed by any mDPPC culture.

		TGFβ-1	IGF-1	PDGF-a	bFGF	VEGF-A	GAPDH
Non – adherent mixed populations	9_7NA1						
	9_7NA3						
	19_8NA1-3						
	7_10BNA1-3						
Total population	14_9TP						
Adherent Clones	19_8A2A						
	7_10BA1B						
	7_10BA2C						
	7_10BA2B						
Non-adherent clones	10_11BNA2B						
	10_11BNA3A						
Controls	RT-ve						
	PCR -ve						
	+ve control						

Figure 3.7 – mRNA expression of growth factors

Rt-PCR was used to detect the expression of TGFβ-1, IGF-1, PDGF-a, bFGF and VEGF-A by different populations of isolated dental pulp cells All populations were found to express TGFβ-1, IGF-1 and VEGF-A, whereas expression of bFGF and PDGF-a was more variable. RNA extracted from murine corpus callosum was used as a positive control.

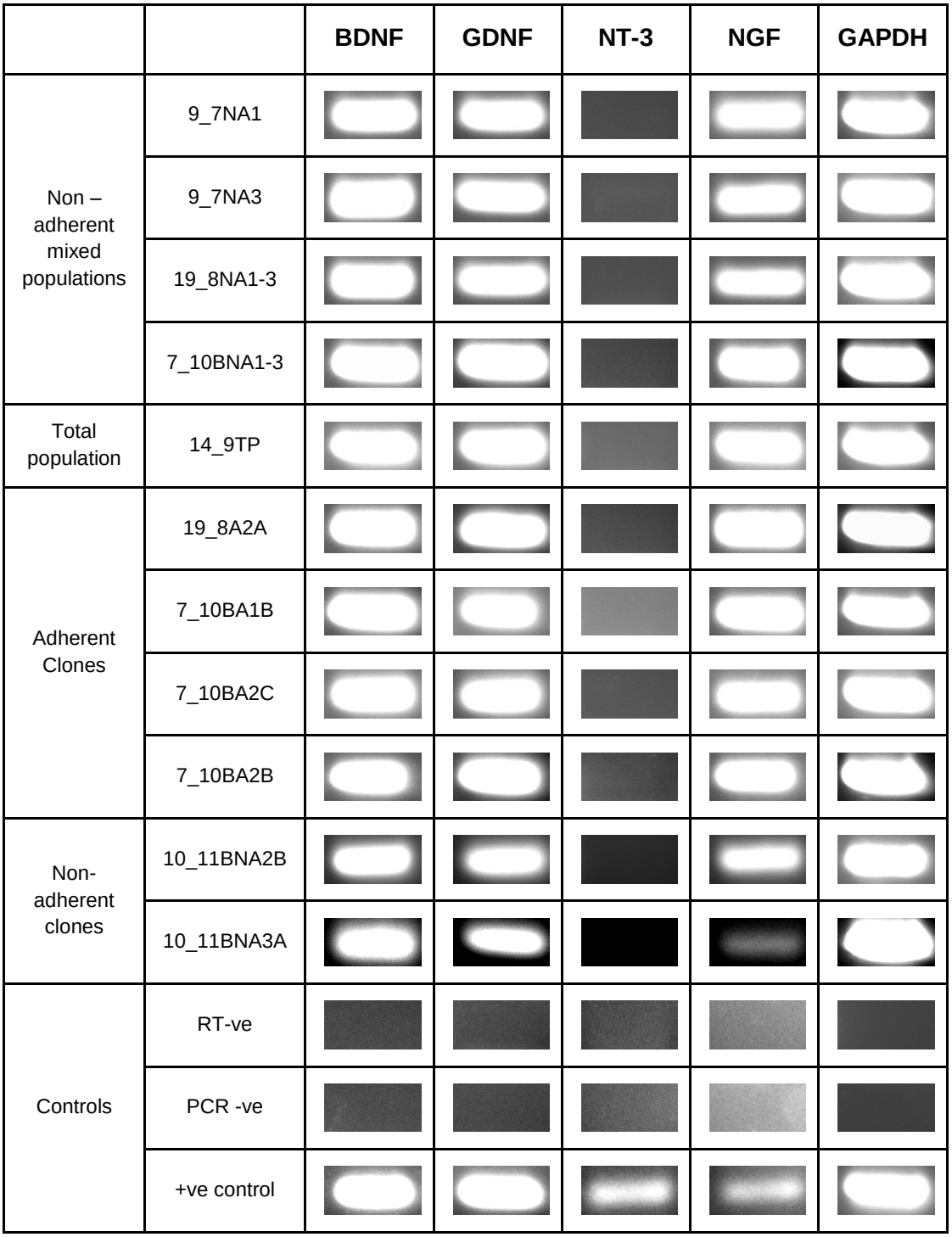

Figure 3.8 – mRNA expression of neurotrophic factors

Rt-PCR was used to detect the expression of BDNF. GDNF, NT-3 and NGF by different populations of isolated dental pulp cells All populations were found to express BDNF, GDNF and NGF. NT-3 expression was not detected in any population. RNA extracted from murine corpus callosum was used as a positive control.

3.5 Discussion

Preferential adherence to fibronectin separates cells based on the functional expression of the $\alpha_5\beta_1$ integrin subunit (Jones and Watt, 1993). This method selects cells of more immature phenotypes, which display increased integrin functionality and, therefore, adhere to fibronectin-coated culture surface in a shorter timeframe, from mixed populations. Variations of this method have been used to successfully isolate purified populations of human epidermal stem cells (Jones and Watt, 1993), articular cartilage progenitor cells (Dowthwaite et al., 2004), oral mucosa lamina propria progenitor cells (Davies *et al*., 2010), cord blood mesenchymal progenitor cells (Maurice *et al*., 2007) and dental pulp progenitor cells (Waddington *et al*., 2009).

One measure for the effectiveness of this selection technique is the calculation of colony forming efficiencies. Cells that adhere to fibronectin within 20 minutes typically possess a greater CFE than non-adherent cells (Jones and Watt, 1993; Dowthwaite et al., 2004). The ability of individual cells to form colonies greater than 32 cells in number is thought to provide a reliable means of identifying progenitor cells. Five population doublings are required to reach this stage and adopting this definition eliminates colonies derived from transit amplifying cells with reduced self-renewal properties (Jones and Watt, 1993). Thus, isolated cultures with higher CFEs should contain a greater proportion of progenitor cells. However, this does not necessarily equate to differentiation potential. No difference was observed in the proportion of epidermal stem cells able to undergo terminal differentiation in cultures of adherent cells with high CFEs, compared to cells that

underwent no selection procedure (Jones and Watt, 1993). In most reports, non-adherent cells are simply disregarded and, as such, these populations of cells remain largely uncharacterised (Maurice *et al*., 2007; Waddington *et al*., 2009; Davies *et al*., 2010).

In this study, no difference in the CFEs of adherent and non-adherent murine dental pulp cells was found, suggesting that not all progenitor cells may have been separated from the initial population (Figure 3.1). Expression of mRNA transcripts for CD90, SCA1 and nestin were detected in both non-adherent clonal and non-adherent heterogeneous cultures (Figure 3.3) confirming that a population of progenitor cells remain unattached at the end of the 20 minute adhesion. The duration of time initially allowed for adherence to fibronectin can prove critical. For the isolation of epidermal stem cells, 5 minutes was identified as an optimal length of time. The CFE ratio between adherent and non-adherent cells began to equalise at longer durations, as transit amplifying cells attached to the fibronectin (Jones and Watt, 1993). This observation may not be applicable to all cell types however. Additional 40 minute steps, after an initial 20 minute adhesion, have proven effective in the further purification of remaining non-adherent progenitor cells from cartilage (Dowthwaite et al., 2004) and oral mucosal lamina propria (Davies *et al*., 2010) tissues. Despite their non-adherent properties, clonal and mixed DPPC cultures not attaching to fibronectin within 20 minutes retained expression of the key marker desired for this study, nestin (Figures 3.3 – 3.6), and so were deemed suitable for further investigation.

Single cell-derived clones typically demonstrated an initial rapid rate of population doubling, followed by a short lag phase, before increasing and remaining at a steady rate (Figure 3.2 B). Heterogeneous cultures, however, tended to proliferate slowly over the first 80-90 days of culture before a sharp increase in doubling rate was observed (Figure 3.2 A). Clonal cultures expressing progenitor markers (Figure 3.3) may possess enhanced self-renewal properties and so maintain a steady rate of doublings over long periods (Gronthos *et al*., 2002; Waddington *et al*., 2009). In heterogeneous cultures, it is likely that only a small number of cells capable of self-renewal are initially present. Other contaminating cell types, capable of only limited renewal, proliferate very slowly, if at all. As an example, primary cultured murine fibroblasts divide approximately 10 times before senescing in serum-containing media at normal oxygen levels (Rohme, 1981; Loo *et al*., 1987; Parrinello *et al*., 2003). Gronthos *et al*., (2002) report that 80% of single cell-derived DPPC clonal cultures fail to proliferate beyond 20 population doublings. During the early stages of culture, the presence of such cells within mixed population masks the higher proliferation of cells with progenitor characteristics. Over the long term, non-proliferating cells may drop out of culture as a result of senescence and/or post-mitotic differentiation and eventually progenitors begin to predominate. This could, perhaps, explain the sharp increase in proliferation rate that can be seen in heterogeneous cultures (Figure 3.2 A), which will eventually consist entirely of progenitor cells.

It is now widely accepted that there may in fact be multiple populations of progenitor cells residing in different locations of the pulp. Different niches have been proposed to exist *in situ* associated with the vasculature, within the pulpal stroma and in the sub-odontoblast layer (Shi and Gronthos, 2003; Lovschall *et al*., 2005; Téclès *et al*., 2005). Depending upon their resident niche, progenitor cells may possess different proliferative and differentiation capababilities. The methods used to isolate cells in this study do not select for cells associated with any specific niche and mixed cultures will likely comprise of progenitor cells from all niches. The clonal differences observed in proliferative abilities (Figure 3.3) and marker expression (Figure 3.4 – 3.8) may be associated with the original niche from which each cell was derived. Without using specific sorting techniques from the very start, it remains a challenge to identify from which niche an *in vitro* cell culture may have originated.

In order to identify the isolated murine pulp cells as progenitor cells, the mRNA expression of different progenitor cell markers was examined (Figure 3.3). Four markers were chosen for investigation. CD90 is an essential marker required for the identification of mesenchymal progenitor cells (Dominici *et al*., 2006). Similarly, no expression of CD45 should be found within mesenchymal cultures as this is indicative of contamination with cells of haematopoietic origin. Together, the expression of CD90 and absence of CD45 indicates that the majority of the isolated populations contained mesenchymal progenitor cells (Figure 3.3). SCA1 represents a more general stem cell marker and has been used to identify haematopoietic cells

(Spangrude *et al*., 1988), as well as progenitor cells found in mammary (Welm *et al*., 2002), prostate (Burger *et al*., 2005), cardiac (Matsuura *et al*., 2004) and dental pulp (Patel *et al*., 2009) tissue. Its expression by every DPPC culture (Figure 3.3) suggests that the isolated cells may have the potential for differentiation into cell types additional to those traditionally associated with mesenchymal cells: osteoblasts, chondrocytes and adipocytes (Dominici *et al*., 2006). The final marker investigated, and key for this study to give an indication of potential for neuronal and glial differentiation, was the early stage neural marker nestin.

The intermediate filament nestin was first used to distinguish neural stem cells from more differentiated cells in the neural tube (Lendahl *et al*., 1990). Although its precise functions are as yet unidentified, knockdown experiments suggest that, rather than a structural role, it is involved in NSC survival and self-renewal (Park *et al*., 2010b). Nestin expression has been identified in progenitor cells from many other ectodermal and mesenchymal tissues including the dermis, bone marrow and dental pulp (Toma *et al*., 2001; Gronthos *et al*., 2002) and its presence may give a reliable indication of neural potential. Nestin expression was examined in isolated murine dental pulp cells in more detail using immunocytochemistry and qPCR. Between 75-90% of cells within heterogeneous cultures were identified as nestin-positive (Figure 3.4), a significantly higher proportion than the 3.5% reported in cultures of total populations from rat incisors (Takeyasu *et al*., 2006). In a differentiation experiment, Takeyasu's mixed population of cells tended towards a more astrocytic than neuronal phenotype, demonstrated by

upregulation of GFAP and unchanged levels of βIII-tubulin and Map2. It is believed the higher percentage of nestin-expressing cells found using the isolation and culture methods described in this chapter may result in a greater tendency towards a neuronal phenotype using similar differentiation conditions. Other studies have reported the isolation of dental pulp progenitor cells with enhanced neural potential based upon the formation of neurosphere-like structures. Rat incisor dental pulp cells can be encouraged to initially grow as enriched nestin-expressing suspended bodies on superhydrophobic plates in a medium containing bFGF and EGF (Sasaki *et al*., 2008). Although neuronal-like differentiation of cells dissociated from the neuropheres was observed, the scalability of this approach is questionable as spheres can only be successfully maintained for one subculture *in vitro*. Mixed and clonal populations of nestin-expressing DPPCs isolated using the methods described in this study, however, have demonstrated the ability to proliferate beyond 40 population doublings (Figure 3.2). Thus, expansion of these DPPCs with neural potential will not suffer from the same scalability issues associated with culture as nestin-expressing neurosphere-like bodies (Sasaki *et al*., 2008).

Two clones, 19_8A2A and 10_11BNA3A, that did not express mRNA transcripts for nestin, as detected by rt-PCR (Figure 3.3), showed weak immunocytochemistry staining compared to the background set using matching isotype controls (Figure 3.5 A – D). qPCR confirmed the presence of nestin mRNA in these clones, but at very low levels in comparison with two other clones, 7_10BA1B and 7_10BA2C (Figure 3.6). The lack of

expression of nestin mRNA detected by rt-PCR may have been due to cycling conditions that, perhaps, weren't fully optimised for the primer pair. These clonal differences in expression levels will allow comparisons to be made between weakly and strongly nestin-positive cells in subsequent differentiation chapters, confirming whether nestin is potentially a useful marker for identifying DPPCs with increased neuronal and glial differentiation capabilities.

The ability of the isolated murine dental pulp progenitor cells to produce a range of growth factors and neurotrophic factors thought to modulate a number of mechanisms involved in neural repair and regeneration was investigated (Figures 3.7 and 3.8). At the mRNA level, DPPCs were found to express TGFβ-1, IGF-1, PDGF-a, bFGF and VEGF-A. Similarly, cells were found to also express NGF, BDNF and GDNF, but not NT-3, matching previous studies demonstrating expression of neurotrophic factors excluding NT-3 by cultured DPPCs (Nosrat *et al*., 2001, 2004; Nesti *et al*., 2011).

The release of NGF, BDNF and GDNF by DPPCs has been measured at the protein level using ELISA techniques (Nesti *et al*., 2011; Soria *et al*., 2011). Similar quantitative measures are required to demonstrate that cultured mDPPCs can produce and release the factors investigated in this study (Figures 3.7 and 3.8). However, their expression at the mRNA level does provide a strong indication of the cells ability to secrete the related growth factors. The release of growth factors by cells of the dental pulp plays important roles *in vivo* to promote trigeminal ganglion innervation of the tooth during development (Luukko *et al*., 1997a, 1997b) and to promote

revascularisation following injury (Tran-Hung *et al*., 2008). Whether these effects are mediated by progenitor cells or other cells resident in the pulp is unclear. The expression of mRNA for these growth factors by mDPPCs suggests that progenitor cells could be responsible, in part, for this. Similar innervation and revascularisation effects would prove instrumental in growth factor-mediated repair of the damaged CNS by transplanted DPPCs. Such trophic effects have been observed *in vivo* following grafting into neural tissue. Chitosan mesh tubes enclosing human pulp explants grafted into the transected sciatic nerve of SD rats act as a conduit for regenerating endogenous axons which can be identified growing through the grafts (Matsushita *et al*., 2012). Porcine side population DPPCs have also demonstrated the potential to promote revascularisation in models of hindlimb and cerebral ischaemia (Iohara *et al*., 2008; Sugiyama *et al*., 2011; Ishikaza *et al*., 2013). These studies demonstrate the ability of DPPCs to exert influences upon endogenous cells of the CNS and PNS following transplantation. Expression of mRNA for a wide range of neurotrophic and growth factors (Figures 3.7 and 3.8), suggests that the isolation and culture methods used in this study are suitable for the derivation of cells with potential to promote repair/regeneration of the injured spinal cord through similar paracrine mechanisms.

Stem cells isolated from the murine dental pulp possess very similar properties to those isolated from human molars, expressing mesenchymal markers (CD73, CD90, CD117, SCA1 and Stro-1) and embryonic markers (SSEA-1 and OCT-4) (Guimarães *et al*., 2011). They also possess

adipogenic, chondrogenic, myogenic and osteogenic differentiation capabilities (Balic and Mina., 2010; Nakatsuka *et al*., 2010; Zainal Ariffin *et al*., 2012). As such, murine DPPCs do not represent an inferior source of cells for laboratory investigations. However, they may be partially removed in some properties from human DPPCs as a result of differences in tooth development between species. Murine incisors continually erupt throughout life due to the abrasive gnawing nature of their eating habits producing significant wear and tear. This necessitates a more active population of resident stem cells in comparison with the human pulp, whose stem cells are more quiescent and reactive in nature. An additional mesenchymal stem cell niche is proposed to exist between the labial and lingual cervical loops of the proximal root of the mouse incisor pulp (Harada *et al*., 1999; Seidel *et al*., 2010; Lapthanasupkul *et al*., 2012). These cells give rise to transit amplifying progeny which further differentiate into dentine-forming odontoblasts and enamel-forming ameloblasts, and migrate distally to sustain continual tooth growth at the root (Harada *et al*., 1999). The continuous turnover of progenitor cells within this location is evidenced by extensive BrdU uptake in the region (Harada *et al.,* 1999; Seidel *et al*., 2010). In contrast, in the pulp of the human molar, BrdU labelling is observed only following pulpal exposure and damage, and is restricted to the perivascular niche (Téclès *et al*., 2005). This suggests the existence of a small population of slowly proliferating stem cells that remain at rest until activated by suitable stimuli (Shi and Gronthos, 2003). Despite the *in situ* differences in turnover rates and niche location, human and murine DPPCs retain similar mesenchymal characteristics *in vitro*. Expression of CD90, SCA1 and nestin by mDPPCs in this study (Figure

3.3) is sufficient to confirm that these cells provide a suitable means of investigating the behaviours of dental pulp-derived mesenchymal progenitor cells.

3.6 Summary

- Clonal and heterogeneous populations of cells were isolated from the dental pulp of murine incisors using the selective adhesion to fibronectin method.

- 20 minutes fibronectin adhesion is insufficient to select for all pulpal progenitor cells evidenced by similar CFEs and the expression of progenitor markers in both adherent and non-adherent cultures.

- Clonal differences were observed in the expression of RNA transcripts for progenitor markers and neurotrophic factors. Clones have been separated into those that express nestin at low (19_8A2A and 10_11BNA3A) and high levels (7_10BA1B and 7_10BA2C) allowing for comparisons in subsequent neuronal and glial differentiation studies.

- Isolated DPPC cultures were found to express mRNA transcripts for a range of neurotrophic and growth factors indicating their potential to promote repair/regeneration of the CNS through the release of soluble factors.

Chapter 4: Development of a protocol for the differentiation of neuronal-like cells from dental pulp progenitor cells

4.1 Introduction

A major goal of any cellular transplantation therapy for SCI is the replacement of dead neurons to reform functional neuronal pathways. *In vitro* differentiation protocols provide a valuable tool to determine the optimal conditions for the derivation of such neuronal-like cells from progenitor cells. Although such protocols may not be directly applicable *in vivo*, they present confirmation of the potential for neuronal differentiation and supply a means of investigating further mechanisms through which transplanted cells could promote spinal regeneration.

As yet, there is no definitive method for the *in vitro* differentiation of neuronal-like cells from DPPCs, although a number of protocols have been published (reviewed by Young *et al*., 2013). Different approaches include the generation of floating neurosphere-like bodies (Iohara *et al*., 2006; Takeyasu *et al*., 2006; Sasaki *et al*., 2008; Govindasamay *et al*., 2010; Osathanon *et al*., 2011; Osathanon *et al*., 2013), stimulation of cAMP and protein kinase C signalling to induce the onset of functional properties (Király *et al*. 2009), and the addition of retinoic acid (Arthur *et al*., 2008) or β-mercaptoethanol and butylated hydroxyanisole (Zhang *et al*., 2006a; Osathanon *et al*., 2013) to culture media.

One issue associated with these reported methods is that, prior to differentiation, DPPCs typically already express a number of the markers used to identify them as neuronal-like cells including: βIII-tubulin, Map2, NF and NeuN (Karaöz *et al*., 2011; Osathanon *et al*., 2011; Sakai *et al*., 2012).

Although the presence of such markers provides strong evidence of the potential for DPPCs to differentiate into neurons, it also necessitates the use of quantitative methods, such as qPCR, to confirm changes in neuronal marker expression. In the literature, such quantitative methods are often not used (Iohara *et al*., 2006; Zhang *et al*., 2006a; Sasaki *et al*., 2008; Karaöz *et al*., 2011; Osathanon *et al*., 2011). Of those studies using appropriate methods, the induction and/or upregulation of glial markers, such as GFAP, is often reported indicating that the differentiated cells may be of a potentially more astrocytic phenotype, rather than true neuronal cells (Takeyasu *et al*., 2006; Király *et al*. 2009; Govindasamy *et al*., 2010; Karaöz *et al*., 2011). As such, these published methods may not be the most suitable, and there remains a requirement for a protocol to definitively derive neuronal-like cells from DPPCs.

In order to act as a direct cell replacement, transplanted cells must be capable of functionally compensating for neurons lost following SCI. Patch clamp techniques can be used to record and assess the functionality of neuronal-like cells by measuring electrical currents under defined conditions. Two leading studies report on the electrophysiological properties of neuronally differentiated DPPCs (Arthur *et al*., 2008; Király *et al*. 2009). Each differentiation protocol derives cells with neuronal-like morphology expressing late stage neuronal markers. In one study, Arthur *et al*. recorded inward-directed voltage-activated Na^+ currents in DPPCs differentiated using their protocol. Király *et al*. identified not only Na^+, but also outward voltage-propagated K^+ currents, albeit only present in a small proportion of

differentiated cells. A follow-up study using Király's protocol reported that DPPCs from only one out of four patient samples were capable of differentiation into neuronal-like cells (Aanismaa *et al*., 2012). No voltage-activated Ca^{2+} currents have been detected in DPPCs differentiated using these protocols and, crucially with regards to neuronal signalling, no signs of spontaneous activity or action potentials evoked using standard voltage ramp protocols have been recorded. The ability to generate a full action potential is a key requirement, which has not yet been achieved, to demonstrate that DPPCs truly can differentiate into functionally active neurons. The development of a protocol to reproducibly derive functional neuronal-like cells from DPPCs would be a significant development.

CNS development and the subsequent onset of neuronal functional properties fall under complex genetic control. Transcription factors, such as SOX1, SOX2, Pax6 and Myelin transcription factor 1-like (Myt1l), in addition to the RNA binding protein Musashi and nestin, are important in regulating self-renewal and regional differentiation of NSCs (Kim *et al*., 1997; Imai *et al*., 2001; Takahashi and Osumi. 2002; Graham *et al*., 2003; Park *et al*., 2010b). Indentifying the expression of such developmental markers by DPPCs could provide a means of determining the most appropriate methods to promote their neuronal-like differentiation. In developing a differentiation protocol it may also be of importance to identify whether DPPCs are closer in phenotype to radial glial or neuroepithelial NSCs. BLBP and GLAST are typically used to identify radial glial cells (Anthony *et al*., 2005), whereas CD133 expression is more indicative of a neuroepithelial phenotype (Corbeil

et al., 2010). A comprehensive comparison of the expression of such developmental markers between DPPCs and NSCs will serve as a foundation for the rational development of a neuronal differentiation protocol underpinned by logic and reasoning.

4.2 Objectives

- To provide a comprehensive characterisation of the expression of developmental and late stage neuronal markers by mDPPCs and compare this with NSCs.

- To develop a definitive protocol for the differentiation of functional neuronal-like cells from DPPCs and confirm phenotype using appropriate quantitative methods.

- To investigate how neuronal differentiation may affect the ability of DPPCs to promote neural repair via trophic mechanisms.

4.3 Materials and methods

4.3.1 Characterisation of neural marker expression

RNA extracted from low-passage DPPC cultures at between 15-25 population doublings was used with rt-PCR (see sections 2.2.2.1 – 2.2.2.5) to identify undifferentiated DPPC expression of developmental neural markers (SOX1, SOX2, Pax6, Myt1l and P75), neural stem cell markers (BLBP, GLAST, Musashi, CD133) and mature neuronal markers (NF-l). RNA extracted from cultured murine NSCs (sections 2.2.1.4 and 2.2.1.5) was used as a positive control. Primer sequences and targets are shown in Table 4.1.

Four single cell-derived clones (19_8A2A, 10_11BNA3A, 7_10BA1B and 7_10BA2C (20-25 PDs)) in culture were further fixed with 4% PFA and immunocytochemically stained (section 2.2.2.7) with antibodies against nestin and Musashi, together with appropriate isotype controls (Tables 2.2 – 2.4).

4.3.2 DPPC differentiation in NSC medium

Culture surfaces were coated with 0.01% poly-l-lysine (Sigma-Aldrich, UK) for 5 minutes at room temperature. This was removed and the surfaces allowed to completely air dry for a minimum of one hour before rinsing with PBS. Laminin (Sigma-Aldrich, UK), diluted to 20µg/ml in PBS, was then used to coat the culture plastics overnight at room temperature. Laminin solution was removed the day after and, following a wash with PBS, the surfaces were ready for seeding with cells.

Four DPPC clones (19_8A2A, 10_11BNA3A, 7_10BA1B and 7_10BA2C (20-30 PDs)) were passaged (sections 2.2.1.1. and 2.2.1.2) and seeded at 4,000 cells/cm^2 on poly-l-lysine/laminin-coated dishes in NSC medium (section 2.2.1.4). Cells seeded in DPPC medium were used as an undifferentiated control. Photos were acquired of the differentiating cells every day to record changes in morphology. After 7 days of differentiation, RNA was extracted (section 2.2.2.1) from each culture, reverse transcribed (section 2.2.2.3) and the resultant cDNA used for qPCR (section 2.2.2.5). Fold change in expression was calculated for the general stem cell marker SCA1 and the neural markers nestin, Map2 and NF-l (Table 4.2).

4.3.3 Maturation in neurotrophin-containing medium

In order to encourage the development of functional properties, a further maturation step was added to the protocol. 7_10BA2C was differentiated in NSC medium on poly-l-lysine/laminin-coated dishes and slides, as described above, for 5 days. After 5 days differentiation, the cells were rinsed with PBS and the medium replaced with a neurotrophin-containing medium: Neurobasal medium supplemented with 1% (v/v) penicillin/streptomycin, 2mM L-glutamine (all Life Technologies, UK), 1x NEAA (Sigma-Aldrich, UK), 10ng/ml BDNF, 10ng/ml NGF and 10ng/ml NT-3 (all Peprotech, UK). Differentiating DPPCs were allowed to mature in neurotrophin-containing medium for up to 15 days (Figure 4.1). qPCR was used to quantify fold changes of expression of SCA1, nestin, Map2, NF-l, SOX2, Pax6, BLBP, Ncam and neurogenic marker Ngn2 (Table 4.2), in addition to neurotrophic and growth factors (Table 2.1), from RNA extracted on days 0, 5, 10 and 15

of differentiation (Figure 4.1). Cells were fixed on day 15 and immunocytochemically stained with antibodies against Map2 and NF-l, together with appropriate isotype controls (Tables 2.2 – 2.4). Cells differentiated for 15-19 days were used for patch clamp functional testing.

As a positive control for ICC staining, NSCs (sections 2.2.1.4 and 2.2.1.5) were seeded on poly-l-lysine/laminin coated chamber slides and differentiated in neurotrophin-containing medium for 10 days before antibody staining.

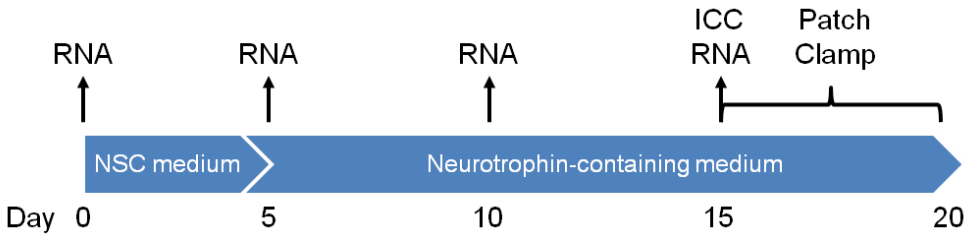

Figure 4.1 – DPPC differentiation experimental design

4.3.4 Patch clamp recordings

Transmembrane currents were recorded in conventional whole-cell configuration from DPPCs after 15-19 days of differentiation. Cells differentiated on poly-l-lysine/laminin-coated glass cover slips were bathed in a continuous wash-through of extracellular solution designed to resemble *in vivo* extracellular fluid, containing: 135mM NaCl, 5mM KCl, 1.2mM $MgCl_2$, 1.25mM $CaCl_2$, 10mM d-glucose, and 5mM N-2-hydroxyethylpiperazine-N′-2-ethanesulfonic acid (HEPES); adjusted to a pH of 7.4 using NaOH. The pipette solution was designed to match intracellular ionic concentrations and

contained: 117mM KCl, 10mM NaCl, 2mM $MgCl_2$, 1mM $CaCl_2$, 2mM Na_2ATP, 1mM Na_2GTP, 11mM HEPES, and 11mM ethylene glycol tetraacetic acid; free $[Ca^{2+}]_i$ was adjusted to 100 nM; pH was adjusted to 7.2 with KOH. A micromanipulator control system was used to manoeuvre fire-polished glass pipettes until contact was made with the cellular membrane and suction applied to form a high resistance seal. Further suction resulted in patch rupture and entrance into whole cell recording mode. All recordings were performed at room temperature (22 ± 0.5 °C) using an Axopatch 200B amplifier and Digidata 1320 A/D interface (Axon Instruments, Forster City, CA, USA). Holding voltage was set to -70 mV and transmembrane currents recorded using a voltage step protocol of 80 ms duration of voltages ranging from -120 to +80 mV. Series resistance and membrane capacitance were compensated ≈ 90 % (11.6 ± 1.5 MΩ and 29.9 ± 3.1 pF, respectively (n = 6)). Pipette resistances were ≈ 5 – 10 MΩ when filled with the pipette solution. All recordings were filtered with an 8-pole Bessel filter at 5 kHz and digitized at 10 kHz. Half-activation voltage (V_{50} = 75.7 ± 3.1 mV) and slope coefficient (h = 23.1 ± 0.8) were obtained from the current-voltage curve.

4.3.5 Tables of primers

Table 4.1 – rt-PCR primer sequences

Product	Accession no.	Primer Sequences (5' → 3)	Product Size (bp)	Tm (°C)
BLBP	NM_021272.3	f: GGACACAATGCACATTCAAGAA r: CCGAACCACAGACTTACAGTTT	101	60
CD133	NM_008935.2	f: GAATGCGCCATGCAGGAGGAAGTGCTT r: GGCTGCTCCCCAGACTGCTTAGGCTTG	542	60
GAPDH	NM_008084.2	f: AGACGGCCGCATCTTCTTGTGCAGTGC r: ACATACTCAGCACCGGCCTCACCCCA	326	60
GLAST	NM_148938.3	f: ACCAAAAGCAACGGAGAAGAG r: GGCATTCCGAAACAGGTAACTC	144	60
Musashi	NM_008629.1	f: GGGGTGGATAAAGTGCTGGCGCAATCG r: CGCTCTACACGGAATTCGGGGAACTGGT	533	60
Myt1l	NM_001093775.1	f: TGGTCACGTCAGTGGCAAATA r: TGCAAATGGTTTTCGCTTGGG	121	60
NF-I	NM_010910.1	f: CAAGAGCCGCTTCACCGTGCTAACCGA r: CGCTGGTTATGCTACCCACGCTGGTGA	392	60
P75	NM_033217.3	f: CTCAGATGAAGCCAACCACG r: CCTTGTGATCCATCGGCCA	133	60
Pax6	NM_001244198.1	f: TACCAGTGTCTACCAGCCAAT r: TGCACGAGTATGAGGAGGTCT	194	60
SOX1	NM_009233.3	f: CCTTGCTAGAAGTTGCGGTCCCAGA r: CCTCCTCTTGTCGGCTCGAAGTCTC	84	60
SOX2	NM_011443.3	f: GCGGAGTGGAAACTTTTGTCC r: CGGGAAGCGTGTACTTATCCTT	157	60

Table 4.2 – qPCR primer sequences

Product	Accession no.	Primer Sequences (5' → 3)	Product Size (bp)	Tm (°C)
BLBP	NM_021272.3	f: GGACACAATGCACATTCAAGAA r: CCGAACCACAGACTTACAGTTT	101	60
GAPDH	NM_008084.2	f: AGGTCGGTGTGAACGGATTTG r: TGTAGACCATGTAGTTGAGGTCA	123	60
Map2	NM_001039934.1	f: TGACACTTGGGACCTGGACGAGTAT r: ACACCACTTCTTCAACCAACGCTCA	105	60
Ncam	NM_001081445.1	f: CAGTGAAGAAAAGACTCTGGATG r: TTCCCTTCCCAAGTGTACACA	213	60
Nestin	NM_016701.3	f: CCAAAGAGGTGTCCGATCATC r: CTCCCTTCTTCTTCATCAGCATCT	147	60
NF-I	NM_010910.1	f: TGAGAAGCACGAAGAGCGAGATGG r: TGAAACTGAGCCTGGTCTCTTCGC	135	60
Ngn2	NM_009718.2	f: AACTCCACGTCCCCATACAG r: GAGGCGCATAACGATGCTTCT	103	60
Pax6	NM_001244198.1	f: TACCAGTGTCTACCAGCCAAT r: TGCACGAGTATGAGGAGGTCT	194	60
SCA1	NM_001271416.1	f: GAGGCAGCAGTTATTGTGGAT r: ACCCAGGATCTCCATACTTTCA	99	60
SOX2	NM_011443.3	f: GCGGAGTGGAAACTTTTGTCC r: CGGGAAGCGTGTACTTATCCTT	157	60

4.4 Results

4.4.1 Expression of neural markers by DPPCs

Prior to differentiation, RNA was extracted from each isolated dental pulp progenitor cell clone and mixed population at the earliest possible population doubling level. This was used to screen for the mRNA expression of a selection of neural stem cell and mature neural markers (Figures 4.2 and 4.3). All isolated DPPC cultures were found to express SOX2, P75, BLBP and Musashi. No clones or mixed populations expressed SOX1 or CD133. Expressions of Pax6, Myt1l, GLAST and NF-l were heterogeneous with differences evident between different cultures. No pattern of marker expression was apparent with regards to adhesion to fibronectin properties.

Individual clones with low (19_8A2A and 10_11BNA3A) and high (7_10BA1B and 7_10BA2C) levels of nestin mRNA expression were immunostained with antibodies against the neural progenitor markers nestin and Musashi (Figures 4.4 and 4.5). All four clones were found to double-stain for both early stage neural markers, at the protein level, with weaker nestin staining observed in 19_8A2A and 10_11BNA3A.

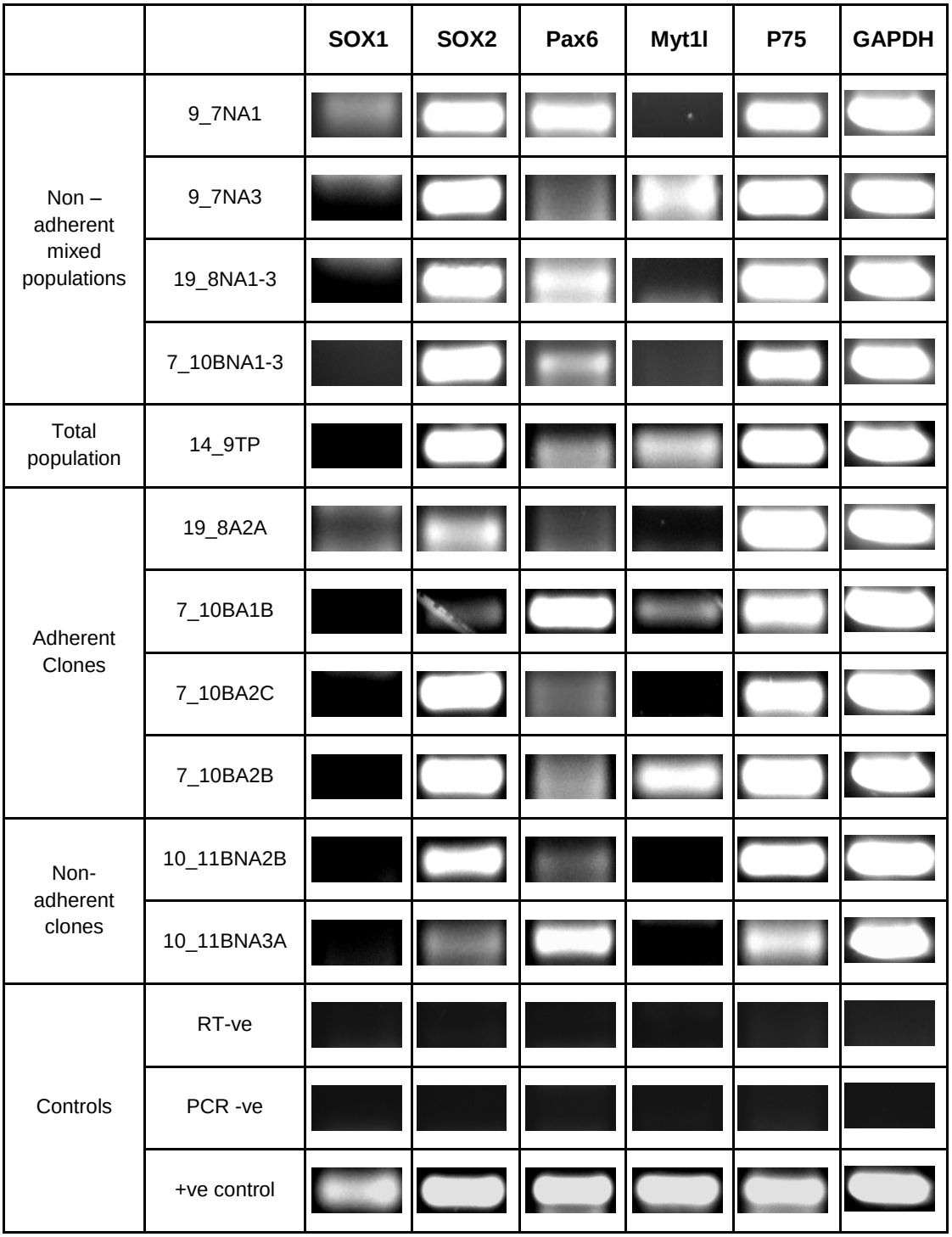

Figure 4.2 – mRNA expression of developmental neural markers

Rt-PCR was used to detect the expression of SOX1, SOX2, Pax6, Myt1l and P75 in undifferentiated DPPCs. SOX2 and P75 expression was identified in all cell populations, whereas Pax6 and Myt1l expression was found to differ between cultures. SOX1 was not expressed by any of the DPPC populations. RNA extracted from primary cultured neural stem cells was used as a positive control.

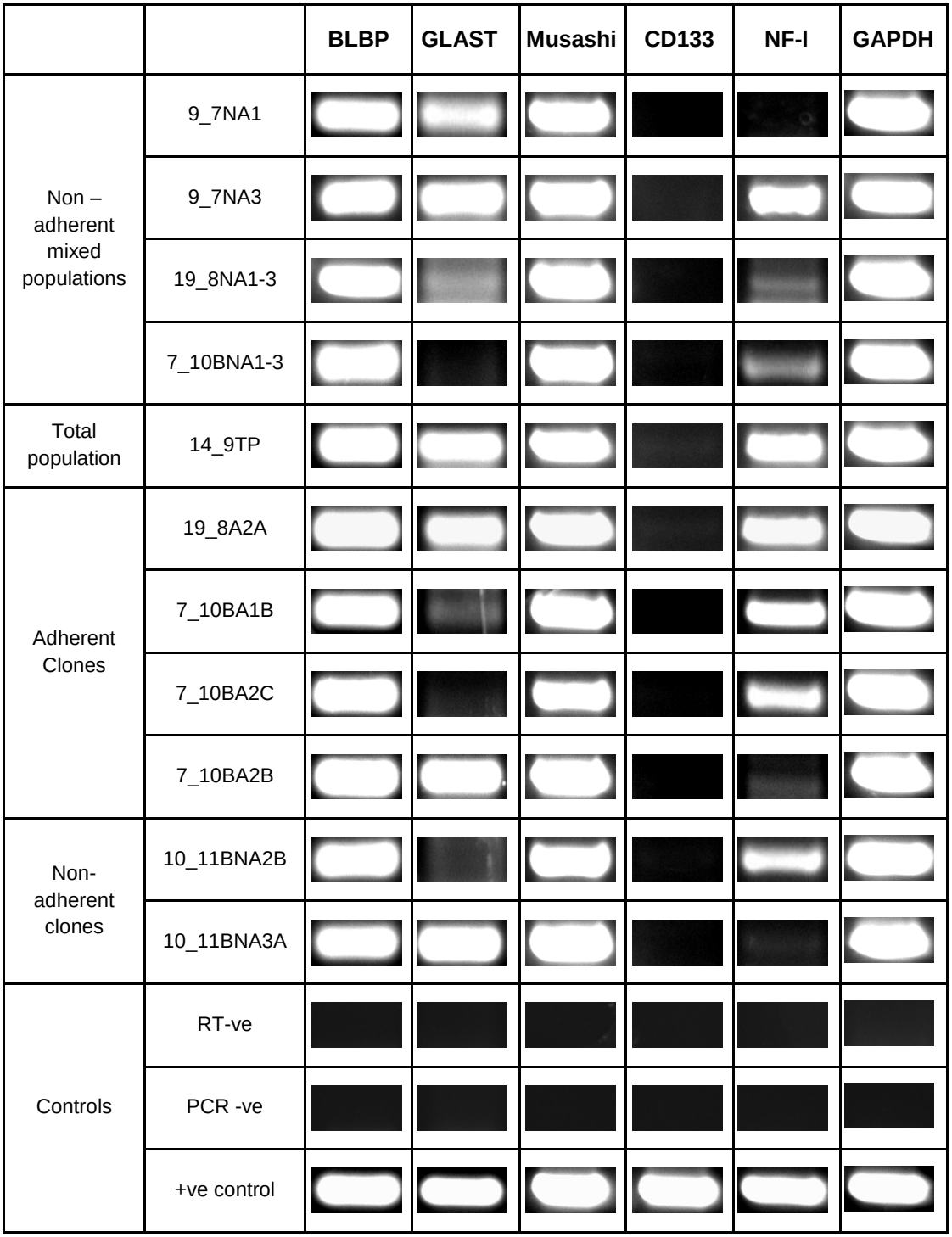

Figure 4.3 – mRNA expression of NSC and mature neural markers

Rt-PCR was used to detect the expression of BLBP, GLAST, Musashi, CD133 and NF-l in undifferentiated DPPCs. BLBP and Musashi expression was identified in all cell populations, whereas GLAST and NF-l expression was found to differ between cultures. CD133 was not expressed by any of the DPPC populations. RNA extracted from primary cultured neural stem cells was used as a positive control.

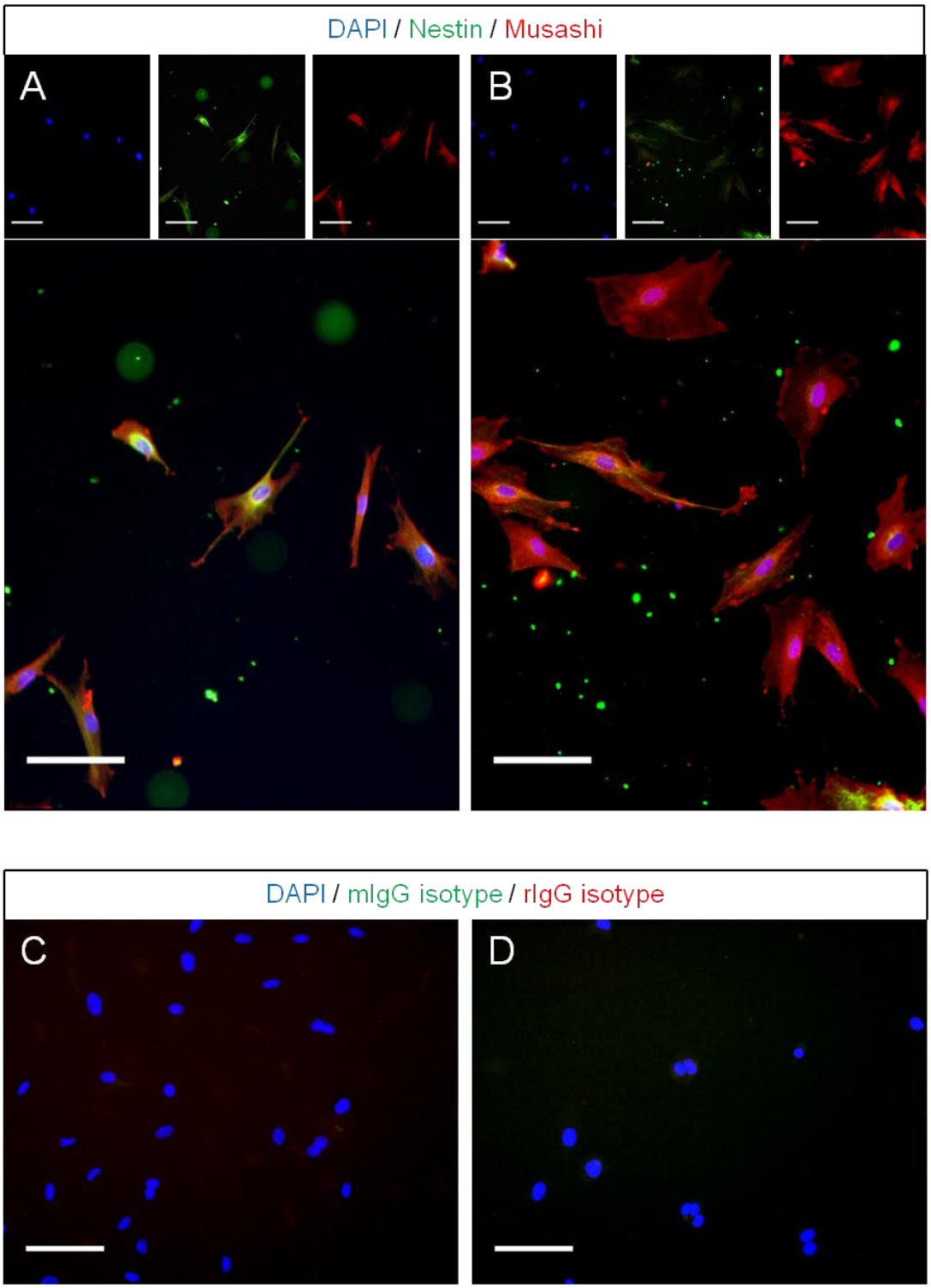

Figure 4.4 – Presence of nestin and Musashi in weakly nestin-expressing clones
Clones with low levels of nestin mRNA expression, 19_8A2A (A) and 10_11BNA3A (B), were fixed and stained with antibodies against the neural stem cell markers nestin (green) and Musashi (red). Nuclei were counterstained with DAPI. Merged images of the respective isotype controls are shown (C & D). Scale bars = 100µm.

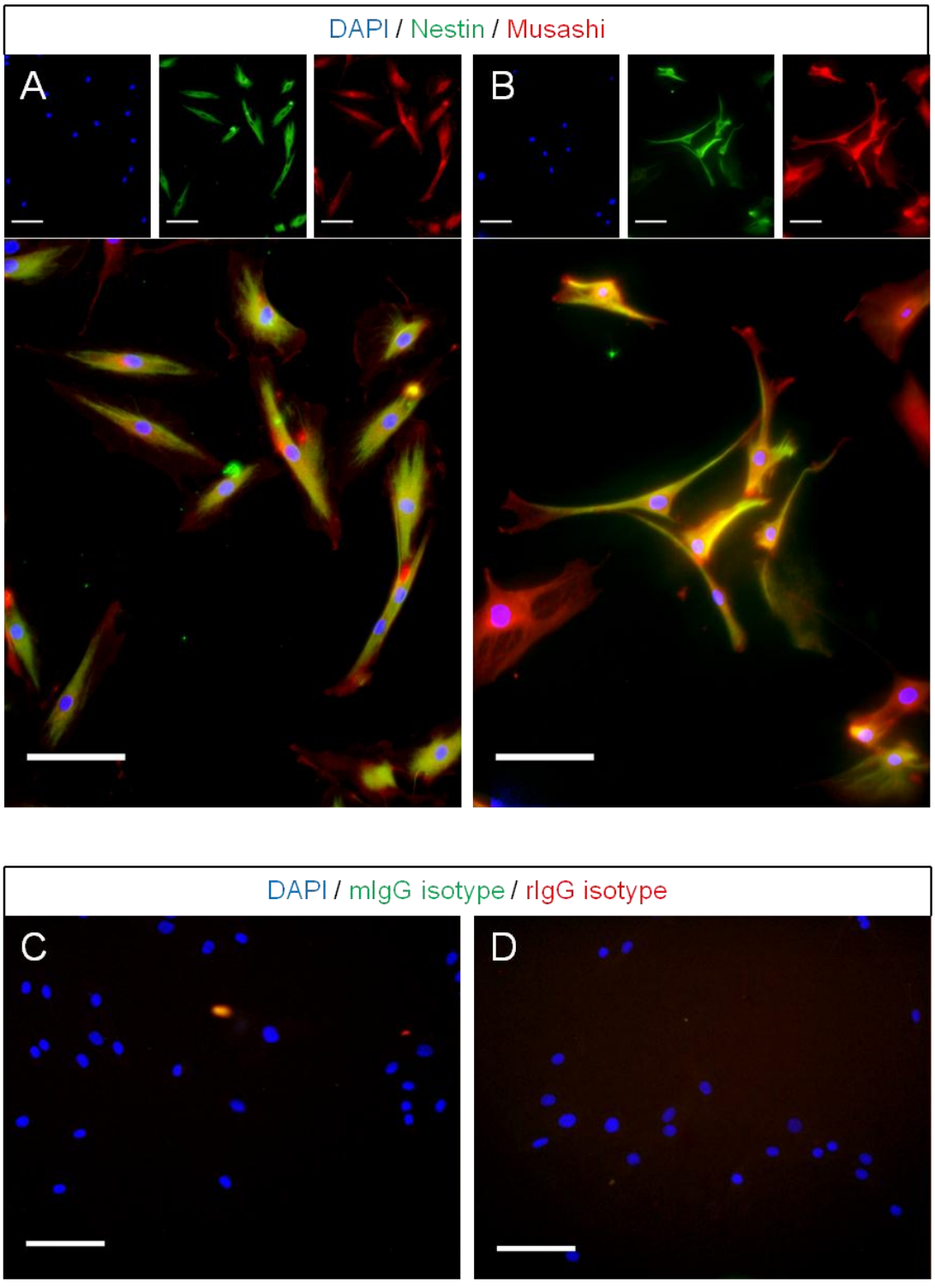

Figure 4.5 – Presence of nestin and Musashi in strongly nestin-expressing clones
Clones with high levels of nestin mRNA expression, 7_10BA1B (A) and 7_10BA2C (B) were fixed and stained with antibodies against the neural stem cell markers nestin (green) and Musashi (red). Nuclei were counterstained with DAPI. Merged images of the respective isotype controls are shown (C & D). Scale bars = 100µm.

4.4.2 DPPC clones cultured in NSC medium

Due to the similarities in marker expression with NSCs, initial attempts to differentiate DPPCs down a neural lineage were based on NSC culture protocols. The four clones (19_8A2A, 10_11BNA3A, 7_10BA1B and 7_10BA2C) were passaged and seeded afresh, in NSC medium, on poly-l-lysine and laminin-coated culture surfaces. Changes in morphology were observed over 7 days culture. mRNA extracted on day 7 was compared with mRNA extracted prior to differentiation to analyse changes in gene expression using qPCR techniques.

Low nestin-expressing clone 19_8A2A appeared morphologically unchanged following culture in NSC medium, remaining bipolar and fibroblastic-like (Figure 4.6 A and B). 10_11BNA3A, also with low levels of nestin mRNA, was similarly unchanged although some cells appeared to show stress fibre formation (Figure 4.6 C and D). Clones with high nestin mRNA levels, 7_10BA1B and 7_10BA2C, appeared similarly fibroblastic-like in DPPC medium (Figure 4.6 E and G, respectively). However, these clones were found to adopt a more neuronal-like morphology in NSC medium, with rounded cell bodies extending multiple long and branched processes (Figure 4.6 F and H). No obvious proliferation in NSC culture medium was observed in any of the four clones tested.

At the end of 7 days culture in NSC medium, changes in expression of SCA1, nestin, Map2 and NF-l were investigated (Figure 4.7). The general stem cell marker SCA1 was downregulated by all four clones. Nestin

expression was downregulated by 19_8A2A, upregulated by 10_11BNA3A and 7_10BA2C but unchanged in 7_10BA2C. Map2 expression increased in 19_8A2A, 7_10BA1B and 7_10BA2C but was unaffected in 10_11BNA3A. Expression of NF-l was found to be unchanged in 19_A2A cells, decreased in 10_11BNA3A but increased in both strong nestin-expressing clones, 7_10BA1B, 7_10BA2C.

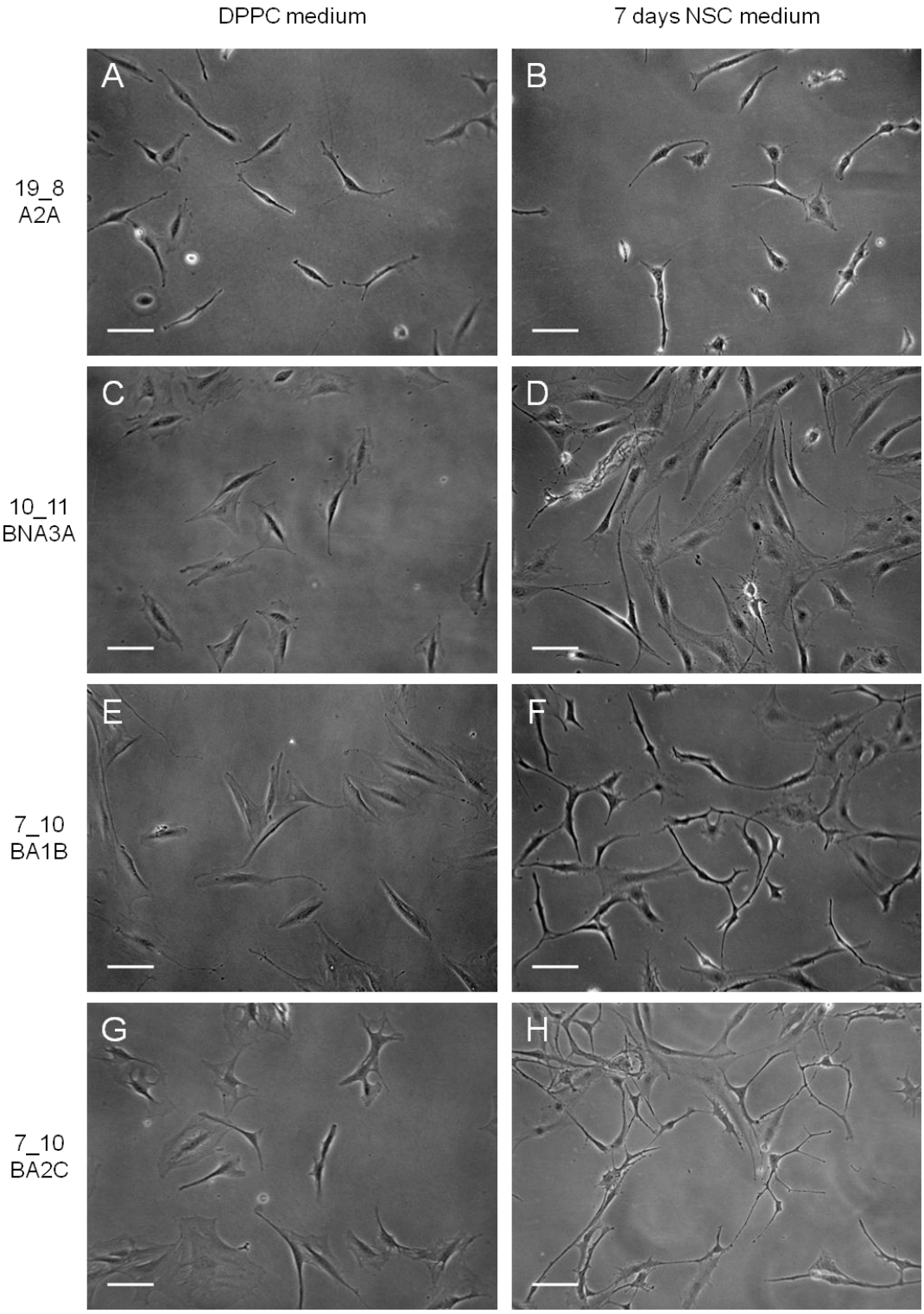

Figure 4.6 – Morphology changes following culture in NSC medium

In DPPC medium 19_8A2A (A), 10_11BNA3A (B), 7_10BA1B (E) and 7_10BA2C (G) displayed bi/tripolar fibroblastic-like morphology, typical of DPPCs. After 7 days culture in NSC medium no significant changes in morphology were observed in 19_8A2A (B), while 10_11BNA3A showed signs of stress (D). Small numbers of cells adopted a more neuronal like phenotype, with small round bodies extending multiple processes in 7_10BA1B (F) and 7_10BA2C (H). Scale bars = 100µm

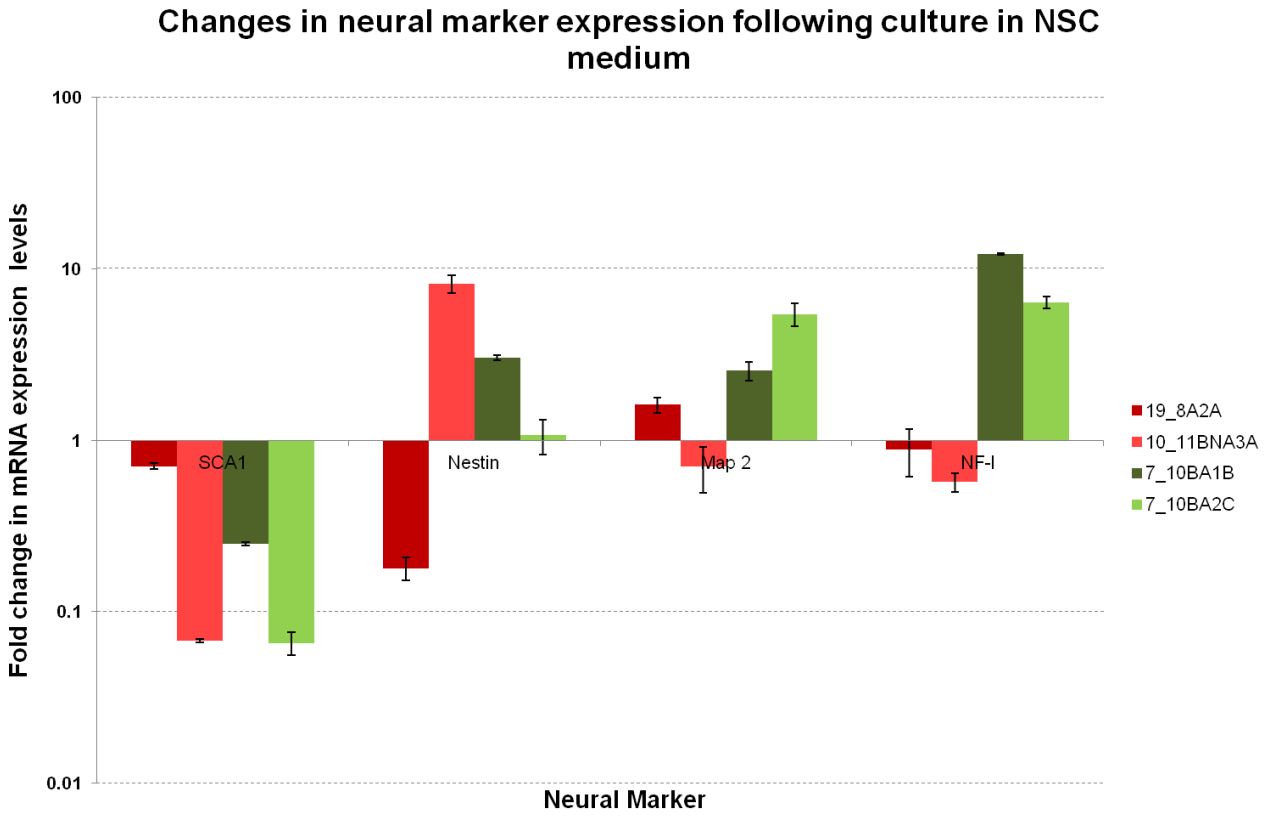

Figure 4.7 – Changes in neural marker expression following culture in NSC medium

RNA was extracted from 19_8A2A, 10_11BNA3A, 7_10BA1B and 7_10BA2C before and after 7 days culture in NSC medium. Fold change (±SD) in mRNA expression levels of SCA1, Nestin, MAP2 and NF-l were calculated using the $2^{-\Delta\Delta ct}$ method for qPCR analysis. All four clones downregulated SCA1 expression in NSC medium. Nestin expression was downregulated by 19_8A2A, unchanged in 7_10BA2C, and upregulated in 10_11BNA3A and 7_10BA1B. Map2 was upregulated by 10_11BNA3A, 7_10BA1B and 7_10BA2C. Expression of NF-l was unchanged in 19_8A2A, downregulated by 10_11BNA3A and upregulated by both 7_10BA1B and 7_10BA2C.

4.4.3 Maturation with neurotrophins

As the clone with the most neuronal-like appearance and mature marker expression profile, 7_10BA2C was used for further analysis to investigate the addition of an extra differentiation step to the protocol. Following 5 days culture in NSC medium, cells were exposed to a maturation medium containing the neurotrophic factors NT-3, NGF and BDNF. RNA was extracted from the cells on days 0, 5, 10 and 15 for qPCR to analyse changes in gene expression. Cells were fixed on day 15 and stained with antibodies against Map2 and NF-l.

In DPPC medium, prior to differentiation, the cells were typically fibroblastic-like in appearance (Figure 4.8 A). After 5 days culture in NSC medium, cell bodies appeared rounder and long processes could be seen branching from the cells (Figure 4.8 B). On day 10, 5 days after switching to the neurotrophin-containing medium, process extensions were longer and appeared to make intercellular connections (Figure 4.8 C). By day 15, the differentiating cells had formed a highly interconnected network of neuronal-like cells (Figure 4.8 D).

By day 5 of differentiation, mRNA expression of SCA1 was strongly downregulated (Figure 4.9). During the same time-period, expression of nestin and NF-l were seen to increase before plateauing. Expression of the intermediate neuronal marker Map2 continued to increase over the 15 day differentiation protocol indicating a more mature neuronal phenotype.

On day 15, presence of Map2 and NF-l proteins were identified in the differentiating DPPCs by immunocytochemical staining (Figure 4.10 A). Neural stem cells, similarly differentiated in neurotrophin-containing medium for 10 days, also stained positively for both markers and showed a comparable morphology, albeit smaller in size (Figure 4.10 B).

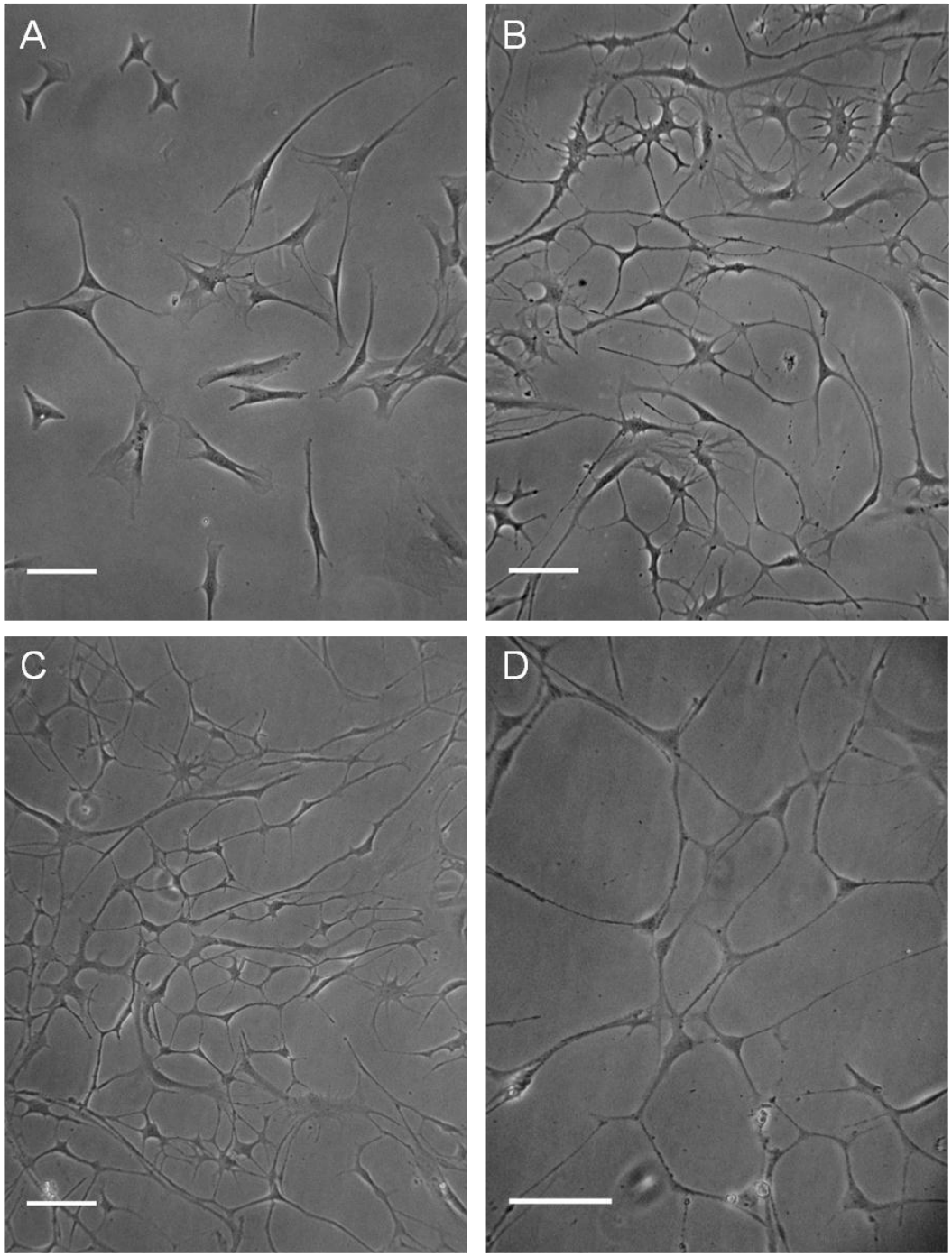

Figure 4.8 – Morphology changes during differentiation in NSC medium followed by neurotrophin-containing medium

7_10BA2C were cultured for 5 days in NSC medium before being transferred to a NGF, NT-3 and BDNF-containing medium for 10 further days. A) In DPPC medium, before differentiation, cells were typically bi/tripolar and fibroblastic-like. B) After 5 days in NSC medium, cell bodies appeared rounder and sprouting of multiple long processes was evident. C) 5 days after transfer to a neurotrophin-containing medium, long processes extended by neuronal-like cells appear to form network like connections. D) Intercellular connections are maintained after 10 days culture in neurotrophin-containing medium, on day 15 of differentiation. Scale bars = 100µm.

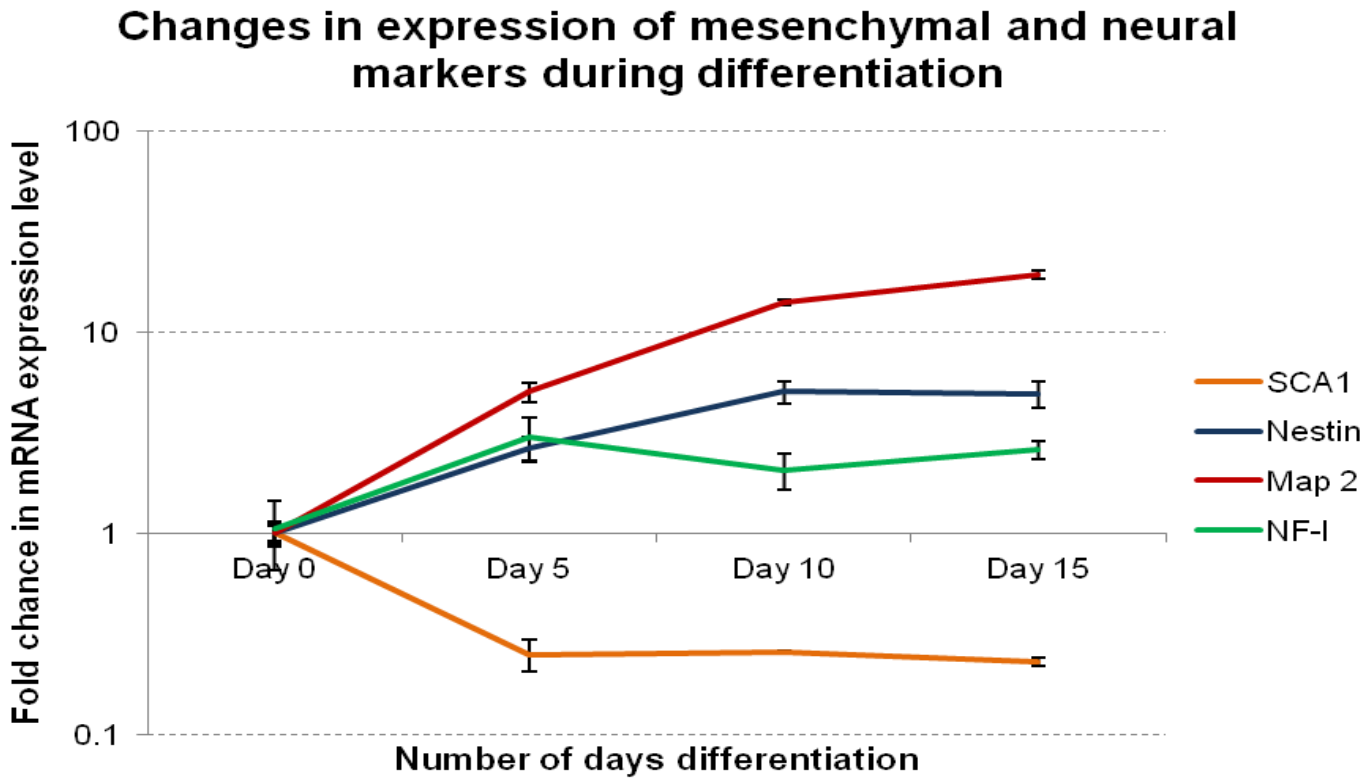

Figure 4.9 – Changes in expression of mesenchymal and neural markers during differentiation

RNA was extracted from 7_10BA2C on days 0, 5, 10 and 15 of differentiation and fold changes in mRNA expression (±SD) of the progenitor cell marker SCA1, the neural precursor marker nestin and the later stage neural markers Map2 and NF-l calculated using the $2^{-\Delta\Delta ct}$ method for qPCR analysis. SCA1 expression was strongly downregulated over the first 5 days of differentiation. Expression of nestin, Map2 and NF-l all increased over 15 days differentiation.

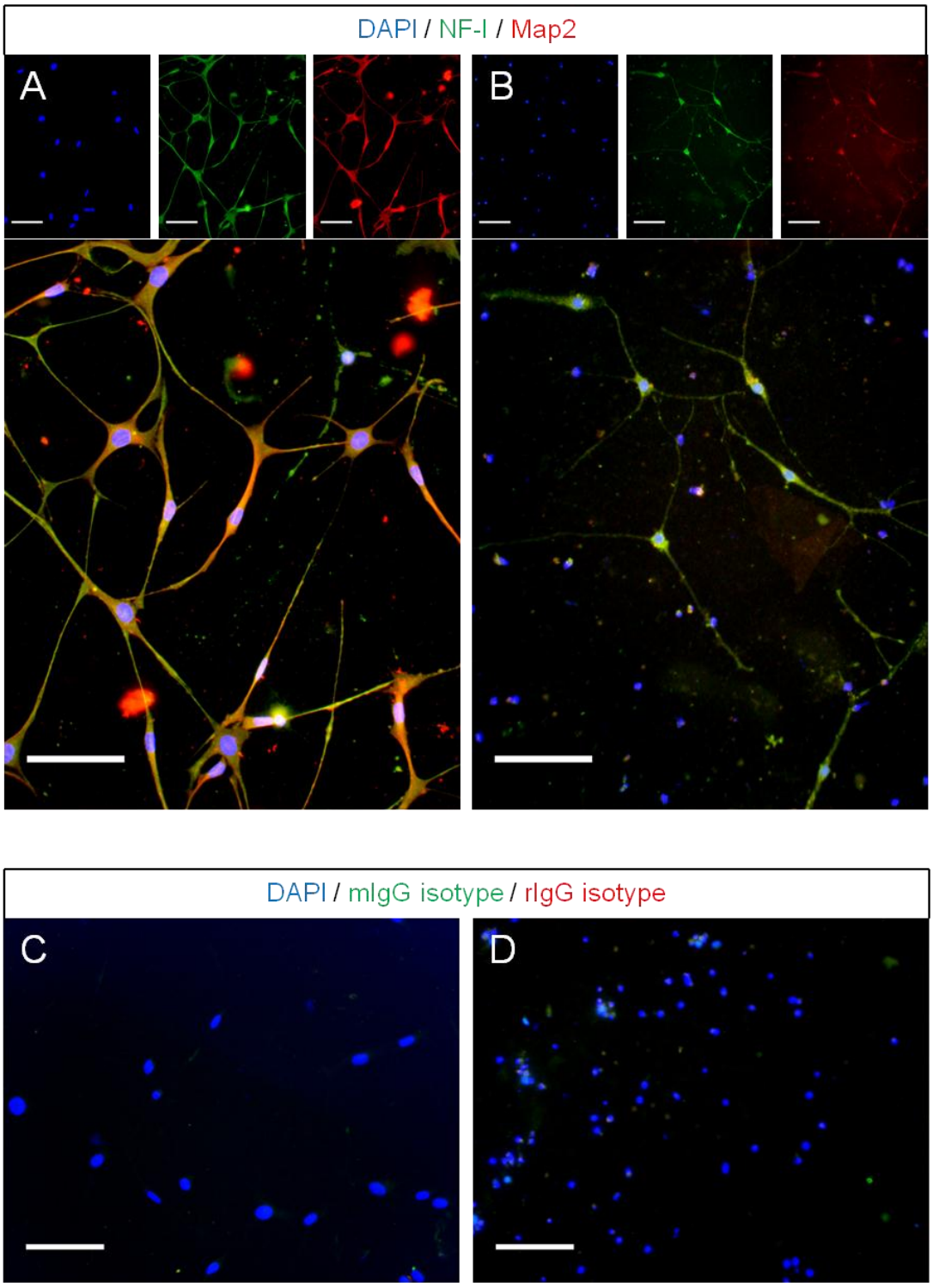

Figure 4.10 – DPPCs show similar morphology to NSCs differentiated in neurotrophin-containing medium

7_10BA2C after 15 days differentiation (A) and NSCs after 10 days culture in neurotrophin-containing medium (B) were fixed and double-stained with antibodies against Map2 (red) and NF-l (green). Cells of both types showed similar morphology and stained positive for both neuronal markers. Appropriate isotype controls are shown for DPPCs (C) and NSCs (D). Scale bars = 100µm.

4.4.4 Functional testing

Patch clamp recording techniques were used to assess the functionality of the neuronal-like cells differentiated from DPPCs using this protocol. Recordings were taken from 6 cells of the clonal population 7_10BA2C after 15 days differentiation. High resting membrane potentials ranging between -6 and -10mV were recorded for the differentiated DPPCs (Figure 4.11 A). Action potentials could not be evoked by 80 ms voltage steps from -120 to +80 mV in incremental steps of 10 mV from a holding potential of -70 mV (Figure 4.11 B). Outward K^+ currents but no inward Na^+ currents were identified in whole cell measurements (Figure 4.11 C and D).

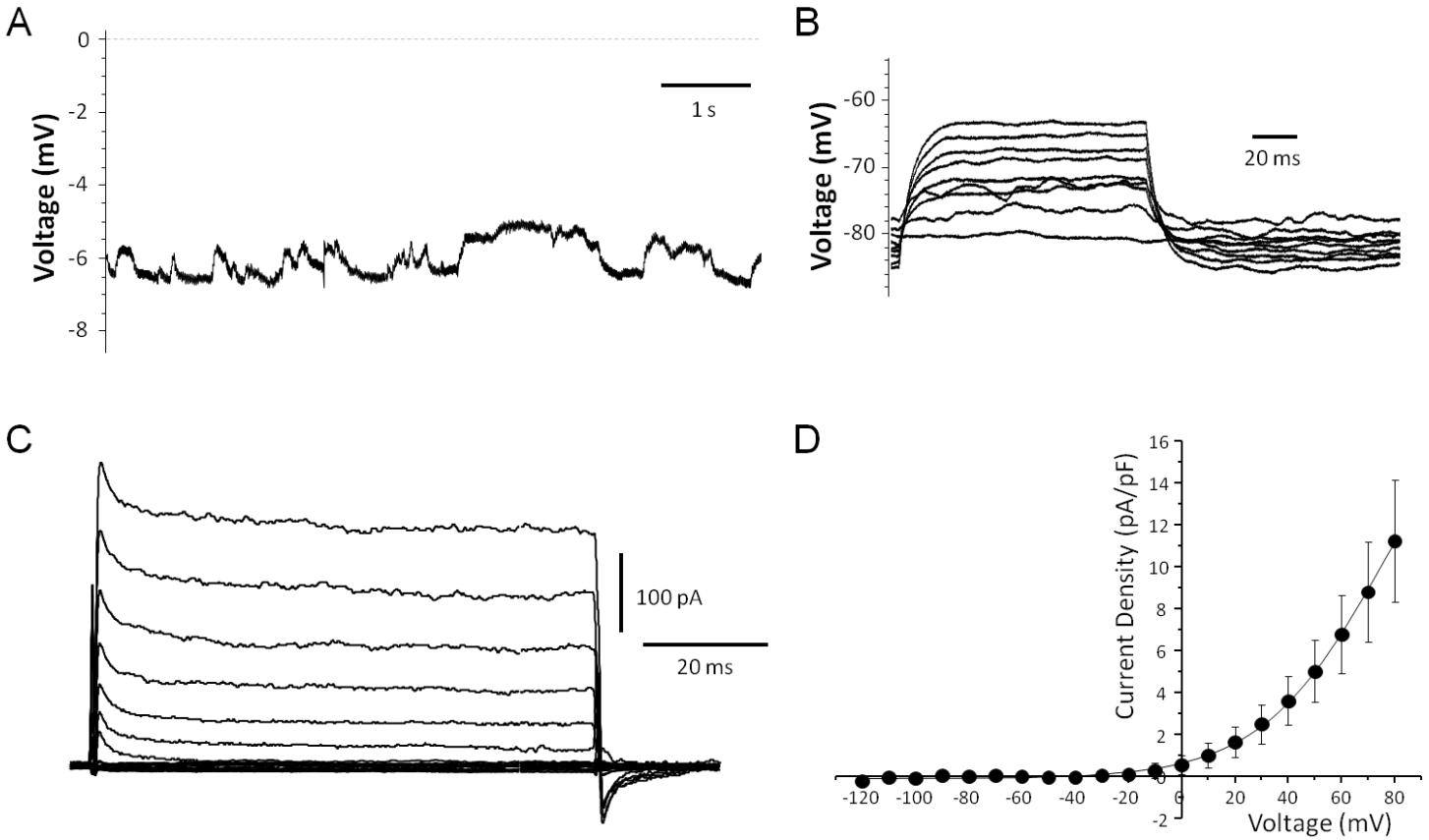

Figure 4.11 – Electrophysiology of differentiated DPPCs

Electrophysiological measurements were recorded using whole cell patch clamp techniques. Currents were generated by 80 ms voltage steps from -120 to +80 mV in incremental steps of 10 mV from a holding potential of -70 mV. A) Differentiated DPPCs showed high resting membrane potentials of ~-6mV. B) Action potentials could not be evoked in voltage clamp mode. C) Representative recording of whole cell currents shows outward K^+ but no inward Na^+ currents. D) Mean current density (pA.pF-1) plotted against command potential (mV). Bars show SEMs (n = 6).

4.4.5 Changes in expression of neural markers during differentiation

Following identification of the non-functional characteristics of differentiated 7_10BA2C, a more detailed analysis was performed on the changes in mRNA expression on days 0, 5, 10 and 15. Expression of SOX2 was continuously upregulated over 15 days differentiation while Pax6 remained unchanged (Figure 4.12 A). BLBP expression decreased over the first 5 days of differentiation, at which point expression of Ncam began to increase. Expression of the neurogenic marker Ngn2 remained constant over 15 days (Figure 4.12 B).

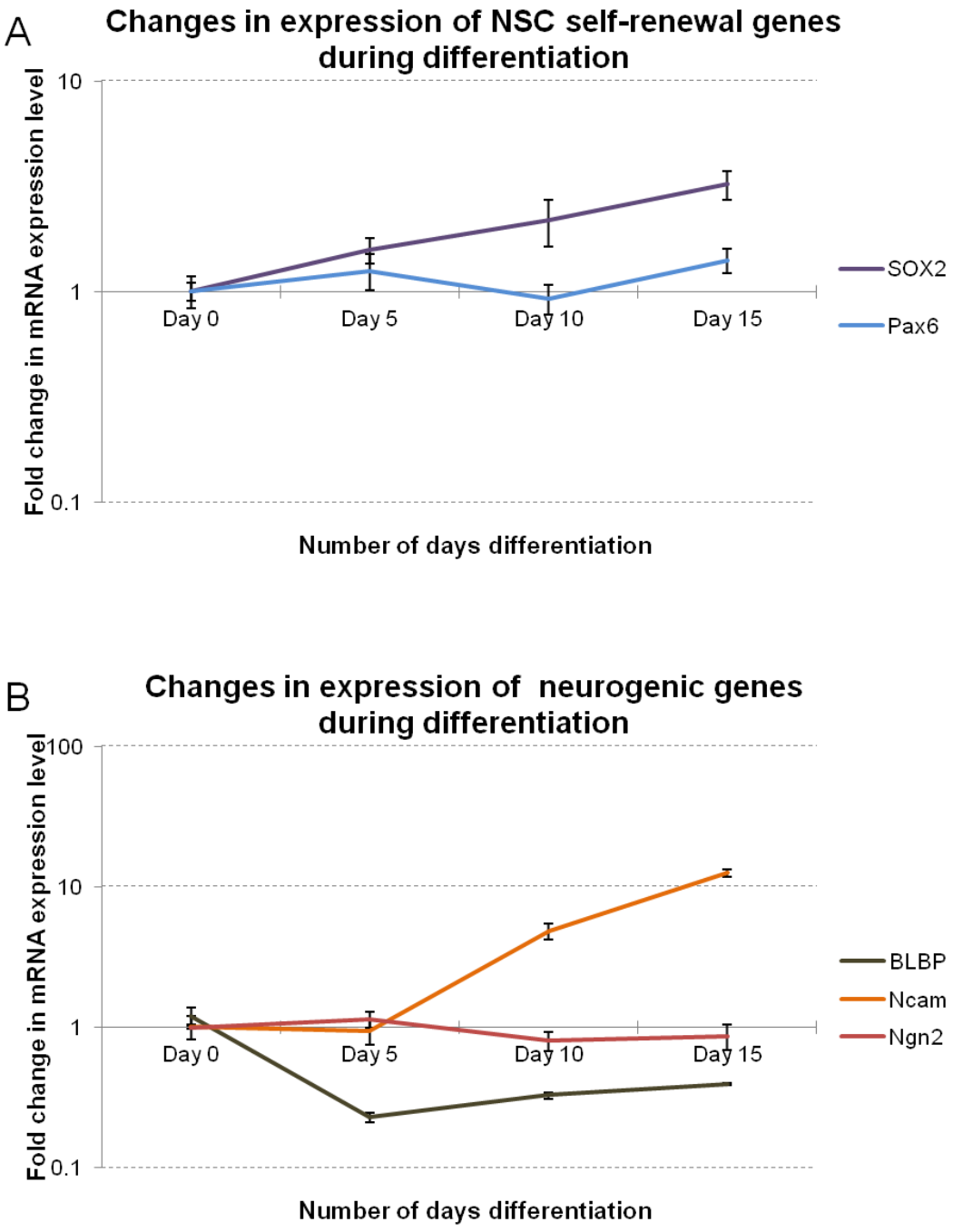

Figure 4.12 – Changes in expression of NSC renewal and neurogenic genes during differentiation

RNA extracted from 7_10BA2C cells on days 0, 5, 10 and 15 of the differentiation protocol was used for quantifying changes in expression of mRNA transcripts (±SD) for genes involved in NSC self-renewal (A) and neurogenesis (B) using the $2^{-\Delta\Delta ct}$ method for qPCR analysis. A) Expression of SOX2 increased over 15 days differentiation, whereas Pax6 remained unchanged. B) Ngn2 expression was unchanged over 15 days, BLBP decreased over the first 5 days of differentiation and Ncam expression increased from day 5 onwards.

4.4.6 Changes in neurotrophin and growth factor expression during differentiation

The changes in expression of neurotrophins and growth factors at days 0, 5 10 and 15 was also investigated using qPCR. At the end of 15 days differentiation, expression of NT-3, NGF and BDNF were unchanged although increased expression of both NT-3 and BDNF was identified on day 10. Expression of GDNF decreased over 15 days (Figure 4.13 A). bFGF expression was strongly upregulated by day 5 of differentiation and remained so until day 15. TGFβ-1 was unchanged over the first 5 days of differentiation before increasing over the next 10 days. A relatively smaller increase was observed in expression of VEGF-A. Expression of PDGF-a and IGF-1 was unchanged at the end of 15 days (Figure 4.13 B).

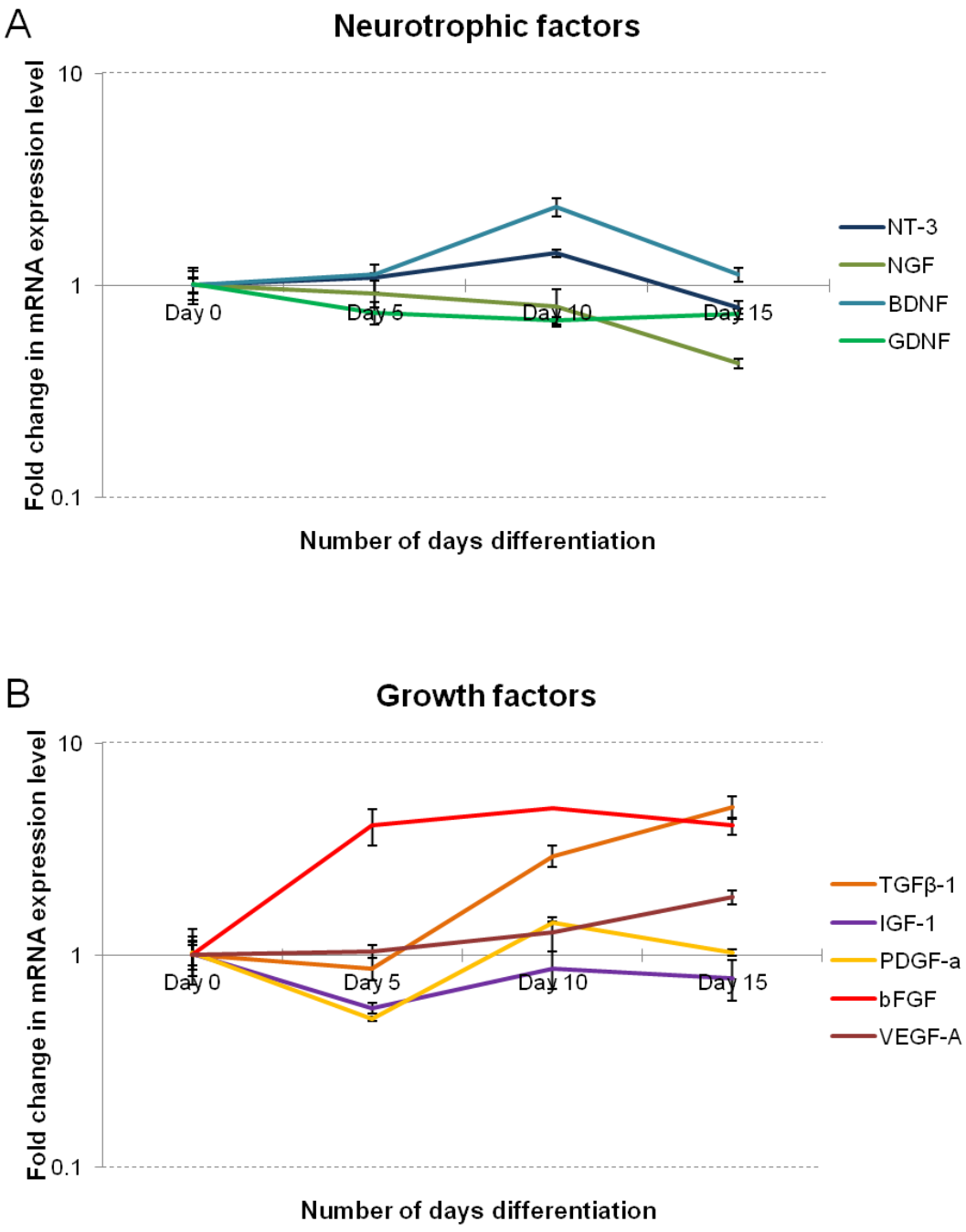

Figure 4.13 – Changes in expression of neurotrophic and growth factors during differentiation

RNA extracted from 7_10BA2C cells on days 0, 5, 10 and 15 of the differentiation protocol was used for quantifying changes in expression of mRNA transcripts (±SD) for neurotrophins (A) and growth factors (B) using the $2^{-\Delta\Delta ct}$ method for qPCR analysis. A) Expression of NT-3, BDNF and GDNF was much unchanged on day 15 although a small increase was seen between days 5 and 10, GDNF slowly decreased over 15 days. B) Expression of TGFβ-1, bFGF and VEGF-A increased during the differentiation protocol, PDGF-a and IGF-1 remained unchanged at the end of 15 days.

4.5 Discussion

Previous studies have identified expression of a handful of NSC markers, such as Musashi and SOX2, in cultured DPPCs (Govindasamy *et al*., 2010; Karaöz *et al*., 2011; Karbanová *et al*. 2011; Aanismaa *et al*., 2012). In fact, DPPCs often express mature neuronal markers, such as Map2, NF and βIII-tubulin, at a basal level (Karaöz *et al*., 2011; Osathanon *et al*., 2011; Sakai *et al*., 2012). This chapter provides a comprehensive characterisation of the expression of further neural lineage markers, demonstrating a degree of heterogeneity between different cell cultures and clones. Prior to differentiation, DPPCs were found to express both developmental and later stage neural markers, with a profile similar to NSCs (Figures 4.2 – 4.5).

The transcription factors SOX1 and SOX2 are important for maintenance of NSC identity and self-renewal properties (Bylund *et al*., 2003; Graham *et al.,* 2003; Kan *et al*., 2004). Expression of SOX2 was identified in all mDPPC cultures tested, but not the closely-related SOX1 (Figure 4.2). There is a degree of functional overlap between the two transcription factors and deficiencies in one can often be compensated for by the other (Graham *et al*., 2003). Thus, the absence of SOX1 in DPPCs does not necessarily imply a less NSC-like phenotype.

During development, Pax6 expression gradients are essential for the regional specification of ventral progenitor cells of the spinal cord and hindbrain (Ericson *et al*., 1997; Takahashi and Osumi, 2002). Pax6 expression is important in regulating the self-renewal and differentiation of

NSCs with transcriptional targets including cell cycle regulators and initiators of neurogenesis (Sansom *et al*., 2009). Pax6 expression in DPPCs was found to be heterogeneous, ranging from complete absence to high levels in different cell cultures (Figure 4.2). With regards to NSCs, increased Pax6 expression drives neuronal differentiation and inhibits self-renewal, whereas reduced Pax6 levels also result in reduced self-renewal (Sansom *et al*., 2009). It is possible that, in this manner, the precise level of Pax6 expression may be a factor determining the neuronal differentiation potential of each individual DPPC culture. Cells with mid to high levels of Pax6 may represent those with a greater propensity for neuronal differentiation. Only four DPPC cultures were found to express the transcription factor Myt1l which is associated with developing neurons of the CNS (Kim *et al*., 1997).

All DPPC cultures showed positive expression of the neural crest-associated marker P75 (Figure 4.2). The dental pulp arises from the neural crest during tooth development (Chai *et al*., 2000) and this observation confirms the cells used in this study are of neural crest origin, similar to those previously described (Waddington *et al*., 2009; Janebodin *et al*., 2011).

BLBP, a marker for radial glial NSCs and a transcriptional target of Notch1 and Notch3 signalling (Anthony *et al*., 2005), was found to be expressed by all DPPCs. Another radial glia marker, GLAST, was found to be more variable in expression (Figure 4.3). The expression of both BLBP and GLAST, together with the absence of CD133, suggests that DPPCs may be closer in characteristics to radial glial NSCs than neuroepithelial NSCs. Given that radial glia are the source of the majority of neurons in the brain

(Anthony *et al*., 2004; Merkle *et al*., 2004), this provides strong indication of a neuronal potential for DPPCs.

Expression of mRNA transcripts for Musashi were identified in all mDPPC cultures and protein was present, together with nestin, in four different single cell-derived DPPC clones (Figures 4.3 – 4.5). Musashi helps to maintain NSC self-renewal properties by binding *m-Numb* RNA to suppress its translation and subsequent inhibition of Notch1 signalling (Imai *et al*., 2001). Notch1 signalling is one of the key pathways involved in NSC self-renewal (Hitoshi *et al*., 2002) and has similarly been implicated in maintaining dental pulp cell progenitor properties (Zhang *et al*., 2008; He *et al*., 2009; Wang *et al*., 2011). Notch1 signalling is induced in the sub-odontoblast layer and perivascular regions of the pulp following capping of rat adult molars, both of which are believed to harbour niches of DPPCs (Lovschall *et al*., 2005). *In vitro,* over-expression of constitutively activated Notch1 intracellular domain or jagged1 ligand inhibits DPPC odontoblastic differentiation, but does not affect proliferation (Zhang *et al*., 2008). Similarly, inhibition of notch signalling by RNA interference of delta-1 ligand promotes differentiation and inhibits the proliferation of DPPCs (Wang *et al*., 2011). Embryonic knockout of Notch1 results in depletion of NSCs, and their *in vitro* differentiation is enhanced following attenuation of notch signalling (Hitoshi *et al*., 2002). The importance of this signalling pathway in maintaining progenitor/stem cell identity of both NSCs and DPPCs suggests that Musashi may perform a similar function in DPPCs by binding RNA transcripts to prevent the translation of Notch inhibitory factors. Immunocytochemical staining of Musashi in DPPCs

indicated a primarily cytoplasmic localisation (Figures 4.4 and 4.5), allowing it to function in mRNA binding. In differentiating NSCs, unbound Musashi tends to translocate to the nucleus (MacNicol *et al*., 2008; Nickerson *et al*., 2011). This cytoplasmic localisation in DPPCs is consistent with early stage proliferating neural cells.

Based upon this initial characterisation data, it is clear that DPPCs share a number of characteristics with NSCs. As such, a differentiation protocol was developed based on procedures used in NSC culture. Four DPPC clones demonstrating low or high levels of nestin mRNA expression were grown in NSC culture medium on poly-l-lysine/laminin coated plates for 7 days. After 7 days differentiation, no significant alterations were observed in the morphology of the weaker nestin mRNA-expressing clones, although 10_11BNA3A showed signs of stress (Figure 4.6 B and D). Stronger nestin-expressing clones, on the other hand, adopted a more neuronal-like phenotype extending a number of long processes (Figure 4.6 F and H). This suggests that nestin expression may be indicative of neuronal differentiation potential using this protocol. In previously published neuronal differentiation studies, NSC culture media, similar to that utilised in this study, has been used to promote the generation of neurosphere-like structures from DPPCs on low attachment culture plates (Iohara *et al*., 2006; Takeyasu *et al*., 2006; Sasaki *et al*., 2008; Govindasamy *et al*., 2010; Osathanon *et al*., 2011). The formation of such spheres is associated with the expression of astrocytic markers, such as S100 (Sasaki *et al*., 2008), and upregulation of GFAP mRNA (Govindasamy *et al*., 2010). This approach, therefore, may not

represent the most effective method for deriving purified populations of neuronal-like cells from DPPCs. In order to minimise the adoption of astrocytic-like phenotypes occurring as a result of neurosphere formation, DPPCs differentiated using the protocol developed in this chapter were encouraged to adhere to poly-lysine/laminin-coated culture surfaces.

qPCR analysis identified clonal differences in gene expression response to NSC medium (Figure 4.7). The general stem cell marker SCA1 was downregulated by all 4 clones, suggesting the neural inductive medium initiated a move away from the default mesenchymal progenitor phenotype. Those clones with stronger levels of nestin mRNA expression, 7_10BA1B and 7_10BA2C, adopted a more neuronal-like phenotype evidenced by the upregulation of neuronal markers Map2 and NF-l (Figure 4.7). On the other hand, in clones with initially lower levels of nestin mRNA expression, 19_8A2A and 10_11BNA3A, expression of these markers was unchanged or downregulated, with only a small increase of Map2 observed in 19_8A2A. Together, these results suggest that mRNA expression levels of nestin may be an important factor in determining the potential of DPPCs for neuronal differentiation. Although the precise function of nestin is as yet unidentified, it is required for NSC self-renewal and survival. Knockdown of nestin in NSCs does not overtly affect their proliferation or differentiation, but does result in increased apoptosis (Park *et al*., 2010b). In contrast, the results presented in this chapter suggest a role for nestin in the differentiation of DPPCs. The formation of neurospheres from DPPCs using similar NSC media has been similarly associated with the upregulation of mRNA transcripts for NF (Iohara

et al., 2006; Govindasamy *et al*., 2010). In these reports, heterogeneous DPPC populations isolated with no selection step were used to generate neurospheres and, thus, it is likely that only a small proportion of cells were responding positively to the NSC medium. This report demonstrates changes in gene expression at a clonal level and suggests a possible means of identifying those cells with a greater potential for neuronal differentiation, based upon mRNA expression levels of nestin. This is a significant finding and may help explain why in previous studies only small numbers of DPPCs within mixed populations were found to adopt mature neuronal phenotypes (Király *et al*., 2009), and why different patient samples do not differentiate equally in the same inductive conditions (Aanismaa *et al*., 2012).

The downregulation of mesenchymal markers and upregulation of neural markers, particularly by the stronger nestin-expressing clones 7_10BA1B and 7_10BA2C (Figure 4.7), suggests a “neuralisation” effect of NSC medium on mDPPCs. As these neuralised DPPCs appear to be more NSC-like in marker expression, a further step was added to the differentiation protocol. 7_10BA2C was neuralised in NSC medium for 5 days, washed with PBS and then changed to a neurotrophin-containing medium for 10+ further days of maturation (Figure 4.1). Exposure of NSCs to BDNF, NGF or NT-3 can promote their neuronal differentiation (Benoit *et al*., 2001; Ito *et al*., 2003; Chen *et al*., 2013). After switching from NSC medium to neurotrophin medium, 7_10BA2C cells became more neuronal-like in appearance with rounded cell bodies and projected multiple long range processes that extended towards other cells to form network-like connections (Figure 4.8).

This morphology was mirrored by NSCs seeded on poly-lysine/laminin-coated dishes and differentiated in the same neurotrophin-containing medium for 10 days (Figure 4.10).

Changes in the expression of SCA1, nestin, Map2 and NF-l were again analysed using quantitative PCR (Figure 4.9). Over the first five days of neuralisation, as seen before (Figure 4.7), levels of SCA1 reduced while the neural markers increased. Map2 continued to increase over the next 10 days differentiation. Expression of nestin and NF-l, increased over the first 5 days of maturation before plateuaing. At the end of 10 days maturation, fixed cells stained positively for Map2 and NF-l demonstrating their presence in both 7_10BA2C and NSCs (Figure 4.10). The presence of both late neuronal markers, at the protein level, confirmed that differentiating DPPCs were of a neuronal-like phenotype, similar to NSCs grown in the same medium. As such, approaches used to encourage the neuronal differentiation of NSCs may represent a simple method of promoting comparable DPPC neuronal-like differentiation. This provides further evidence of the similarities between DPPCs and NSCs.

In order to test the functionality of DPPC-derived neuronal-like cells, patch clamp techniques were used to provide electrophysiology readings for 7_10BA2C cells after 5 days neuralisation followed by 10-15 days maturation. Previous studies have shown the passive membrane potential of NSCs typically ranges from -40 to -85mV, depending upon tissue of origin and developmental stage at the time of isolation, and is around -70mV in terminally differentiated neurons (Gritti *et al*., 1996; Yasuda and Adams,

2010). Neuronally differentiated DPPCs possessed highly depolarised membrane potentials ranging between -6 and -10mV (Figure 4.11 A). Such high resting potentials are typically associated with unexcitable cell types. No action potentials could be evoked using a voltage step protocol from a holding potential set to -70 mV (Figure 4.11 B). The influx of Na^+ ions through voltage-gated channels is a key event in triggering action potentials. Outward voltage-activated K^+ currents but not inward currents propagated through voltage-activated Na^+ channels were identified in differentiated DPPCs (Figure 4.11 C and D). Previous studies using different approaches for the neuronal differentiation of DPPCs have recorded both Na^+ and K^+ currents, however, this is still insufficient for the generation of true action potentials (Arthur *et al*., 2008; Király *et al*., 2009; Aanismaa *et al*., 2012). Despite the presence of mature markers and appropriate morphology, the neuronal-like cells obtained using the protocol developed in this chapter are electrophysiologically unexcitable and, thus, unable to function like true neurons. This finding is similar to a previous report of skin-derived progenitor cells (Collo *et al*., 2006). Following neuronal differentiation, these cells adopted a neuronal-like morphology, comparable with that observed in DPPCs, and expressed both βIII-tubulin and Map2. As with DPPCs, voltage-activated K^+, but not Na^+ currents were recorded to indicate a functionally immature neuronal phenotype.

In order to ascertain why DPPC-derived neuronal-like cells were not functional, a more detailed qPCR analysis of the changes in gene expression during differentiation was performed. Throughout 15 days of differentiation,

expression of SOX2 was seen to steadily increase (Figure 4.12 A). SOX2 actively inhibits NSC differentiation, helping to maintain pluripotency (Graham *et al*., 2003). It is only as SOX2 expression is downregulated during differentiation, that key transcription factors initiating the onset of neuronal functional properties, such as neurogenin-2 (Ngn2) and Mash1, become expressed (Bylund *et al*., 2003). Ngn2 was expressed at a low basal level by 7_10BA2C, prior to differentiation, but its expression did not change during 15 days differentiation (Figure 4.12 B). No expression of Mash1 was identified at any stage of differentiation. The induction of such proneural factors is unlikely while SOX2 remains expressed at high levels. Expression of Pax6 was largely unaltered during differentiation (Figure 4.12 A). Increased levels of Pax6 in NSCs are associated with neurogenesis (Sansom *et al*., 2009) and, as such, this provides further evidence that the onset of functional properties in DPPCs is unlikely at this stage of the protocol. Expression of neural cell adhesion molecule (Ncam) was found to increase sharply from day 5 of differentiation onwards, correlating with the transfer to neurotrophin-containing medium (Figure 4.12 B). Ncam is associated with neurite outgrowth and cell-cell interactions (Kolkova *et al*., 2000; Kleene *et al*., 2010) and from day 5 of differentiation onwards, the extension of neuronal-like processes from DPPCs becomes more pronounced and synapse-like connections appear between cells (Figure 4.8). These process extensions are likely promoted by the addition of NGF, NT3 and BDNF to the maturation medium which are known to induce expression of Ncam via binding to P75 (already expressed by DPPCs (Figure 4.2)) (Mirnics *et al*., 2005; Thornton *et al*., 2008). Despite the presence of more

mature neural markers, such as Ncam, Map2 and NF-l (Figure 4.10), the high levels of SOX2 expression and lack of proneural gene induction, in addition to electrophysiological readings, confirmed that the neuronal-like DPPCs were still of an immature phenotype. The protocol developed in this chapter, although simple and based upon the shared properties of NSCs and DPPCs, is insufficient to promote terminal functional differentiation of DPPCs and further steps will be required.

More often thought of as a target for neurotrophic and growth factors to promote their proliferation and differentiation (Benoit *et al*., 2001; Chen *et al*., 2013; Supeno *et al*., 2013), only limited information is available regarding the production and release of such factors by NSCs as they differentiate. In culture, NSCs express mRNA transcripts for a wide range of neurotrophic and growth factors, including NGF, NT-3, BDNF, GDNF, bFGF, PDGF-a, IGF-1, TGFβ-1 and VEGF-a (Hawryluk *et al*., 2012b). In the rat spinal cord, secretion of NGF, BDNF and GDNF by transplanted NSCs is associated with increased host axonal regrowth and myelination (Lu *et al*., 2003; Yan *et al*., 2004). As NSCs differentiate in the presence of serum *in vitro,* transcripts for all the neurotrophic and growth factors investigated in this study, with the exception of PDGF-a and VEGF-A, are upregulated (Hawryluk *et al*., 2012b). Using the 15 day protocol developed in this chapter, only TGFβ-1, bFGF and VEGF-A increased in expression as DPPCs differentiated into neuronal-like cells (Figure 4.13). TGFβ-1 began to increase from day 5 onwards, at which point exogenous neurotrophic factors were added to the medium. Increased expression of VEGF-A, bFGF and TGFβ-1 by neuronally differentiated

DPPCs could potentially promote recovery from SCI by helping to maintain blood vessel architecture (Widenfalk *et al*., 2003) and protect against death of endogenous neuronal cells (Ho *et al*., 2000; Zhang *et al*., 2013).

Based on the results presented in this chapter, the production of neurotrophic and growth factors should be taken into account when considering DPPCs as a source of cells to directly replace endogenous neurons following SCI. Although neuronal differentiation is observed following NSC transplantation into *in vivo* models of SCI, increased expression of neurotrophic factors by grafted cells provides a secondary mechanism, through which recovery is promoted, by recruiting endogenous oligodendrocyte cells (Amemori *et al*., 2013). In fact, the regenerative effects of NSC transplantation can be enhanced using NSCs genetically engineered to overexpress NT-3 (Lu *et al*., 2003). At this current point in time, recovery following DPPC transplantation into *in vivo* SCI models is attributed to similar secondary neurotrophic mechanisms (de Almeida *et al*., 2011; Sakai *et al*., 2012). This chapter has demonstrated that the expression of neurotrophic and growth factor mRNA transcripts changes during DPPC neuronal-like differentiation, potentially altering the mechanisms through which they can promote secondary regeneration. A similar neurotrophic and growth factor expression profile of DPPCs, following definitive differentiation into functional neuronal-like cells, would help to identify what further roles, in addition to direct cellular replacement, they can play in promoting spinal cord repair.

4.6 Summary

- Undifferentiated DPPCs were found to express a range of developmental and mature neural markers demonstrating shared characteristics with NSCs.

- Following culture in NSC medium, DPPCs become “neuralised”, as demonstrated by a more neuronal-like morphology, decreased expression of mesenchymal markers and increased expression of neuronal markers. The level of nestin expression, prior to differentiation, may be indicative of DPPCs ability to neuralise in NSC medium.

- The addition of a further maturation stage, in the presence of neurotrophins, results in further increases of neural marker expression and morphology analagous to NSCs differentiated in the same medium.

- DPPCs differentiated using this method show no indications of electrical functionality and are still of an immature neuronal-like phenotype. The differentiation protocol will require further development to promote functional maturation.

- The expression of neurotrophic and growth factors by DPPCs is altered by differentiation into neuronal-like cells and this will prove important in considering the use of DPPCs to treat SCI.

Chapter 5: Development of a protocol for the differentiation of oligodendrocyte-like cells from dental pulp progenitor cells

5.1 Introduction

If cell replacement therapies are to result in complete functional recovery following SCI then, in addition to the replacement of neuronal cells, new sources of glial cells are also required. Oligodendrocytes are among the cell types most severely depleted following SCI, resulting in the chronic demyelination of axons to impair neuronal signalling (Li *et al*., 1999; Grossman *et al*., 2001; Totoiu and Keirstead, 2005). Replacement of oligodendrocytes with myelinating cells from alternative sources can help to improve recovery by restoring myelination and, thereby, facilitating axonal conduction.

Transplantation of exogenous myelinating glial cells has proven successful in experimental models of SCI. Grafting of OPCs differentiated from human embryonic stem cells results in increased remyelination of endogenous axonal fibres accompanied with improved recovery of hindlimb function (Keirstead *et al*., 2005; Nistor *et al*., 2005). Alternatively, myelinating cells from other sources have demonstrated similar recovery and remyelination effects. Transplantation of PNS Schwann cells, either alone or in combination with olfactory ensheathing cells, a similar glial cell type found specifically in the olfactory bulb, has demonstrated efficacy at promoting functional recovery following SCI (Takami *et al*., 2002). The ability of olfactory ensheathing cells to promote this type of recovery remains controversial due to a number of contradicting studies (Ramón-Cueto *et al*., 2000; Takami *et al*., 2002; Pearse *et al*., 2007). Schwann cells differentiated from BMSCs promote the sparing of spinal cord tissue and are associated

with improved functional recovery following SCI (Someya *et al*., 2008; Kamada *et al*., 2011). If DPPCs can similarly demonstrate the ability to differentiate into myelinating glial cells, their ease of isolation would endow them with a distinct advantage over other cell types for SCI transplantation.

Cells of oligodendrocytic lineage are typically identified by the expression of the transcription factors Olig1 and Olig2 (Zhou *et al*., 2000). During development and differentiation from OPCs, the expression of oligodendrocyte markers follows a well-defined progression. At the earliest stages oligodendrocyte precursors can be identified by expression of the alpha subunit of platelet-derived growth factor receptor (PDGFR-α) (Pringle *et al*., 1992) and the neural crest glial-specific transcription factor SOX10 (Kuhlbrodt *et al*., 1998). The cell surface ganglioside A2B5 is found on early/mid stage proliferative oligodendrocytes (Gard and Pfeiffer, 1990). As they continue to mature, expression of 2',3'-cyclic-nucleotide 3'-phosphodiesterase (CNPase) develops (Yu *et al*., 1994). Expression of myelin-associated proteins, such as myelin basic protein (MBP), myelin/oligodendrocyte specific protein (MOSP) and galactocerebroside (GalC), indicates a terminal, functional myelinating phenotype (Dyer and Matthieu, 1994).

Heterogeneous populations of dental pulp progenitor cells have been reported to express, at a basal level, various proteins associated with early stage glial cell types including A2B5, CNPase and GFAP (Gronthos *et al*., 2002; Sakai *et al*., 2012) indicating potential for differentiation. As yet, however, no protocols have been developed for the specific differentiation of

glial cells from DPPCs. Expression of astrocytic markers, such as GFAP and S100 (Takeyasu *et al*., 2006; Sasaki *et al*., 2008; Janebodin *et al*., 2011; Karaöz *et al*., 2011), are often induced or found to increase during some neuronal differentiation protocols *in vitro*. Similarly, the unexpected differentiation of small numbers of GalC-positive, but Olig2-negative, oligodendrocyte-like cells has been reported as a side-product of a neuronal differentiation protocol (Aanismaa *et al*., 2012). The absence of Olig2 raises questions of whether these cells truly were of oligodendrocyte lineage. *In vivo,* the spontaneous differentiation of MBP-positive mature oligodendrocytes has been reported following transplantation of SHEDS into the injured rat spinal cord (Sakai *et al*., 2012) and GFAP/S100b-positive astrocytes derived from DPPCs transplanted into a mouse model of SCI (De Almeida *et al*., 2011). The development of a protocol for the specific differentiation of glial cells *in vitro* would provide a valuable model for investigating the roles that DPPCs have already demonstrated in promoting regeneration and repair in *in vivo* SCI studies. Furthermore, the DPPC-derived oligodendrocytes, themselves, could provide a more suitable source of transplantable cells of a restricted lineage.

5.2 Objectives

- To identify the expression of a range of glial-associated markers by murine dental pulp progenitor cells

- To develop a protocol demonstrating the ability of DPPCs to differentiate into oligodendrocyte-like cells *in vitro* and confirm phenotype using appropriate methods.

- To investigate how oligodendrocyte differentiation may affect the ability of DPPCs to promote neural repair via trophic mechanisms

5.3 Materials and methods

5.3.1 Characterisation of glial marker expression

RNA extracted from low-passage DPPC cultures at between 15-25 population doublings was used with rt-PCR (sections 2.2.2.1, 2.2.2.3 – 2.2.2.5) to identify expression of range of glial markers by undifferentiated DPPCs, including those for early-mid stage oligodendrocytes (PDGFR-α and CNPase) and astrocytes/Schwann cells (GFAP and S100b). RNA extracted from murine corpus callosum tissue (section 2.2.2.2), a brain region enriched with glial cells, was used as a positive control. Primer sequences and targets are shown in Table 5.2

Four single cell-derived clones (19_8A2A, 10_11BNA3A, 7_10BA1B and 7_10BA2C (20-25 PDs)) were further fixed with 4% PFA and immunocytochemically stained (section 2.2.2.7) with antibodies against A2B5 and SOX10, together with appropriate isotype controls (Tables 2.2 – 2.4).

5.3.2 Oligodendrocyte progenitor cell medium

OPC medium was composed as outlined below in Table 5.1.

Table 5.1 – OPC medium

Component	Comments	Supplier
DMEM	L-glutamine 40mM Glucose	Sigma-Aldrich, UK
1 x SATO supplement	16µg/ml putrescine 62ng/ml progesterone 5ng/ml sodium selenite 100µg/ml BSA	all Sigma-Aldrich, UK
Holo-transferrin	50µg/ml	Sigma-Aldrich, UK
Insulin	5µg/ml	Sigma-Aldrich, UK
PDGFaa	10ng/ml	Peprotech, UK
bFGF	20ng/ml	Peprotech, UK
Penicillin/Streptomycin	1% (v/v)	Life Technologies, UK

5.3.3 DPPC differentiation in OPC medium

8-well chamber slides (BD Biosciences, USA) were coated with 0.01% poly-l-lysine (Sigma-Aldrich, UK) for 5 minutes at room temperature. This was removed and the surfaces allowed to completely air dry for a minimum of one hour before rinsing with PBS. During culture (sections 2.2.1.1 and 2.2.1.2), four DPPC clones (19_8A2A, 10_11BNA3A, 7_10BA1B and 7_10BA2C (20-30 PDs)) were seeded at 10,000cells/cm^2 in OPC medium. Cells seeded in DPPC medium were used as an undifferentiated control. Medium changes were performed every other day and phase contrast images acquired to record changes in cellular morphology. After 7 days differentiation, the

chamber slides were fixed with 4% (w/v) PFA and immunocytyochemically stained (section 2.2.2.8) with primary antibodies against the oligodendrocyte-associated markers Olig2, MBP and MOSP together with appropriate isotype controls (Tables 2.2 – 2.4).

To keep consistent with the neuronal differentiation studies (see Chapter 4), 7_10BA2C was selected for further analysis and a direct comparison made between glass and plastic surfaces for differentiation. Plastic tissue culture dishes and 8-chamber glass slides were coated with poly-l-lysine, as described above, and seeded with 7_10BA2C cells in OPC medium at 10,000 cells/cm^2. RNA was extracted (section 2.2.2.1) on days 0 (as an undifferentiated control), 5 and 10. qPCR measurements(section 2.2.2.5) were used to calculate the fold change in expression of oligodendrocyte-associated CNPase and astrocyte/Schwann cell-associated S100b (for primers see Table 5.3), in addition to neurotrophins and growth factors (for primers see Table 2.1). Additionally, cells were fixed on differentiation days 0 and 10 and immunostained with antibodies (Tables 2.2 – 2.4) against the oligodendrocyte markers Olig1 or Olig2, together with β-actin to demonstrate morphology, prior to, and after, 10 days of differentiation. Antibodies against GFAP and S100b were also used to investigate the expression of astrocytic and Schwann cell markers. Matching isotype control antibody (Table 2.3) stains were performed in parallel.

5.3.4 Tables of primers

Table 5.2 – rt-PCR primer sequences

Product	Accession no.	Primer Sequences (5' → 3)	Product Size (bp)	Tm (°C)
CNPase	NM_001146318.1	f: TTTACCCGCAAAAGCCACACA r: CACCGTGTCCTCATCTTGAAG	117	60
GAPDH	NM_008084.2	f: AGACGGCCGCATCTTCTTGTGCAGTGC r: ACATACTCAGCACCGGCCTCACCCCAT	326	60
GFAP	NM_001131020.1	f: CAACTTTGCACAGGACCTCGGCACCCT r: GGCGGCGATAGTCGTTAGCTTCGTGCT	437	60
PDGFR-α	NM_011058.2	f: GGCCGCAGTGTTGGTGCTGTTGGTGAT r: TGGTGCAGGCTCCCAGCAAGTTCACAAT	413	60
S100b	NM_009115.3	f: TGGTTGCCCTCATTGATGTCT r: CCCATCCCCATCTTCGTCC	179	60

Table 5.3 – qPCR primer sequences

Product	Accession no.	Primer Sequences (5' → 3)	Product Size (bp)	Tm (°C)
CNPase	NM_001146318.1	f: TTTACCCGCAAAAGCCACACA r: CACCGTGTCCTCATCTTGAAG	117	60
GAPDH	NM_008084.2	f: AGGTCGGTGTGAACGGATTTG r: TGTAGACCATGTAGTTGAGGTCA	123	60
S100b	NM_009115.3	f: TGGTTGCCCTCATTGATGTCT r: CCCATCCCCATCTTCGTCC	179	60

5.4 Results

5.4.1 Expression of glial cell markers by DPPCs

Prior to differentiation, RNA was extracted from each isolated DPPC clone and mixed population at the earliest possible population doubling level and used to screen for mRNA expression of a selection of glial cell markers (Figure 5.1). All isolated DPPC cultures were found to express markers associated with oligodendrocytes at progenitor (PDGFR-α) and later (CNPase) stages. Similarly, the astrocytic marker GFAP was also expressed by all cultures. S100b, associated with both astrocytes and Schwann cells, was found to be expressed in all cultures with the exception of one non-adherent mixed population: 19_8NA1-3.

Clones with low (19_8A2A and 10_11BNA3A) and high (7_10BA1B and 7_10BA2C) levels of nestin expression were further immunostained with antibodies against the OPC cell surface marker A2B5 and SOX10, a glial-associated transcription factor (Figures 5.2 and 5.3). All four clones were found to stain positive for both early stage oligodendrocyte markers A2B5 and SOX10.

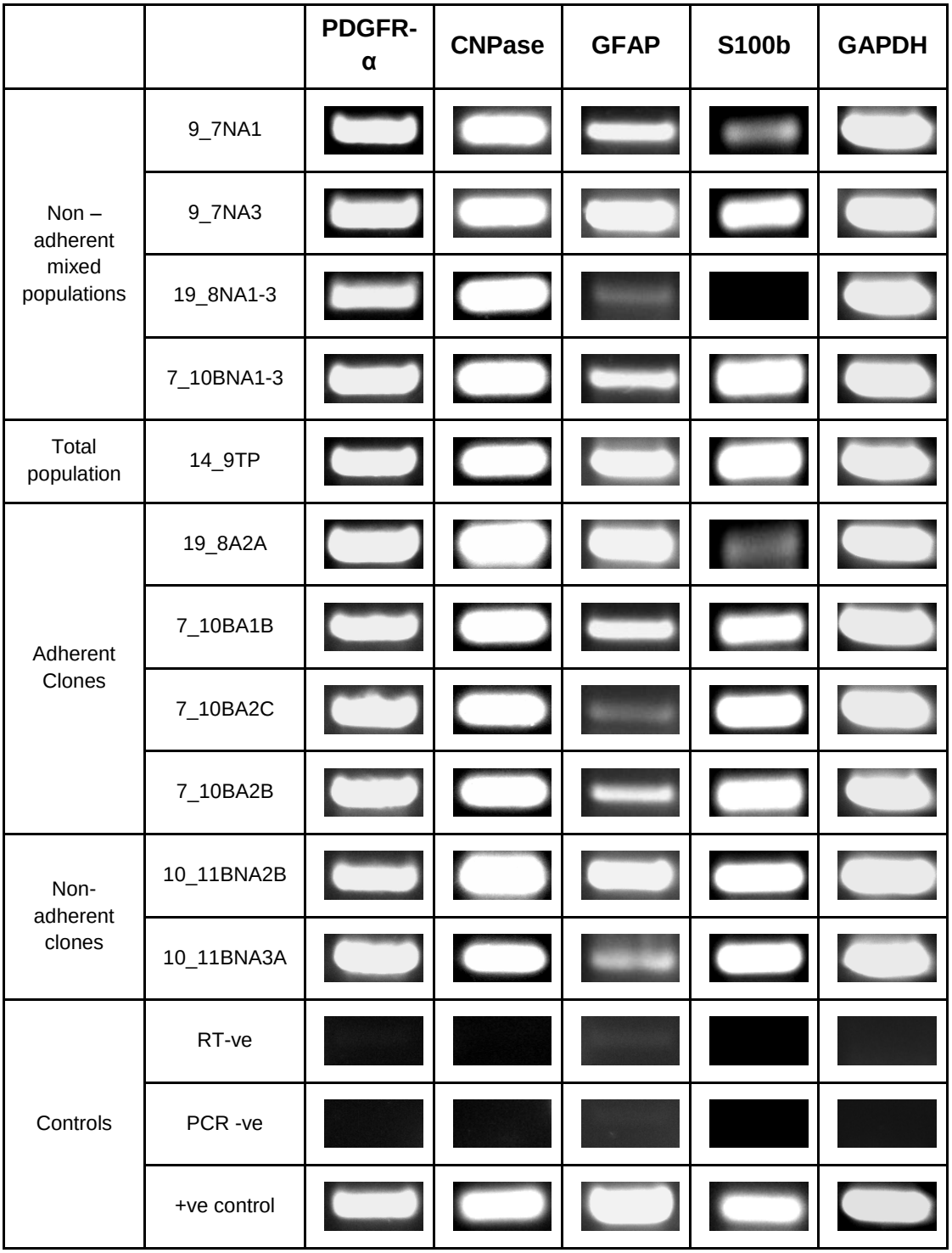

Figure 5.1 – mRNA expression of glial cell markers.

Rt-PCR was used to detect the expression of PDGFR-α, CNPase, GFAP and S100b in isolated dental pulp progenitor cells. PDGFR-α, CNPase and GFAP expression was identified in all cell populations, whereas S100b expression was found to be more variable. RNA extracted from mouse corpus callosum tissue was used as a positive control.

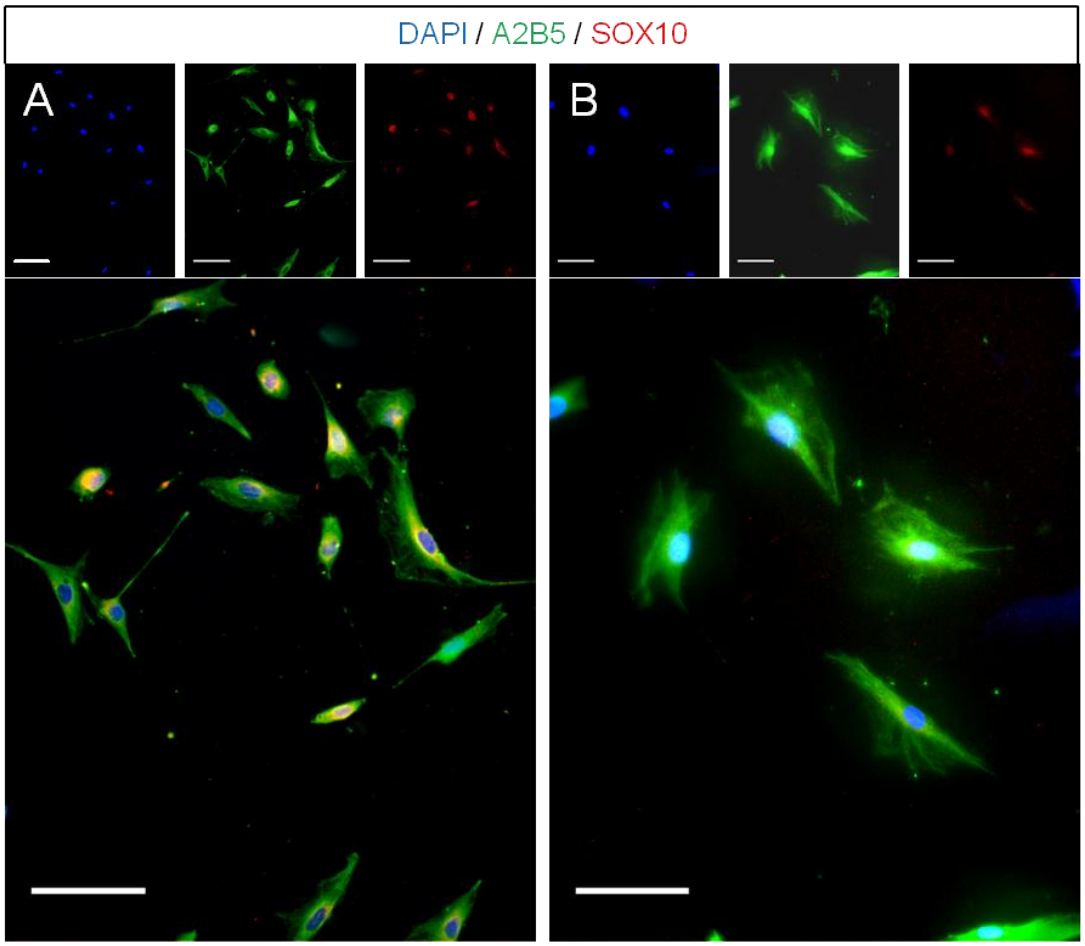

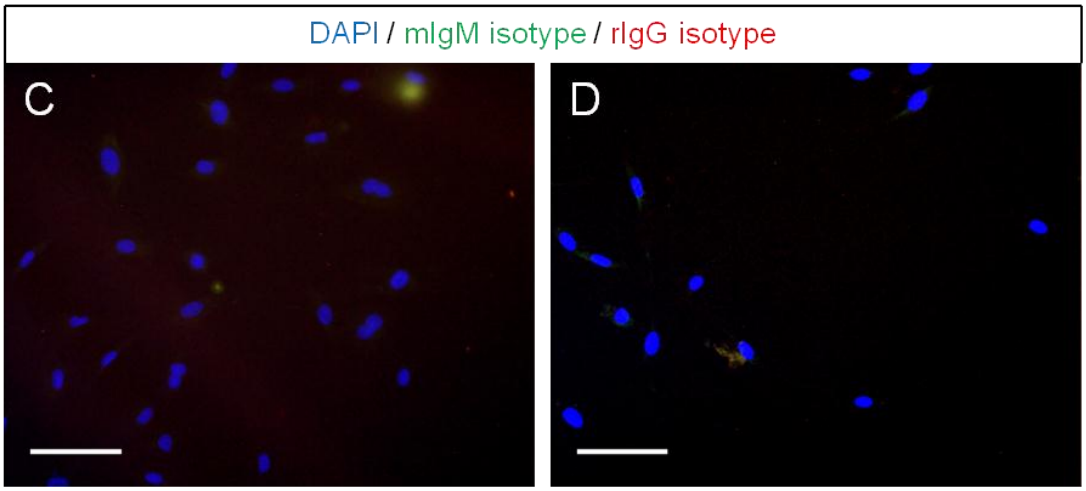

Figure 5.2 – Presence of A2B5 and SOX10 in weakly nestin-expressing clones
Clones with low levels of nestin mRNA expression, 19_8A2A (A) and 10_11BNA3A (B), were fixed and stained with antibodies against the early stage glial markers A2B5 (green) and SOX10 (red). Nuclei were counterstained with DAPI. Merged images of the respective isotype controls are shown (C & D). Scale bars = 100µm.

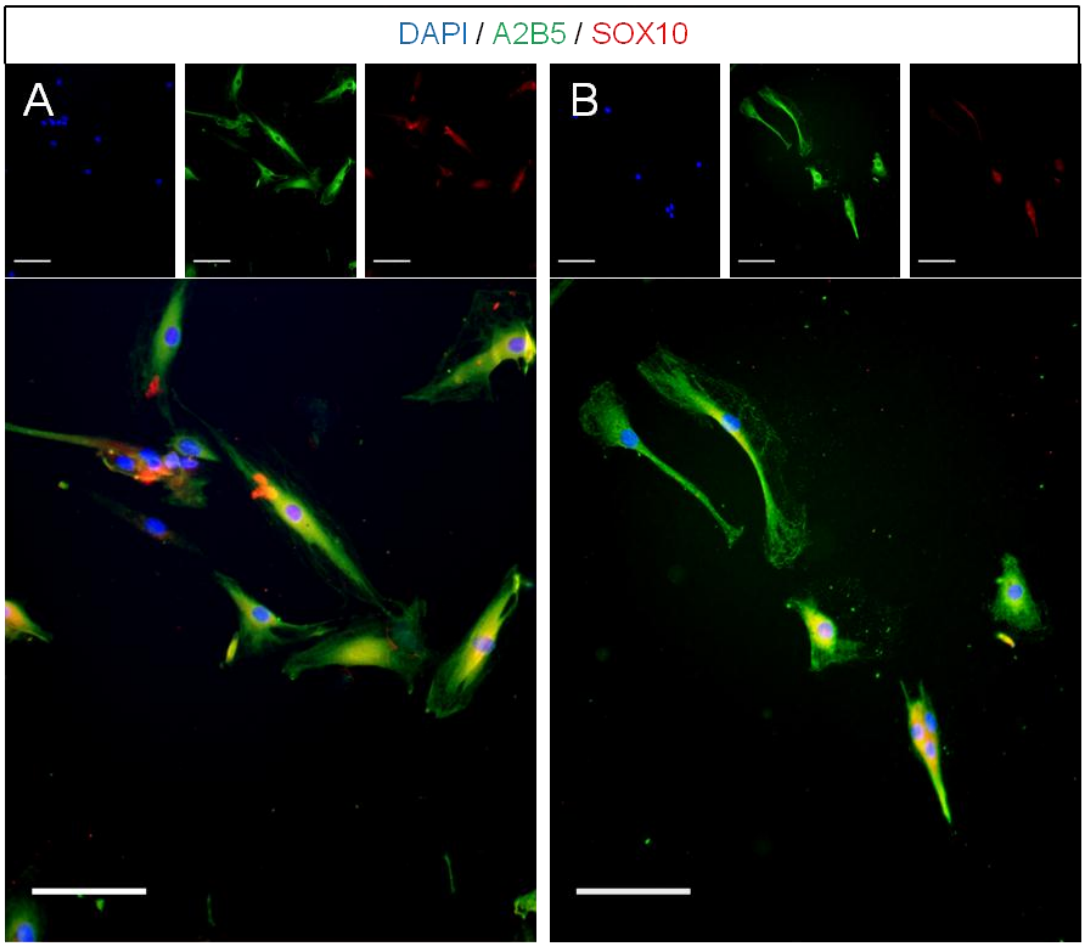

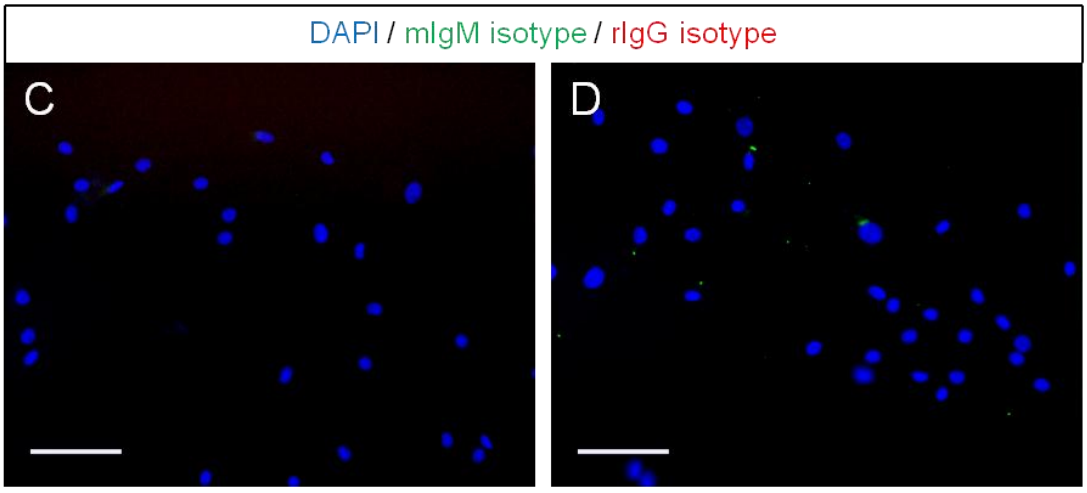

Figure 5.3 – Presence of A2B5 and SOX10 in strongly nestin-expressing clones
Clones with high levels of nestin mRNA expression, 7_10BA1B (A) and 7_10BA2C (B), were fixed and stained with antibodies against the early stage glial markers A2B5 (green) and SOX10 (red). Nuclei were counterstained with DAPI. Merged images of the respective isotype controls are shown (C & D). Scale bars = 100µm.

5.4.2 DPPC clones cultured in OPC medium

Due to the similarities in marker expression with OPCs, initial attempts to differentiate DPPCs down an oligodendrocyte lineage were based on media used in the culture of OPCs (O'Meara *et al*., 2011; Jagielska *et al*., 2012) The four clones (19_8A2A, 10_11BNA3A, 7_10BA1B and 7_10BA2C) were passaged and seeded afresh, at 10, 000 cells/cm^2 in OPC medium, on poly-l-lysine-coated chamber slides. Changes in morphology were observed over 7 days culture before fixation for characterisation by immunocytochemistry.

Low nestin-expressing clones 19_8A2A and 10_11BNA3A were observed to transform from their typical bi/tripolar fibroblastic-like morphology in DPPC culture medium (Figure 5.4 A and C, respectively) to a more branched phenotype in OPC medium (Figure 5.4 B and D). However, few cells were found to adhere and survive over the course of the 7 day culture period. Clones 7_10BA1B and 7_10BA2C appeared similarly fibroblastic in DPPC medium (Figure 5.4 E and G) but, on the other hand, were found to adopt a comparatively more highly branched glial-cell like morphology in OPC medium (Figure 5.4 F and H). No obvious proliferation was observed in any of the four clones tested.

.

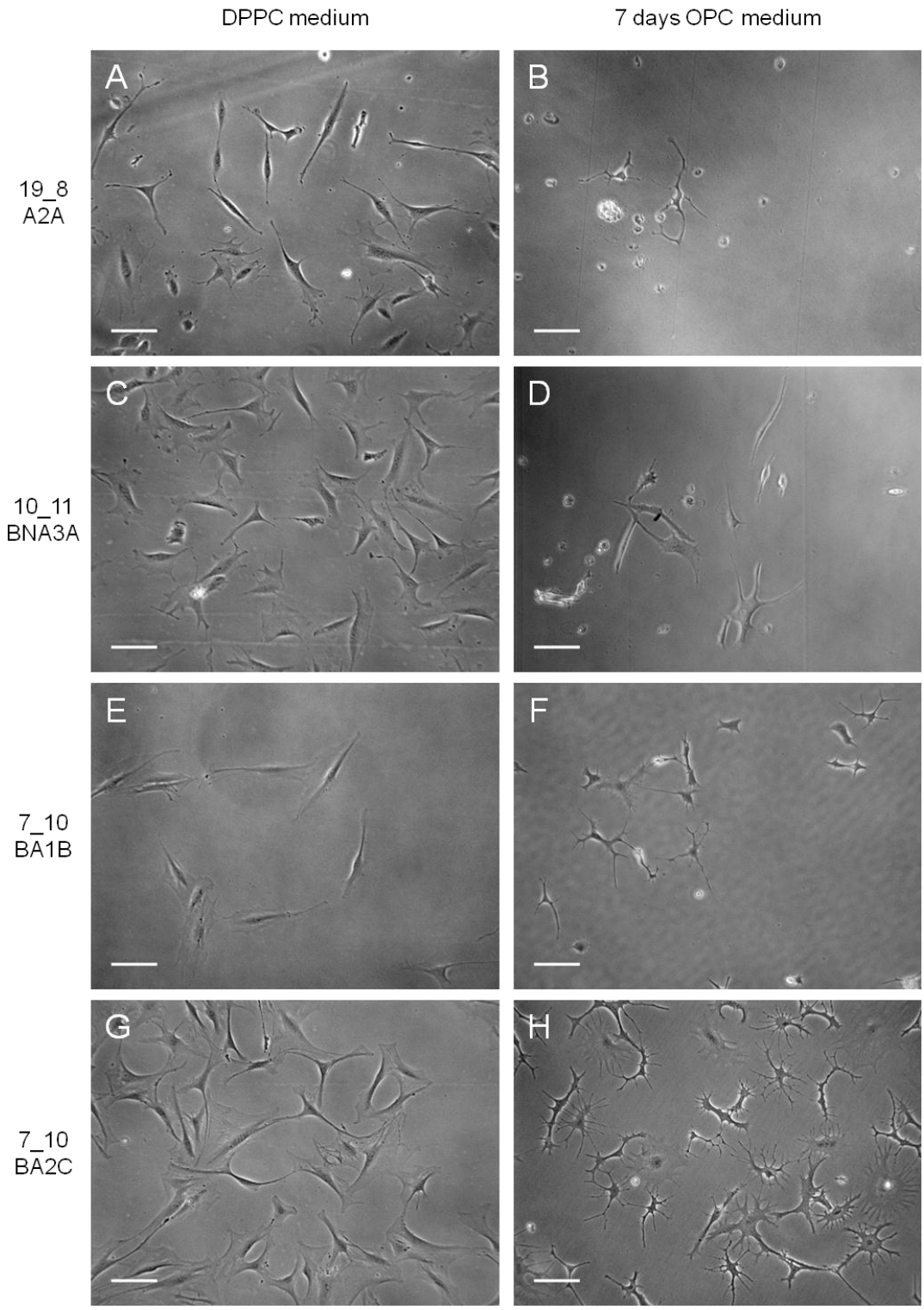

Figure 5.4 – Morphology changes following culture in OPC medium

In DPPC culture medium 19_8A2A (A), 10_11BNA3A (B), 7_10BA1B (E) and 7_10BA2C (G) displayed bi/tripolar fibroblastic-like morphology, typical of dental pulp progenitor cells. After 7 days culture in oligodendrocyte progenitor cell medium, however, all 4 clones (B, D, F & H, respectively) adopted a highly branched, more glial-like, phenotype. Scale bars = 100µm

At the end of 7 days culture in OPC medium the presence of mature oligodendrocyte markers Olig2, MBP and MOSP was investigated. Olig2 was identified in all four clones following culture in OPC medium (Figure 5.5). MBP-positivity was not observed in either 19_8A2A or 10_11BNA3A (Figure 5.6 B and D), but was identified in both 7_10BA1B and 7_10BA2C (Figure 5.6 F and H, respectively). Presence of another myelin-associated protein, MOSP, was demonstrated in all cells of all four clones (Figure 5.7). The expression of mature oligodendrocyte markers strongly suggested that the differentiation of oligodendrocyte-like cells from DPPCs was induced using OPC medium.

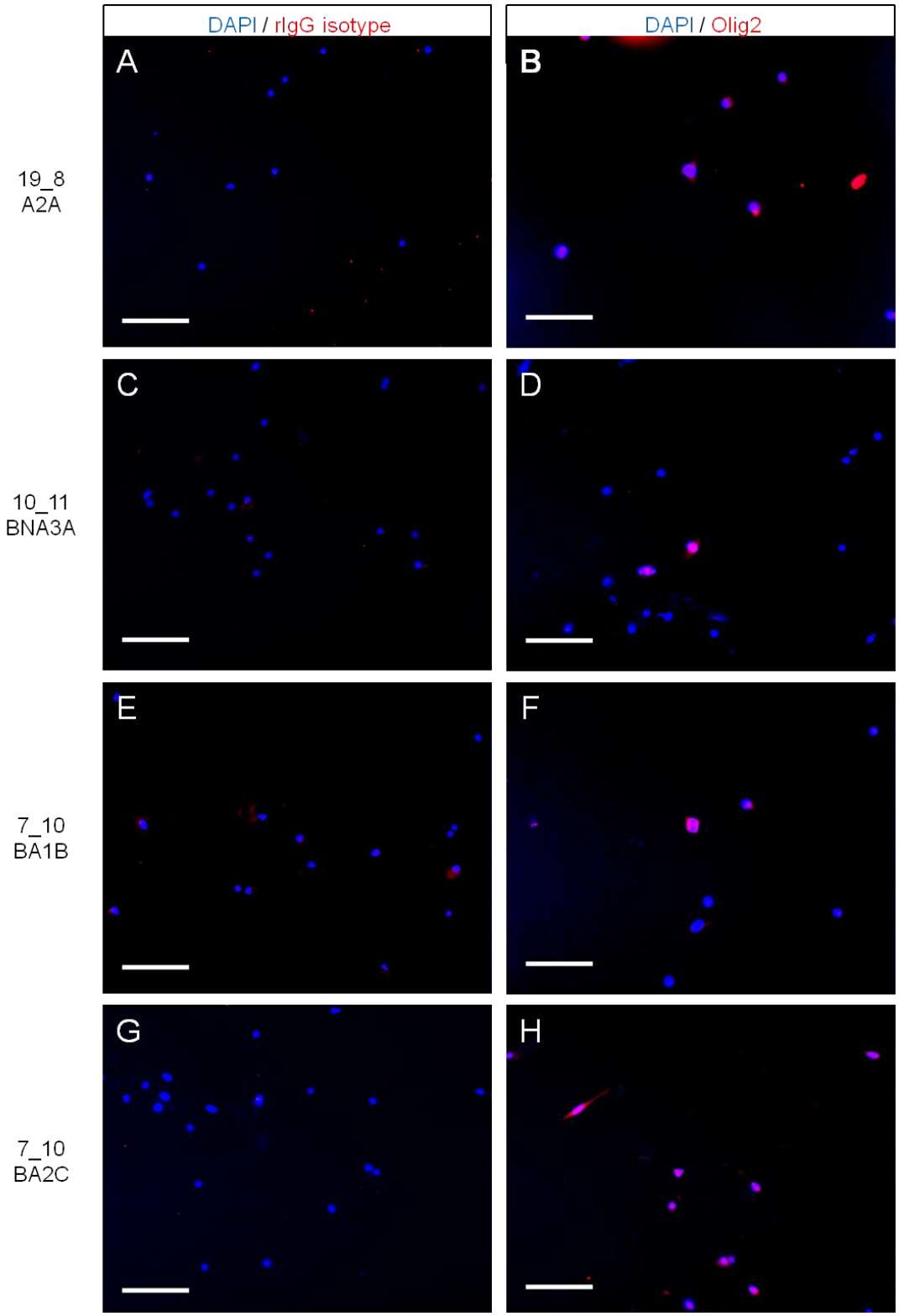

Figure 5.5 – Olig2-positivity following culture in OPC medium

After 7 days culture in OPC medium, 19_8A2A (A & B), 10_11BNA3A (C & D), 7_10BA1B (E & F) and 7_10BA2C (G & H) were fixed with 4% paraformaldehyde. The fixed cells were subsequently stained with rabbit IgG antibodies as an isotype control (A, C, E & G) and antibodies against Olig2 (B, D, F & H). Presence of Olig2 was identified in all 4 clones. Scale bars = 100µm

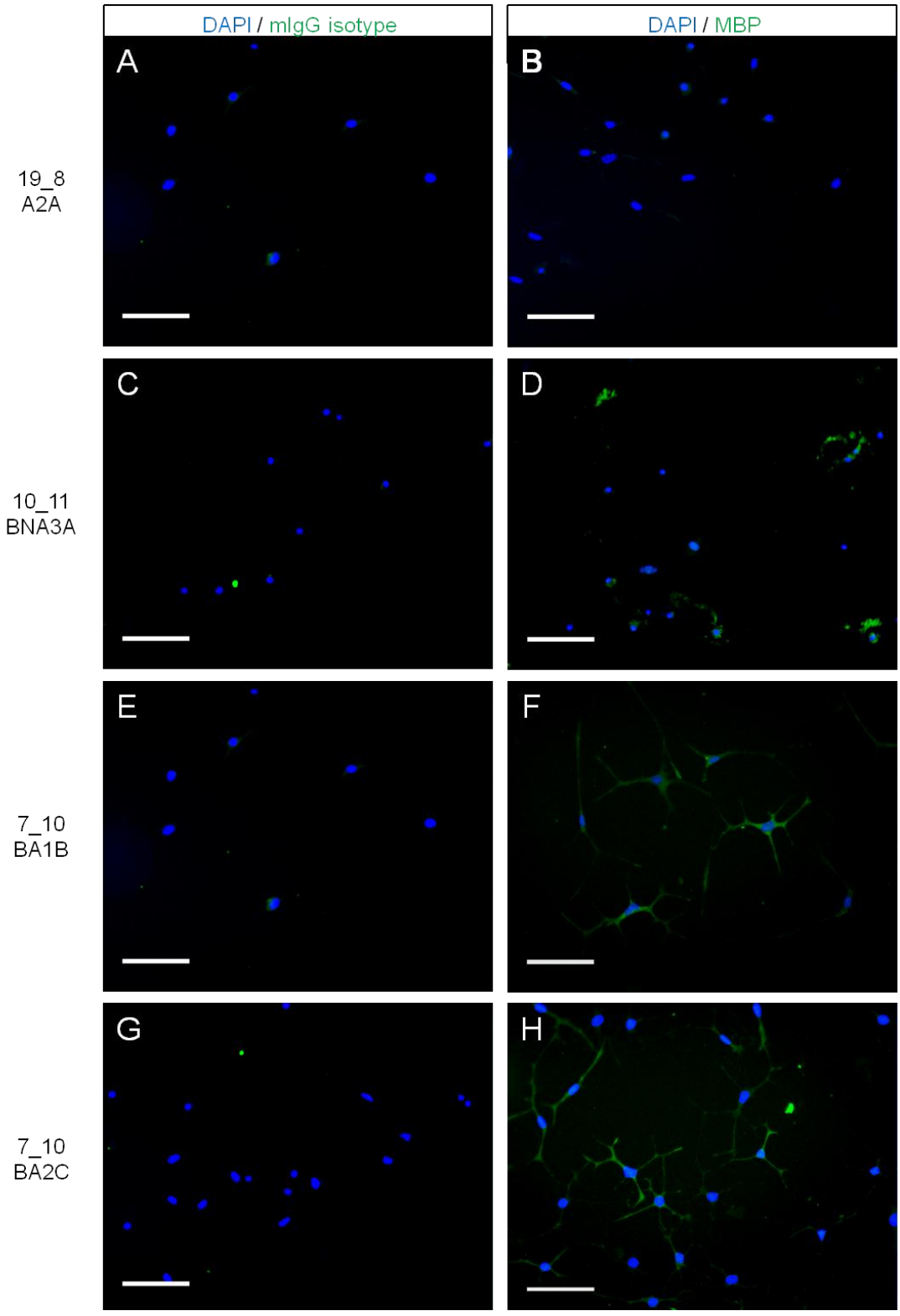

Figure 5.6 – MBP-positivity following culture in OPC medium

After 7 days culture in OPC medium, 19_8A2A (A & B), 10_11BNA3A (C & D), 7_10BA1B (E & F) and 7_10BA2C (G & H) were fixed with 4% paraformaldehyde. The fixed cells were subsequently stained with mouse IgG antibodies as an isotype control (A, C, E & G) and antibodies against MBP (B, D, F & H). Only the strongly nestin-expressing clones, 7_10BA1B and 7_10BA2C, were identified as being MBP-positive. Scale bars = 100µm

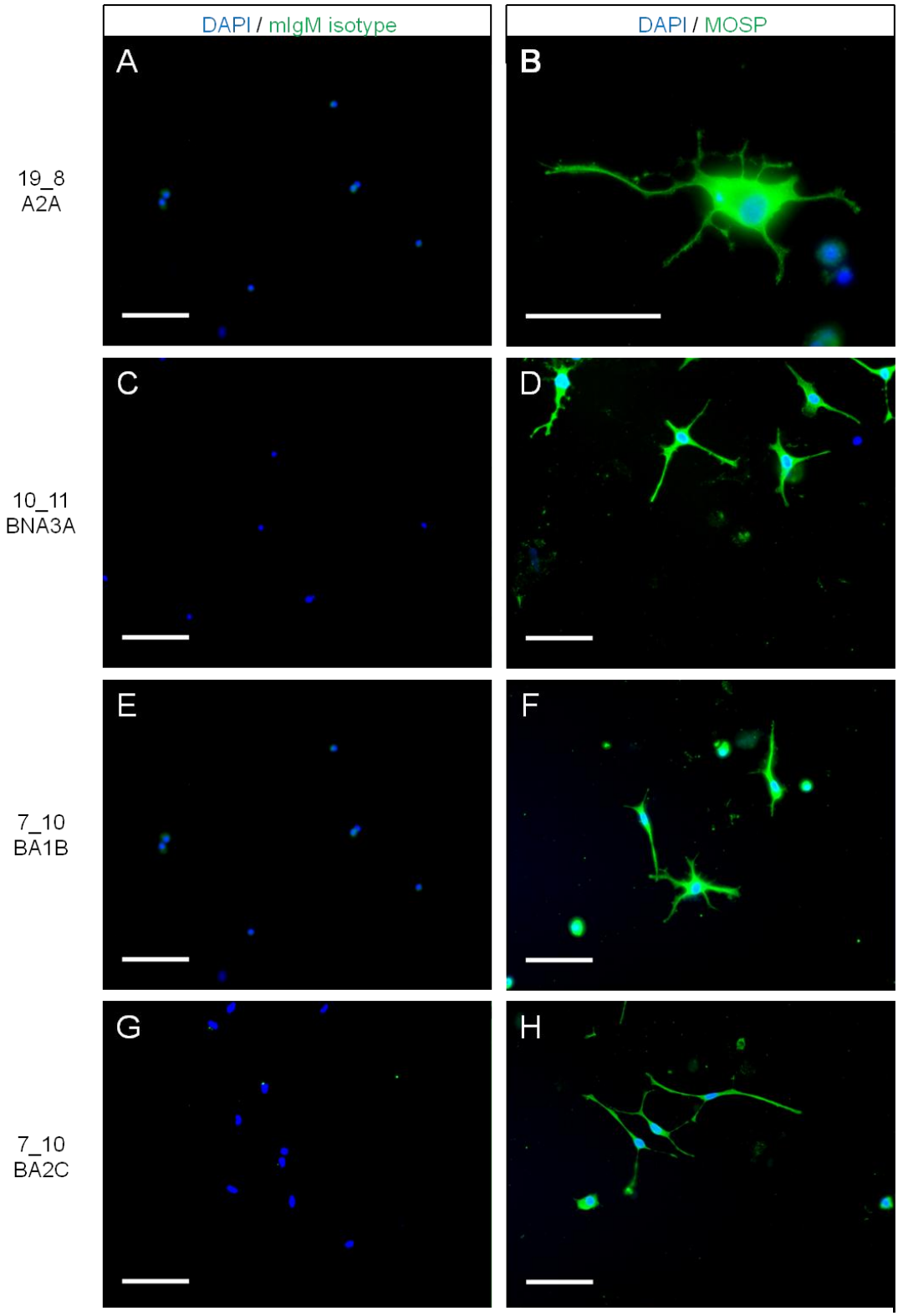

Figure 5.7 – MOSP-positivity following culture in OPC medium

After 7 days culture in OPC medium, 19_8A2A (A & B), 10_11BNA3A (C & D), 7_10BA1B (E & F) and 7_10BA2C (G & H) were fixed with 4% paraformaldehyde. The fixed cells were subsequently stained with mouse IgM antibodies as an isotype control (A, C, E & G) and antibodies against MOSP (B, D, F & H). Presence of MOSP was identified in all 4 clones. Scale bars = 100µm

5.4.3 Optimisation of culture surface for differentiation

Having demonstrated the greatest ability for oligodendrocyte differentiation based upon cell survival, morphology and specific marker positivity, 7_10BA2C was selected for further analysis to investigate the effects of different culture surfaces and increased duration of differentiation. Cells were differentiated on poly-l-lysine-coated glass or plastic culture surfaces for 10 days in OPC medium. Those cells grown on plastic for 10 days (Figure 5.8 C - G) displayed a demonstrably more highly branched oligodendrocyte-like morphology than those on glass chamber slides (Figure 5.8 A and B).

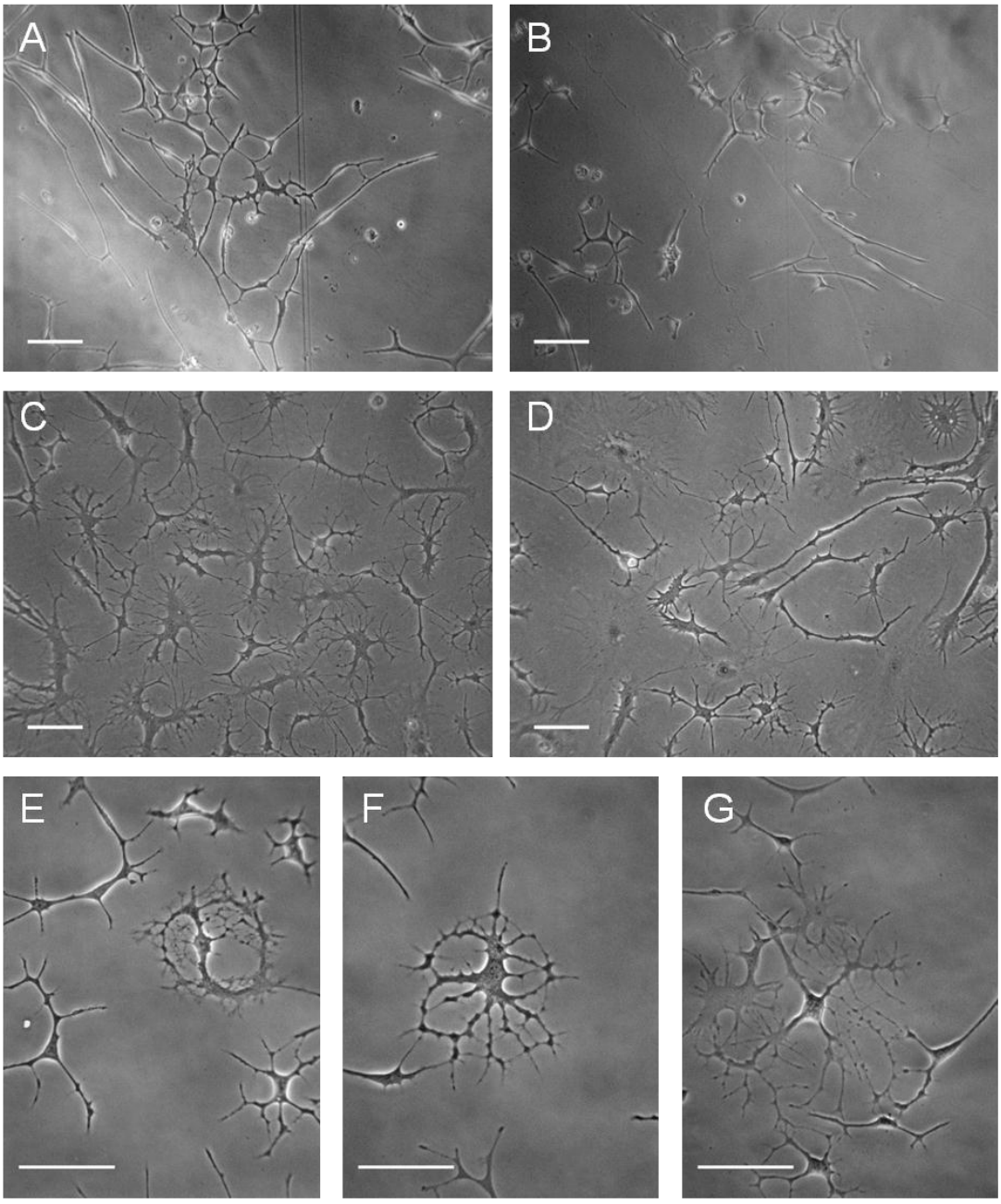

Figure 5.8 – Optimisation of culture surface for differentiation
7_10BA2C was cultured in OPC medium for 10 days on poly-l-lysine-coated glass (A & B) and plastic (C – G) culture surfaces. Cells grown on plastic display a more highly branched morphology. Scale bars = 100µm

5.4.4 Changes in expression of glial markers during differentiation

As dental pulp progenitor cells have been shown to express a number of markers associated with different developmental stages and types of glial cells prior to differentiation (Figure 5.1), the changes in expression of some of these during differentiation was investigated.

7_10BA2C cells did not stain positive for the oligodendrocyte-specific transcription factor Olig1 before differentiation (Figure 5.9 A). After 10 days culture in OPC medium, however, Olig1 was identified both in the nucleus and the surrounding perinuclear cytoplasm (Figure 5.9 B). Nuclear staining of Olig2, on the other hand, was observed both prior to and following differentiation (Figures 5.10 A and B, respectively). Expression of GFAP, at the protein level, was not identified at either stage, whereas S100b was seen before, but not after, differentiation (Figure 5.11 A and B). Quantitative PCR demonstrated that, over 10 days differentiation, CNPase expression increased in conjunction with a downregulation of S100b (Figure 5.12). Together, these characterisation results confirm that OPC culture medium results in the upregulation/induction of oligodendrocyte-associated markers together with the downregulation of other glial cell markers in DPPCs.

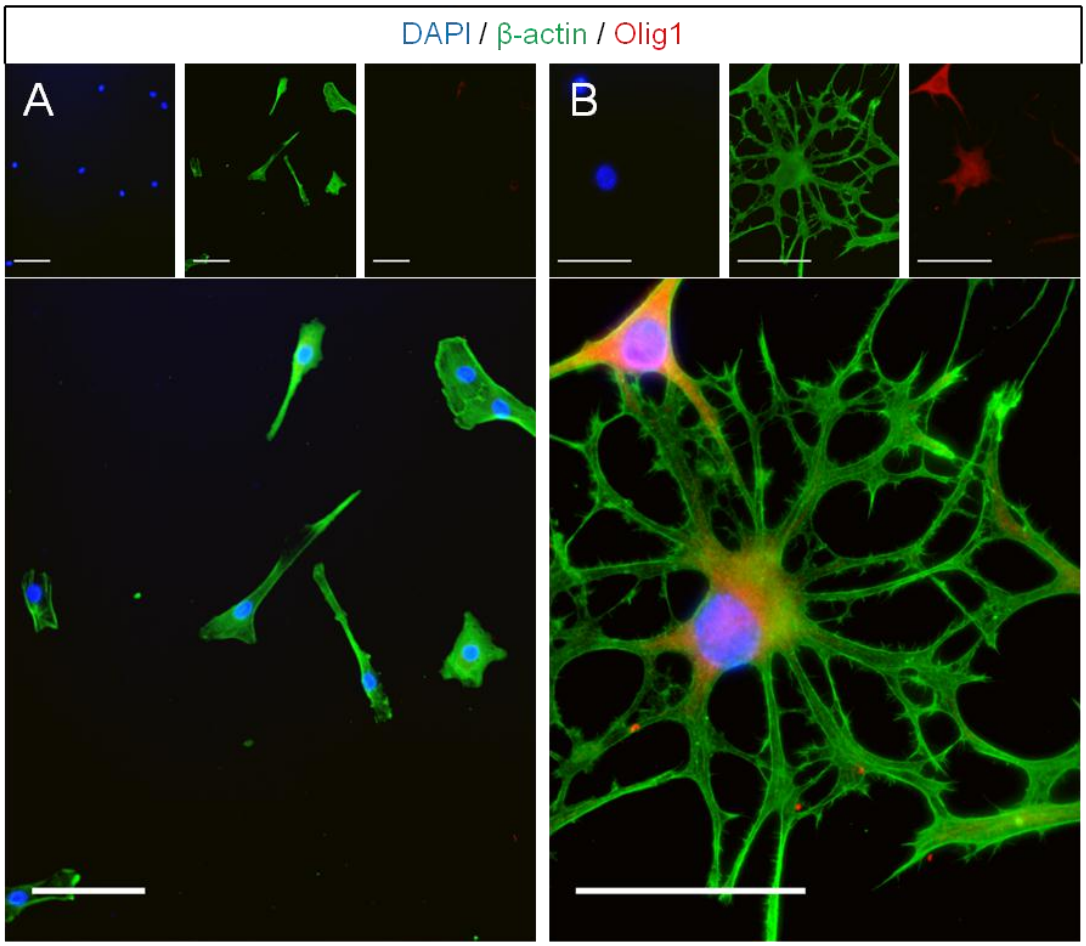

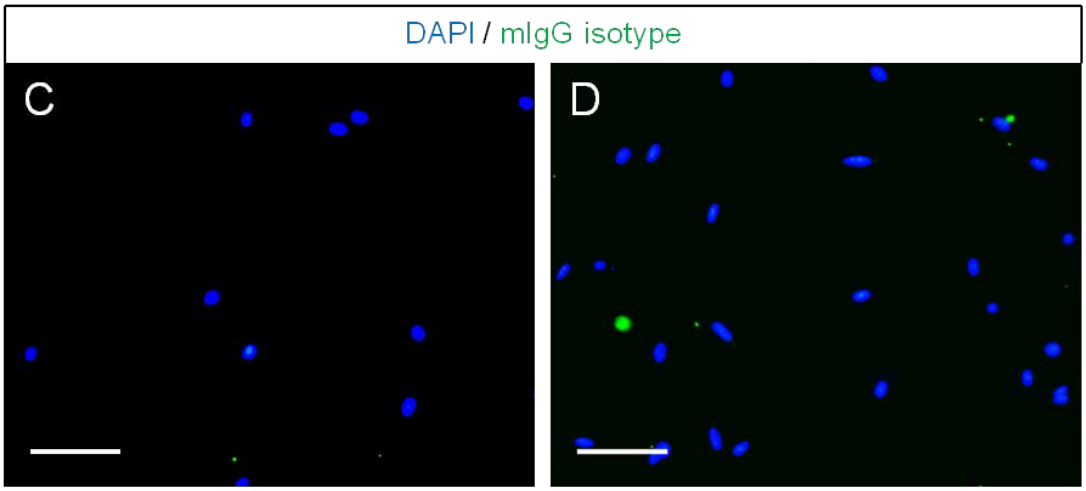

Figure 5.9 - Olig1 immunocytochemistry

Undifferentiated 7_10BA2C cells cultured in standard DPPC medium (A & C) and after 10 days differentiation in OPC medium (B & D) were fixed with 4% PFA before antibody staining. Olig1 positivity (red) was not found in undifferentiated cells (A) but was induced following differentiation (B). β-actin (green) was used to visualise cell morphology. Mouse IgG isotype controls for β-actin antibody are shown before (C) and after (D) differentiation. Rabbit IgG as an isotype control for Olig1 is shown in Figure 5.10 (C & D). Scale bars = 100µm.

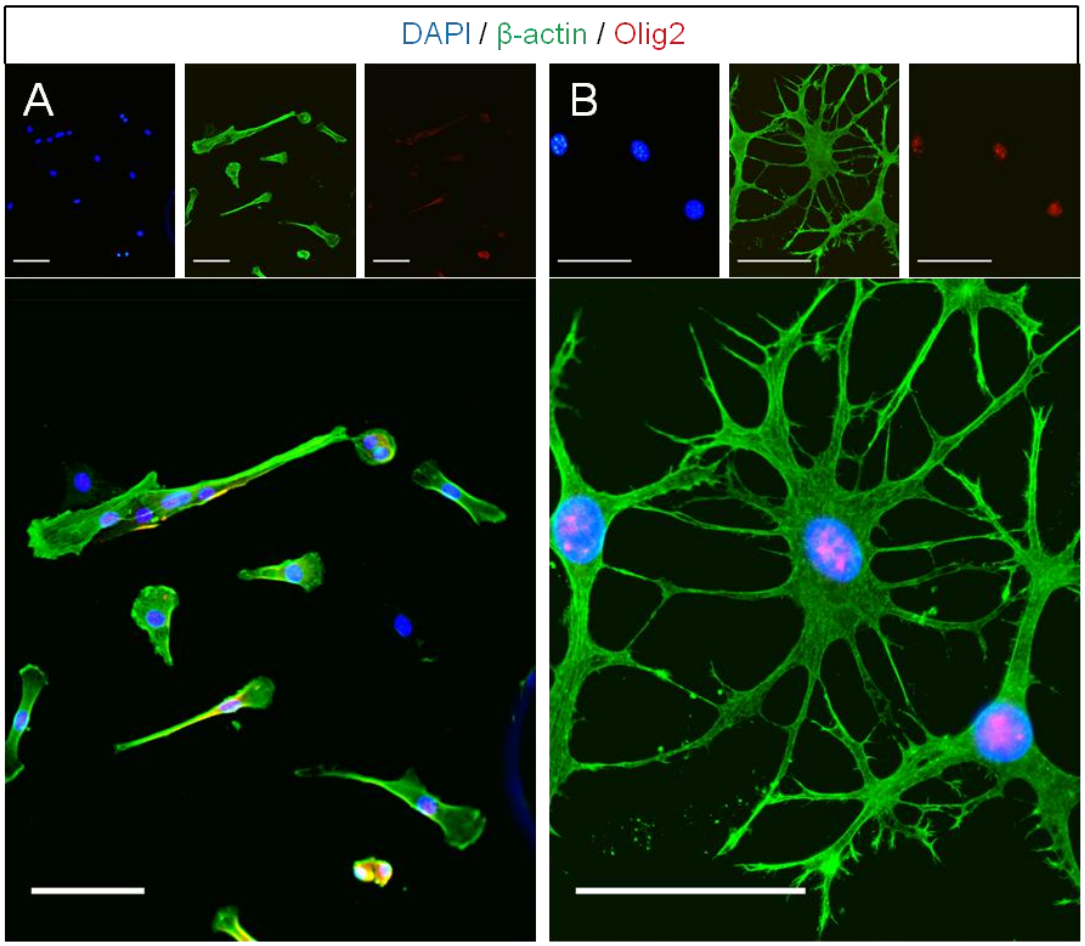

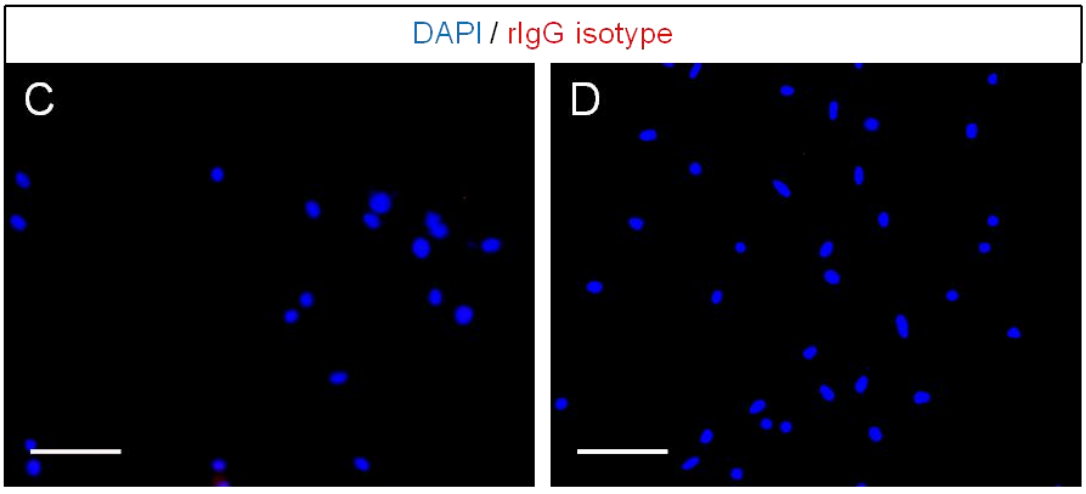

Figure 5.10 - Olig2 immunocytochemistry

Undifferentiated 7_10BA2C cells cultured in standard DPPC medium (A & C) and after 10 days differentiation in OPC medium (B & D) were fixed with 4% PFA before antibody staining. Olig2 positivity (red) was found at low levels in undifferentiated cells (A) and further induced following differentiation (B). β-actin (green) was used to visualise cell morphology. Rabbit IgG as an isotype control for Olig1 & Olig2 is shown before (C) and after (D) differentiation. Scale bars = 100µm.

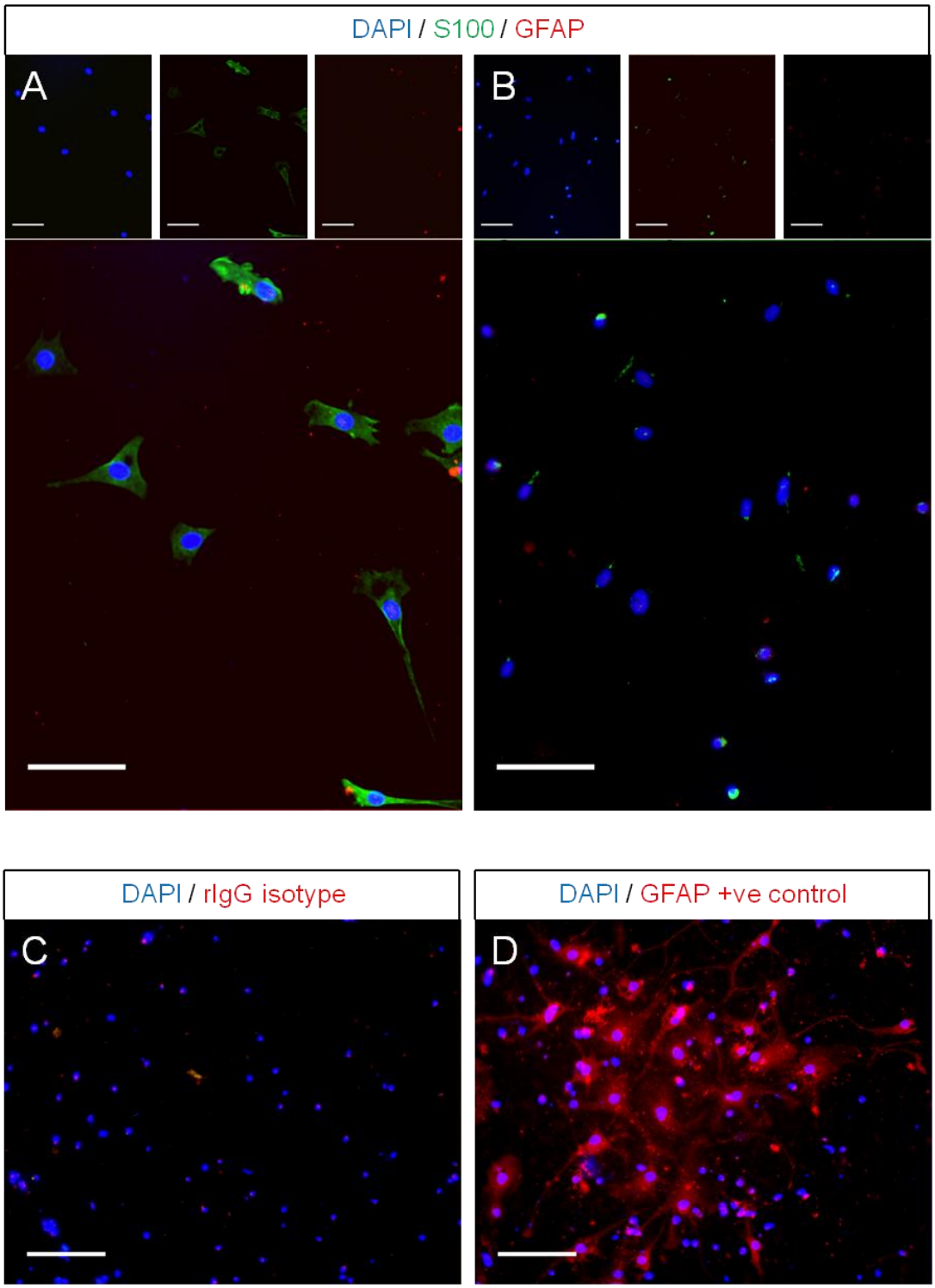

Figure 5.11 – GFAP and S100b immunocytochemistry

Undifferentiated 7_10BA2C cells cultured in standard DPPC medium (A & C) and after 10 days differentiation in OPC medium (B & D) were fixed with 4% PFA before antibody staining. S100b positivity (green) was found at low levels in undifferentiated cells (A) but reduced following differentiation (B) while GFAP staining was not observed at either stage. C & D) Differentiated neural progenitor cells provided a positive control for GFAP expression. Scale bars = 100µm.

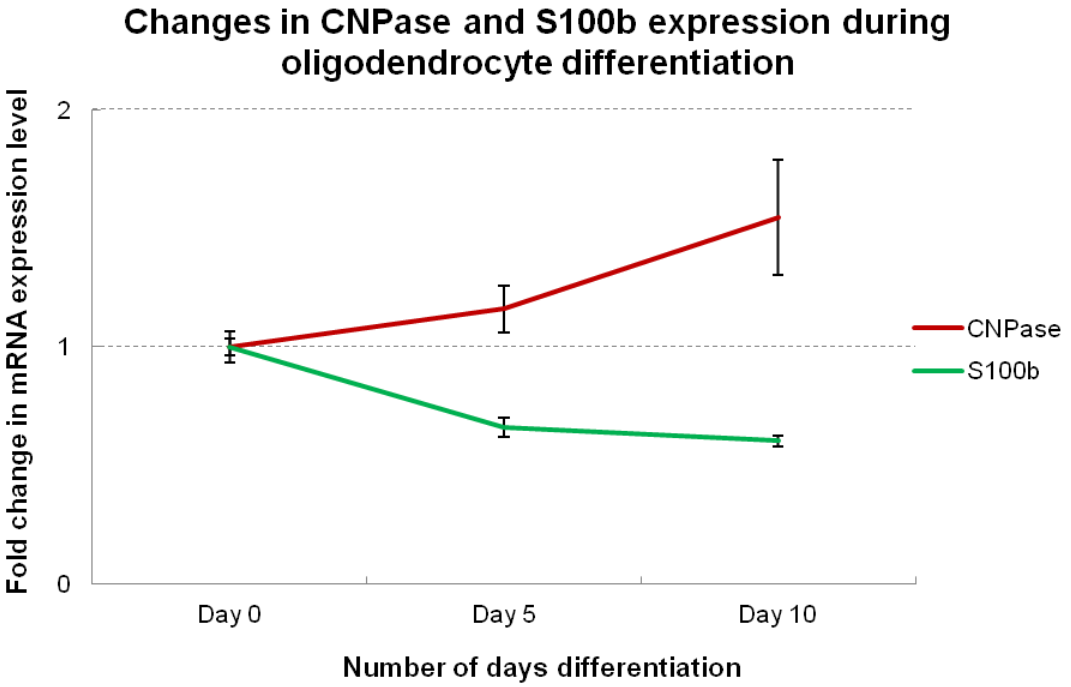

Figure 5.12 – Changes in expression of CNPase and S100b during differentiation
RNA extracted from 7_10BA2C cells on days 0, 5 and 10 of the differentiation protocol was used for quantifying changes in expression of mRNA transcripts for the oligodendrocyte marker CNPase and the astrocytic marker S100b using the $2^{-\Delta\Delta ct}$ method for qPCR analysis. Expression of CNPase was found to increase during differentiation over 10 days accompanied by a concurrent decrease in S100b expression.

5.4.5 Changes in neurotrophin and growth factor expression during differentiation

The changes in expression of neurotrophins and growth factors at days 0, 5 and 10 were also investigated using qPCR. Both BDNF and GDNF were strongly downregulated over the first 5 days of differentiation before plateauing. Expression of NGF marginally decreased over 10 days while NT-3 expression began to increase between day 5 and 10 (Figure 5.13 A). bFGF slowly decreased in expression over 10 days. TGFβ-1 was strongly induced over the first 5 days of differentiation, while relatively smaller increases were observed in expression of VEGF-A, IGF-1 and PDGF-a. Between days 5 and 10 PDGF-a expression reduced to pre-differentiation levels and VEGF-A similarly decreased while TGFβ-1 and IGF-1 remained unchanged (Figure 5.13 B).

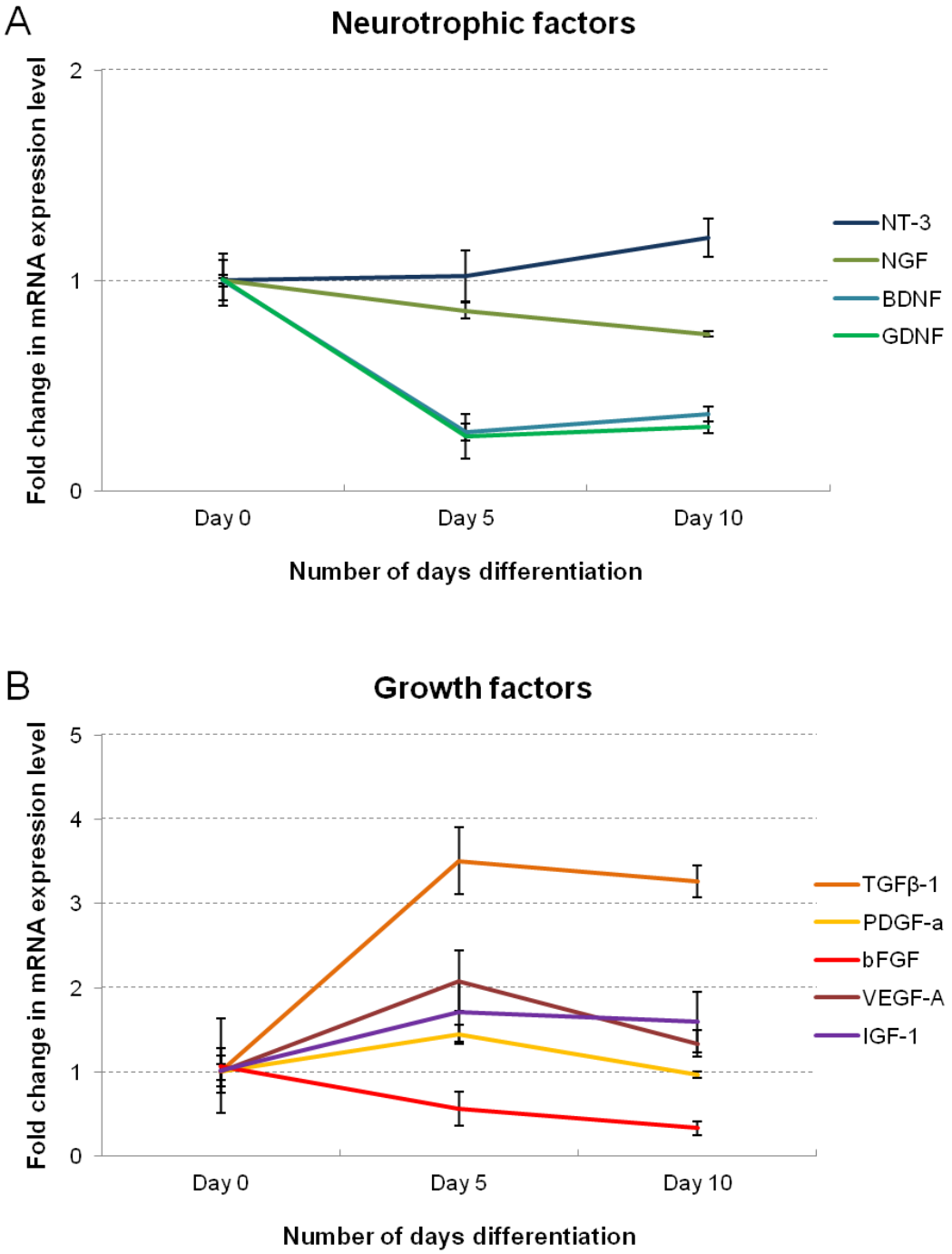

Figure 5.13 – Changes in expression of neurotrophic and growth factors during differentiation

RNA extracted from 7_10BA2C cells on days 0, 5 and 10 of the differentiation protocol was used for quantifying changes in expression of mRNA transcripts for neurotrophins (A) and growth factors (B) using the $2^{-\Delta\Delta ct}$ method for qPCR analysis. A) Expression of neurotrophins tended to decrease with the exception of NT-3 which showed a marginal increase by day 10. B) Expression of TGFβ-1, IGF-1, VEGF-A increased during the differentiation protocol, PDGF-a remained unchanged and bFGF was downregulated.

5.5 Discussion

This chapter provides the first in-depth characterisation of the expression of glial markers by DPPCs. Before differentiation, all isolated DPPCs populations were screened for the expression of glial cell markers by rt-PCR and immunocytochemistry. Undifferentiated DPPCs were found to express markers associated with glial-precursor cells, astrocytes, Schwann cells and early-mid stage oligodendrocytes (Figures 5.1 – 5.3).

Glial-restricted precursors, with the potential for astrocytic or oligodendroytic differentiation, arise from neural stem cells during development and are neural crest in origin. Appearance of the A2B5 antigen, is believed to represent the transition from NSC to a glial-restricted phenotype (Rao and Mayer-Proschel, 1997). However, A2B5-positive cells may still retain the ability for multipotential neuronal differentiation (Nunes *et al*., 2003). A2B5 expression was identified in all four clones used in this study together with SOX10 (Figures 5.2 and 5.3). SOX10 expression is associated with the neural crest during development and, as such, its appearance within DPPCs (Figures 5.2 and 5.3) is not unexpected given the developmental origins of the pulp (Chai *et al*., 2000). Multipotent neural crest cells migrate away from the neural tube into developing craniofacial tissues. At initiation of tooth morphogenesis these cells populate the underlying mesenchyme, eventually giving rise to the cellular components of pulpal tissue. Populations of progenitor cells retaining neural crest stem cell characteristics have been previously isolated from the pulp (Waddington *et al*. 2009; Janebodin *et al*., 2011). These may represent a source of cells with greater potential for

neuronal and glial differentiation due to their neural tube origin, which gives rise to the adult CNS. Upon reaching adulthood, SOX10 expression is restricted to glial progenitor cells and mature oligodendrocytes in the CNS and Schwann cells in the PNS (Kuhlbrodt *et al*., 1998). Presence of A2B5 and SOX10 together in DPPCs (Figures 5.2 and 5.3) suggests a possible glial precursor-like phenotype.

Expression of GFAP by undifferentiated DPPCs has previously been reported at both the mRNA (Gronthos *et al*., 2002) and protein levels, as measured by fluorescence activated cell sorting and immunocytochemistry (Takeyasu *et al*., 2006; Sakai *et al*., 2012). In this study, the expression of mRNA transcripts for GFAP was detected (Figure 5.1) but no protein was identified by antibody-staining (Figure 5.11 A). Multiple isoforms of GFAP have been identified and many more may exist (Boyd *et al*., 2012). As such, this inconsistency between gene and protein expression may be due to differing specificities of the primer pair and antibody used in this study. The antibody has been demonstrated to work with differentiated NSCs (Figure 5.11 D) and primary cultured astrocytes, but may not react with the specific isoform expressed by DPPCs. In addition to GFAP, DPPCs also expressed another astrocytic marker, S100b (Figures 5.1 and 5.11 A). S100 expression has been only previously been reported in DPPCs that have been induced to grow as neurospheres (Sasaki *et al*., 2008). Together, co-expression of both S100b and GFAP would appear to indicate a potential astrocytic phenotype of undifferentiated DPPCs. However, neither of these markers is entirely astrocyte-specific. GFAPs role is primarily structural in astrocytes and its

knockdown results in significant disruption of CNS extracellular architecture (Liedtke *et al*., 1996). The function of GFAP is less well defined for the many other cell types by which it is expressed including fibroblasts, chondrocytes, Schwann cells and BMSCs (Hainfellner *et al*., 2001). In addition to astrocytes, calcium-binding protein S100b expression is also strongly associated with Schwann cell identification. Furthermore, there is increasing evidence of S100b expression in subtypes of oligodendrocytes at both immature and mature stages of development (Hachem *et al*., 2005; Steiner *et al*., 2007 and 2008), bringing into question its suitability as a definitive marker for astrocytes/Schwann cells. Thus, the expression of S100b and GFAP mRNA by undifferentiated DPPCs (Figure 5.1) may not be indicative of a glial differentiation potential that is purely restricted to astrocytes or Schwann cells.

Prior to differentiation, murine DPPCs were found to express a number of early-mid oligodendrocyte markers including PDGFR-α, CNPase, A2B5 and SOX10 (Figures 5.1 – 5.3). Within the CNS, expression of PDGFR-α subunits is restricted to cells of oligodendrocyte lineage (Pringle *et al*., 1992). CNPase forms a major constituent of CNS myelin, although its exact physiological role is unknown. It is implicated in the regulation of oligodendrocyte maturation and development of myelinating properties (Gravel *et al*., 1996). DPPC expression of CNPase and A2B5 has previously been reported for cells which were found to spontaneously differentiate into oligodendrocyte-like cells following transplantation into the injured spinal cord

(Sakai *et al*., 2012). As such, the presence of these markers in the DPPCs used in this study could provide evidence of oligodendrocytic potential.

The glial marker expression profile of undifferentiated DPPCs gives a strong indication of their potential for glial differentiation (Figure 5.1). The *in vivo* differentiation of glial cells following transplantation of progenitor cells from the dental pulp into the injured spinal cord has been described in two contrasting studies, each reporting improvements in functional outcome. De Almeida *et al*. (2011) identified $GFAP^+/S100^+$ astrocytes derived from transplanted DPPCs, but no $GalC^+$ oligodendrocytes, eight weeks after transplantation. Conversely, Sakai *et al*. (2012) report that eight weeks after grafting, 90% of surviving SHEDs had differentiated into MBP^+ oligodendrocytes with no detectable GFAP expression among the remaining unidentified cells. These conflicting results may be explained due to the differences in the injury environment at the time of transplantation, 7 days after or immediately following injury, respectively. The cytokine and growth factor profile of the injured spinal cord will vary significantly at each time point. Transplantation in the sub-acute stages of injury, after 7 days, represents a more clinically relevant timeframe, but one that will be less conducive for growth and regeneration due to production of neuronal growth inhibitory molecules and the presence of myelin breakdown products (McKeon *et al*., 1991; Sandvig *et al.,* 2004). It may be that this more hostile environment favours spontaneous differentiation towards an astrocytic phenotype. Alternatively, SHEDs are believed to represent a population of progenitor cells that are more immature in comparison to progenitor cells

isolated from the adult pulp based upon their odontogenic/osteogenic differentiation properties following transplantation into immunocomprimised mice (Miura *et al*., 2003). As with DPPCs (Gronthos *et al*., 2000), SHEDs have been shown to differentiate into odontoblastic-like cells and produce ectopic dentine. However, SHEDs were unable to produce similar dentine-pulp complexes, but could induce bone formation by host cells, a property not associated with DPPCs (Miura *et al*., 2003). How such differences in the potential of SHEDs and DPPCs for mineralised tissue formation may translate to neural tissue regeneration is unclear. Regardless, these *in vivo* SCI studies demonstrate that glial differentiation of progenitor cells from the dental pulp can help improve functional outcome in experimental models of SCI.

This study reports, for the first time, the development of a protocol for the specific differentiation of oligodendrocytes from DPPCs *in vitro*. Due to similarities with OPCs in the expression of PDGFR-α, SOX10, A2B5 and CNPase, a differentiation medium similar to that used in the culture of oligodendrocyte cells was adopted (O'Meara *et al*., 2011; Jagielska *et al*., 2012). Four DPPC clones were cultured in OPC medium and changes in morphology observed over 7 days before the cells were fixed for immunocytochemistry. Clones with low levels of nestin mRNA expression (19_8A2A and 10_11BNA3A) showed lower attachment and reduced branching under the differentiation conditions than stronger nestin-expressing clones (Figure 5.4). All four clones stained positive for Olig2 and MOSP following differentiation (Figures 5.5 and 5.7), whereas only the

stronger nestin-expressing 7_10BA1B and 7_10BA2C were positive for MBP (Figure 5.6). This suggests that nestin expression may be indicative of DPPCs potential for oligodendrocyte differentiation. Although not traditionally associated with cells of the oligodendrocyte lineage, nestin expression may be identified along with A2B5 in some subtypes of proliferating OPCs, and is downregulated upon maturation (Almazán *et al*., 2001). Despite the expression of MBP and MOSP in differentiated DPPCs, there was no observation of the membranous sheets associated with the production of myelin by mature oligodendrocytes *in vitro* (Dyer and Matthieu., 1994; Jagielska *et al*., 2012). This suggests that the differentiated DPPCs are not terminally differentiated, but are of a less mature pre-myelinating phenotype. The production of myelin membrane sheets *in vitro* requires perfectly optimised culture conditions and, as such, further work is needed to determine the precise conditions required to achieve this with DPPCs.

7_10BA2C, as the clone with the most highly-branched oligodendrocyte-like morphology and MBP-positivity was selected for further investigation and optimisation. It was found that 7_10BA2C demonstrated greater attachment and a more complex branched morphology when differentiated on poly-l-lysine-coated plastic culture surfaces, as an alternative to glass (Figure 5.8). This observation conflicts with recent work by Jagielska *et al*. (2012) who demonstrated the importance of culture surface mechanical properties on the attachment, survival, migration and differentiation of OPCs. They found that OPCs adopt a more complex branched phenotype, with enhanced MBP expression, when differentiated on stiffer substrates, such as glass.

However, both glass and plastic represent culture surfaces that are many orders of magnitude stiffer than the extracellular matrix of the CNS. The authors additionally investigated different concentrations of polyacrylamide hydrogels to cover a physiological range of mechanical stiffness. Optimal OPC attachment, survival, proliferation and differentiation was found on gels of stiffness equivalent to that of CNS tissue. The use of similar polymers in the differentiation of DPPCs may provide the optimisation required to elicit a membranous myelinating phenotype.

Oligodendrocyte transcription factor Olig1 was found to be induced in 7_10BA2C following differentiation (Figure 5.9). Olig1 expression is essential for the remyelination of demyelinated CNS axons in a multiple sclerosis model (Arnett *et al*., 2004) and, thus, its presence in differentiated DPPCs indicates potential for remyelination of the injured spinal cord. Furthermore, Olig1 was not localised exclusively within the nucleus of differentiated DPPCs, but also found within the perinuclear cytoplasm (Figure 5.9 B). Cellular localisation of Olig1 varies with oligodendrocyte developmental stage: being found exclusively nuclear in progenitor cells but almost completely cytoplasmic in mature myelinating cells (Arnett *et al*., 2004). Both nuclear and cytoplasmic expression of Olig1 in differentiated DPPCs provides further evidence that the cells are of an intermediate pre-myelinating stage, prior to terminal differentiation, and may require further differentiation steps. The closely related Olig2 was expressed by 7_10BA2C prior to, and after, differentiation (Figure 5.10 A). Olig2 is one of three factors that have recently been used to convert fibroblasts to induced

oligodendrocyte precursor cells via direct lineage conversion, along with SOX10 and Zfp536 (Yang *et al*., 2013). Expression of both Olig2 and SOX10 (Figure 5.2 and 5.3) by undifferentiated DPPCs provides further evidence of an inherent capacity for oligodendrocyte differentiation. Olig1 and Olig2 are involved in the specification of motor neurons and oligodendrocytes that may arise from a shared precursor within the spinal cord (Lu *et al*., 2002; Zhou and Anderson, 2002). Genetic deletion of both Olig transcription factors results in the ablation of motor neurons and oligodendrocytes. However, when knocked out separately, loss of Olig2 results in the loss of motor neurons and Olig1 deletion delays oligodendrocyte maturation (Lu *et al*., 2002). Based on these findings and the presence of other oligodendrocyte-associated markers in differentiated DPPCs, expression of Olig2 does not indicate motor neuron differentiation in this case. The only previous report of oligodendrocyte differentiation of DPPCs *in vitro* (Aanismaa *et al*., 2012) identified small numbers of GalC-positive cells when subjected to a previously published neuronal differentiation protocol (Király *et al*., 2009). However, none of the oligodendrocyte-like cells identified by Aanismaa *et al.* were found to express Olig2, unlike DPPCs differentiated using the specific protocol for oligodendrocyte derivation developed in this chapter.

No staining of GFAP, a marker of astrocytic differentiation, was observed either before, or after, differentiation (Figure 5.11). S100b staining was identified in undifferentiated DPPCs (Figure 5.11 A), but not following differentiation (Figure 5.11 B). qPCR confirmed the downregulation of S100b mRNA over 10 days differentiation (Figure 5.12). The non-expression and

downregulation of astrocytic genes in combination with an up-regulation of oligodendrocyte-associated CNPase (Figure 5.12) confirms that during differentiation, DPPCs are favouring a differentiation pathway towards an oligodendrocyte-like phenotype.

Progenitor cells isolated from tissues other than the CNS could provide further alternative sources of glial-like cells. Bone marrow stromal cells can be readily encouraged to differentiate into Schwann cells using a well-defined protocol (Someya *et al*., 2008; Park *et al*., 2010a; Kamada *et al*., 2011). Unlike oligodendrocytes differentiated from DPPCs, BMSC-derived Schwann cells are bipolar in morphology and can be stained immunocytochemically for GFAP. In contrast to observations from this study (Figure 5.12), RNA expression of CNPase and S100 does not change during Schwann cell differentiation of BMSCs (Park *et al*., 2010a). Transplantation of these cells into SCI models reduces size of injury sites via increased neuronal survival, promotes remyelination and improves hindlimb locomotion recovery (Someya *et al*., 2008; Kamada *et al*., 2011). Alternatively, CNPase and MBP-expressing cells with oligodendrocyte-like morphology, capable of myelinating neurons in co-culture, can be selectively isolated from umbilical cord stem cells by gradient centrifugation and selective culture media (Tracy *et al*., 2008). Circulating foetal mesenchymal stem cells can be encouraged to adopt oligodendrocyte-like morphology and marker expression using neuroblastoma cell line-conditioned medium (Kennea *et al*., 2009). The dental pulp represents a more easily accessible source of progenitor cells than bone marrow or umbilical cord blood, as it is often discarded following

routine orthodontic treatment. Furthermore, the relative simplicity of the protocol for oligodendrocyte differentiation of DPPCs gives the dental pulp a distinct advantage as an alternative source of myelinating glial cells as a treatment for SCI.

Although not traditionally viewed as a neurotrophin-secreting cell type, literature suggests that oligodendrocytes may function in this capacity. Rat embryonic cortical and forebrain-derived primary cultured neurons demonstrate enhanced survival and increased axonal length when grown in medium conditioned by primary cultured oligodendrocytes. These effects can be attenuated by antibodies to BDNF, NGF, NT-3 (Dai *et al*., 2003), GDNF (Wilkins *et al*., 2003) or IGF-1 (Wilkins *et al*., 2001). Similar neurotrophic effects are observed using hESC-derived OPC-conditioned medium containing measurable levels of BDNF, NGF, NT-3, IGF-1, TGFβ-1 and VEGF (Zhang *et al*., 2006b). Changes in mRNA expression of these factors were investigated during the differentiation of DPPCs into oligodendrocytes (Figure 13). The observation that GDNF expression is downregulated during differentiation contrasts with previously published work where detectable levels of GDNF are observed in mature oligodendrocyte-cultured medium but not in OPC-conditioned medium (Wilkins *et al*., 2003). It may be that GDNF is already released at high levels by DPPCs prior to differentiation and downregulation results in levels that are comparable with mature oligodendrocytes. Based upon the methods used for detecting GDNF release into culture media in the literature, it is not possible to perform such a direct comparison at this time. GDNF release by undifferentiated DPPCs has been

quantified through ELISA assays (Soria *et al*., 2011), whereas GDNF release by OPCs and mature oligodendrocytes was determined by western blotting (Wilkins *et al*., 2003). Using an identical method on each cell type during differentiation would allow a valid comparative analysis of changes in GDNF production to be made. IGF-1 expression levels, on the other hand, remain unchanged between oligodendrocytes and OPCs (Wilkins *et al*., 2001), which is replicated by the DPPC differentiation data from this current study (Figure 5.13 B). TGFβ-1 was identified as the growth factor showing the largest change in expression level during the differentiation of DPPCs into oligodendrocyte-like cells. This observation is supported by previous reports of increased mRNA transcript expression for TGFβ-1 by mature oligodendrocytes compared to OPCs (McKinnon *et al*., 1993). The same study reports that TGFβ-1 inhibits OPC proliferation and promotes their differentiation. This suggests that, in addition to trophic effects on neuronal cells, growth factor release may help to modulate oligodendrocyte maturation via auto/paracrine mechanisms.

Based on observations from this study the production of neurotrophins and growth factors by oligodendrocytes derived from DPPCs should not be overlooked when considering the use of DPPCs as a treatment for SCI. Not only does this suggest potential for DPPCs to act as a cell replacement for oligodendrocytes to remyelinate axons, but the cells could simultaneously promote endogenous regeneration through trophic mechanisms. Such observations have been made following the transplantation of hESC-derived OPCs into an *in vivo* SCI model to promote functional recovery (Keirstead *et*

al., 2005). Only 55% of oligendrocyte-remyelinated axons were physically associated with transplanted cells, suggesting the recruitment of native oligodendrocytes to the injury site. In the same manner, transplanted DPPCs may possess the potential to act synergistically to improve functional outcome.

5.6 Summary

- Murine dental pulp progenitor cells were found to express a range of markers associated with astrocytes, Schwann cells and oligodendrocytes.

- DPPCs cultured in OPC medium adopt a highly branched oligodendrocyte-like morphology and express mature oligodendrocyte markers.

- Astrocyte marker expression is downregulated during differentiation, confirming an oligodendrocyte-like phenotype.

- Neurotrophic factor release by DPPCs may be altered as a result of oligodendrocyte differentiation and will prove important in considering the use of DPPCs to treat SCI.

- This is the first report of a protocol developed for the specific differentiation of oligodendrocyte-like cells from DPPCs.

Chapter 6: The behaviour of dental pulp progenitor cells transplanted into spinal cord ex vivo and in vivo models

6.1 Introduction

Undifferentiated DPPCs have been reported to respond well to CNS transplantation, surviving over sustained periods and exerting influences upon endogenous cells whilst simultaneously responding to environmental cues (Huang *et al*., 2008; Arthur *et al*., 2008 and 2009). Functional improvements mediated by DPPC transplantation have been reported for *in vivo* models of stroke (Yang *et al*., 2009; Sugiyama *et al*., 2011; Fang *et al*., 2013; Yamagata *et al*., 2013) and spinal cord injury (de Almeida *et al*., 2011; Sakai *et al*., 2012). In these studies, the protective/regenerative effects appear to be mediated by neurotrophic and/or growth factor release rather than direct cell replacement. The differentiation of transplanted DPPCs into neurons *in vivo* has not yet been confirmed, although oligodendrocyte-like (Sakai *et al*., 2012) and astrocyte-like (de Almeida *et al*., 2011) phenotypes have been observed.

Pre-differentiation of cells prior to transplantation enables researchers a degree of control over cell fate, restricting the potential for differentiation into undesirable cell types. Directing cells partially down a specific lineage allows the possibility of natural maturation in response to endogenous environmental factors *ex vivo/in vivo*. This approach to cellular transplantation has only been investigated in one DPPC *in vivo* study. DPPCs, neuronally pre-differentiated using the protocol described by Király *et al*. (2009), retain a degree of electrophysiological functionality, as measured by patch clamp recordings, following injection into the cerebrospinal fluid of newborn rats (Király *et al*. 2011). This suggests that the

pre-differentiation of DPPCs prior to spinal cord transplantation may prove a viable option for investigating whether DPPCs truly can act as a direct cell replacement option for SCI therapy.

Ex vivo tissue culture systems are a valuable research tool to provide multiple insights at the cellular and tissue levels. Spinal cord slice cultures are a well established model and have been used in a range of investigations into aspects of neuroscience as diverse as: electrophysiology (Yoshimura and Nishi, 1993), inflammatory and neurodegenerative disease processes (Zhang *et al*., 2011; Ravikumar *et al*., 2012) and cellular migration (Meng *et al*., 2012). *Ex vivo* spinal cord slice cultures serve as a useful "stepping stone" before progressing onto *in vivo* SCI models, allowing researchers to obtain large amounts of data with reduced costs, time requirements and animal numbers. Such model systems also allow the live imaging and monitoring of cells within the spinal cord which is not possible *in vivo.*

Three techniques are commonly used to generate *in vivo* models of SCI. Compression injury models, such as that used by de Almeida *et al*. (2011), are induced by the application of a vascular clip to the exposed spinal cord. Injuries can be generated by transection of the cord with a surgical scalpel, mimicking a laceration type injury, such as the approach used by Sakai *et al*. (2012). As spinal cord contusion is the type of injury most commonly observed among humans, the most clinically relevant method of generating *in vivo* models involves a direct impact onto the cord itself. This may be performed with a simple weight-drop set-up or an electronically-driven impact

device that allows precise control over force and speed parameters to create a highly reproducible model, as used in this investigation.

The timing of cellular transplantation following SCI is important in determining whether any functional improvement is through protective or reparative mechanisms. Transplantation of cells immediately following injury, as performed by Sakai *et al.* (2012), suggests that improvements are likely to be a protective effect. True regeneration is more likely to be observed following stem cell grafting a number of days post-injury. This approach was adopted by de Almeida *et al*. (2011). In this investigation, DPPC transplantation 7 days after spinal cord contusion represents a clinically feasible timeframe and ensures that any improvements will be a result of true spinal repair.

6.2 Objectives

- To explore the behaviour of DPPCs injected into *ex vivo* spinal cord slice models. Three conditions will be investigated: undifferentiated cells, DPPCs pre-differentiated into oligodendrocyte-like cells using the protocol developed in chapter 6, and DPPCs neuralised as described in chapter 5.

- To develop and transfer these findings to a clinically relevant *in vivo* mouse model of contusive SCI, as a pilot study, and determine if any hindlimb functional recovery can be attributed to direct cell replacement with transplanted DPPCs.

6.3 Materials and methods

6.3.1 *Ex vivo* spinal cord slice model

6.3.1.1 Preparation of *ex vivo* spinal cord slice cultures

Spinal cord slice cultures were prepared as previously described (Meng *et al*., 2012). Briefly, complete spinal cords were dissected from 4 week old C57BL/6 mice on ice. Meninges were carefully removed, so as not to damage the cord, under a dissecting microscope. A McIlwain Tissue Chopper (Mickle Laboratory Engineering, UK) was used to slice the cords into 500µm thick sections. Intact slices were selected and transferred to the centres of 35mm tissue culture dishes, two per dish. 30µl of Matrigel (BD Biosciences, UK) was pipetted over the slices in each dish and the plates transferred to a tissue culture incubator for 1 hour until the Matrigel polymerised. 1.5ml of pre-warmed DMEM/F-12 medium containing 25 mM HEPES buffer and 20% heat-inactivated FBS (all Life Technologies, UK) was added to each dish, ensuring the surface of the slices remained exposed to the air. Spinal slice sections were then returned to the incubator for 24-72 hours before cell injection.

6.3.1.2 Preparation of cells for injection

To allow for easy identification of transplanted cells, DPPCs were isolated from transgenic mice expressing green fluorescent protein (GFP) under control of the chicken β-actin promoter (Okabe *et al*., 1997). Cells were isolated and purified using the fibronectin adhesion assay, as previously

described (sections 3.3.1 and 3.3.2). A mixed population of fibronectin-adherent cells was used for all experiments in this chapter.

Three culture conditions were investigated for transplantation into *ex vivo* spinal cord slice cultures: undifferentiated cells grown in standard DPPC culture medium (section 2.2.1.1), cells pre-differentiated in OPC culture medium for 5 days (sections 5.3.1 and 5.3.2) and cells neuralised in NSC medium for 5 days (section 4.3.2).

6.3.1.3 Injection of cells into spinal cord slice cultures

Prior to injection, cells were dissociated from culture surfaces and counted, as previously described (section 2.2.1.2), and the cell pellet resuspended at a concentration of 100,000 cells/µl in DMEM/F12 +20% FBS. 2µl of cell suspension was injected per slice using a 10µl Hamilton syringe (Hamilton Company, USA). Before loading with cells, the syringe was sterilised by washing through with 70% (w/v) ethanol (Sigma-Aldrich, UK) three times. Traces of ethanol were then removed by washing through a further 5 times with sterile Hank's Balanced Salt Solution (Life Technologies, UK). 10µl cell suspension was then loaded into the syringe and 2µl carefully injected at the junction between grey and white matter on the right hand side of one slice per dish. The remaining slice in each dish was left as a non-injected control. Injected slice cultures were maintained for 10-14 days, with medium changes every other day, before fixation for immunohistochemistry.

6.3.1.4 Immunohistochemical staining of spinal slice cultures

Before staining with antibodies, spinal slice cultures were fixed with a paraformaldehyde and gluteraldehyde fixative. Culture medium was removed from the dishes and the slices were washed three times for 10 minutes on a see-saw rocker with PBS, pre-warmed to 37°C so as not to melt the matrigel. Slices were then immersed for 1 hour in a fixative solution composed of 2% (w/v) paraformaldehyde and 0.1% (w/v) gluteraldhyde (both Sigma-Aldrich, UK) in PBS, also pre-warmed to 37°C. After two further 10 minute PBS washing steps, aldehyde autofluorescense was quenched by immersion of the slices in 50mM ammonium chloride (Sigma-Aldrich, UK) for 2 hours. Slices were then washed with PBS for 10 minutes before a ring was created around each slice using a hydrophobic pap pen (Sigma-Aldrich, UK) in order to minimise antibody wastage. Slices were permeabilised by bathing in 0.5% (v/v) Triton X-100 and 1% (w/v) BSA for 30 minutes. Permeabilisation solution was then removed and unreacted groups blocked by incubating in 0.3% (v/v) Triton X-100 and 3% (w/v) BSA overnight at 4°C. The following day, blocking solution was removed and replaced with antibodies against βIII-tubulin or synaptophysin, alongside respective isotype control antibodies (Tables 2.2 and 2.3) diluted in blocking solution. Spinal cord slices were returned to the fridge and incubated for 3 days. After three days, primary antibody solution was removed and the slices washed with PBS 4 times for 30 minutes. Dishes were then incubated at 4°C overnight with complementary matched secondary antibodies (Table 2.4) diluted in blocking solution. The following day, after 5 x 30 minute PBS washes, the dishes were filled with PBS and the slices taken for confocal and/or two-photon imaging.

6.3.1.5 Imaging of spinal slice cultures

6.3.1.5.1 Live imaging

Phase contrast and fluorescent images of live cells and slice cultures were captured using an Olympus IX71 inverted microscope with an automated stage system and camera (Applied Precision, USA). The imaging equipment was enclosed within a custom-designed temperature control chamber that maintained conditions at 37°C. Photography was controlled using Deltavision imaging software with X/Y/Z multiple position recording (Applied Precision, USA).

6.3.1.5.2 Confocal microscopy

Laser scanning confocal imaging of both live and fixed slice cultures was performed using a Leica SP5 Confocal Microscope and LAS AF imaging software in a temperature controlled environmental chamber (Leica Microsystems, Germany).

6.3.1.5.3 Two-photon microscopy

The two-photon setup consisted of a MaiTai DeepSee tunable Ti:Sapphire laser (Newport Spectra Physics, UK) and a movable objective microscope (Sutter Instruments, USA). R6357 photomultipliers were used (Hamamatsu, Japan). Freeware ScanImage software (developed by Karel Svoboda and colleagues) was used for data acquisition and scanning control.

6.3.1.5.4 Image processing

Acquired images and Z stacks were processed and analysed using ImageJ software.

6.3.2 *In vivo* spinal cord contusion injury model

6.3.2.1 Animals and drug dosage regimen

Adult female C57Bl/6 mice weighing 19-23g (mean = 20.7g) were used in this study. Two days prior to surgery, Enrofloxacin antibiotic solution (Baytril (Bayer Healthcare, UK)) was added to the drinking water at a concentration of 0.04% (v/v) and administered until 10 days after cellular transplantation. Starting one day prior to impact surgery, until 10 days after cell transplantation, mice were subcutaneously injected daily with Meloxicam anti-inflammatory analgesic (Metacam (Boehringer Ingelheim, UK)) at a dosage of 1mg/kg (Figure 6.1).

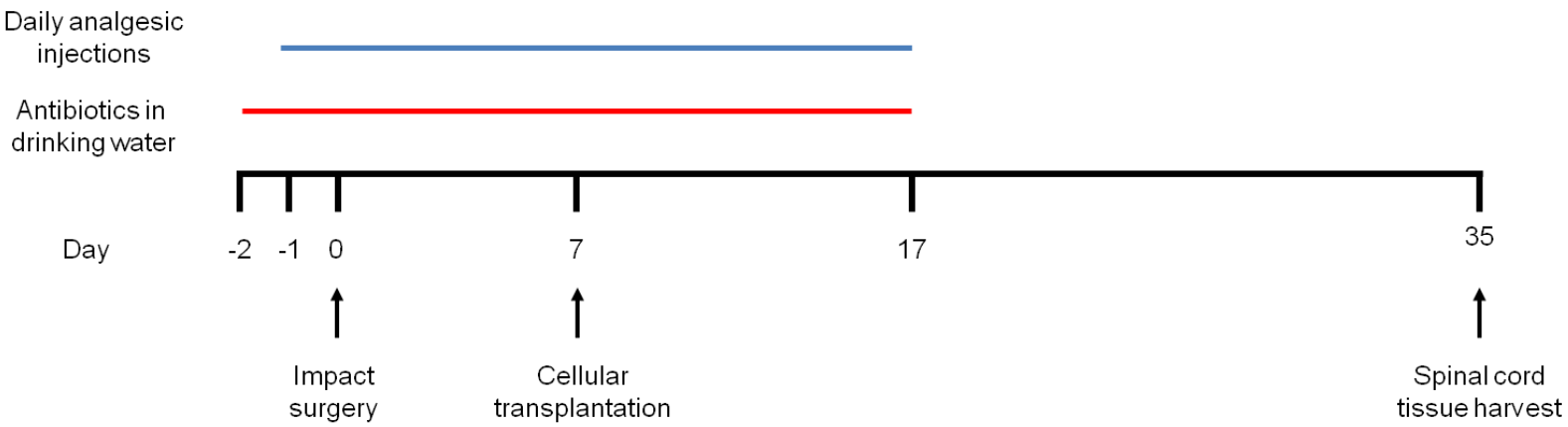

Figure 6.1 – Experimental timeline for transplantation of DPPCs into *in vivo* spinal cord injury model

6.3.2.2 Surgical procedure

Mice were anaesthetised in an induction chamber to which 4% isofluorane in a continuous oxygen flow of 2l/min was applied. Once anaesthetised, animals were maintained on an anaesthetic mask with 2% isofluorane in a continuous oxygen flow of 2l/min. The dorsal area between the neck and hindlimbs, extending ~1cm bilaterally from the spine, was shaved and disinfected with Clorhexadine surgical scrub (Hydrex (EcoLabs, UK)). Using sterilised surgical instruments a longitudinal dorsal midline incision was made on the skin and underlying muscle layers to expose the spinal column from T7-T11. A laminectomy was then performed using fine-point scissors to remove the dorsal portion of the vertebrae and expose a single segment of the spinal cord between T8-T10. An Infinite Horizons IH-0400 spinal cord impactor (Precision Systems and Instrumentation, USA) was used to deliver contusion injuries of a controlled 50kdyn force through a 1.3mm impactor tip with 1 second dwell time on the cord. Following impact, the muscle and skin layers were sutured separately using absorbable Vicryl sutures (Johnson and Johnson, UK) and sealed externally using Vetbond tissue adhesive (3M, UK). 0.5ml saline solution was injected intraperitoneally to account for fluid loss during surgery and animals were then placed in a recovery chamber and monitored closely until fully alert. As a surgical control group, sham impact animals underwent laminectomy without subsequent spinal cord impact.

6.3.2.3 Post-operative care

Following surgery, mice were caged individually on warm paper bedding with a wet mash diet. Animals were monitored closely and bladders manually emptied twice daily.

6.3.2.4 DPPC transplantation

Cell transplantations were performed in the sub-acute phase of injury, 7 days after spinal contusion (Figure 6.1). Prior to transplantation, GFP mDPPCs were neuralised in NSC medium for 5 days, as previously described. Following harvesting, cells were resuspended in PBS at 200,000cells/µl and placed on ice. Mice were anaesthetised, as described previously, and the injury site re-exposed. 5µl of cell suspension (1×10^6 cells) was injected at two locations on the spinal cord midline: 1-1.5mm rostral and 1-1.5mm caudal to the impact. Cells were injected to a depth of between 0.5 and 1mm at a rate of 1µl/minute controlled by a Quintessential Stereotactic Injection system (Stoelting Co, USA) mounted on a manipulable platform. Following completion of each injection, 1 minute was allowed before withdrawal of the 10µl Hamilton syringe to prevent leakage of cells. After both injections, the muscle and skin layers were sutured individually and the animals allowed to recover. As a vehicle control group, injured animals were injected with 5µl PBS alone.

6.3.2.5 Experimental groups

Mice were randomly assigned to three experimental groups used in this experiment: A) Sham impacts (n = 3) underwent laminectomy surgery

without impact. At the time of cellular transplantation, injury sites were surgically exposed but no injections performed before resuturing the wound. B) GFP mDPPC transplants (n=3) underwent laminectomy and contusion injury with DPPC transplantation 7 days later. C) PBS control animals (n=3) underwent laminectomy and contusion injury surgery before injection with PBS alone after 7 days.

6.3.2.6 Analysis of hindlimb locomotor function

Hindlimb motor function was assessed using the Basso, Beattie and Bresnahan (BBB) locomotor scale (Table 6.1) (Basso *et al*., 1995). Two observers recorded BBB scores for each individual animal twice weekly. Mean scores ± standard error were calculated for each treatment group. Statistical analysis was performed using repeated-measures ANOVA with Tukey's multiple comparison tests at each time point.

Table 6.1 – Basso, Beattie and Bresnahan (BBB) locomotor scale

0. No observable hindlimb (HL) movement
1. Slight movement of one or two joints, usually the hip and/or knee
2. Extensive movement of one joint or extensive movement of one joint and slight mov of one other joint
3. Extensive movement of two joints
4. Slight movement of all three joints of the HL
5. Slight movement of two joints and extensive movement of the third
6. Extensive movement of two joints and slight movement of the third
7. Extensive movement of all three joints of the HL
8. Sweeping with no weight support or plantar placement of the paw with no weight support
9. Plantar placement of the paw with weight support in stance only (i.e., when stationary) or occasional, frequent, or consistent weight-supported dorsal stepping and no plantar stepping
10. Occasional weight-supported plantar steps; no FL–HL coordination
11. Frequent to consistent weight-supported plantar steps and no FL–HL coordination
12. Frequent to consistent weight-supported plantar steps and occasional FL–HL coordination
13. Frequent to consistent weight-supported plantar steps and frequent FL–HL coordination
14. Consistent weight-supported plantar steps, consistent FL–HL coordination, and predominant paw position during locomotion is rotated (internally or externally) when it makes initial contact with the surface as well as just before it is lifted off at the end of stance; or frequent plantar stepping, consistent FL–HL coordination, and occasional dorsal stepping
15. Consistent plantar stepping and consistent FL–HL coordination and no toe clearance or occasional toe clearance during forward limb advancement; predominant paw position is parallel to the body at initial contact
16. Consistent plantar stepping and consistent FL–HL coordination during gait and toe clearance occurs frequently during forward limb advancement; predominant paw position is parallel at initial contact and rotated at lift off
17. Consistent plantar stepping and consistent FL–HL coordination during gait and toe clearance occurs frequently during forward limb advancement; predominant paw position is parallel at initial contact and lift off
18. Consistent plantar stepping and consistent FL–HL coordination during gait and toe clearance occurs consistently during forward limb advancement; predominant paw position is parallel at initial contact and rotated at lift off
19. Consistent plantar stepping and consistent FL–HL coordination during gait, toe clearance occurs consistently during forward limb advancement, predominant paw position is parallel at initial contact and lift off, and tail is down part or all of the time
20. Consistent plantar stepping and consistent coordinated gait, consistent toe clearance, predominant paw position is parallel at initial contact and lift off, and trunk instability; tail consistently up
21. Consistent plantar stepping and coordinated gait, consistent toe clearance, predominant paw position is parallel throughout stance, and consistent trunk stability; tail consistently up

6.3.2.7 Preparation of spinal cord tissue samples for cryosectioning

Four weeks after cellular transplantation, animals were sacrificed by CO_2 asphyxiation and transcardially perfused with PBS followed by 4% (w/v) PFA solution. Complete spinal cords were carefully dissected and post-fixed overnight at 4°C in 4% PFA. The following day, cords were washed for 3 x 10 minutes in PBS and then transferred to 30% (w/v) sucrose (Sigma-Aldrich, UK) solution for 3 days to provide cryoprotection. Spinal cord tissue was then mounted in OCT embedding matrix (Thermoscientific, UK) and stored at -80°C before cryosectioning. 16µm-thick transverse sections were cut using a Leica CM3050 S cryostat (Leica Microsystems, Germany) and mounted onto 0.01% (v/v) poly-l-lysine-coated glass microscope slides (Sigma-Aldrich, UK). Glass slides were stored at -80°C until required for immunohistochemical staining.

6.3.2.8 Immunohistochemical staining of cryosections

Slides were removed from the -80°C freezer and air dried at room temperature for 20 minutes. Sections were post-fixed in a 1:1 mixture of acetone and methanol (both Sigma-Aldrich, UK), pre-cooled to -20°C, for 2 minutes. Acetone/methanol solution was then removed and the slides allowed to air dry for 15 minutes. Following a 5 minute wash with PBS, sections were incubated in 50mM ammonium chloride for 5 minutes. After a further 5 minute PBS wash, non-specific antibody binding was blocked with 3% (w/v) BSA and 1% (v/v) Triton X-100 in PBS for 1 hour. Glass slides were then incubated overnight at 4°C with primary antibodies against synaptophysin and βIII-tubulin (Table 2.2) alongside appropriate isotype

controls (Table 2.3) diluted in 0.1% (w/v) BSA and 0.1% (v/v) Triton X-100 in PBS. The following day 3 x 5 minute washes were performed before incubation with complementary alexa fluor-594 conjugated secondary antibodies (Table 2.4) diluted in 0.1% BSA and 0.1% Triton X-100 for 1 hour at room temperature. Sections were then washed 4 x 5 minutes with PBS before mounting. Fluorescent (section 2.1.3.2) and confocal (section 6.1.3.5.2) images were then acquired of the stained spinal cord tissue.

6.4 Results

6.4.1 Injection of DPPCs into *ex vivo* spinal slice cultures

Progenitor cells were isolated from the dental pulps of 4 week old transgenic "GFP mice" (Okabe *et al*., 1997) and purified using the fibronectin preferential adhesion assay. Mixed populations of adherent cells characterised as $CD90^{+}/CD45^{-}/Nestin^{+}/SCA1^{+}$ (see Appendix III) were micro-injected into *ex vivo* spinal cord slice cultures prepared from 2-4 week old mice. 200,000 cells were injected per slice and cultured for 14 days. Undifferentiated GFP mDPPCs were found to survive within spinal slice cultures, showing signs of proliferation (Figure 6.2), migration (Figure 6.3) and varying morphology (Figure 6.4).

One day after injection, small numbers of cells were typically observed localised to the site of injection (Figure 6.2 B and C). During culture these visibly increased in density, suggesting cellular proliferation, and spread from the initial injection site (Figure 6.2 E and F).

Cells were found to follow distinct migratory pathways within spinal slices. In instances where injected cells did not initially adhere within the tissue, but rather embedded within the matrigel adjacent to the slice, cells were identified migrating into the spinal tissue (Figure 6.3 A – D). Cells appeared to migrate along pre-defined pathways in a column-like fashion. Confocal scanning microscopy identified cells migrating in 3D, indicating that migration was through the tissue as opposed to over the surface of the slice (Figure 6.3 E and F).

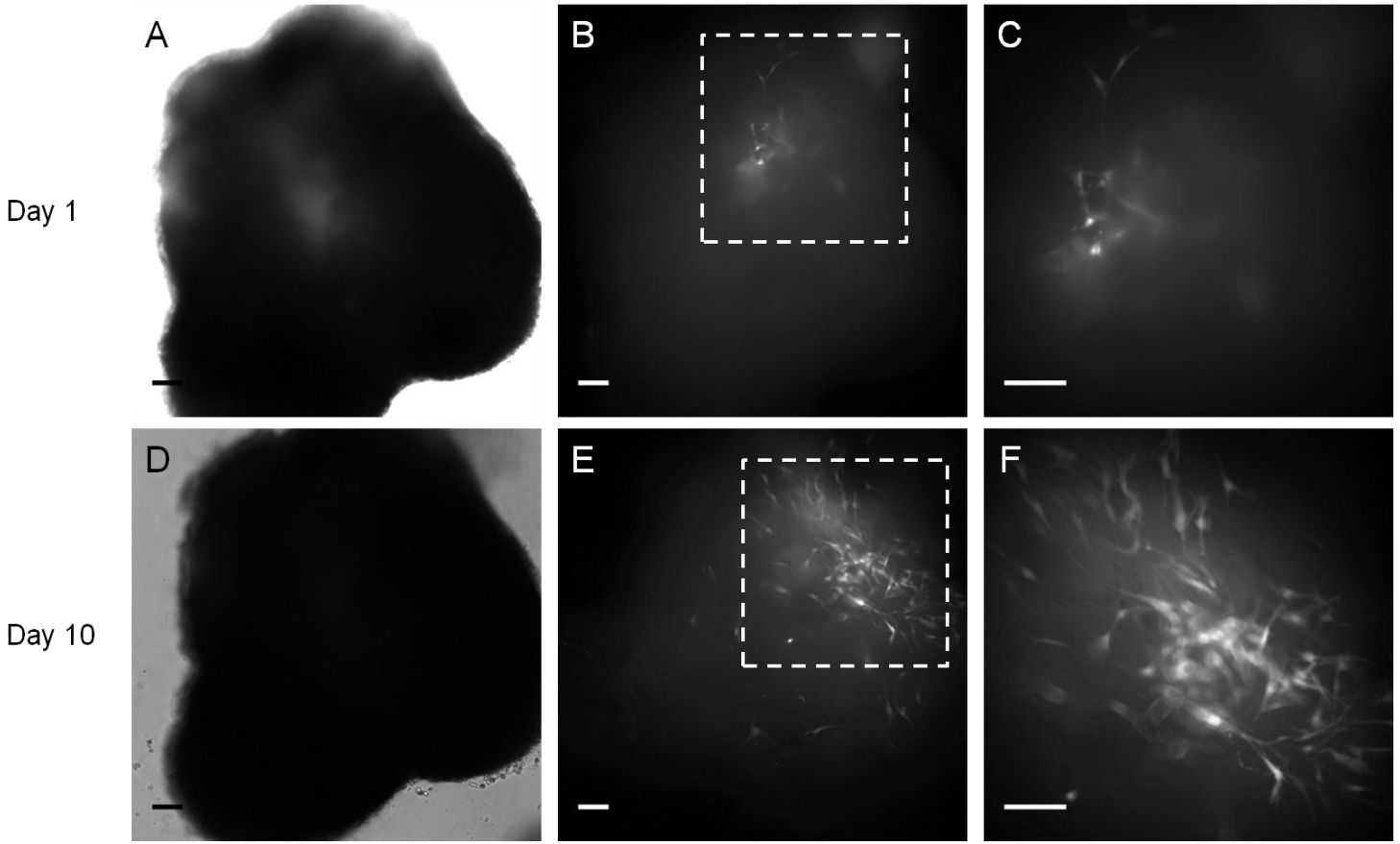

Figure 6.2 – Proliferation of mDPPCs in spinal cord slice cultures

Phase contrast (A & D) and corresponding green fluorescent channel (B, C, E & F) images of *ex vivo* spinal cord slice cultures injected with GFP mDPPCs. A–C) One day after injection, small clusters of concentrated GFP mDPPCs were visible. D – F) By day 10 after injection, increased numbers of cells, which had spread from the original site of injection, were observed. C & F) Higher magnification images of regions represented by boxes (B & E, respectively). Scale bars = 100µm.

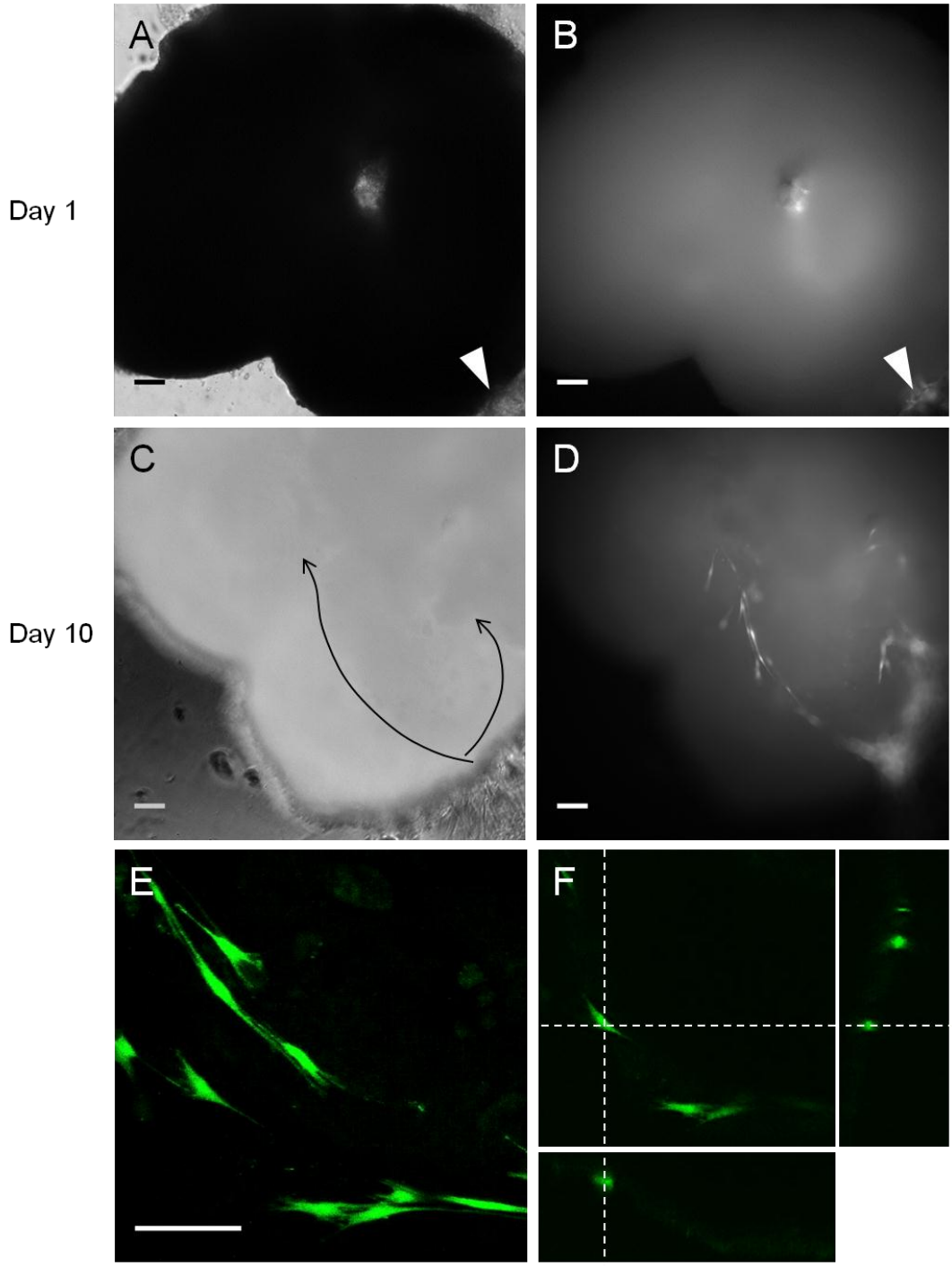

Figure 6.3 – Migration of mDPPCs in spinal cord slice cultures

Phase contrast (A & C) and corresponding green fluorescent channel (B & D) images of *ex vivo* spinal cord slice cultures. A & B) On day 1 following injection, no GFP mDPPCs were visible directly within the slice but a cluster of cells could be seen growing in the matrigel on the periphery (arrowheads). C & D) Over 10 days culture, mDPPCs were observed migrating into the slice following clearly-defined pathways (arrows). E) Maximum projection image of migrating cells acquired from confocal Z scan over a depth of 144µm. F) Image 20 of 72 of the Z stack (E), including XZ and YZ axes, demonstrates migration on different planes, and therefore, through the tissue and not over the surface. Scale bars = 100µm.

Following injection into spinal cord slices, a range of different cellular morphologies were identified amongst GFP mDPPCs. A proportion of cells adopted the branched appearance of astrocytes (Figure 6.4 A), while other cells remained bipolar and fibroblastic-like, typical of undifferentiated DPPCs (Figure 6.4 B). Some interneuron-like long bipolar cells with branched terminals were also identified (Figure 6. 4 C – E).

After 14 days culture, injected spinal slices were fixed and immunohistochemically stained with antibodies against βIII-tubulin to visualise endogenous axonal architecture. Injected DPPCs typically aligned parallel with axons and could be identified interspersed amongst endogenous neuronal cells (Figure 6.5). Long axonal-like projections from DPPCs (Figure 6.5 B, arrowhead) were consistent in size and direction with endogenous neuronal fibres, but βIII-tubulin counter-staining could not be confirmed.

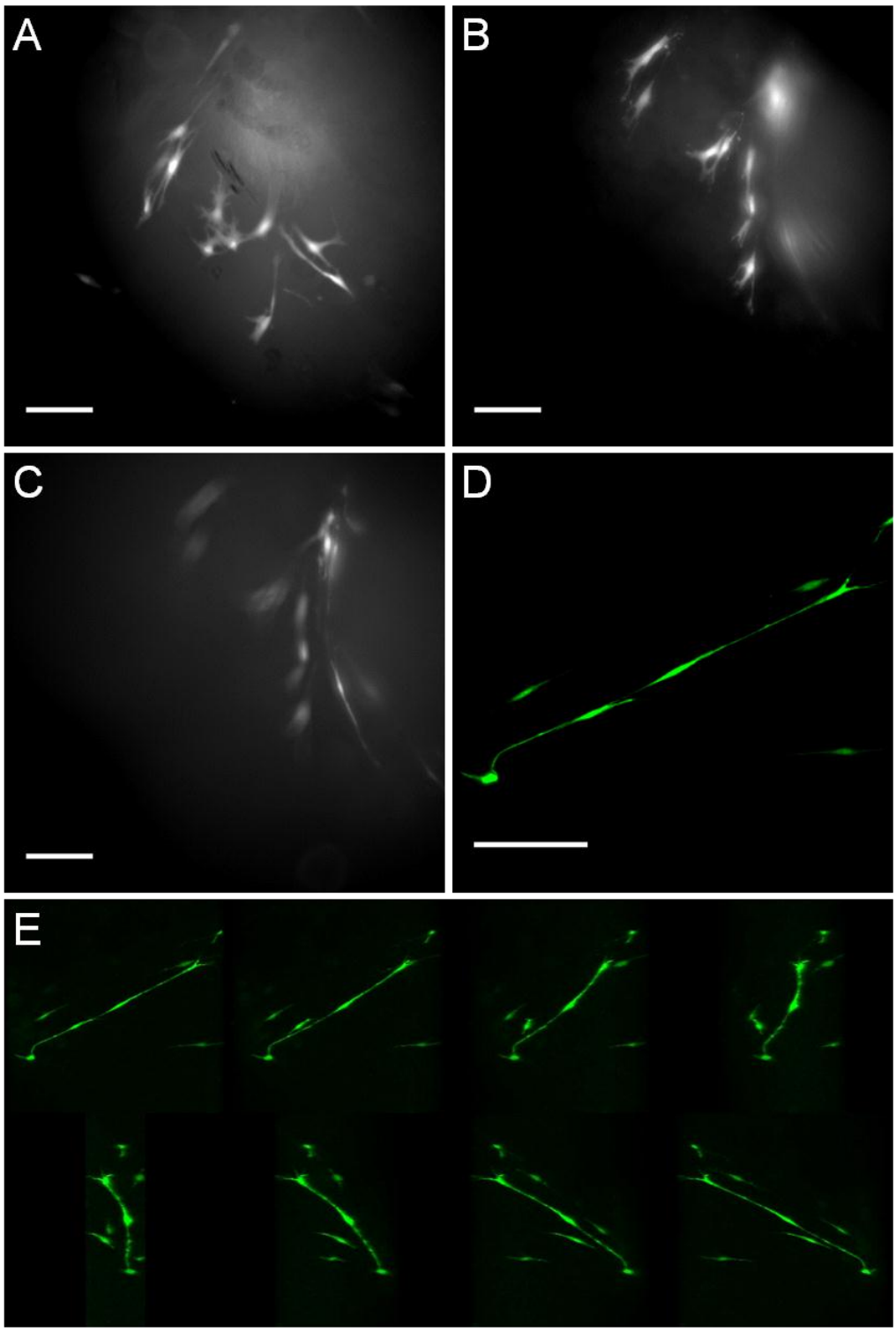

Figure 6.4 – Varied morphologies of mDPPCs in spinal cord slice cultures
10 days after injection into *ex vivo* spinal cord slices GFP mDPPCs were found to adopt a range of different morphologies including: (A) highly-branched astrocyte-like cells, (B) fibroblast-like cells and (C) long bipolar interneuron-like cells. D) Maximum projection image of long bipolar cells acquired from confocal Z scan over a depth of 108µm. E) 20° rotations of a 180° 3D reconstruction of confocal Z scan shown in (D). Scale bars = 100µm.

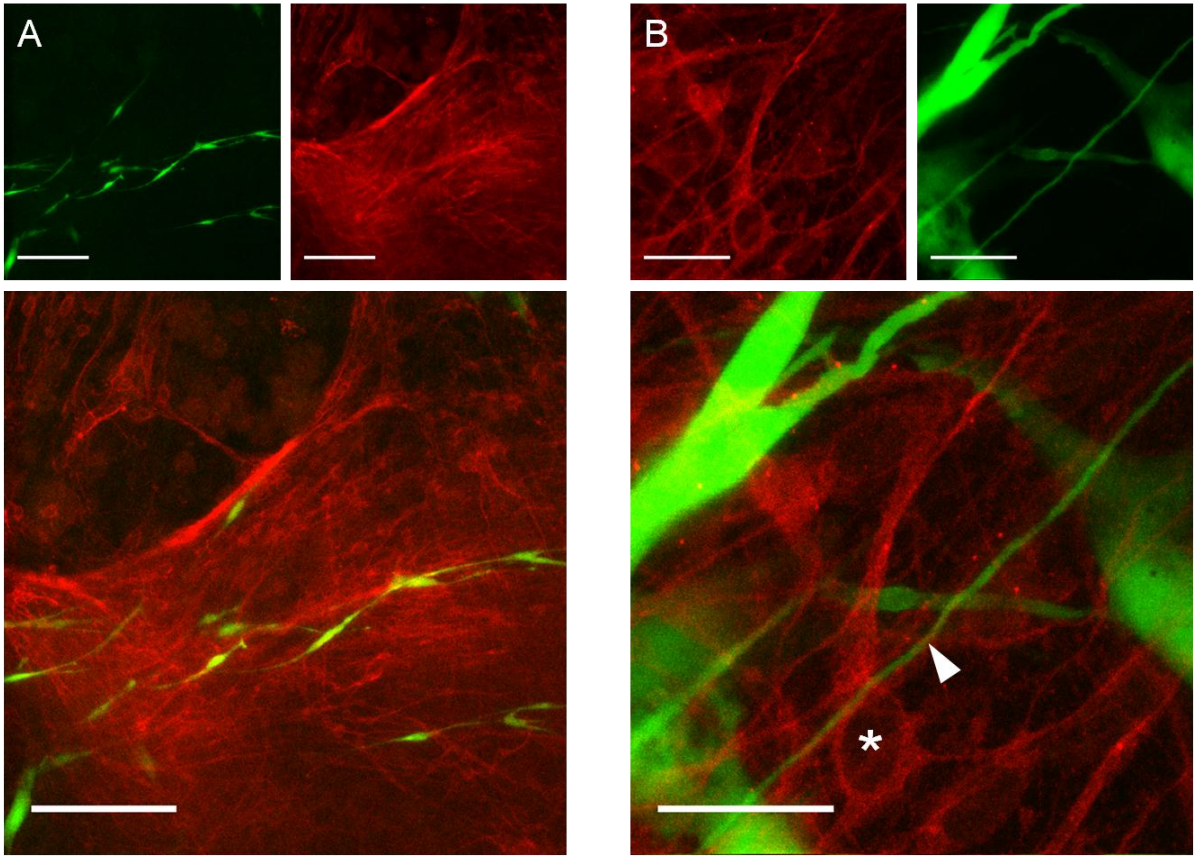

Figure 6.5 – Alignment of GFP mDPPCs along endogenous axonal fibres

Endogenous axons were stained with antibodies against βIII-tubulin (red) 14 days after GFP mDPPC injection into spinal cord slice cultures. A) Maximum projection image of confocal Z stack shows long bipolar DPPCs aligned parallel with axonal fibres. B) Higher magnification two-photon image shows GFP mDPPC axonal-like projection (arrowhead) interspersed among endogenous axons. The cell body of an adjacent interneuron can be easily identified (asterisk). Rabbit IgG isotype control images are shown in Appendix IV. Scale bars = 100µm (A) and 20µm (B).

6.4.2 Injection of oligodendrocyte pre-differentiated DPPCs into *ex vivo* spinal slice cultures

To investigate the effect of pre-differentiation, GFP DPPCs were pre-differentiated into oligodendrocyte-like cells for 5 days prior to injection into spinal cord slices.

As with the injection of undifferentiated DPPCs, concentrated clusters of cells were localised to the site of injection one day after transplantation (Figure 6.6 C and D). However, these cells failed to survive within *ex vivo* spinal slices, reducing in number until only small numbers of viable cells remained after 12 days (Figure 6.6 E and F).

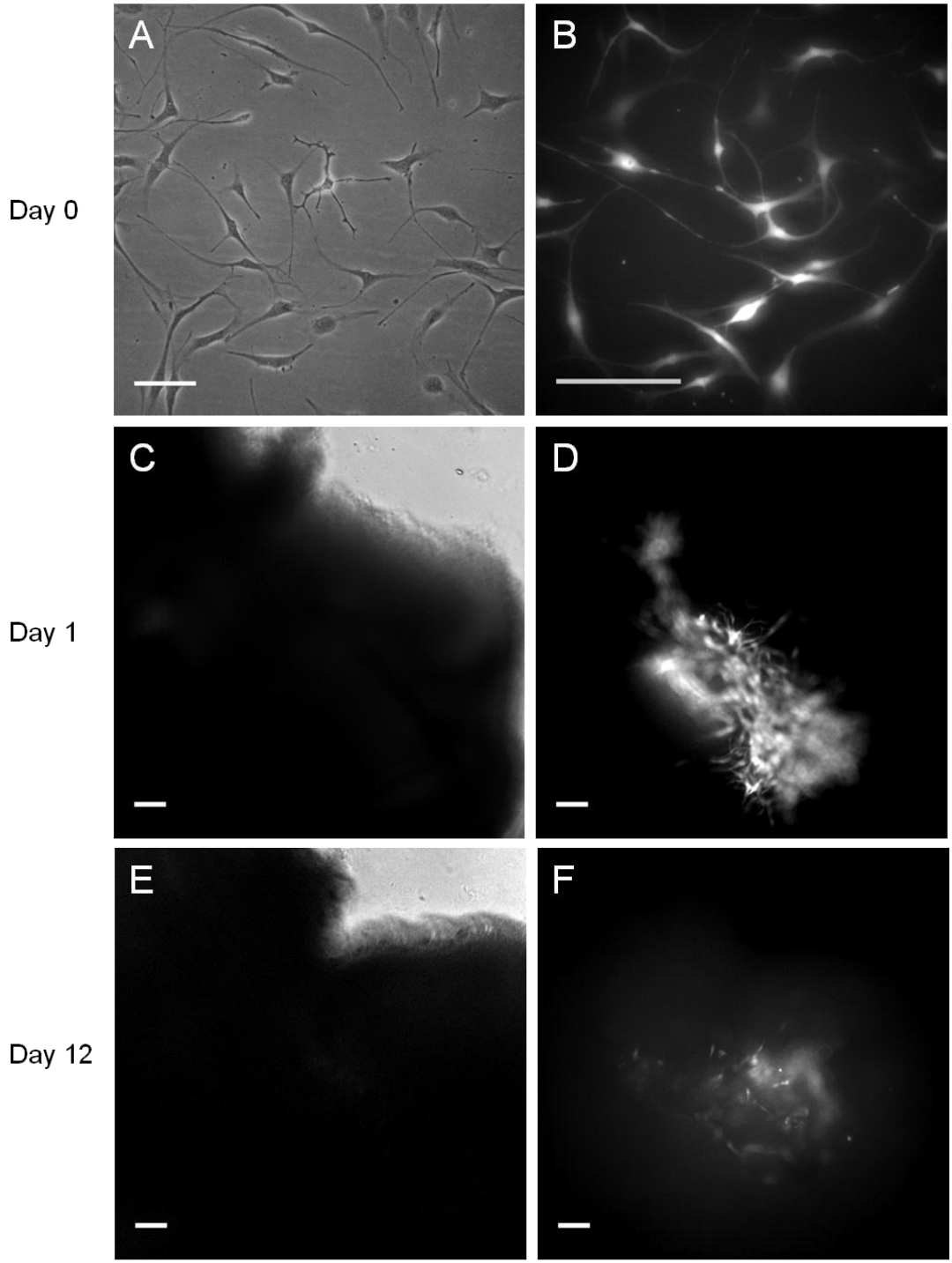

Figure 6.6 – Injection of oligodendrocyte pre-differentiated DPPCs into spinal cord slices
Phase contrast (A) and GFP (B) images of mDPPCs pre-differentiated in OPC medium for 5 days prior to injection into *ex vivo* spinal cord slices. C & D) One day after injection large clusters of cells were visible at the injection site. E & F) By day 12 only small numbers of pre-differentiated cells were left. Scale bars = 100µm.

6.4.3 Injection of neuralised DPPCs into *ex vivo* spinal slice cultures

As an alternative to oligodendrocyte pre-differentiated cells, GFP DPPCs neuralised in NSC medium for 5 days were also injected into spinal slice cultures. Neuralised cells survived and, over 12 days culture, spread from the site of injection (Figure 6.7).

To investigate the integration of injected neuralised cells, after 14 days slice cultures were immunohistochemically stained for synaptophysin, a synaptic vesicle protein, to identify neuronal synapses. In non-injected slices, synaptophysin expression was identified projecting radially from the grey matter (Figure 6.8 A). Synaptophysin expression was more evenly spread throughout the grey matter of injected slices, particularly in regions densely populated with neuralised GFP DPPCs (Figure 6.8 B – D). Higher magnification imaging confirmed the localisation of synaptophysin staining at sites where injected cells came together in close contact, but could not confirm expression by transplanted cells (Figure 6.8 E).

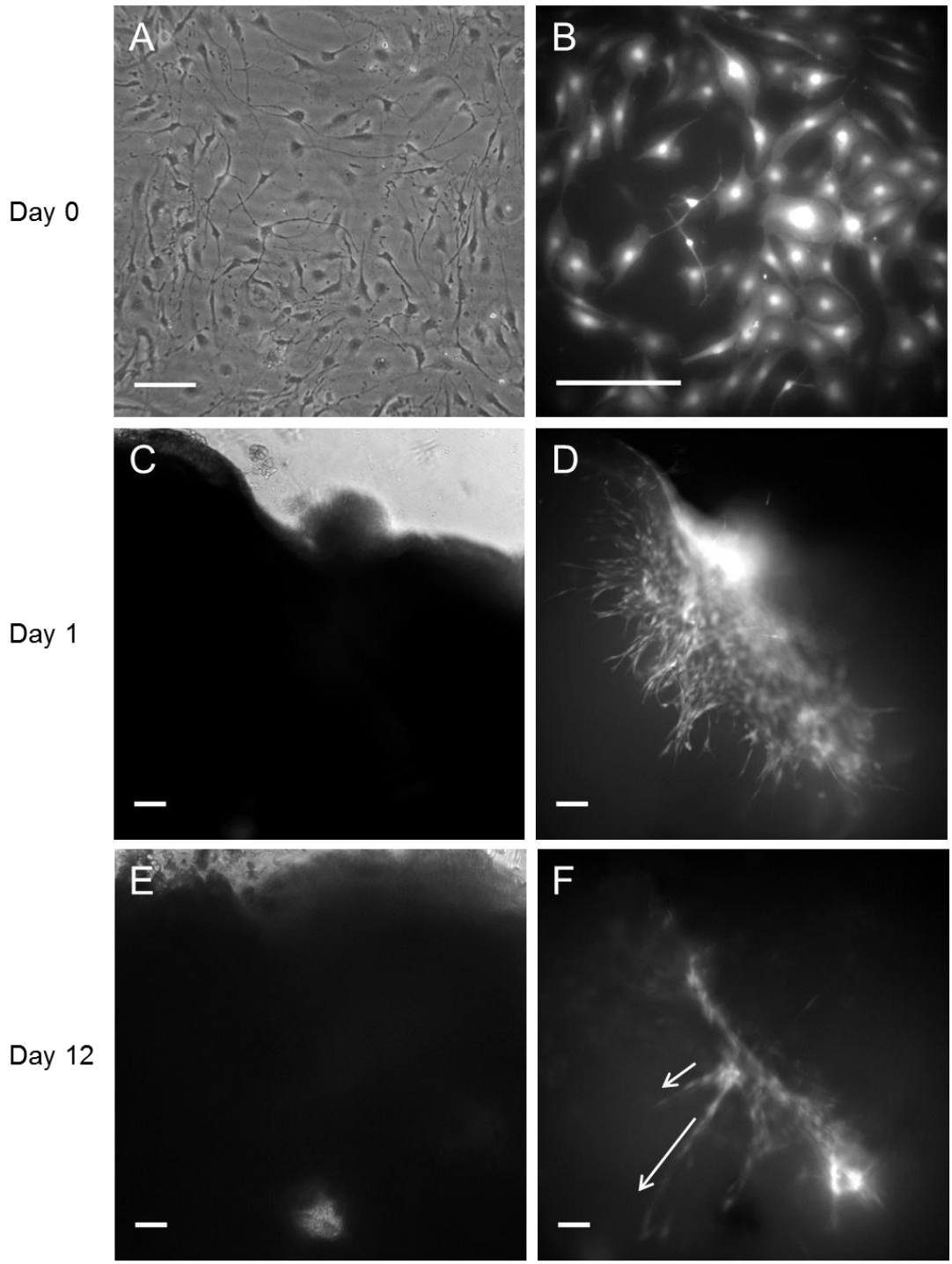

Figure 6.7 – Injection of neuralised mDPPCs into spinal cord slices

Phase contrast (A) and GFP (B) images of mDPPCs neuralised in NSC medium for 5 days prior to injection into *ex vivo* spinal cord slices. C & D) One day after injection large clusters of cells were visible. E & F) By day 12, the transplanted cells were seen extending from injection sites in clearly defined pathways (arrows). Scale bars = 100µm.

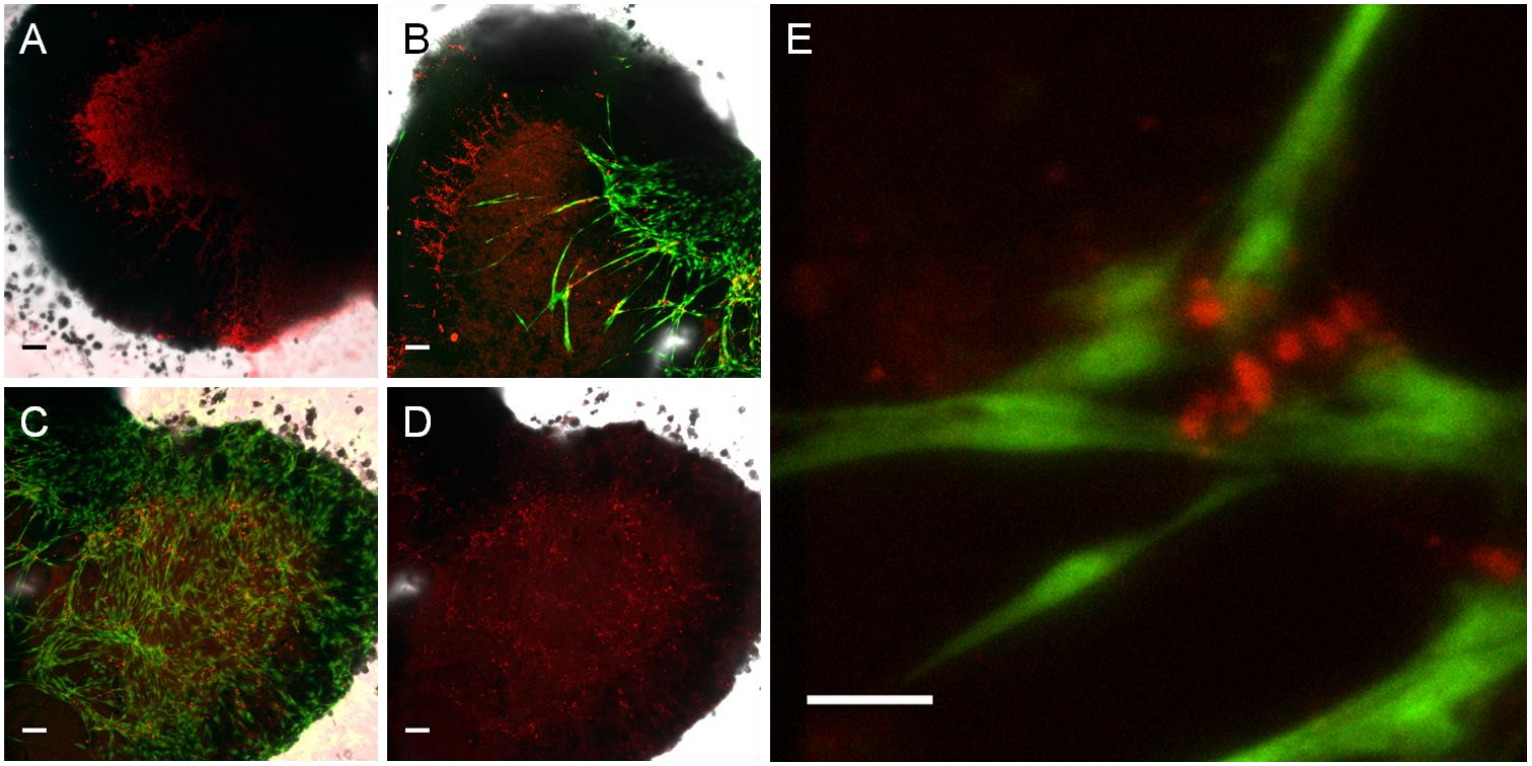

Figure 6.8 – Expression of synaptophysin following neuralised mDPPC injection

Neuronal synapses were stained with antibodies against synaptophysin (red) 14 days after the injection of neuralised GFP mDPPCs into spinal cord slice cultures. A) Maximum projection image of confocal Z scan shows of synaptophysin expression at grey/white matter boundary of a non-injected slice. B) A similar pattern of expression was evident in injected slices with additional staining observed amongst injected GFP DPPCs. C & D) Synaptophysin staining was distributed more evenly throughout the grey matter of densely populated slice cultures, (D) represents the same field of view as (C) with the green fluorescent channel not shown. E) Higher magnification images identified synaptophysin staining localised at cell-cell junctions. Mouse IgG isotype control images are shown in Appendix IV. Scale bars = 100µm (A - D) and 20µm (E).

6.4.4 Injection of neuralised DPPCs into an *in vivo* model of mouse spinal cord injury

As neuralised DPPCs showed signs of promise in *ex vivo* spinal cord slice cultures, surviving and becoming associated with neuronal synapses, this transplantation approach was adopted for an *in vivo* model of spinal cord injury as a pilot study. One week after the induction of a spinal contusion injury in mice, 1 x 10^6 neuralised GFP DPPCs were stereotactically injected at two locations, rostral and caudal to the site of injury. Hindlimb motor functionality was assessed over 4 weeks post-transplantation before spinal tissue was removed and processed for immunohistochemistry.

One day following the induction of SCI, BBB scores of 0 or 1 indicated hindlimb paralysis and, therefore, successful impact surgery (Figure 6.9). No significant reduction in score was observed for the sham surgical treatment group, confirming that paralysis was a result of the impact rather than the surgical procedure itself. One week after impact, no increase in BBB scores was observed and the paralysed mice were randomly divided into two groups: those that received injections of DPPCs and those that were injected with sterile PBS, as a vehicle control. Over 4 weeks following cellular transplantation, locomotor function was found to marginally improve in both DPPC and PBS groups, indicated by increased BBB scores (Figure 6.9). No statistically significant difference in recovery was observed between the groups at any time point.

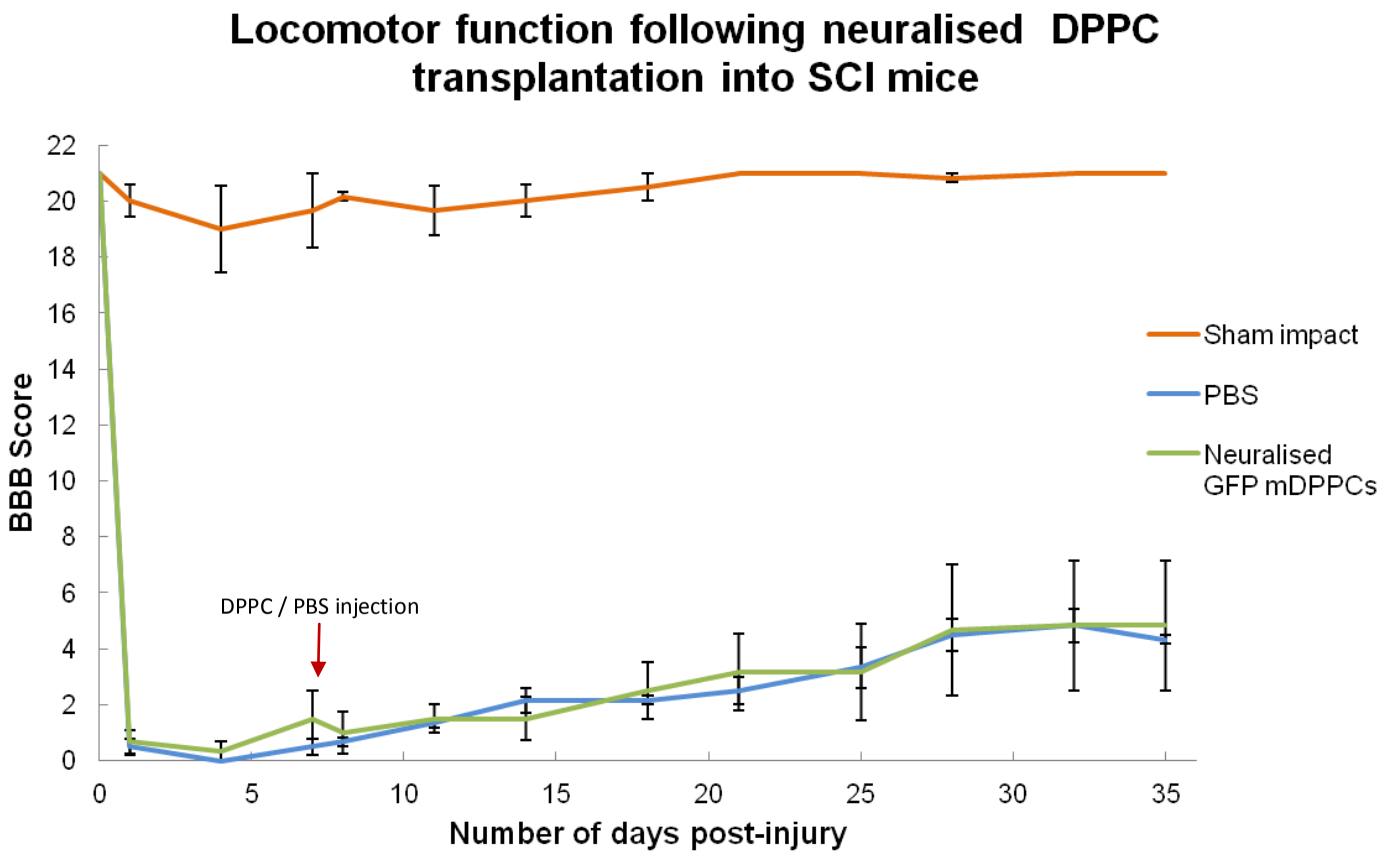

Figure 6.9 – Locomotor function following transplantation of neuralised DPPCs into SCI mice

Neuralised GFP DPPCs were injected into the spinal cords of mice 7 days after induction of an *in vivo* contusion injury. Mice injected with DPPCs (green (n=3)) showed no improvement in functional recovery over PBS injection controls (blue (n=3)). No significant decrease in hindlimb function occured as a result of laminectomy surgery without impact (orange (n=3)). Error bars depict standard error.

Following tissue harvest and cryosectioning, DPPCs were easily identified as having survived within the injured spinal cord for 4 weeks (Figure 6.10). Large clusters of cells were observed localised at the grafting site (Figure 6.10 A – E). Additionally, small numbers of cells were seen to have migrated laterally, over relatively large distances (arrowheads, Figure 6.10 B and D).

Cryosections of spinal tissue were stained immunohistochemically with antibodies against βIII-tubulin and synaptophysin to identify neuronal cells/axonal fibres and synaptic connections, respectively (Figures 6.11 and 6.12). Transplanted neuralised DPPCs were found to stain positive for the neuronal marker βIII-tubulin (Figure 6.11 A – C). Endogenous axonal fibres were identified passing through the grafting site densely populated with transplanted DPPCs (Figure 6.11 A) and appearing to project towards individual cells (Figure 6.11 B and C). As with *ex vivo* cultures (Figure 6.5), GFP mDPPCs were observed to align parallel with endogenous neuronal fibres (Figure 6.11 D). Synaptophysin was associated with transplanted cells (Figure 6.12). However, synaptophysin was not expressed by the DPPCs, but rather localised around individual cells (Figure 6.12 B – D).

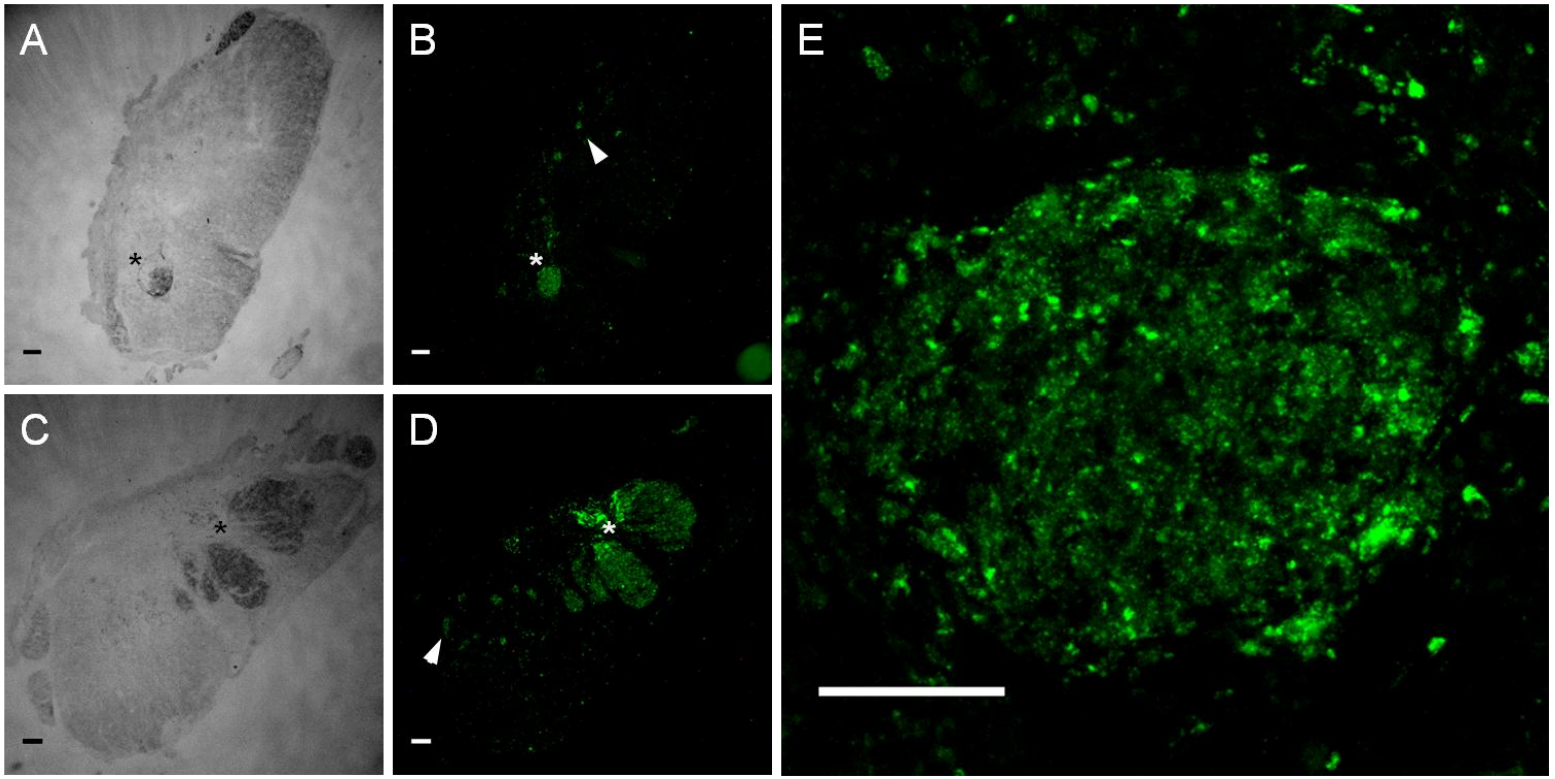

Figure 6.10 – Localisation of neuralised DPPCs following transplantation into SCI mice

Bright field (A & C) and corresponding green fluorescent channel (B & D, respectively) images of 16um-thick cryosections prepared from the spinal cords of SCI mice 4 weeks after transplantation of neuralised DPPCs. Injection sites (asterisks) were easily identified as darker regions of tissue (A & C). B & D) Large numbers of GFP-labelled cells were visible at the grafting sites while small clusters of cells appeared to have migrated laterally over distance (arrowheads). E) High magnification confocal image shows large cluster of cells still present at the site of injection. Scale bars = 100µm (A – D) and 50µm (E).

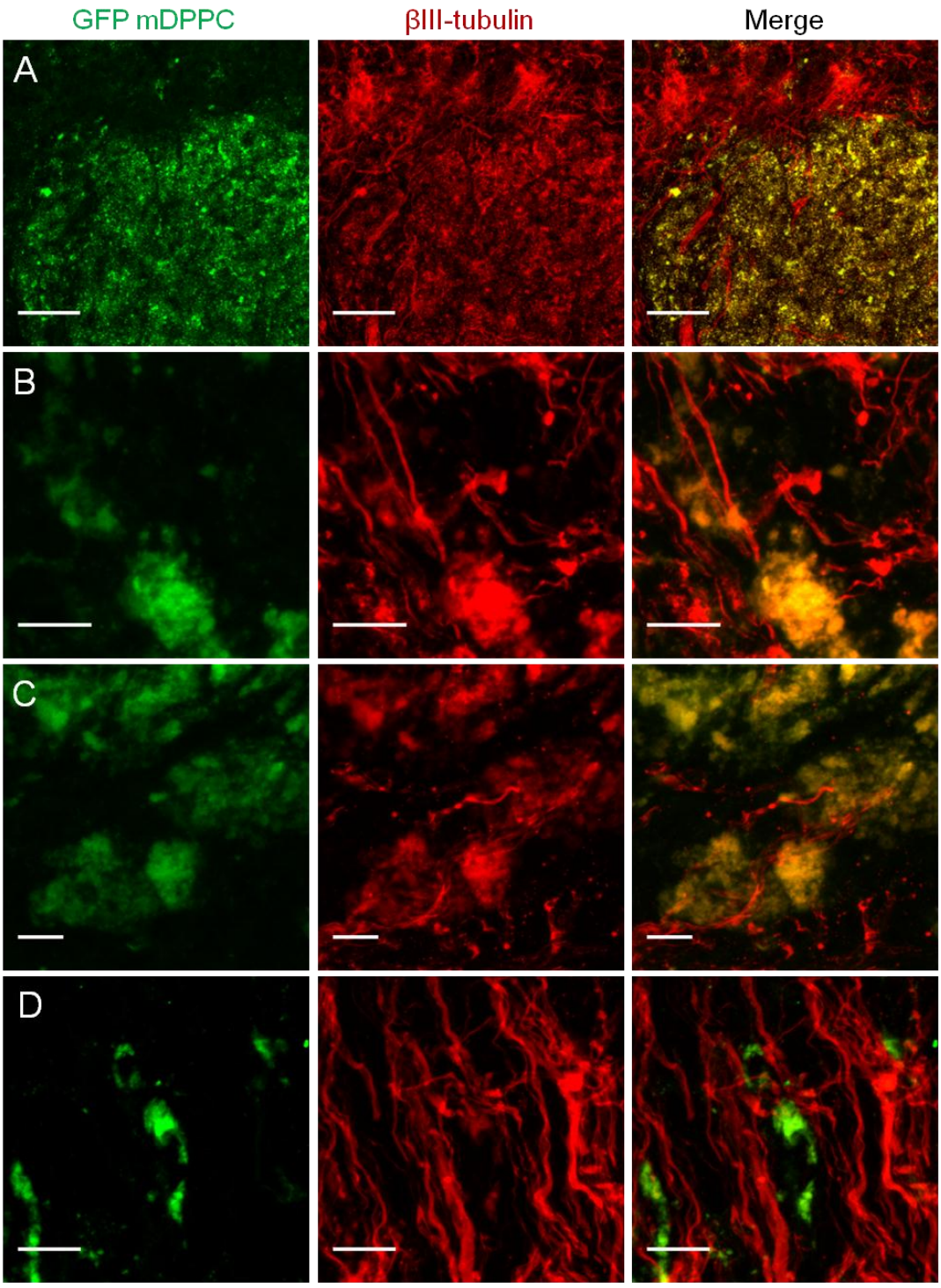

Figure 6.11 – βIII-tubulin staining of transplanted DPPCs

Cryosections prepared from the spinal cords of SCI mice transplanted with neuralised DPPCs were immunohistochemically stained with antibodies against βIII-tubulin (red) and images acquired using confocal microscopy. A) Injected DPPCs were found to stain positive for the neuronal marker βIII-tubulin. B & C) Higher magnification images show endogenous axonal fibres projecting towards transplanted cells. D) DPPCs were identified aligning parallel with neuronal fibres. Isotype controls and images for sham-treated mice can be found in Appendix V. Scale bars = 50µm (A) and 10µm (B – D).

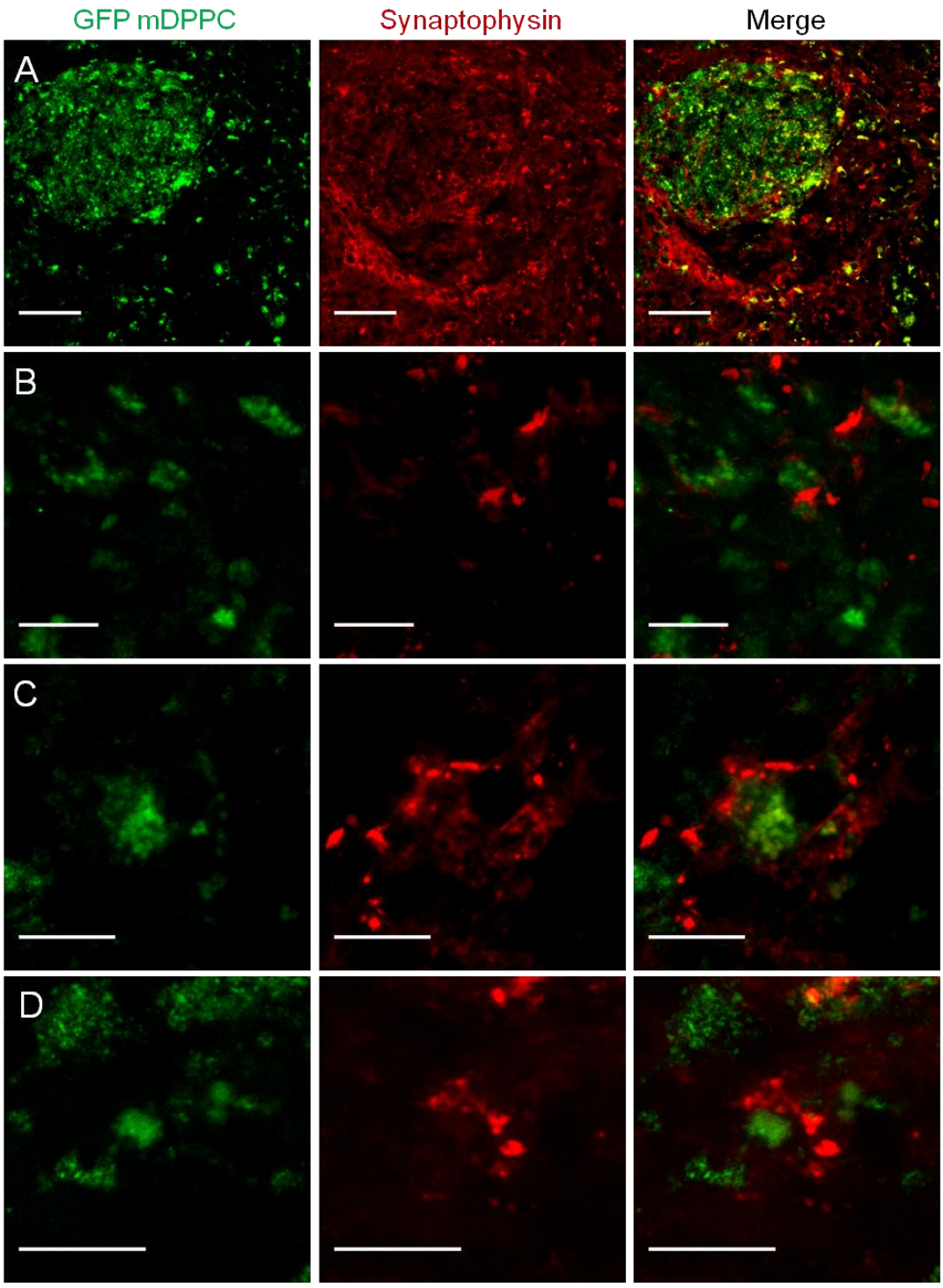

Figure 6.12 – Synaptophysin positivity associated with transplanted DPPCs
Cryosections prepared from the spinal cords of SCI mice transplanted with neuralised DPPCs were immunohistochemically stained with antibodies against synaptophysin (red) and images acquired using confocal microscopy. A) Synaptophysin staining was detected amongst injected DPPCs. B – D) Higher magnification images identified synaptophysin localised around individual transplanted cells but not expressed by the DPPCs themselves. Isotype controls and images for sham-treated mice can be found in Appendix V. Scale bars = 50µm (A) and 10µm (B – D).

6.5 Discussion

This chapter provides the first detailed investigation into the cellular behaviour of DPPCs, both undifferentiated and pre-differentiated, transplanted into spinal cord tissue. This was made possible through the adoption of *ex vivo* slice cultures to allow live imaging of cells. Such regular observations were not possible in previous *in vivo* SCI DPPC studies where detailed analysis could only be performed following tissue harvest at experimental end-points (de Almeida *et al*., 2011; Sakai *et al* 2012).

Undifferentiated DPPCs survived within spinal cord slices showing signs of apparent proliferation, migration, and changes in morphology to suggest differentiation (Figures 6.2 – 6.4). Similar observations have been found after the injection of DPPCs into various regions of the rodent and avian CNS at different developmental stages (Huang *et al*., 2008; Arthur *et al*., 2008 and 2009; Király *et al*., 2011; Fang *et al*., 2013).

GFP mDPPCs appeared to proliferate within spinal cord slices over 14 days culture, as suggested by increased cellular density at the site of grafting (Figure 6.2). Contrastingly, DPPCs isolated from rhesus monkeys showed signs of apoptosis following injection into the mouse hippocampus, indicated by decreases in graft size between days 5 and 30, together with cellular fragmentation (Huang *et al*., 2008). *Ex vivo* slice cultures are avascular and as such, reduced apoptosis as a result of inflammatory defence responses may be expected. A technique, such as BrdU uptake and labelling, would provide scientific confirmation of whether the GFP DPPCs truly did proliferate

within spinal cord slice cultures. This method was adopted by Huang *et al.*, and no labelling of transplanted DPPCs was identified. In a neonatal rat model of cerebral ischaemia, on the other hand, BrdU staining of transplanted DPPCs was observed (Fang *et al*., 2013). The survival and proliferation of DPPCs within the CNS will be dependent upon many environmental factors. Their ability to do this within spinal slice cultures, which mimic hostile conditions of the damaged spinal cord, offers promise for SCI treatment.

Transplanted DPPCs migrated within spinal slice cultures, spreading from the site of injection (Figure 6.3). Often, cells were observed to migrate over long distances along linear clearly-defined pathways (Figures 6.3 and 6.5 D and F). At this stage, it is only possible to speculate on the mechanism promoting such a distinct pattern of migration. One possibility is migration along the border separating the white and grey matter of the spinal cord. Certainly, DPPCs are able to sense and respond to endogenous migratory cues as demonstrated by the localisation of transplanted cells amongst regions of migrating cranial neural crest cells in the developing avian hindbrain (Arthur *et al*., 2008). Similarly, DPPCs injected into cerebrospinal fluid settle and localise within neurogenic regions of newborn rats when healthy (Király *et al*., 2011) or in a model of cerebral ischaemia (Fang *et al*., 2013). The coating of culture plastics with laminin, a major constituent of CNS extracellular matrix, increases the migratory capacity of DPPCs *in vitro* (Howard *et al*., 2010). Additionally, DPPCs produce a number of matrix metalloproteinases (Suri *et al*., 2008; Miyagi *et al*., 2012) that may assist in

three-dimensional migration through tissues. These could potentially help transplanted DPPCs to penetrate the glial scar, of which collagen is a major component (Klapka and Müller, 2006), and enter the site of injury. If the precise mechanisms controlling the observed migration of DPPCs through spinal cord tissue can be elucidated, they could perhaps be harnessed to direct transplanted cells to where they will prove most effective at promoting repair.

Three different morphologies were identified amongst the undifferentiated DPPCs injected into spinal cord slice cultures: branched astrocyte-like cells (Figure 6.4 A), bipolar fibroblastic-like cells (Figure 6.4 B) and long bipolar neuronal-like cells (Figure 6.4 C – E). Although unconfirmed by characterisation techniques, it appears that a proportion of cells may have spontaneously differentiated into astrocytes and neurons, while others remained undifferentiated. The differentiation of astrocyte-like cells, based upon expression of GFAP and/or S100, from DPPCs transplanted into the CNS *in vivo* has been previously reported (de Almeida *et al*., 2011; Fang *et al*., 2013) and so this would not be unexpected. Bipolar neuronal-like cells, similar in appearance to those observed in this chapter, have been identified amongst DPPCs grafted into developing chicken embryos (Arthur *et al*., 2008). Furthermore, these cells express the neuronal markers βIII-tubulin and NF. When *ex vivo* spinal slice cultures were similarly stained with βIII-tubulin antibodies, its expression by transplanted cells could not be confirmed using this immunohistochemical protocol (Figure 6.5). Instead, injected DPPCs were found aligning parallel alongside endogenous neuronal

fibres stained with βIII-tubulin (Figure 6.5 A) and were seen to extend axon-like projections consistent in size and directionality with resident axons (Figure 6.5 B). Further optimisation of the staining protocol would help to confirm whether or not the DPPCs had spontaneously differentiated into βIII-tubulin-positive neuronal-like cells, as their appearance suggests. No differentiation of cells oligodendrocyte-like in morphology was observed in spinal slice cultures. DPPCs expressing oligodendrocyte-associated markers, such as GalC and 04, have been identified following the transplantation of DPPCs into *in vivo* models of SCI (Sakai *et al*., 2012) and stroke (Fang *et al*., 2013).

The pre-differentiation of progenitor/stem cells prior to transplantation enforces a lineage restriction, reducing the potential for differentiation into cell types that may prove detrimental. This approach is commonly adopted with ESCs which may be pre-differentiated into oligodendrocyte (Keirstead *et al*., 2005; Sharp *et al*., 2010) or motorneuron (Deshpande *et al*., 2006; Lee *et al*., 2007) precursor cells prior to injection into SCI models. This methodology provides the advantage that cells partially pre-differentiated can be allowed to mature naturally and integrate in response to endogenous environmental conditions. This study explored the possibility of using a similar approach with DPPCs for SCI. Cells were pre-differentiated for 5 days into neuronal-like cells and oligodendrocyte-like cells using the protocols developed in chapters 4 and 5, respectively, prior to injection into *ex vivo* spinal cord slices.

Oligodendrocyte differentiated DPPCs failed to survive over 12 days in spinal slice cultures (Figure 6.6). Pre-differentiation of DPPCs for 5 days may have resulted in a phenotype that is too mature to withstand the stresses involved in dissociation from culture surfaces and transplantation into spinal tissue. Similar to DPPC derived oligodendrocyte-like cells (chapter 5), hESC-derived oligodendrocyte precursors express SOX10, PDGFRα, A2B5 and Olig1 (Nistor *et al*., 2005; Sharp *et al*., 2010). However, the bipolar morphology of the ESC-derived cells would suggest that they are of a more immature phenotype in comparison to the highly-branched DPPC-derived cells. A shorter period of pre-differentiation in future work could potentially result in greater cell survival, allowing further research into interactions between DPPC-derived oligodendrocyte-cells and the spinal cord.

Neuralised DPPCs, on the other hand, fared better within spinal slice cultures and survived up to 14 days culture in large numbers (Figure 6.7). The neuronal pre-differentiation of DPPCs prior to transplantation has only been described once prior to this study (Király *et al*., 2011). DPPCs, pre-differentiated using a previously published protocol (Király *et al*., 2009), were injected into the cerebrospinal fluid of neonatal rats. Transplanted cells were found to settle within NSC-associated niches and retained a degree of electrophysiological functionality. The authors reported expression of synaptophysin, a protein associated with vesicle release at synapses, nearby grafted cells to suggest integration into neuronal networks. Similarly, following immunohistochemical staining of spinal slice cultures injected with neuralised DPPCs, synaptophysin expression was identified amongst grafted

cells localised at sites of cell-cell contact (Figure 6.8). This expression did not correlate spatially with GFP fluorescence suggesting that it is the endogenous neuronal cells that are trying to form connections with transplanted cells. Synaptophysin expression is associated with the mid-late stages of synaptogenesis (Knaus *et al*., 1986; Liebau *et al*., 2007) and its expression near to transplanted DPPCs suggests a possible integration within neuronal networks.

The *ex vivo* spinal cord slice system used in this chapter proved invaluable for early investigations into the behaviour of transplanted DPPCs and their potential ability to act as a direct replacement for neural cells. However, the model is not without its limitations. During culture, a handful of slices showed signs of significant tissue degradation. This, in itself, does not prove a problem for investigations focusing on neurodegeneration and improving neuronal cell survival (Cho *et al*., 2009; Ravikumar *et al*., 2012). For the exploration of cellular differentiation and replacement, on the other hand, the endogenous tissue architecture should remain intact and therefore spinal cord slices were only maintained in culture for a maximum of 14 days. In addition to the tissue degeneration associated with *ex vivo* slice cultures, no information can be gathered regarding how the findings translate to functionality at the whole body level. *In vivo* animal models allow a longer timeframe for cellular differentiation and integration, as well as enabling the assessment of hindlimb locomotor recovery. As neuralised cells had demonstrated the most promise *ex vivo*, showing signs of potential neuronal

integration, this pre-differentiation approach was selected for transplantation into a murine *in vivo* model of sub-acute contusive SCI.

In the pilot *in vivo* study, no improvements in hindlimb functional recovery were observed as a result of neuralised DPPC transplantation over vehicle controls (Figure 6.9). This contrasts with other studies where functional improvement was observed following the transplantation of DPPCs into SCI injured rodents (de Almeida *et al*., 2011; Sakai *et al*., 2012). Of importance when trying to compare with these reports are the different models of SCI used, the timing of cellular transplantation and the numbers of experimental animals.

Sakai *et al*. (2012) adopted a model where rat spinal cords were subjected to a complete transection injury. Cellular transplantation was performed immediately following the injury and so the improved functional outcomes are almost certainly achieved through neuroprotective mechanisms, rather than regeneration and/or cellular replacement. de Almeida *et al*. (2011) induced an injury in mice through the application of a vascular clip to the exposed spinal cord for 1 minute. Cell transplantation was then performed in the sub-acute (7 days post-injury) or chronic (28 days post-injury) stages. As such, the improvements seen were likely mediated through cell replacement and/or regeneration.

In each of these studies, larger numbers of animals were used for each experimental group than the 3 per group in this chapter. This proves of significance when looking at individual differences between animals of the

same treatment group in the pilot study described in this chapter. At the end of the experiment, 4 weeks after transplantation, each of the 3 vehicle control mice scored BBB ratings of 4 or 5. Mice in the neuralised DPPC transplant group, on the other hand, showed less consistency with scores of 1, 5 and 9 introducing a degree of uncertainty and explaining the large error bars (Figure 6.9). The use of larger numbers of animals would reduce the magnitude of error and allow the identification and removal of any outliers within each group, thereby increasing the chance of finding statistical significance.

The ability of transplanted DPPCs to migrate over large distances in *ex vivo* spinal cord tissue (Figure 6.3) was replicated *in vivo* (Figure 6.10). In addition to large numbers of cells found at the site of grafting (Figure 6.10 E), small groups were identified having migrated laterally from the injection site (arrowheads, Figure 6.10 B and D). Similar observations have been made following transplantation of DPPCs into models of cerebral ischaemia (Yang *et al*., 2009; Sugiyama *et al*., 2011).

Immunohistochemical staining of cryosectioned spinal cord tissue identified βIII-tubulin positivity of transplanted DPPCs (Figure 6.11) suggesting early stage neuronal differentiation. A comprehensive characterisation of the expression of more mature neuronal markers, such as Map2, NF, NeuN or specific neurotransmitter synthesis/receptor proteins, would help to confirm differentiation. This is the first report of the expression of neuronal markers by DPPCs transplanted into the injured spinal cord. Previously, expression of astrocytic and Schwann cell (de Almeida *et al*., 2011) or oligodendrocytic

(Sakai *et al*., 2012), but not neuronal markers, has been detected. Neuralising the cells prior to transplantation will have restricted the potential for differentiation down lineages other than neuronal. This approach could prove feasible for the replacement of dead/damaged neuronal cells with DPPCs in SCI.

As with *ex vivo* spinal cord tissue (Figure 6.8), synaptophysin expression was detected around transplanted neuralised DPPCs (Figure 6.12). This, together with the projection of endogenous axonal fibres in between and towards injected cells (Figure 6.11 A – C), re-enforces the suggestion that endogenous cells are trying to form synaptic connections with transplanted DPPCs. Such a phenomenon has been observed following the transplantation of NSCs into the injured mouse spinal cord, where synaptogenesis with grafted cells resulted in hindlimb functional improvement (Cummings *et al*., 2005). If the neuralised cells truly are integrating within neuronal networks, as this may suggest, then this demonstrates great potential for the use of neuralised DPPCs to repair damaged neuronal-signalling pathways following SCI.

6.6 Summary

- Undifferentiated DPPCs survive within *ex vivo* spinal slice cultures showing signs of proliferation, aligning parallel with endogenous axonal fibres and adopting astrocyte-like and neuron-like morphologies.

- Oligodendrocyte pre-differentiated DPPCs fail to survive following injection into spinal cord slices.

- Neuralised DPPCs survive and may integrate with endogenous cells of the *ex vivo* spinal cord.

- No improvement in functional recovery was observed in a pilot study investigating the transplantation of neuralised DPPCs into an *in vivo* model of mouse SCI.

- Nevertheless, the expression of βIII-tubulin and synaptophysin suggests that DPPCs have neuronally differentiated and may have integrated with endogenous neuronal cells.

Chapter 7: General Discussion

This project set out to identify the ability of DPPCs to directly replace neuronal and oligodendrocyte cells, thereby restoring functionality following a spinal cord injury. Although this question has not been fully answered, significant progress has been made to demonstrate that, at the very least, DPPCs possess great potential to function in this manner. Novel protocols have been developed showcasing the ability of DPPCs to differentiate *in vitro* into oligodendrocyte-like and immature non-functional neuronal-like cells. Using an *ex vivo* model, live imaging of DPPCs injected into spinal cord tissue was performed for the first time, providing fascinating insights into their behaviour. Transplanted DPPCs were demonstrated to possess the ability to proliferate, migrate in response to environmental cues, align parallel with endogenous axonal fibres and adopt neuronal and glial-like morphology, suggesting spontaneous differentiation. Although oligodendrocyte pre-differentiated cells failed to survive post-transplantation, neuronally pre-differentiated cells fared better. Identical observations were made in a clinically relevant *in vivo* model of SCI where transplanted neuralised DPPCs survived following injection into the injured spinal cord and maintained expression of early stage neuronal markers. Endogenous axonal projections towards grafted cells and the expression of synaptophysin suggested possible integration into neuronal signalling pathways, albeit without an associated statistical functional improvement.

The first chapter focused on the isolation and characterisation of both mixed and clonal populations of progenitor cells from the murine dental pulp. Individual differences in the potential for odontoblastic differentiation of clonal

DPPC cultures has previously been reported (Gronthos *et al*., 2002). With regards to neuronal differentiation, individual populations within heterogeneous cultures have been reported to reach different stages of maturity, with only a small proportion (reported as 5 out of 38 cells tested) acquiring the most highly developed phenotype (Király *et al*., 2009). Similarly, outcomes may differ between patient samples subjected to the same differentiation protocol (Aanismaa *et al*., 2012). The extensive characterisation of DPPCs at the clonal level presented in this thesis has, for the first time, enabled the identification of a possible means of distinguishing those cells with enhanced neural differentiation capabilities. DPPC clones with comparatively higher levels of nestin mRNA expression showed greater potential for both neuronal-like and oligodendrocyte-like differentiation, based upon morphology and marker expression. However, the use of single cell-derived clones is unlikely to be therapeutically applicable due to scalability issues within short timeframes. Therefore, in the final chapter of this thesis, focusing on the translational aspects of the work, a heterogeneous population of DPPCs, selected for fibronectin adherence properties was used. The isolation and culture methods used in this study were shown to derive mixed populations with much higher proportions of nestin-expressing cells than the 3.5% previously described for whole pulp cultures (Takeyasu *et al*., 2006). Despite this, cells with little to no nestin expression still remained within the heterogeneous cultures. The ability to purify cells with high levels of nestin mRNA expression immediately following pulpal extraction would provide a population of cells that possess greater potential for functional replacement of neuronal and oligodendrocytes. However, as an

intracellular structural protein, nestin is an unsuitable target for traditional antibody-based fluorescent or magnetic sorting techniques. A potentially similar alternative could be provided by the cell surface antigen A2B5 which is expressed by glial progenitors (Rao and Mayer-Proschel, 1997), neuronal progenitors (Nunes *et al*., 2003) and DPPCs. Selection of DPPCs based on expression of this antigen immediately following pulpal extraction may provide a heterogeneous population of cells with greater potential for neuronal and oligodendrocytic differentiation that may not suffer from scalability issues.

Previous studies have reported functional characteristics of neuronally differentiated DPPCs (Arthur *et al*., 2008; Király *et al*., 2009; Aanismaa *et al*., 2012), but no action potentials or spontaneous electrical activity has been recorded. This project was unsuccessful in the specific objective of developing a definitive protocol for deriving truly functional neuronal-like cells from DPPCs, despite achieving appropriate morphology and marker expression. The initial neuralisation stage of the protocol resulted in downregulation of mesenchymal markers while neuronal-like characteristics concurrently increased. However, the subsequent maturation step failed to elicit an appropriate induction of neurogenic markers. Further optimisation and/or the addition of extra steps to the protocol may be required to induce full functionality. One such possibility would be natural maturation in response to the environmental conditions of the CNS. This was explored in the final chapter by injecting neuralised DPPCs into spinal cord tissue *ex vivo* and *in vivo*. The expression of βIII-tubulin, outgrowth of axonal-like

projections and apparent integration within endogenous neuronal pathways, based upon synaptophysin co-localisation, suggests there may be a degree of functionality in transplanted neuralised DPPCs. Although technically challenging and requiring complicated set-ups, patch clamp recordings can be taken from specific cells within *ex vivo* spinal slice cultures (Yoshimura and Nishi, 1993; Deng and Xu, 2012; Mitra and Brownstone, 2012). Applying such methods to injected *ex vivo* spinal cord slices would provide definitive evidence for whether neuralised DPPCs are capable of replacing, and functionally compensating, for dead neurons following SCI. Certainly, further characterisation of the transplanted cells is required and cryosectioned tissue from the *in vivo* experiment remains available for this purpose.

This thesis presents the first described protocol for the specific differentiation of oligodendrocyte-like cells from DPPCs. Oligodendrocyte-like differentiation *in vitro* has only ever been previously reported as a side effect of neuronal differentiation (Aanismaa *et al*., 2012). This is a significant finding in demonstrating the potential of DPPCs to differentiate into a further cell lineage, additional to mesenchymal cell types, reinforcing their multipotent characteristics. The functionality of the DPPC-derived oligodendrocyte-like cells has yet to be elucidated, although MBP-positivity shows promise for this aspect. The development of a co-culture system with primary neuronal cells, similar to that described by O'Meara *et al*. (2012), would help to determine the ability of oligodendrocyte-like cells to attach to and insulate axons with myelin, demonstrating their functionality. One intriguing prospect would be exploring the possibility of DPPC-derived oligodendrocyte-like cells to

myelinate DPPC-derived neuronal-like cells. Although such a system could prove technically challenging to derive, it would demonstrate great potential for promoting spinal repair through functional cellular replacement. The co-transplantation of ESC-derived oligodendrocyte progenitors and motorneuron progenitors has proven more effective at improving functional outcomes in a rodent model of SCI than either cell type individually (Erceg *et al*., 2010) and this approach could be replicated for DPPC transplantation.

DPPC-derived oligodendrocyte-like cells failed to survive for any significant length of time following injection into *ex vivo* spinal cord tissue. Oligodendrocytes are particularly susceptible to apoptosis within the CNS, being one of the first cell types lost following injury, and can be identified apoptosing at long distances away from actual site of injury (Li *et al*., 1999; Grossman *et al*., 2001). If a method of promoting their survival within spinal slice cultures can be devised, and subsequently applied *in vivo,* enabling the myelination of endogenous axons, DPPC-derived oligodendrocyte-like cells may not only prove successful for promoting recovery after SCI, but could also be applied in demyelinating disorders, such as multiple sclerosis. Optimising the duration of pre-differentiation would provide a solid starting point for increasing transplanted oligodendrocyte-like cell survival in *ex vivo* slice cultures. The addition of growth factors, such as PDGF-aa, may also potentially reduce transplanted cell death. Nevertheless, the development of a specific protocol to derive oligodendrocytes from DPPCs is a significant finding. Not only does it provide a potential new source of cells for CNS transplantation therapies, but it also serves as a useful model for

investigating new mechanisms and roles that DPPCs can play in promoting CNS repair and regeneration.

Previous reports of improved outcome following the transplantation of DPPCs into rodent models of SCI have demonstrated neuroprotective/regenerative effects through the release of soluble factors (de Almeida *et al*., 2011; Sakai *et al*., 2012). The pre-differentiation of DPPCs prior to transplantation, in order to facilitate their ability to directly replace endogenous cells, will not necessarily hinder such paracrine mechanisms of repair. This study has demonstrated changes in the mRNA expression of a range of neurotrophic and growth factors during *in vitro* differentiation into neuronal-like and oligodendrocyte-like cells. Thus, the growth factor release profile of transplanted DPPCs would be altered by pre-differentiation, leading to changes in the precise trophic mechanisms of repair. Quantitative techniques, such as ELISA, should be used to confirm the release of growth factors *in vitro* by DPPCs and the changes that occur as a result of pre-differentiation.

The small scale of the pilot *in vivo* study presented in this thesis did not allow the detection of any statistical improvements in hindlimb function as a result of neuralised DPPC transplantation. This does not mean to say that the cell transplantation was ineffective, rather that more animals may be required for differences to become apparent. If such an experiment was to be performed, alternative avenues of investigation, such as the seeding of cells on a biocompatible scaffold, could be explored as a technique for enhancing the regenerative effects of transplanted DPPCs.

Embryonic stem cells, neural stem cells and bone marrow and adipose tissue-derived mesenchymal stem cells have demonstrated promise in promoting spinal repair, primarily through trophic neuroprotective actions, and have been subject to phase I clinical trials (Keirstead *et al*., 2005; Ra *et al*., 2011; Gupta *et al*., 2012; Park *et al*., 2012). DPPCs possess a distinct advantage over each of these cell types due to the ability to access pulp tissue during routine dental procedures and cryogenically preserve to provide a pool of patient-matched progenitor cells available for use if required (Woods *et al*., 2009). However, a number of challenges remain for the future application of the work presented in this thesis.

In the short term, priority should be given to advancing DPPC oligodendrocyte differentiation to demonstrate their functionality and ability to survive within spinal cord tissue. This work has the potential to open up a range of exciting novel avenues of research. At the same time it would be beneficial to investigate the effects of the differentiation protocols developed in this study on human DPPCs. Although limited experiments have been performed on human cells during these investigations, the differentiation protocols remain to be fully optimised and validated. Transferring to the use of primarily human DPPCs will drastically shorten the length of time between any potential translation of the work into a more clinical setting.

The challenges faced over the long term are less well defined but can be equally applied to the wider research field of stem cells and their potential applications in promoting spinal repair. Namely: the upscaling and isolation of purified stem cells, together with identifying the optimal approach for

cellular transplantation into the injured spinal cord. Progenitor cells represent only a minute fraction of the total pulpal population, and those with potential for neuronal and oligodendrocyte differentiation, based upon expression of nestin, even less so. Reliable ways of extracting, purifying, and expanding cells with these desirable properties on a therapeutic scale have to be devised. Although using neuronally pre-differentiated cells demonstrated promise in the *in vivo* pilot study, this may not be the most effective DPPC phenotype at promoting functional recovery. Undifferentiated or oligodendrocyte pre-differentiated DPPCs represent alternative cell populations that remain to be explored in this model. It may be that co-transplantation of DPPCs at a number of different stages of differentiation, or even in combination with a completely different cell type, such as NSCs, could prove optimal. Despite the need for such future investigations, taken together the results presented in this thesis provide a strong case for DPPCs being able to facilitate functional recovery following SCI through direct cell replacement mechanisms.

References

AANISMAA, R., HAUTALA, J., VUORINEN, A., MIETTINEN, S. & NARKILAHTI, S. 2012. Human dental pulp stem cells differentiate into neural precursors but not into mature functional neurons. *Stem Cell Discovery,* 2**,** 85-91.

ALL, A. H., BAZLEY, F. A., GUPTA, S., PASHAI, N., HU, C., POURMORTEZA, A. & KERR, C. 2012. Human Embryonic Stem Cell-Derived Oligodendrocyte Progenitors Aid in Functional Recovery of Sensory Pathways following Contusive Spinal Cord Injury. *PLoS ONE,* 7.

ALMAZÁN, G., VELA, J. M., MOLINA-HOLGADO, E. & GUAZA, C. 2001. Re-evaluation of nestin as a marker of oligodendrocyte lineage cells. *Microscopy research and technique,* 52**,** 753-765.

AMEMORI, T., ROMANYUK, N., JENDELOVA, P., HERYNEK, V., TURNOVCOVA, K., PROCHAZKA, P., KAPCALOVA, M., COCKS, G., PRICE, J. & SYKOVA, E. 2013. Human conditionally immortalized neural stem cells improve locomotor function after spinal cord injury in the rat. *Stem Cell Research and Therapy,* 4.

ANGHILERI, E., MARCONI, S., PIGNATELLI, A., CIFELLI, P., GALIÉ, M., SBARBATI, A., KRAMPERA, M., BELLUZZI, O. & BONETTI, B. 2008. Neuronal differentiation potential of human adipose-derived mesenchymal stem cells. *Stem Cells and Development,* 17**,** 909-916.

ANTHONY, T. E., KLEIN, C., FISHELL, G. & HEINTZ, N. 2004. Radial glia serve as neuronal progenitors in all regions of the central nervous system. *Neuron,* 41**,** 881-890.

ANTHONY, T. E., MASON, H. A., GRIDLEY, T., FISHELL, G. & HEINTZ, N. 2005. Brain lipid-binding protein is a direct target of Notch signaling in radial glial cells. *Genes and Development,* 19**,** 1028-1033.

ARANA-CHAVEZ, V. E. & MASSA, L. F. 2004. Odontoblasts: The cells forming and maintaining dentine. *International Journal of Biochemistry and Cell Biology,* 36**,** 1367-1373.

ARNETT, H. A., FANCY, S. P. J., ALBERTA, J. A., ZHAO, C., PLANT, S. R., KAING, S., RAINE, C. S., ROWITCH, D. H., FRANKLIN, R. J. M. &

STILES, C. D. 2004. bHLH transcription factor Olig1 is required to repair demyelinated lesions in the CNS. *Science,* 306**,** 2111-2115.

ARSENIJEVIC, Y., VILLEMURE, J. G., BRUNET, J. F., BLOCH, J. J., DÉGLON, N., KOSTIC, C., ZURN, A. & AEBISCHER, P. 2001. Isolation of multipotent neural precursors residing in the cortex of the adult human brain. *Experimental Neurology,* 170**,** 48-62.

ARTHUR, A., RYCHKOV, G., SHI, S., KOBLAR, S. A. & GRONTHOS, S. 2008. Adult human dental pulp stem cells differentiate toward functionally active neurons under appropriate environmental cues. *Stem Cells,* 26**,** 1787-1795.

ARTHUR, A., SHI, S., ZANNETTINO, A. C. W., FUJII, N., GRONTHOS, S. & KOBLAR, S. A. 2009. Implanted adult human dental pulp stem cells induce endogenous axon guidance. *Stem Cells,* 27**,** 2229-2237.

BABCOCK, A. A., KUZIEL, W. A., RIVEST, S. & OWENS, T. 2003. Chemokine expression by glial cells directs leukocytes to sites of axonal injury in the CNS. *Journal of Neuroscience,* 23**,** 7922-7930.

BALIC, A. & MINA, M. 2005. Analysis of developmental potentials of dental pulp in vitro using GFP transgenes. *Orthodontics & craniofacial research.,* 8**,** 252-258.

BALIC, A. & MINA, M. 2010. Characterization of progenitor cells in pulps of murine incisors. *Journal of Dental Research,* 89**,** 1287-1292.

BALIC, A., AGUILA, H. L., CAIMANO, M. J., FRANCONE, V. P. & MINA, M. 2010. Characterization of stem and progenitor cells in the dental pulp of erupted and unerupted murine molars. *Bone,* 46**,** 1639-1651.

BARNABÉ-HEIDER, F., GÖRITZ, C., SABELSTRÖM, H., TAKEBAYASHI, H., PFRIEGER, F. W., MELETIS, K. & FRISÉN, J. 2010. Origin of new glial cells in intact and injured adult spinal cord. *Cell Stem Cell,* 7**,** 470-482.

BASSO, D. M., BEATTIE, M. S. & BRESNAHAN, J. C. 1995. A sensitive and reliable locomotor rating scale for open field testing in rats. *Journal of Neurotrauma,* 12**,** 1-21.

BEAN, B. P. 2007. The action potential in mammalian central neurons. *Nature Reviews Neuroscience,* 8**,** 451-465.

BENOIT, B. O., SAVARESE, T., JOLY, M., ENGSTROM, C. M., PANG, L., REILLY, J., RECHT, L. D., ROSS, A. H. & QUESENBERRY, P. J. 2001. Neurotrophin channeling of neural progenitor cell differentiation. *Journal of Neurobiology,* 46**,** 265-280.

BERNHARD, M., GRIES, A., KREMER, P. & BÖTTIGER, B. W. 2005. Spinal cord injury (SCI) - Prehospital management. *Resuscitation,* 66**,** 127-139.

BOTTAI, D., CIGOGNINI, D., MADASCHI, L., ADAMI, R., NICORA, E., MENARINI, M., DI GIULIO, A. M. & GORIO, A. 2010. Embryonic stem cells promote motor recovery and affect inflammatory cell infiltration in spinal cord injured mice. *Experimental Neurology,* 223**,** 452-463.

BOYD, S. E., NAIR, B., NG, S. W., KEITH, J. M. & ORIAN, J. M. 2012. Computational characterization of 3′ splice variants in the GFAP isoform family. *PLoS ONE,* 7.

BREGMAN, B. S., MCATEE, M., DAI, H. N. & KUHN, P. L. 1997. Neurotrophic factors increase axonal growth after spinal cord injury and transplantation in the adult rat. *Experimental Neurology,* 148**,** 475-494.

BUCHET, D. & BARON-VAN EVERCOOREN, A. 2009. In search of human oligodendroglia for myelin repair. *Neuroscience Letters,* 456**,** 112-119.

BURGER, P. E., XIONG, X., COETZEE, S., SALM, S. N., MOSCATELLI, D., GOTO, K. & WILSON, E. L. 2005. Sca-1 expression identifies stem cells in the proximal region of prostatic ducts with high capacity to reconstitute prostatic tissue. *Proceedings of the National Academy of Sciences of the United States of America,* 102**,** 7180-7185.

BYLUND, M., ANDERSSON, E., NOVITCH, B. G. & MUHR, J. 2003. Vertebrate neurogenesis is counteracted by Sox1-3 activity. *Nature Neuroscience,* 6**,** 1162-1168.

CACERES, A., BANKER, G. A. & BINDER, L. 1986. Immunocytochemical localization of tubulin and microtubule-associated protein 2 during the development of hippocampal neurons in culture. *Journal of Neuroscience,* 6**,** 714-722.

CAO, Q., XU, X. M., DEVRIES, W. H., ENZMANN, G. U., PING, P., TSOULFAS, P., WOOD, P. M., BUNGE, M. B. & WHITTEMORE, S. R. 2005. Functional recovery in traumatic spinal cord injury after transplantation of multineurotrophin-expressing glial-restricted precursor cells. *Journal of Neuroscience,* 25**,** 6947-6957.

CASHA, S., YU, W. R. & FEHLINGS, M. G. 2001. Oligodendroglial apoptosis occurs along degenerating axons and is associated with FAS and p75 expression following spinal cord injury in the rat. *Neuroscience,* 103**,** 203-218.

CASHA, S., ZYGUN, D., MCGOWAN, M. D., BAINS, I., YONG, V. W. & JOHN HURLBERT, R. 2012. Results of a phase II placebo-controlled randomized trial of minocycline in acute spinal cord injury. *Brain,* 135**,** 1224-1236.

CHAI, Y., JIANG, X., ITO, Y., BRINGAS JR, P., HAN, J., ROWITCH, D. H., SORIANO, P., MCMAHON, A. P. & SUCOV, H. M. 2000. Fate of the mammalian cranial neural crest during tooth and mandibular morphogenesis. *Development,* 127**,** 1671-1679.

CHEN, B. Y., WANG, X., WANG, Z. Y., WANG, Y. Z., CHEN, L. W. & LUO, Z. J. 2013. Brain-derived neurotrophic factor stimulates proliferation and differentiation of neural stem cells, possibly by triggering the Wnt/β-catenin signaling pathway. *Journal of Neuroscience Research,* 91**,** 30-41.

CHIBA, Y., KURODA, S., MARUICHI, K., OSANAI, T., HOKARI, M., YANO, S., SHICHINOHE, H., HIDA, K. & IWASAKI, Y. 2009. Transplanted bone

marrow stromal cells promote axonal regeneration and improve motor function in a rat spinal cord injury model. *Neurosurgery,* 64**,** 991-999.

CHO, J. S., PARK, H. W., PARK, S. K., ROH, S., KANG, S. K., PAIK, K. S. & CHANG, M. S. 2009. Transplantation of mesenchymal stem cells enhances axonal outgrowth and cell survival in an organotypic spinal cord slice culture. *Neuroscience Letters,* 454**,** 43-48.

COLLO, G., GOFFI, F., MERLO PICH, E., BALDELLI, P., BENFENATI, F. & SPANO, P. 2006. Immature neuronal phenotype derived from mouse skin precursor cells differentiated in vitro. *Brain Research,* 1109**,** 32-36.

CORBEIL, D., MARZESCO, A. M., WILSCH-BRÄUNINGER, M. & HUTTNER, W. B. 2010. The intriguing links between prominin-1 (CD133), cholesterol-based membrane microdomains, remodeling of apical plasma membrane protrusions, extracellular membrane particles, and (neuro)epithelial cell differentiation. *FEBS Letters,* 584**,** 1659-1664.

CORFAS, G., VELARDEZ, M. O., KO, C. P., RATNER, N. & PELES, E. 2004. Mechanisms and roles of axon-Schwann cell interactions. *Journal of Neuroscience,* 24**,** 9250-9260.

CUMMINGS, B. J., UCHIDA, N., TAMAKI, S. J., SALAZAR, D. L., HOOSHMAND, M., SUMMERS, R., GAGE, F. H. & ANDERSON, A. J. 2005. Human neural stem cells differentiate and promote locomotor recovery in spinal cord-injured mice. *Proceedings of the National Academy of Sciences of the United States of America,* 102**,** 14069-14074.

DAI, X., LERCHER, L. D., CLINTON, P. M., DU, Y., LIVINGSTON, D. L., VIEIRA, C., YANG, L., SHEN, M. M. & DREYFUS, C. F. 2003. The trophic role of oligodendrocytes in the basal forebrain. *Journal of Neuroscience,* 23**,** 5846-5853.

DAVIES, L. C., LOCKE, M., WEBB, R. D. J., ROBERTS, J. T., LANGLEY, M., THOMAS, D. W., ARCHER, C. W. & STEPHENS, P. 2010. A multipotent neural crest-derived progenitor cell population is resident within the oral mucosa lamina propria. *Stem Cells and Development,* 19**,** 819-830.

DE ALMEIDA, F. M., MARQUES, S. A., RAMALHO, B. D. S., RODRIGUES, R. F., CADILHE, D. V., FURTADO, D., KERKIS, I., PEREIRA, L. V., REHEN, S. K. & MARTINEZ, A. M. B. 2011. Human dental pulp cells: A new source of cell therapy in a mouse model of compressive spinal cord injury. *Journal of Neurotrauma,* 28**,** 1939-1949.

DENG, P. & XU, Z. C. 2012. Whole-cell patch-clamp recordings on spinal cord slices.

DEMIRCAN, P. C., SARIBOYACI, A. E., UNAL, Z. S., GACAR, G., SUBASI, C. & KARAOZ, E. 2011. Immunoregulatory effects of human dental pulp-derived stem cells on T cells: Comparison of transwell co-culture and mixed lymphocyte reaction systems. *Cytotherapy,* 13**,** 1205-1220.

DESHPANDE, D. M., KIM, Y. S., MARTINEZ, T., CARMEN, J., DIKE, S., SHATS, I., RUBIN, L. L., DRUMMOND, J., KRISHNAN, C., HOKE, A., MARAGAKIS, N., SHEFNER, J., ROTHSTEIN, J. D. & KERR, D. A. 2006. Recovery from paralysis in adult rats using embryonic stem cells. *Annals of Neurology,* 60**,** 32-44.

DOETSCH, F., CAILLE, I., LIM, D. A., GARCIA-VERDUGO, J. M. & ALVAREZ-BUYLLA, A. 1999. Subventricular zone astrocytes are neural stem cells in the adult mammalian brain. *Cell,* 97**,** 703-716.

DOMINICI, M., LE BLANC, K., MUELLER, I., SLAPER-CORTENBACH, I., MARINI, F. C., KRAUSE, D. S., DEANS, R. J., KEATING, A., PROCKOP, D. J. & HORWITZ, E. M. 2006. Minimal criteria for defining multipotent mesenchymal stromal cells. The International Society for Cellular Therapy position statement. *Cytotherapy,* 8**,** 315-317.

DOWTHWAITE, G. P., BISHOP, J. C., REDMAN, S. N., KHAN, I. M., ROONEY, P., EVANS, D. J. R., HAUGHTON, L., BAYRAM, Z., BOYER, S., THOMSON, B., WOLFE, M. S. & ARCHER, C. W. 2004. The surface of articular cartilage contains a progenitor cell populations. *Journal of Cell Science,* 117**,** 889-897.

DREYFUS, C. F., DAI, X., LERCHER, L. D., RACEY, B. R., FRIEDMAN, W. J. & BLACK, I. B. 1999. Expression of neurotrophins in the adult spinal cord in vivo. *Journal of Neuroscience Research,* 56**,** 1-7.

DYER, C. A. & MATTHIEU, J. M. 1994. Antibodies to myelin/oligodendrocyte-specific protein and myelin/oligodendrocyte glycoprotein signal distinct changes in the organization of cultured oligodendroglial membrane sheets. *Journal of Neurochemistry,* 62**,** 777-787.

EL KARIM, I. A., LINDEN, G. J., CURTIS, T. M., ABOUT, I., MCGAHON, M. K., IRWIN, C. R., KILLOUGH, S. A. & LUNDY, F. T. 2011. Human dental pulp fibroblasts express the "cold-sensing" transient receptor potential channels TRPA1 and TRPM8. *Journal of Endodontics,* 37**,** 473-478.

ENGEL, U. & WOLSWIJK, G. 1996. Oligodendrocyte-type-2 astrocyte (O-2A) progenitor cells derived from adult rat spinal cord: In vitro characteristics and response to PDGF, bFGF and NT-3. *GLIA,* 16**,** 16-26.

ERCEG, S., RONAGHI, M., ORIA, M., ROSELLÓ, M. G., ARAGÓ, M. A. P., LOPEZ, M. G., RADOJEVIC, I., MORENO-MANZANO, V., RODRÍGUEZ-JIMÉNEZ, F. J., BHATTACHARYA, S. S., CORDOBA, J. & STOJKOVIC, M. 2010. Transplanted oligodendrocytes and motoneuron progenitors generated from human embryonic stem cells promote locomotor recovery after spinal cord transection. *Stem Cells,* 28**,** 1541-1549.

ERICSON, J., RASHBASS, P., SCHEDL, A., BRENNER-MORTON, S., KAWAKAMI, A., VAN HEYNINGEN, V., JESSELL, T. M. & BRISCOE, J. 1997. Pax6 controls progenitor cell identity and neuronal fate in response to graded Shh signaling. *Cell,* 90**,** 169-180.

FANG, C. Z., YANG, Y. J., WANG, Q. H., YAO, Y., ZHANG, X. Y. & HE, X. H. 2013. Intraventricular Injection of Human Dental Pulp Stem Cells Improves Hypoxic-Ischemic Brain Damage in Neonatal Rats. *PLoS ONE,* 8.

FAULKNER, J. & KEIRSTEAD, H. S. 2005. Human embryonic stem cell-derived oligodendrocyte progenitors for the treatment of spinal cord injury. *Transplant Immunology,* 15**,** 131-142.

FEHLINGS, M. G., THEODORE, N., HARROP, J., MAURAIS, G., KUNTZ, C., SHAFFREY, C. I., KWON, B. K., CHAPMAN, J., YEE, A., TIGHE, A. & MCKERRACHER, L. 2011. A phase I/IIa clinical trial of a recombinant Rho protein antagonist in acute spinal cord injury. *Journal of Neurotrauma,* 28**,** 787-796.

FEHLINGS, M. G., WILSON, J. R., FRANKOWSKI, R. F., TOUPS, E. G., AARABI, B., HARROP, J. S., SHAFFREY, C. I., HARKEMA, S. J., GUEST, J. D., TATOR, C. H., BURAU, K. D., JOHNSON, M. W. & GROSSMAN, R. G. 2012. Riluzole for the treatment of acute traumatic spinal cord injury: rationale for and design of the NACTN Phase I clinical trial. *Journal of Neurosurgery. Spine,* 17**,** 151-156.

FLEMING, J. C., NORENBERG, M. D., RAMSAY, D. A., DEKABAN, G. A., MARCILLO, A. E., SAENZ, A. D., PASQUALE-STYLES, M., DIETRICH, W. D. & WEAVER, L. C. 2006. The cellular inflammatory response in human spinal cords after injury. *Brain,* 129**,** 3249-3269.

FOGARTY, M., RICHARDSON, W. D. & KESSARIS, N. 2005. A subset of oligodendrocytes generated from radial glia in the dorsal spinal cord. *Development,* 132**,** 1951-1959.

GARD, A. L. & PFEIFFER, S. E. 1990. Two proliferative stages of the oligodendrocyte lineage (A2B5+O4- and O4+GalC-) under different mitogenic control. *Neuron,* 5**,** 615-625.

GENOVESE, T. & CUZZOCREA, S. 2008. Role of free radicals and poly (ADP-Ribose)Polymerase-1 in the development of spinal cord injury: New potential therapeutic targets. *Current Medicinal Chemistry,* 15**,** 477-487.

GOLDBERG, M., FARGES, J. C., LACERDA-PINHEIRO, S., SIX, N., JEGAT, N., DECUP, F., SEPTIER, D., CARROUEL, F., DURAND, S., CHAUSSAIN-MILLER, C., DENBESTEN, P., VEIS, A. & POLIARD, A.

2008. Inflammatory and immunological aspects of dental pulp repair. *Pharmacological Research,* 58**,** 137-147.

GONZALEZ-MARTINEZ, T., PEREZ-PIÑERA, P., DÍAZ-ESNAL, B. & VEGA, J. A. 2003. S-100 proteins in the human peripheral nervous system. *Microscopy research and technique,* 60**,** 633-638.

GOVINDASAMY, V., ABDULLAH, A. N., RONALD, V. S., MUSA, S., CHE AB. AZIZ, Z. A., ZAIN, R. B., TOTEY, S., BHONDE, R. R. & ABU KASIM, N. H. 2010. Inherent Differential Propensity of Dental Pulp Stem Cells Derived from Human Deciduous and Permanent Teeth. *Journal of Endodontics,* 36**,** 1504-1515.

GRAHAM, V., KHUDYAKOV, J., ELLIS, P. & PEVNY, L. 2003. SOX2 functions to maintain neural progenitor identity. *Neuron,* 39**,** 749-765.

GRAVEL, M., PETERSON, J., YONG, V. W., KOTTIS, V., TRAPP, B. & BRAUN, P. E. 1996. Overexpression of 2',3'-cyclic nucleotide 3'-phosphodiesterase in transgenic mice alters oligodendrocyte development and produces aberrant myelination. *Molecular and Cellular Neurosciences,* 7**,** 453-466.

GREGORI, N., PRÖSCHEL, C., NOBLE, M. & MAYER-PRÖSCHEL, M. 2002. The tripotential glial-restricted precursor (GRP) cell and glial development in the spinal cord: Generation of bipotential oligodendrocyte-type-2 astrocyte progenitor cells and dorsal-ventral differences in GRP cell function. *Journal of Neuroscience,* 22**,** 248-256.

GRITTI, A., PARATI, E. A., COVA, L., FROLICHSTHAL, P., GALLI, R., WANKE, E., FARAVELLI, L., MORASSUTTI, D. J., ROISEN, F., NICKEL, D. D. & VESCOVI, A. L. 1996. Multipotential stem cells from the adult mouse brain proliferate and self-renew in response to basic fibroblast growth factor. *Journal of Neuroscience,* 16**,** 1091-1100.

GRONTHOS, S., MANKANI, M., BRAHIM, J., ROBEY, P. G. & SHI, S. 2000. Postnatal human dental pulp stem cells (DPSCs) in vitro and in vivo. *Proceedings of the National Academy of Sciences of the United States of America,* 97**,** 13625-13630.

GRONTHOS, S., BRAHIM, J., LI, W., FISHER, L. W., CHERMAN, N., BOYDE, A., DENBESTEN, P., ROBEY, P. G. & SHI, S. 2002. Stem cell properties of human dental pulp stem cells. *Journal of Dental Research,* 81**,** 531-535.

GROS, T., SAKAMOTO, J. S., BLESCH, A., HAVTON, L. A. & TUSZYNSKI, M. H. 2010. Regeneration of long-tract axons through sites of spinal cord injury using templated agarose scaffolds. *Biomaterials,* 31**,** 6719-6729.

GROSSMAN, S. D., ROSENBERG, L. J. & WRATHALL, J. R. 2001. Temporal-spatial pattern of acute neuronal and glial loss after spinal cord contusion. *Experimental Neurology,* 168**,** 273-282.

GUIMARÃES, E. T., CRUZ, G. S., DE JESUS, A. A., LACERDA DE CARVALHO, A. F., ROGATTO, S. R., PEREIRA, L. D. V., RIBEIRO-DOS-SANTOS, R. & SOARES, M. B. P. 2011. Mesenchymal and embryonic characteristics of stem cells obtained from mouse dental pulp. *Archives of Oral Biology,* 56**,** 1247-1255.

GUPTA, N., HENRY, R. G., STROBER, J., KANG, S. M., LIM, D. A., BUCCI, M., CAVERZASI, E., GAETANO, L., MANDELLI, M. L., RYAN, T., PERRY, R., FARRELL, J., JEREMY, R. J., ULMAN, M., HUHN, S. L., BARKOVICH, A. J. & ROWITCH, D. H. 2012. Neural stem cell engraftment and myelination in the human brain. *Science Translational Medicine,* 4**,** 155ra137.

GUTH, L., ZHANG, Z. & STEWARD, O. 1999. The unique histopathological responses of the injured spinal cord. Implications for neuroprotective therapy. *Annals of the New York Academy of Sciences,* 890**,** 366-384.

HACHEM, S., AGUIRRE, A., VIVES, V., MARKS, A., GALLO, V. & LEGRAVEREND, C. 2005. Spatial and temporal expression of S100B in cells of oligodendrocyte lineage. *GLIA,* 51**,** 81-97.

HAINFELLNER, J. A., VOIGTLÄNDER, T., STRÖBEL, T., MAZAL, P. R., MADDALENA, A. S., AGUZZI, A. & BUDKA, H. 2001. Fibroblasts can express glial fibrillary acidic protein (GFAP) in vivo. *Journal of Neuropathology and Experimental Neurology,* 60**,** 449-461.

HAN, S. S. W., LIU, Y., TYLER-POLSZ, C., RAO, M. S. & FISCHER, I. 2004. Transplantation of Glial-Restricted Precursor Cells into the Adult Spinal Cord: Survival, Glial-Specific Differentiation, and Preferential Migration in White Matter. *GLIA,* 45**,** 1-16.

HARADA, H., KETTUNEN, P., JUNG, H. S., MUSTONEN, T., WANG, Y. A. & THESLEFF, I. 1999. Localization of putative stem cells in dental epithelium and their association with Notch and FGF signaling. *Journal of Cell Biology,* 147**,** 105-120.

HATAMI, M., MEHRJARDI, N. Z., KIANI, S., HEMMESI, K., AZIZI, H., SHAHVERDI, A. & BAHARVAND, H. 2009. Human embryonic stem cell-derived neural precursor transplants in collagen scaffolds promote recovery in injured rat spinal cord. *Cytotherapy,* 11**,** 618-630.

HAWRYLUK, G. W. J., MOTHE, A., WANG, J., WANG, S., TATOR, C. & FEHLINGS, M. G. 2012a. An in vivo characterization of trophic factor production following neural precursor cell or bone marrow stromal cell transplantation for spinal cord injury. *Stem Cells and Development,* 21**,** 2222-2238.

HAWRYLUK, G. W. J., MOTHE, A. J., CHAMANKHAH, M., WANG, J., TATOR, C. & FEHLINGS, M. G. 2012b. In vitro characterization of trophic factor expression in neural precursor cells. *Stem Cells and Development,* 21**,** 432-447.

HE, F., YANG, Z., TAN, Y., YU, N., WANG, X., YAO, N. & ZHAO, J. 2009. Effects of Notch ligand Delta1 on the proliferation and differentiation of human dental pulp stem cells in vitro. *Archives of Oral Biology,* 54**,** 216-222.

HIRASAWA, T., OHSAWA, K., IMAI, Y., ONDO, Y., AKAZAWA, C., UCHINO, S. & KOHSAKA, S. 2005. Visualization of microglia in living tissues using Iba1-EGFP transgenic mice. *Journal of Neuroscience Research,* 81**,** 357-362.

HITOSHI, S., ALEXSON, T., TROPEPE, V., DONOVIEL, D., ELIA, A. J., NYE, J. S., CONLON, R. A., MAK, T. W., BERNSTEIN, A. & VAN DER

KOOY, D. 2002. Notch pathway molecules are essential for the maintenance, but not the generation, of mammalian neural stem cells. *Genes and Development,* 16**,** 846-858.

HO, T. W., BRISTOL, L. A., COCCIA, C., LI, Y., MILBRANDT, J., JOHNSON, E., JIN, L., BAR-PELED, O., GRIFFIN, J. W. & ROTHSTEIN, J. D. 2000. TGFβ trophic factors differentially modulate motor axon outgrowth and protection from excitotoxicity. *Experimental Neurology,* 161**,** 664-675.

HODGKIN, A. L. & HUXLEY, A. F. 1952. A quantitative description of membrane current and its application to conduction and excitation in nerve. *The Journal of physiology,* 117**,** 500-544.

HOLLAND, G. R. 1994. Morphological features of dentine and pulp related to dentine sensitivity. *Archives of Oral Biology,* 39**,** S3-S11.

HOLTHOFF, K. & WITTE, O. W. 2000. Directed spatial potassium redistribution in rat neocortex. *GLIA,* 29**,** 288-292.

HOWARD, C., MURRAY, P. E. & NAMEROW, K. N. 2010. Dental pulp stem cell migration. *Journal of Endodontics,* 36**,** 1963-1966.

HSIEH, J., AIMONE, J. B., KASPAR, B. K., KUWABARA, T., NAKASHIMA, K. & GAGE, F. H. 2004. IGF-I instructs multipotent adult neural progenitor cells to become oligodendrocytes. *Journal of Cell Biology,* 164**,** 111-122.

HUANG, A. H. C., SNYDER, B. R., CHENG, P. H. & CHAN, A. W. S. 2008. Putative dental pulp-derived stem/stromal cells promote proliferation and differentiation of endogenous neural cells in the hippocampus of mice. *Stem Cells,* 26**,** 2654-2663.

IANNOTTI, C., PING ZHANG, Y., SHIELDS, C. B., HAN, Y., BURKE, D. A. & XU, X. M. 2004. A neuroprotective role of glial cell line-derived neurotrophic factor following moderate spinal cord contusion injury. *Experimental Neurology,* 189**,** 317-332.

IMAI, T., TOKUNAGA, A., YOSHIDA, T., HASHIMOTO, M., MIKOSHIBA, K., WEINMASTER, G., NAKAFUKU, M. & OKANO, H. 2001. The neural

RNA-binding protein musashi1 translationally regulates mammalian numb gene expression by interacting with its mRNA. *Molecular and Cellular Biology,* 21**,** 3888-3900.

IOHARA, K., ZHENG, L., ITO, M., TOMOKIYO, A., MATSUSHITA, K. & NAKASHIMA, M. 2006. Side population cells isolated from porcine dental pulp tissue with self-renewal and multipotency for dentinogenesis, chondrogenesis, adipogenesis, and neurogenesis. *Stem Cells,* 24**,** 2493-2503.

IOHARA, K., ZHENG, L., WAKE, H., ITO, M., NABEKURA, J., WAKITA, H., NAKAMURA, H., INTO, T., MATSUSHITA, K. & NAKASHIMA, M. 2008. A novel stem cell source for vasculogenesis in ischemia: Subfraction of side population cells from dental pulp. *Stem Cells,* 26**,** 2408-2418.

IOHARA, K., MURAKAMI, M., TAKEUCHI, N., OSAKO, Y., ITO, M., ISHIZAKA, R., UTUNOMIYA, S., NAKAMURA, H., MATSUSHITA, K. & NAKASHIMA, M. 2013. A novel combinatorial therapy with pulp stem cells and granulocyte colony-stimulating factor for total pulp regeneration. *Stem Cells Translational Medicine,* 2**,** 521-533.

ISHIZAKA, R., HAYASHI, Y., IOHARA, K., SUGIYAMA, M., MURAKAMI, M., YAMAMOTO, T., FUKUTA, O. & NAKASHIMA, M. 2013. Stimulation of angiogenesis, neurogenesis and regeneration by side population cells from dental pulp. *Biomaterials,* 34**,** 1888-1897.

ISHKITIEV, N., YAEGAKI, K., IMAI, T., TANAKA, T., NAKAHARA, T., ISHIKAWA, H., MITEV, V. & HAAPASALO, M. 2012. High-purity hepatic lineage differentiated from dental pulp stem cells in serum-free medium. *Journal of Endodontics,* 38**,** 475-480.

ITO, H., NAKAJIMA, A., NOMOTO, H. & FURUKAWA, S. 2003. Neurotrophins facilitate neuronal differentiation of cultured neural stem cells via induction of mRNA expression of basic helix-loop-helix transcription factors Mash1 and Math1. *Journal of Neuroscience Research,* 71**,** 648-658.

IWANAMI, A., KANEKO, S., NAKAMURA, M., KANEMURA, Y., MORI, H., KOBAYASHI, S., YAMASAKI, M., MOMOSHIMA, S., ISHII, H., ANDO, K., TANIOKA, Y., TAMAOKI, N., NOMURA, T., TOYAMA, Y. & OKANO, H. 2005. Transplantation of human neural stem cells for spinal cord injury in primates. *Journal of Neuroscience Research,* 80**,** 182-190.

JACOBS, P. L. & NASH, M. S. 2004. Exercise recommendations for individuals with spinal cord injury. *Sports Medicine,* 34**,** 727-751.

JAGIELSKA, A., NORMAN, A. L., WHYTE, G., VLIET, K. J. V., GUCK, J. & FRANKLIN, R. J. M. 2012. Mechanical environment modulates biological properties of oligodendrocyte progenitor cells. *Stem Cells and Development,* 21**,** 2905-2914.

JANEBODIN, K., HORST, O. V., IERONIMAKIS, N., BALASUNDARAM, G., REESUKUMAL, K., PRATUMVINIT, B. & REYES, M. 2011. Isolation and characterization of neural crest-derived stem cells from dental pulp of neonatal mice. *PLoS ONE,* 6.

JONES, P. H. & WATT, F. M. 1993. Separation of human epidermal stem cells from transit amplifying cells on the basis of differences in integrin function and expression. *Cell,* 73**,** 713-724.

KAMADA, T., KODA, M., DEZAWA, M., ANAHARA, R., TOYAMA, Y., YOSHINAGA, K., HASHIMOTO, M., KOSHIZUKA, S., NISHIO, Y., MANNOJI, C., OKAWA, A. & YAMAZAKI, M. 2011. Transplantation of human bone marrow stromal cell-derived Schwann cells reduces cystic cavity and promotes functional recovery after contusion injury of adult rat spinal cord. *Neuropathology,* 31**,** 48-58.

KAN, L., ISRASENA, N., ZHANG, Z., HU, M., ZHAO, L. R., JALALI, A., SAHNI, V. & KESSLER, J. A. 2004. Sox1 acts through multiple independent pathways to promote neurogenesis. *Developmental Biology,* 269**,** 580-594.

KARAÖZ, E., DEMIRCAN, P. C., SAFLAM, O., AKSOY, A., KAYMAZ, F. & DURUKSU, G. 2011. Human dental pulp stem cells demonstrate better

neural and epithelial stem cell properties than bone marrow-derived mesenchymal stem cells. *Histochemistry and Cell Biology,* 136**,** 455-473.

KARBANOVÁ, J., SOUKUP, T., SUCHÁNEK, J., PYTLÍK, R., CORBEIL, D. & MOKRÝ, J. 2011. Characterization of dental pulp stem cells from impacted third molars cultured in low serum-containing medium. *Cells Tissues Organs,* 193**,** 344-365.

KEIRSTEAD, H. S., NISTOR, G., BERNAL, G., TOTOIU, M., CLOUTIER, F., SHARP, K. & STEWARD, O. 2005. Human embryonic stem cell-derived oligodendrocyte progenitor cell transplants remyelinate and restore locomotion after spinal cord injury. *Journal of Neuroscience,* 25**,** 4694-4705.

KENNEA, N. L., WADDINGTON, S. N., CHAN, J., O'DONOGHUE, K., YEUNG, D., TAYLOR, D. L., AL-ALLAF, F. A., PIRIANOV, G., THEMIS, M., EDWARDS, A. D., FISK, N. M. & MEHMET, H. 2009. Differentiation of human fetal mesenchymal stem cells into cells with an oligodendrocyte phenotype. *Cell Cycle,* 8**,** 1069-1079.

KERKIS, I., AMBROSIO, C. E., KERKIS, A., MARTINS, D. S., ZUCCONI, E., FONSECA, S. A. S., CABRAL, R. M., MARANDUBA, C. M. C., GAIAD, T. P., MORINI, A. C., VIEIRA, N. M., BROLIO, M. P., SANT'ANNA, O. A., MIGLINO, M. A. & ZATZ, M. 2008. Early transplantation of human immature dental pulp stem cells from baby teeth to golden retriever muscular dystrophy (GRMD) dogs: Local or systemic? *Journal of Translational Medicine,* 6.

KERN, S., EICHLER, H., STOEVE, J., KLÜTER, H. & BIEBACK, K. 2006. Comparative analysis of mesenchymal stem cells from bone marrow, umbilical cord blood, or adipose tissue. *Stem Cells,* 24**,** 1294-1301.

KESSARIS, N., PRINGLE, N. & RICHARDSON, W. D. 2008. Specification of CNS glia from neural stem cells in the embryonic neuroepithelium. *Philosophical Transactions of the Royal Society B: Biological Sciences,* 363**,** 71-85.

KIM, J. G., ARMSTRONG, R. C., AGOSTON, D. V., ROBINSKY, A., WIESE, C., NAGLE, J. & HUDSON, L. D. 1997. Myelin transcription factor 1 (Myt1) of the oligodendrocyte lineage, along with a closely related CCHC zinc finger, is expressed in developing neurons in the mammalian central nervous system. *Journal of Neuroscience Research,* 50**,** 272-290.

KIM, S. U. & DE VELLIS, J. 2009. Stem cell-based cell therapy in neurological diseases: A review. *Journal of Neuroscience Research,* 87**,** 2183-2200.

KIRÁLY, M., PORCSALMY, B., PATAKI, A., KADAR, K., JELITAI, M., MOLNAR, B., HERMANN, P., GERA, I., GRIMM, W. D., GANSS, B., ZSEMBERY, A. & VARGA, G. 2009. Simultaneous PKC and cAMP activation induces differentiation of human dental pulp stem cells into functionally active neurons. *Neurochemistry International,* 55**,** 323-332.

KIRÁLY, M., KÁDÁR, K., HORVÁTHY, D. B., NARDAI, P., RÁCZ, G. Z., LACZA, Z., VARGA, G. & GERBER, G. 2011. Integration of neuronally predifferentiated human dental pulp stem cells into rat brain in vivo. *Neurochemistry International,* 59**,** 371-38.

KLAPKA, N. & MÜLLER, H. W. 2006. Collagen matrix in spinal cord injury. *Journal of Neurotrauma,* 23**,** 422-435.

KLEENE, R., MZOUGHI, M., JOSHI, G., KALUS, I., BORMANN, U., SCHULZE, C., XIAO, M. F., DITYATEV, A. & SCHACHNER, M. 2010. NCAM-induced neurite outgrowth depends on binding of calmodulin to NCAM and on nuclear import of NCAM and fak fragments. *Journal of Neuroscience,* 30**,** 10784-10798.

KNAUS, P., BETZ, H. & REHM, H. 1986. Expression of synaptophysin during postnatal development of the mouse brain. *Journal of Neurochemistry,* 47**,** 1302-1304.

KODA, M., MURAKAMI, M., INO, H., YOSHINAGA, K., IKEDA, O., HASHIMOTO, M., YAMAZAKI, M., NAKAYAMA, C. & MORIYA, H. 2002. Brain-derived neurotrophic factor suppresses delayed apoptosis of

oligodendrocytes after spinal cord injury in rats. *Journal of Neurotrauma,* 19**,** 777-785.

KOLKOVA, K., NOVITSKAYA, V., PEDERSEN, N., BEREZIN, V. & BOCK, E. 2000. Neural cell adhesion molecule-stimulated neurite outgrowth depends on activation of protein kinase C and the Ras-mitogen-activated protein kinase pathway. *Journal of Neuroscience,* 20**,** 2238-2246.

KUKEKOV, V. G., LAYWELL, E. D., SUSLOV, O., DAVIES, K., SCHEFFLER, B., THOMAS, L. B., O'BRIEN, T. F., KUSAKABE, M. & STEINDLER, D. A. 1999. Multipotent stem/progenitor cells with similar properties arise from neurogenic regions of adult human brain. *Experimental Neurology,* 156**,** 333-344.

KUHLBRODT, K., HERBARTH, B., SOCK, E., HERMANS-BORGMEYER, I. & WEGNER, M. 1998. Sox10, a novel transcriptional modulator in glial cells. *Journal of Neuroscience,* 18**,** 237-250.

LAPTHANASUPKUL, P., FENG, J., MANTESSO, A., TAKADA-HORISAWA, Y., VIDAL, M., KOSEKI, H., WANG, L., AN, Z., MILETICH, I. & SHARPE, P. T. 2012. Ring1a/b polycomb proteins regulate the mesenchymal stem cell niche in continuously growing incisors. *Developmental Biology,* 367**,** 140-153.

LEE, M. K. & CLEVELAND, D. W. 1996. Neuronal intermediate filaments. *Annual Reviews in Neuroscience,* 19**,** 187-217.

LEE, H., AL SHAMY, G., ELKABETZ, Y., SCHOFIELD, C. M., HARRSION, N. L., PANAGIOTAKOS, G., SOCCI, N. D., TABAR, V. & STUDERA, L. 2007. Directed differentiation and transplantation of human embryonic stem cell-derived motoneurons. *Stem Cells,* 25**,** 1931-1939.

LEE, B. B., CRIPPS, R. A., FITZHARRIS, M. & WING, P. C. 2013. The global map for traumatic spinal cord injury epidemiology: update 2011, global incidence rate. *Spinal Cord*.

LENDAHL, U., ZIMMERMAN, L. B. & MCKAY, R. D. G. 1990. CNS stem cells express a new class of intermediate filament protein. *Cell,* 60**,** 585-595.

LEVI, A. D., CASELLA, G., GREEN, B. A., DIETRICH, W. D., VANNI, S., JAGID, J. & WANG, M. Y. 2010. Clinical outcomes using modest intravascular hypothermia after acute cervical spinal cord injury. *Neurosurgery,* 66**,** 670-677.

LI, G. L., FAROOQUE, M., HOLTZ, A. & OLSSON, Y. 1999. Apoptosis of oligodendrocytes occurs for long distances away from the primary injury after compression trauma to rat spinal cord. *Acta Neuropathologica,* 98**,** 473-480.

LIEBAU, S., VAIDA, B., STORCH, A. & BOECKERS, T. M. 2007. Maturation of synaptic contacts in differentiating neural stem cells. *Stem Cells,* 25**,** 1720-1729.

LIEDTKE, W., EDELMANN, W., BIERI, P. L., CHIU, F. C., COWAN, N. J., KUCHERLAPATI, R. & RAINE, C. S. 1996. GFAP is necessary for the integrity of CNS white matter architecture and long-term maintenance of myelination. *Neuron,* 17**,** 607-615.

LIESI, P., DAHL, D. & VAHERI, A. 1983. Laminin is produced by early rat astrocytes in primary culture. *Journal of Cell Biology,* 96**,** 920-924.

LIU, J., CHEN, J., LIU, B., YANG, C., XIE, D., ZHENG, X., XU, S., CHEN, T., WANG, L., ZHANG, Z., BAI, X. & JIN, D. 2013. Acellular spinal cord scaffold seeded with mesenchymal stem cells promotes long-distance axon regeneration and functional recovery in spinal cord injured rats. *Journal of the Neurological Sciences,* 325**,** 127-136.

LIVAK, K. J. & SCHMITTGEN, T. D. 2001. Analysis of relative gene expression data using real-time quantitative PCR and the 2 -ΔΔCT method. *Methods,* 25**,** 402-408.

LIZIER, N. F., KERKIS, A., GOMES, C. M., HEBLING, J., OLIVEIRA, C. F., CAPLAN, A. I. & KERKIS, I. 2012. Scaling-up of dental pulp stem cells isolated from multiple niches. *PLoS ONE,* 7**,** e39885.

LOBSIGER, C. S., SMITH, P. M., BUCHSTALLER, J., SCHWEITZER, B., FRANKLIN, R. J. M., SUTER, U. & TAYLOR, V. 2001. A role for

oligodendrocyte-derived IGF-1 in trophic support of cortical neurons. *GLIA,* 36**,** 48-57.

LOO, D. T., FUQUAY, J. I., RAWSON, C. L. & BARNES, D. W. 1987. Extended culture of mouse embryo cells without senescence: Inhibition by serum. *Science,* 236**,** 200-202.

LOVSCHALL, H., TUMMERS, M., THESLEFF, I., FÜCHTBAUER, E. M. & POULSEN, K. 2005. Activation of the Notch signaling pathway in response to pulp capping of rat molars. *European Journal of Oral Sciences,* 113**,** 312-317.

LU, Q. R., SUN, T., ZHU, Z., MA, N., GARCIA, M., STILES, C. D. & ROWITCH, D. H. 2002. Common developmental requirement for Olig function indicates a motor neuron/oligodendrocyte connection. *Cell,* 109**,** 75-86.

LU, P., JONES, L. L., SNYDER, E. Y. & TUSZYNSKI, M. H. 2003. Neural stem cells constitutively secrete neurotrophic factors and promote extensive host axonal growth after spinal cord injury. *Experimental Neurology,* 181**,** 115-129.

LU, P., JONES, L. L. & TUSZYNSKI, M. H. 2005. BDNF-expressing marrow stromal cells support extensive axonal growth at sites of spinal cord injury. *Experimental Neurology,* 191**,** 344-360.

LUBETZKI, C., DEMERENS, C., ANGLADE, P., VILLARROYA, H., FRANKFURTER, A., LEE, V. M. Y. & ZALC, B. 1993. Even in culture, oligodendrocytes myelinate solely axons. *Proceedings of the National Academy of Sciences of the United States of America,* 90**,** 6820-6824.

LUO, Y., ZOU, Y., YANG, L., LIU, J., LIU, S., ZHOU, X., ZHANG, W. & WANG, T. 2013. Transplantation of NSCs with OECs alleviates neuropathic pain associated with NGF downregulation in rats following spinal cord injury. *Neuroscience Letters*.

LUUKKO, K., ARUMÄE, U., KARAVANOV, A., MOSHNYAKOV, M., SAINIO, K., SARIOLA, H., SAARMA, M. & THESLEFF, I. 1997a. Neurotrophin

mRNA expression in the developing tooth suggests multiple roles in innervation and organogenesis. *Developmental Dynamics,* 210**,** 117-129.

LUUKKO, K., SUVANTO, P., SAARMA, M. & THESLEFF, I. 1997b. Expression of GDNF and its receptors in developing tooth is developmentally regulated and suggests multiple roles in innervation and organogenesis. *Developmental Dynamics,* 210**,** 463-471.

MA, L., MAKINO, Y., YAMAZA, H., AKIYAMA, K., HOSHINO, Y., SONG, G., KUKITA, T., NONAKA, K., SHI, S. & YAMAZA, T. 2012. Cryopreserved Dental Pulp Tissues of Exfoliated Deciduous Teeth Is a Feasible Stem Cell Resource for Regenerative Medicine. *PLoS ONE,* 7.

MACNICOL, A. M., WILCZYNSKA, A. & MACNICOL, M. C. 2008. Function and regulation of the mammalian Musashi mRNA translational regulator. *Biochemical Society Transactions,* 36**,** 528-530.

MALATESTA, P. & GÖTZ, M. 2013. Radial glia - From boring cables to stem cell stars. *Development (Cambridge),* 140**,** 483-486.

MARQUES, S. A., ALMEIDA, F. M., FERNANDES, A. M., DOS SANTOS SOUZA, C., CADILHE, D. V., REHEN, S. K. & MARTINEZ, A. M. B. 2010. Predifferentiated embryonic stem cells promote functional recovery after spinal cord compressive injury. *Brain Research,* 1349**,** 115-128.

MATSUSHITA, K., WANG, W., ITOH, S., DOMON, T., FUNAHASHI, M. & TOTSUKA, Y. 2012. Dental pulp can be a good candidate for nerve grafting in a xeno-graft model. *Journal of Neuroscience Methods,* 205**,** 246-251.

MATSUURA, K., NAGAI, T., NISHIGAKI, N., OYAMA, T., NISHI, J., WADA, H., SANO, M., TOKO, H., AKAZAWA, H., SATO, T., NAKAYA, H., KASANUKI, H. & KOMURO, I. 2004. Adult Cardiac Sca-1-positive Cells Differentiate into Beating Cardiomyocytes. *Journal of Biological Chemistry,* 279**,** 11384-11391.

MAURICE, S., SROUJI, S. & LIVNE, E. 2007. Isolation of progenitor cells from cord blood using adhesion matrices. *Cytotechnology,* 52**,** 125-137.

MCDONALD, J. W., LIU, X. Z., QU, Y., LIU, S., MICKEY, S. K., TURETSKY, D., GOTTLIEB, D. I. & CHOI, D. W. 1999. Transplanted embryonic stem cells survive, differentiate and promote recovery in injured rat spinal cord. *Nature Medicine,* 5**,** 1410-1412.

MCKEON, R. J., SCHREIBER, R. C., RUDGE, J. S. & SILVER, J. 1991. Reduction of neurite outgrowth in a model of glial scarring following CNS injury is correlated with the expression of inhibitory molecules on reactive astrocytes. *Journal of Neuroscience,* 11**,** 3398-3411.

MCKINNON, R. D., PIRAS, G., IDA JR, J. A. & DUBOIS-DALCQ, M. 1993. A role for TGF-β in oligodendrocyte differentiation. *Journal of Cell Biology,* 121**,** 1397-1408.

MCTIGUE, D. M., HORNER, P. J., STOKES, B. T. & GAGE, F. H. 1998. Neurotrophin-3 and brain-derived neurotrophic factor induce oligodendrocyte proliferation and myelination of regenerating axons in the contused adult rat spinal cord. *Journal of Neuroscience,* 18**,** 5354-5365.

MENG, X., LI, W., YOUNG, F., GAO, R., CHALMERS, L., ZHAO, M. & SONG, B. 2012. Electric field-controlled directed migration of neural progenitor cells in 2D and 3D environments. *Journal of visualized experiments : JoVE*.

MERKLE, F. T., TRAMONTIN, A. D., GARCÍA-VERDUGO, J. M. & ALVAREZ-BUYLLA, A. 2004. Radial glia give rise to adult neural stem cells in the subventricular zone. *Proceedings of the National Academy of Sciences of the United States of America,* 101**,** 17528-17532.

MIRNICS, Z. K., YAN, C., PORTUGAL, C., KIM, T. W., SARAGOVI, H. U., SISODIA, S. S., MIRNICS, K. & SCHOR, N. F. 2005. P75 neurotrophin receptor regulates expression of neural cell adhesion molecule 1. *Neurobiology of Disease,* 20**,** 969-985.

MITRA, P. & BROWNSTONE, R. M. 2012. An in vitro spinal cord slice preparation for recording from lumbar motoneurons of the adult mouse. *Journal of Neurophysiology,* 107**,** 728-741.

MITSUI, T., SHUMSKY, J. S., LEPORE, A. C., MURRAY, M. & FISCHER, I. 2005. Transplantation of neuronal and glial restricted precursors into contused spinal cord improves bladder and motor functions, decreases thermal hypersensitivity, and modifies intraspinal circuitry. *Journal of Neuroscience,* 25**,** 9624-9636.

MIURA, M., GRONTHOS, S., ZHAO, M., LU, B., FISHER, L. W., ROBEY, P. G. & SHI, S. 2003. SHED: Stem cells from human exfoliated deciduous teeth. *Proceedings of the National Academy of Sciences of the United States of America,* 100**,** 5807-5812.

MIYAGI, S. P. H., MARANDUBA, C. M. C., SILVA, F. S. & MARQUES, M. M. 2012. Dental pulp stem cells express proteins involved in the local invasiveness of odontogenic myxoma. *Brazilian Oral Research,* 26**,** 139-144.

NAGHDI, M., TIRAIHI, T., NAMIN, S. A. M. & ARABKHERADMAND, J. 2009. Transdifferentiation of bone marrow stromal cells into cholinergic neuronal phenotype: A potential source for cell therapy in spinal cord injury. *Cytotherapy,* 11**,** 137-152.

NAKATSUKA, R., NOZAKI, T., UEMURA, Y., MATSUOKA, Y., SASAKI, Y., SHINOHARA, M., OHURA, K. & SONODA, Y. 2010. 5-Aza-2-deoxycytidine treatment induces skeletal myogenic differentiation of mouse dental pulp stem cells. *Archives of Oral Biology,* 55**,** 350-357.

NAPOLI, I. & NEUMANN, H. 2009. Microglial clearance function in health and disease. *Neuroscience,* 158**,** 1030-1038.

NAVARRO, X. 2009. Chapter 27 Neural Plasticity After Nerve Injury and Regeneration. *International Reviews in Neurobiology,* 87**,** 483-505.

NESS, J. K. & WOOD, T. L. 2002. Insulin-like growth factor I, but not neurotrophin-3, sustains Akt activation and provides long-term protection of immature oligodendrocytes from glutamate-mediated apoptosis. *Molecular and Cellular Neuroscience,* 20**,** 476-488.

NESTI, C., PARDINI, C., BARACHINI, S., D'ALESSANDRO, D., SICILIANO, G., MURRI, L., PETRINI, M. & VAGLINI, F. 2011. Human dental pulp stem

cells protect mouse dopaminergic neurons against MPP+ or rotenone. *Brain Research,* 1367**,** 94-102.

NICKERSON, P. E. B., MYERS, T., CLARKE, D. B. & CHOW, R. L. 2011. Changes in Musashi-1 subcellular localization correlate with cell cycle exit during postnatal retinal development. *Experimental Eye Research,* 92**,** 344-352.

NISTOR, G. I., TOTOIU, M. O., HAQUE, N., CARPENTER, M. K. & KEIRSTEAD, H. S. 2005. Human embryonic stem cells differentiate into oligodendrocytes in high purity and myelinate after spinal cord transplantation. *GLIA,* 49**,** 385-396.

NOCTOR, S. C., MARTINEZ-CERDEÑO, V., IVIC, L. & KRIEGSTEIN, A. R. 2004. Cortical neurons arise in symmetric and asymmetric division zones and migrate through specific phases. *Nature Neuroscience,* 7**,** 136-144.

NOLTE, C., MATYASH, M., PIVNEVA, T., SCHIPKE, C. G., OHLEMEYER, C., HANISCH, U. K., KIRCHHOFF, F. & KETTENMANN, H. 2001. GFAP promoter-controlled EGFP-expressing transgenic mice: A tool to visualize astrocytes and astrogliosis in living brain tissue. *GLIA,* 33**,** 72-86.

NOSRAT, I. V., WIDENFALK, J., OLSON, L. & NOSRAT, C. A. 2001. Dental pulp cells produce neurotrophic factors, interact with trigeminal neurons in vitro, and rescue motoneurons after spinal cord injury. *Developmental Biology, 2*38**,** 120-132.

NOSRAT, I. V., SMITH, C. A., MULLALLY, P., OLSON, L. & NOSRAT, C. A. 2004. Dental pulp cells provide neurotrophic support for dopaminergic neurons and differentiate into neurons in vitro; implications for tissue engineering and repair in the nervous system. *European Journal of Neuroscience,* 19**,** 2388-2398.

NOVIKOVA, L. N., BROHLIN, M., KINGHAM, P. J., NOVIKOV, L. N. & WIBERG, M. 2011. Neuroprotective and growth-promoting effects of bone marrow stromal cells after cervical spinal cord injury in adult rats. *Cytotherapy,* 13**,** 873-887.

NUNES, M. C., ROY, N. S., KEYOUNG, H. M., GOODMAN, R. R., MCKHANN II, G., JIANG, L., KANG, J., NEDERGAARD, M. & GOLDMAN, S. A. 2003. Identification and isolation of multipotential neural progenitor cells from the subcortical white matter of the adult human brain. *Nature Medicine,* 9**,** 439-447.

OGATA, K. & KOSAKA, T. 2002. Structural and quantitative analysis of astrocytes in the mouse hippocampus. *Neuroscience,* 113**,** 221-233.

OKABE, M., IKAWA, M., KOMINAMI, K., NAKANISHI, T. & NISHIMUNE, Y. 1997. 'Green mice' as a source of ubiquitous green cells. *FEBS Letters,* 407**,** 313-319.

OLSON, H. E., ROONEY, G. E., GROSS, L., NESBITT, J. J., GALVIN, K. E., KNIGHT, A., CHEN, B., YASZEMSKI, M. J. & WINDEBANK, A. J. 2009. Neural stem cell- and schwann cell-loaded biodegradable polymer scaffolds support axonal regeneration in the transected spinal cord. *Tissue Engineering - Part A,* 15**,** 1797-1805.

O'MEARA, R. W., RYAN, S. D., COLOGNATO, H. & KOTHARY, R. 2011. Derivation of enriched oligodendrocyte cultures and oligodendrocyte/neuron myelinating co-cultures from post-natal murine tissues. *Journal of Visualized Experiments*.

OSATHANON, T., NOWWAROTE, N. & PAVASANT, P. 2011. Basic fibroblast growth factor inhibits mineralization but induces neuronal differentiation by human dental pulp stem cells through a FGFR and PLCγ signaling pathway. *Journal of Cellular Biochemistry,* 112**,** 1807-1816.

OSATHANON, T., SAWANGMAKE, C., NOWWAROTE, N. & PAVASANT, P. 2013. Neurogenic differentiation of human dental pulp stem cells using different induction protocols. *Oral Diseases,* IN PRESS.

PAINO, F., RICCI, G., DE ROSA, A., D'AQUINO, R., LAINO, L., PIROZZI, G., TIRINO, V. & PAPACCIO, G. 2010. Ecto-mesenchymal stem cells from dental pulp are committed to differentiate into active melanocytes. *European cells & materials,* 20**,** 295-305.

PAL, R., VENKATARAMANA, N. K., BANSAL, A., BALARAJU, S., JAN, M., CHANDRA, R., DIXIT, A., RAUTHAN, A., MURGOD, U. & TOTEY, S. 2009. Ex vivo-expanded autologous bone marrow-derived mesenchymal stromal cells in human spinal cord injury/paraplegia: A pilot clinical study. *Cytotherapy,* 11**,** 897-911.

PAPADOPOULOS, S. M., SELDEN, N. R., QUINT, D. J., PATEL, N., GILLESPIE, B. & GRUBE, S. 2002. Immediate spinal cord decompression for cervical spinal cord injury: Feasibility and outcome. *Journal of Trauma - Injury, Infection and Critical Care,* 52**,** 323-332.

PARK, H. W., LIM, M. J., JUNG, H., LEE, S. P., PAIK, K. S. & CHANG, M. S. 2010a. Human mesenchymal stem cell-derived Schwann cell-like cells exhibit neurotrophic effects, via distinct growth factor production, in a model of spinal cord injury. *GLIA,* 58**,** 1118-1132.

PARK, D., XIANG, A. P., MAO, F. F., ZHANG, L., DI, C. G., LIU, X. M., SHAO, Y., MA, B. F., LEE, J. H., HA, K. S., WALTON, N. & LAHN, B. T. 2010b. Nestin is required for the proper self-renewal of neural stem cells. *Stem Cells,* 28**,** 2162-2171.

PARK, J. H., KIM, D. Y., SUNG, I. Y., CHOI, G. H., JEON, M. H., KIM, K. K. & JEON, S. R. 2012. Long-term results of spinal cord injury therapy using mesenchymal stem cells derived from bone marrow in humans. *Neurosurgery,* 70**,** 1238-1247.

PARR, A. M., KULBATSKI, I., ZAHIR, T., WANG, X., YUE, C., KEATING, A. & TATOR, C. H. 2008. Transplanted adult spinal cord-derived neural stem/progenitor cells promote early functional recovery after rat spinal cord injury. *Neuroscience,* 155**,** 760-770.

PARRINELLO, S., SAMPER, E., KRTOLICA, A., GOLDSTEIN, J., MELOV, S. & CAMPISI, J. 2003. Oxygen sensitivity severely limits the replicative lifespan of murine fibroblasts. *Nature Cell Biology,* 5**,** 741-747.

PATEL, M., SMITH, A. J., SLOAN, A. J., SMITH, G. & COOPER, P. R. 2009. Phenotype and behaviour of dental pulp cells during expansion culture. *Archives of Oral Biology,* 54**,** 898-908.

PEARSE, D. D., SANCHEZ, A. R., PEREIRA, F. C., ANDRADE, C. M., PUZIS, R., PRESSMAN, Y., GOLDEN, K., KITAY, B. M., BLITS, B., WOOD, P. M. & BUNGE, M. B. 2007. Transplantation of Schwann cells and/or olfactory ensheathing glia into the contused spinal cord: Survival, migration, axon association, and functional recovery. *GLIA,* 55**,** 976-1000.

PIERDOMENICO, L., BONSI, L., CALVITTI, M., RONDELLI, D., ARPINATI, M., CHIRUMBOLO, G., BECCHETTI, E., MARCHIONNI, C., ALVIANO, F., FOSSATI, V., STAFFOLANI, N., FRANCHINA, M., GROSSI, A. & BAGNARA, G. P. 2005. Multipotent mesenchymal stem cells with immunosuppressive activity can be easily isolated from dental pulp. *Transplantation,* 80**,** 836-842.

PITTENGER, M. F., MACKAY, A. M., BECK, S. C., JAISWAL, R. K., DOUGLAS, R., MOSCA, J. D., MOORMAN, M. A., SIMONETTI, D. W., CRAIG, S. & MARSHAK, D. R. 1999. Multilineage potential of adult human mesenchymal stem cells. *Science,* 284**,** 143-147.

PRIEBE, M. M., CHIODO, A. E., SCELZA, W. M., KIRSHBLUM, S. C., WUERMSER, L. A. & HO, C. H. 2007. Spinal Cord Injury Medicine. 6. Economic and Societal Issues in Spinal Cord Injury. *Archives of Physical Medicine and Rehabilitation,* 88**,** S84-S88.

PRINGLE, N. P., MUDHAR, H. S., COLLARINI, E. J. & RICHARDSON, W. D. 1992. PDGF receptors in the rat CNS: During late neurogenesis, PDGF alpha-receptor expression appears to be restricted to glial cells of the oligodendrocyte lineage. *Development,* 115**,** 535-551.

PURVES, D., AUGUSTINE, G. J. & FITZPATRICK, D. 2001. Increased Conduction Velocity as a Result of Myelination. *Neuroscience.* 2nd ed.: Sunderland (MA): Sinauer Associates.

QUARLES, R. H., MACKLIN, W. B. & MORELL, P. 2005. Myelin Formation, Structure and Biochemistry. *In:* BRADY, S., SIEGEL, G., ALBERS, W. R. & PRICE, D. (eds.) *Basic Neurochemistry: Molecular, Cellular and Medical Aspects.* 7th Edition ed.: Academic Press.

QUERTAINMONT, R., CANTINIEAUX, D., BOTMAN, O., SID, S., SCHOENEN, J. & FRANZEN, R. 2012. Mesenchymal stem cell graft improves recovery after spinal cord injury in adult rats through neurotrophic and pro-angiogenic actions. *PLoS ONE,* 7.

RA, J. C., SHIN, I. S., KIM, S. H., KANG, S. K., KANG, B. C., LEE, H. Y., KIM, Y. J., JO, J. Y., YOON, E. J., CHOI, H. J. & KWON, E. 2011. Safety of intravenous infusion of human adipose tissue-derived mesenchymal stem cells in animals and humans. *Stem Cells and Development,* 20**,** 1297-1308.

RABCHEVSKY, A. G., FUGACCIA, I., TURNER, A. F., BLADES, D. A., MATTSON, M. P. & SCHEFF, S. W. 2000. Basic fibroblast growth factor (bFGF) enhances functional recovery following severe spinal cord injury to the rat. *Experimental Neurology,* 164**,** 280-291.

RADTKE, C., SCHMITZ, B., SPIES, M., KOCSIS, J. D. & VOGT, P. M. 2009. Peripheral glial cell differentiation from neurospheres derived from adipose mesenchymal stem cells. *International Journal of Developmental Neuroscience,* 27**,** 817-823.

RAMÓN-CUETO, A., CORDERO, M. I., SANTOS-BENITO, F. F. & AVILA, J. 2000. Functional recovery of paraplegic rats and motor axon regeneration in their spinal cords by olfactory ensheathing glia. *Neuron,* 25**,** 425-435.

RAO, M. S. & MAYER-PROSCHEL, M. 1997. Glial-restricted precursors are derived from multipotent neuroepithelial stem cells. *Developmental Biology,* 188**,** 48-63.

RAVIKUMAR, M., JAIN, S., MILLER, R. H., CAPADONA, J. R. & SELKIRK, S. M. 2012. An organotypic spinal cord slice culture model to quantify neurodegeneration. *Journal of Neuroscience Methods,* 211**,** 280-288.

REUBINOFF, B. E., ITSYKSON, P., TURETSKY, T., PERA, M. F., REINHARTZ, E., ITZIK, A. & BEN-HUR, T. 2001. Neural progenitors from human embryonic stem cells. *Nature Biotechnology,* 19**,** 1134-1140.

ROHME, D. 1981. Evidence for a relationship between longevity of mammalian species and life spans of normal fibroblasts in vitro and

erythrocytes in vivo. *Proceedings of the National Academy of Sciences of the United States of America,* 78**,** 5009-5013.

RUSAKOV, D. A. 2006. Ca2+-dependent mechanisms of presynaptic control at central synapses. *Neuroscientist,* 12**,** 317-326.

SAKAI, K., YAMAMOTO, A., MATSUBARA, K., NAKAMURA, S., NARUSE, M., YAMAGATA, M., SAKAMOTO, K., TAUCHI, R., WAKAO, N., IMAGAMA, S., HIBI, H., KADOMATSU, K., ISHIGURO, N. & UEDA, M. 2012. Human dental pulp-derived stem cells promote locomotor recovery after complete transection of the rat spinal cord by multiple neuro-regenerative mechanisms. *Journal of Clinical Investigation,* 122**,** 80-90.

SANDVIG, A., BERRY, M., BARRETT, L. B., BUTT, A. & LOGAN, A. 2004. Myelin-, reactive glia-, and scar-derived CNS axon growth inhibitors: Expression, receptor signaling, and correlation with axon regeneration. *GLIA,* 46**,** 225-251.

SANSOM, S. N., GRIFFITHS, D. S., FAEDO, A., KLEINJAN, D. J., RUAN, Y., SMITH, J., VAN HEYNINGEN, V., RUBENSTEIN, J. L. & LIVESEY, F. J. 2009. The level of the transcription factor Pax6 is essential for controlling the balance between neural stem cell self-renewal and neurogenesis. *PLoS Genetics,* 5.

SASAKI, R., AOKI, S., YAMATO, M., UCHIYAMA, H., WADA, K., OKANO, T. & OGIUCHI, H. 2008. Neurosphere generation from dental pulp of adult rat incisor. *European Journal of Neuroscience,* 27**,** 538-548.

SAYER, F. T., KRONVALL, E. & NILSSON, O. G. 2006. Methylprednisolone treatment in acute spinal cord injury: the myth challenged through a structured analysis of published literature. *Spine Journal,* 6**,** 335-343.

SEDGWICK, J. D., SCHWENDER, S., IMRICH, H., DORRIES, R., BUTCHER, G. W. & TER MEULEN, V. 1991. Isolation and direct characterization of resident microglial cells from the normal and inflamed central nervous system. *Proceedings of the National Academy of Sciences of the United States of America,* 88**,** 7438-7442.

SEIDEL, K., AHN, C. P., LYONS, D., NEE, A., TING, K., BROWNELL, I., CAO, T., CARANO, R. A. D., CURRAN, T., SCHOBER, M., FUCHS, E., JOYNER, A., MARTIN, G. R., DE SAUVAGE, F. J. & KLEIN, O. D. 2010. Hedgehog signaling regulates the generation of ameloblast progenitors in the continuously growing mouse incisor. *Development,* 137**,** 3753-3761.

SEKHON, L. H. S. & FEHLINGS, M. G. 2001. Epidemiology, demographics, and pathophysiology of acute spinal cord injury. *Spine,* 26**,** S2-S12.

SHARP, J., FRAME, J., SIEGENTHALER, M., NISTOR, G. & KEIRSTEAD, H. S. 2010. Human embryonic stem cell-derived oligodendrocyte progenitor cell transplants improve recovery after cervical spinal cord injury. *Stem Cells,* 28**,** 152-163.

SHI, S., ROBEY, P. G. & GRONTHOS, S. 2001. Comparison of human dental pulp and bone marrow stromal stem cells by cDNA microarray analysis. *Bone,* 29**,** 532-539.

SHI, S. & GRONTHOS, S. 2003. Perivascular niche of postnatal mesenchymal stem cells in human bone marrow and dental pulp. *Journal of Bone and Mineral Research,* 18**,** 696-704.

SKAPER, S. D. 2012. The neurotrophin family of neurotrophic factors: An Overview. *Methods in Molecular Biology,* 846**,** 1-12.

SMITH, A. J., CASSIDY, N., PERRY, H., BEGUE-KIRN, C., RUCH, J. V. & LESOT, H. 1995. Reactionary dentinogenesis. *International Journal of Developmental Biology,* 39**,** 273-280.

SOBUE, K., YAMAMOTO, N., YONEDA, K., HODGSON, M. E., YAMASHIRO, K., TSURUOKA, N., TSUDA, T., KATSUYA, H., MIURA, Y., ASAI, K. & KATO, T. 1999. Induction of blood-brain barrier properties in immortalized bovine brain endothelial cells by astrocytic factors. *Neuroscience Research,* 35**,** 155-164.

SOMEYA, Y., KODA, M., DEZAWA, M., KADOTA, T., HASHIMOTO, M., KAMADA, T., NISHIO, Y., KADOTA, R., MANNOJI, C., MIYASHITA, T., OKAWA, A., YOSHINAGA, K. & YAMAZAKI, M. 2008. Reduction of cystic cavity, promotion of axonal regeneration and sparing, and functional

recovery with transplanted bone marrow stromal cell-derived Schwann cells after contusion injury to the adult rat spinal cord: Laboratory investigation. *Journal of Neurosurgery: Spine,* 9**,** 600-610.

SORIA, J. M., SANCHO-TELLO, M., ESPARZA, M. A. G., MIRABET, V., BAGAN, J. V., MONLEÓN, M. & CARDA, C. 2011. Biomaterials coated by dental pulp cells as substrate for neural stem cell differentiation. *Journal of Biomedical Materials Research - Part A,* 97 A**,** 85-92.

SPANGRUDE, G. J., HEIMFELD, S. & WEISSMAN, I. L. 1988. Purification and characterization of mouse hematopoietic stem cells. *Science,* 241**,** 58-62.

SPATH, L., ROTILIO, V., ALESSANDRINI, M., GAMBARA, G., DE ANGELIS, L., MANCINI, M., MITSIADIS, T. A., VIVARELLI, E., NARO, F., FILIPPINI, A. & PAPACCIO, G. 2010. Explant-derived human dental pulp stem cells enhance differentiation and proliferation potentials. *Journal of Cellular and Molecular Medicine,* 14**,** 1635-1644.

STEINER, J., BERNSTEIN, H. G., BIELAU, H., BERNDT, A., BRISCH, R., MAWRIN, C., KEILHOFF, G. & BOGERTS, B. 2007. Evidence for a wide extra-astrocytic distribution of S100B in human brain. *BMC Neuroscience,* 8.

STEINER, J., BERNSTEIN, H. G., BOGERTS, B., GOS, T., RICHTER-LANDSBERG, C., WUNDERLICH, M. T. & KEILHOFF, G. 2008. S100B is expressed in, and released from, OLN-93 oligodendrocytes: Influence of serum and glucose deprivation. *Neuroscience,* 154**,** 496-503.

STEVENS, A., ZULIANI, T., OLEJNIK, C., LEROY, H., OBRIOT, H., KERR-CONTE, J., FORMSTECHER, P., BAILLIEZ, Y. & POLAKOWSKA, R. R. 2008. Human dental pulp stem cells differentiate into neural crest-derived melanocytes and have label-retaining and sphere-forming abilities. *Stem Cells and Development,* 17**,** 1175-1184.

STOKOLS, S. & TUSZYNSKI, M. H. 2006. Freeze-dried agarose scaffolds with uniaxial channels stimulate and guide linear axonal growth following spinal cord injury. *Biomaterials,* 27**,** 443-451.

SUBERVIOLA, B., GONZÁLEZ-CASTRO, A., LLORCA, J., ORTIZ-MELÓN, F. & MIÑAMBRES, E. 2008. Early complications of high-dose methylprednisolone in acute spinal cord injury patients. *Injury,* 39**,** 748-752.

SUDA, Y., SUZUKI, M., IKAWA, Y. & AIZAWA, S. 1987. Mouse embryonic stem cells exhibit indefinite proliferative potential. *Journal of Cellular Physiology,* 133**,** 197-201.

SUGIYAMA, M., IOHARA, K., WAKITA, H., HATTORI, H., UEDA, M., MATSUSHITA, K. & NAKASHIMA, M. 2011. Dental pulp-derived CD31 -/CD146 - side population stem/progenitor cells enhance recovery of focal cerebral ischemia in rats. *Tissue Engineering - Part A,* 17**,** 1303-1311.

SULLIVAN, P. G., KRISHNAMURTHY, S., PATEL, S. P., PANDYA, J. D. & RABCHEVSKY, A. G. 2007. Temporal characterization of mitochondrial bioenergetics after spinal cord injury. *Journal of Neurotrauma,* 24**,** 991-999.

SUN, D., LYE-BARTHEL, M., MASLAND, R. H. & JAKOBS, T. C. 2010. Structural remodeling of fibrous astrocytes after axonal injury. *Journal of Neuroscience,* 30**,** 14008-14019.

SUPENO, N. E., PATI, S., HADI, R. A., IZANI, A. R. G., MUSTAFA, Z., ABDULLAH, J. M., IDRIS, F. M., HAN, X. & JAAFAR, H. 2013. IGF-1 acts as controlling switch for long-term proliferation and maintenance of EGF/FGF-responsive striatal neural stem cells. *International Journal of Medical Sciences,* 10**,** 522-531.

SURI, L., DAMOULIS, P. D., LE, T. & GAGARI, E. 2008. Expression of MMP-13 (collagenase-3) in long-term cultures of human dental pulp cells. *Archives of Oral Biology,* 53**,** 791-799.

SYKOVA, E. & JENDELOVA, P. 2005. Magnetic resonance tracking of implanted adult and embryonic stem cells in injured brain and spinal cord. *Annals of the New York Academy of Sciences,* 1049**,** 146-160.

TAKAHASHI, M. & OSUMI, N. 2002. Pax6 regulates specification of ventral neurone subtypes in the hindbrain by establishing progenitor domains. *Development,* 129**,** 1327-1338.

TAKAMI, T., OUDEGA, M., BATES, M. L., WOOD, P. M., KLEITMAN, N. & BUNGE, M. B. 2002. Schwann cell but not olfactory ensheathing glia transplants improve hindlimb locomotor performance in the moderately contused adult rat thoracic spinal cord. *Journal of Neuroscience,* 22**,** 6670-6681.

TAKEYASU, M., NOZAKI, T. & DAITO, M. 2006. Differentiation of dental pulp stem cells into a neuronal lineage. *Pediatric Dental Journal,* 16**,** 154-162.

TATOR, C. H. & KOYANAGI, I. 1997. Vascular mechanisms in the pathophysiology of human spinal cord injury. *Journal of Neurosurgery,* 86**,** 483-492.

TÉCLÈS, O., LAURENT, P., ZYGOURITSAS, S., BURGER, A. S., CAMPS, J., DEJOU, J. & ABOUT, I. 2005. Activation of human dental pulp progenitor/stem cells in response to odontoblast injury. *Archives of Oral Biology,* 50**,** 103-108.

THOMSON, J. A. 1998. Embryonic stem cell lines derived from human blastocysts. *Science,* 282**,** 1145-1147.

THORNTON, M. R., SHAWCROSS, S. G., MANTOVANI, C., KINGHAM, P. J., BIRCHALL, M. A. & TERENGHI, G. 2008. Neurotrophins 3 and 4 differentially regulate NCAM, LI and N-cadherin expression during peripheral nerve regeneration. *Biotechnology and Applied Biochemistry,* 49**,** 165-174.

THUMBIKAT, P., HUSSAIN, N. & MCCLELLAND, M. R. 2009. Acute spinal cord injury. *Surgery,* 27**,** 280-286.

TOMA, J. G., AKHAVAN, M., FERNANDES, K. J. L., BARNABÉ-HEIDER, F., SADIKOT, A., KAPLAN, D. R. & MILLER, F. D. 2001. Isolation of multipotent adult stem cells from the dermis of mammalian skin. *Nature Cell Biology,* 3**,** 778-784.

TOTOIU, M. O. & KEIRSTEAD, H. S. 2005. Spinal cord injury is accompanied by chronic progressive demyelination. *Journal of Comparative Neurology,* 486**,** 373-383.

TRACY, E., ALDRINK, J., PANOSIAN, J., BEAM, D., THACKER, J., REESE, M. & KURTZBERG, J. 2008. Isolation of oligodendrocyte-like cells from human umbilical cord blood. *Cytotherapy,* 10**,** 518-525.

TRAN-HUNG, L., LAURENT, P., CAMPS, J. & ABOUT, I. 2008. Quantification of angiogenic growth factors released by human dental cells after injury. *Archives of Oral Biology,* 53**,** 9-13.

TROPEL, P., PLATET, N., PLATEL, J. C., NOËL, D., ALBRIEUX, M., BENABID, A. L. & BERGER, F. 2006. Functional neuronal differentiation of bone marrow-derived mesenchymal stem cells. *Stem Cells,* 24**,** 2868-2876.

TYSSELING, V. M., SAHNI, V., PASHUCK, E. T., BIRCH, D., HEBERT, A., CZEISLER, C., STUPP, S. I. & KESSLER, J. A. 2010. Self-assembling peptide amphiphile promotes plasticity of serotonergic fibers following spinal cord injury. *Journal of Neuroscience Research,* 88**,** 3161-3170.

WACHS, F. P., COUILLARD-DESPRES, S., ENGELHARDT, M., WILHELM, D., PLOETZ, S., VROEMEN, M., KAESBAUER, J., UYANIK, G., KLUCKEN, J., KARL, C., TEBBING, J., SVENDSEN, C., WEIDNER, N., KUHN, H. G., WINKLER, J. & AIGNER, L. 2003. High efficacy of clonal growth and expansion of adult neural stem cells. *Laboratory Investigation,* 83**,** 949-962.

WADDINGTON, R. J., YOUDE, S. J., LEE, C. P. & SLOAN, A. J. 2009. Isolation of distinct progenitor stem cell populations from dental pulp. *Cells Tissues Organs,* 189**,** 268-274.

WANG, X., HE, F., TAN, Y., TIAN, W. & QIU, S. 2011. Inhibition of Delta1 promotes differentiation of odontoblasts and inhibits proliferation of human dental pulp stem cell in vitro. *Archives of Oral Biology,* 56**,** 837-845.

WEISS, S., DUNNE, C., HEWSON, J., WOHL, C., WHEATLEY, M., PETERSON, A. C. & REYNOLDS, B. A. 1996. Multipotent CNS stem cells

are present in the adult mammalian spinal cord and ventricular neuroaxis. *Journal of Neuroscience,* 16**,** 7599-7609.

WELM, B. E., TEPERA, S. B., VENEZIA, T., GRAUBERT, T. A., ROSEN, J. M. & GOODELL, M. A. 2002. Sca-1pos cells in the mouse mammary gland represent an enriched progenitor cell population. *Developmental Biology,* 245**,** 42-56.

WENDER, R., BROWN, A. M., FERN, R., SWANSON, R. A., FARRELL, K. & RANSOM, B. R. 2000. Astrocytic glycogen influences axon function and survival during glucose deprivation in central white matter. *Journal of Neuroscience,* 20**,** 6804-6810.

WIDENFALK, J., LIPSON, A., JUBRAN, M., HOFSTETTER, C., EBENDAL, T., CAO, Y. & OLSON, L. 2003. Vascular endothelial growth factor improves functional outcome and decreases secondary degeneration in experimental spinal cord contusion injury. *Neuroscience,* 120**,** 951-960.

WILHELMSSON, U., BUSHONG, E. A., PRICE, D. L., SMARR, B. L., PHUNG, V., TERADA, M., ELLISMAN, M. H. & PEKNY, M. 2006. Redefining the concept of reactive astrocytes as cells that remain within their unique domains upon reaction to injury. *Proceedings of the National Academy of Sciences of the United States of America,* 103**,** 17513-17518.

WILKINS, A., CHANDRAN, S. & COMPSTON, A. 2001. A Role for Oligodendrocyte-Derived IGF-1 in Trophic Support of Cortical Neurons. *GLIA,* 36**,** 48-57.

WILKINS, A., MAJED, H., LAYFIELD, R., COMPSTON, A. & CHANDRAN, S. 2003. Oligodendrocytes promote neuronal survival and axonal length by distinct intracellular mechanisms: A novel role for oligodendrocyte-derived glial cell line-derived neurotrophic factor. *Journal of Neuroscience,* 23**,** 4967-4974.

WOODS, E. J., PERRY, B. C., HOCKEMA, J. J., LARSON, L., ZHOU, D. & GOEBEL, W. S. 2009. Optimized cryopreservation method for human dental pulp-derived stem cells and their tissues of origin for banking and clinical use. *Cryobiology,* 59**,** 150-157.

WRATHALL, J. R., TENG, Y. D. & CHOINIERE, D. 1996. Amelioration of functional deficits from spinal cord trauma with systemically administered NBQX, an antagonist of non-N-methyl-D-aspartate receptors. *Experimental Neurology,* 137**,** 119-126.

YAMAGATA, M., YAMAMOTO, A., KAKO, E., KANEKO, N., MATSUBARA, K., SAKAI, K., SAWAMOTO, K. & UEDA, M. 2013. Human dental pulp-derived stem cells protect against hypoxic-ischemic brain injury in neonatal mice. *Stroke,* 44**,** 551-554.

YAN, J., WELSH, A. M., BOKA, S. H., SNYDER, E. Y. & KOLIATSOS, V. E. 2004. Differentiation and tropic/trophic effects of exogenous neural precursors in the adult spinal cord. *Journal of Comparative Neurology,* 480**,** 101-114.

YANASE, M., SAKOU, T. & FUKUDA, T. 1995. Role of N-methyl-D-aspartate receptor in acute spinal cord injury. *Journal of Neurosurgery,* 83**,** 884-888.

YANG, X., ZHANG, W., VAN DEN DOLDER, J., FRANK WALBOOMERS, X., BIAN, Z., FAN, M. & JANSEN, J. A. 2007. Multilineage potential of STRO-1+ rat dental pulp cells in vitro. *Journal of Tissue Engineering and Regenerative Medicine,* 1**,** 128-135.

YANG, K. L., CHEN, M. F., LIAO, C. H., PANG, C. Y. & LIN, P. Y. 2009. A simple and efficient method for generating Nurr1-positive neuronal stem cells from human wisdom teeth (tNSC) and the potential of tNSC for stroke therapy. *Cytotherapy,* 11**,** 606-617.

YANG, N., ZUCHERO, J. B., AHLENIUS, H., MARRO, S., NG, Y. H., VIERBUCHEN, T., HAWKINS, J. S., GEISSLER, R., BARRES, B. A. & WERNIG, M. 2013. Generation of oligodendroglial cells by direct lineage conversion. *Nature Biotechnology,* 31**,** 434-439.

YASUDA, T. & ADAMS, D. J. 2010. Physiological roles of ion channels in adult neural stem cells and their progeny. *Journal of Neurochemistry,* 114**,** 946-959.

YOSHIMURA, M. & NISHI, S. 1993. Blind patch-clamp recordings from substantia gelatinosa neurons in adult rat spinal cord slices:

Pharmacological properties of synaptic currents. *Neuroscience,* 53**,** 519-526.

YOUNG, F., SLOAN, A. J. & SONG, B. 2013. Dental pulp stem cells and their potential roles in central nervous system regeneration and repair. *Journal of Neuroscience Research,*91, 1383-1393.

YU, W. P., COLLARINI, E. J., PRINGLE, N. P. & RICHARDSON, W. D. 1994. Embryonic expression of myelin genes: Evidence for a focal source of oligodendrocyte precursors in the ventricular zone of the neural tube. *Neuron,* 12**,** 1353-1362.

YU, J., HE, H., TANG, C., ZHANG, G., LI, Y., WANG, R., SHI, J. & JIN, Y. 2010. Differentiation potential of STRO-1+ dental pulp stem cells changes during cell passaging. *BMC Cell Biology,* 11.

ZAINAL ARIFFIN, S. H., KERMANI, S., MEGAT ABDUL WAHAB, R., SENAFI, S., ZAINAL ARIFFIN, Z. & ABDUL RAZAK, M. 2012. In vitro chondrogenesis transformation study of mouse dental pulp stem cells. *The Scientific World Journal,* 2012.

ZHANG, S. C., WERNIG, M., DUNCAN, I. D., BRÜSTLE, O. & THOMSON, J. A. 2001. In vitro differentiation of transplantable neural precursors from human embryonic stem cells. *Nature Biotechnology,* 19**,** 1129-1133.

ZHANG, W., WALBOOMERS, X. F., SHI, S., FAN, M. & JANSEN, J. A. 2006a. Multilineage differentiation potential of stem cells derived from human dental pulp after cryopreservation. *Tissue Engineering,* 12**,** 2813-2823.

ZHANG, Y. W., DENHAM, J. & THIES, R. S. 2006b. Oligodendrocyte progenitor cells derived from human embryonic stem cells express neurotrophic factors. *Stem Cells and Development,* 15**,** 943-952.

ZHANG, C., CHANG, J., SONOYAMA, W., SHI, S. & WANG, C. Y. 2008. Inhibition of human dental pulp stem cell differentiation by notch signaling. *Journal of Dental Research,* 87**,** 250-255.

ZHANG, H., BENNETT, J. L. & VERKMAN, A. S. 2011. Ex vivo spinal cord slice model of neuromyelitis optica reveals novel immunopathogenic mechanisms. *Annals of Neurology,* 70**,** 943-954.

ZHANG, H. Y., ZHANG, X., WANG, Z. G., SHI, H. X., WU, F. Z., LIN, B. B., XU, X. L., WANG, X. J., FU, X. B., LI, Z. Y., SHEN, C. J., LI, X. K. & XIAO, J. 2013. Exogenous Basic Fibroblast Growth Factor Inhibits ER Stress-Induced Apoptosis and Improves Recovery from Spinal Cord Injury. *CNS Neuroscience and Therapeutics,* 19**,** 20-29.]

ZHAO, Y., WANG, L., JIN, Y. & SHI, S. 2012. Fas ligand regulates the immunomodulatory properties of dental pulp stem cells. *Journal of Dental Research,* 91**,** 948-954.

ZHOU, Q., WANG, S. & ANDERSON, D. J. 2000. Identification of a novel family of oligodendrocyte lineage-specific basic helix-loop-helix transcription factors. *Neuron,* 25**,** 331-343.

ZHOU, Q. & ANDERSON, D. J. 2002. The bHLH transcription factors OLIG2 and OLIG1 couple neuronal and glial subtype specification. *Cell,* 109**,** 61-73.

ZÖRNER, B. & SCHWAB, M. E. 2010. Anti-Nogo on the go: From animal models to a clinical trial. *Annals of the New York Academy of Sciences,* 1198**,** E22-E34.

ZUK, P. A., ZHU, M., ASHJIAN, P., DE UGARTE, D. A., HUANG, J. I., MIZUNO, H., ALFONSO, Z. C., FRASER, J. K., BENHAIM, P. & HEDRICK, M. H. 2002. Human adipose tissue is a source of multipotent stem cells. *Molecular Biology of the Cell,* 13**,** 4279-4295.

ZWIMPFER, T. J. & BERNSTEIN, M. 1990. Spinal cord concussion. *Journal of Neurosurgery,* 72**,** 894-900.

Appendix I: qPCR dissociation curves

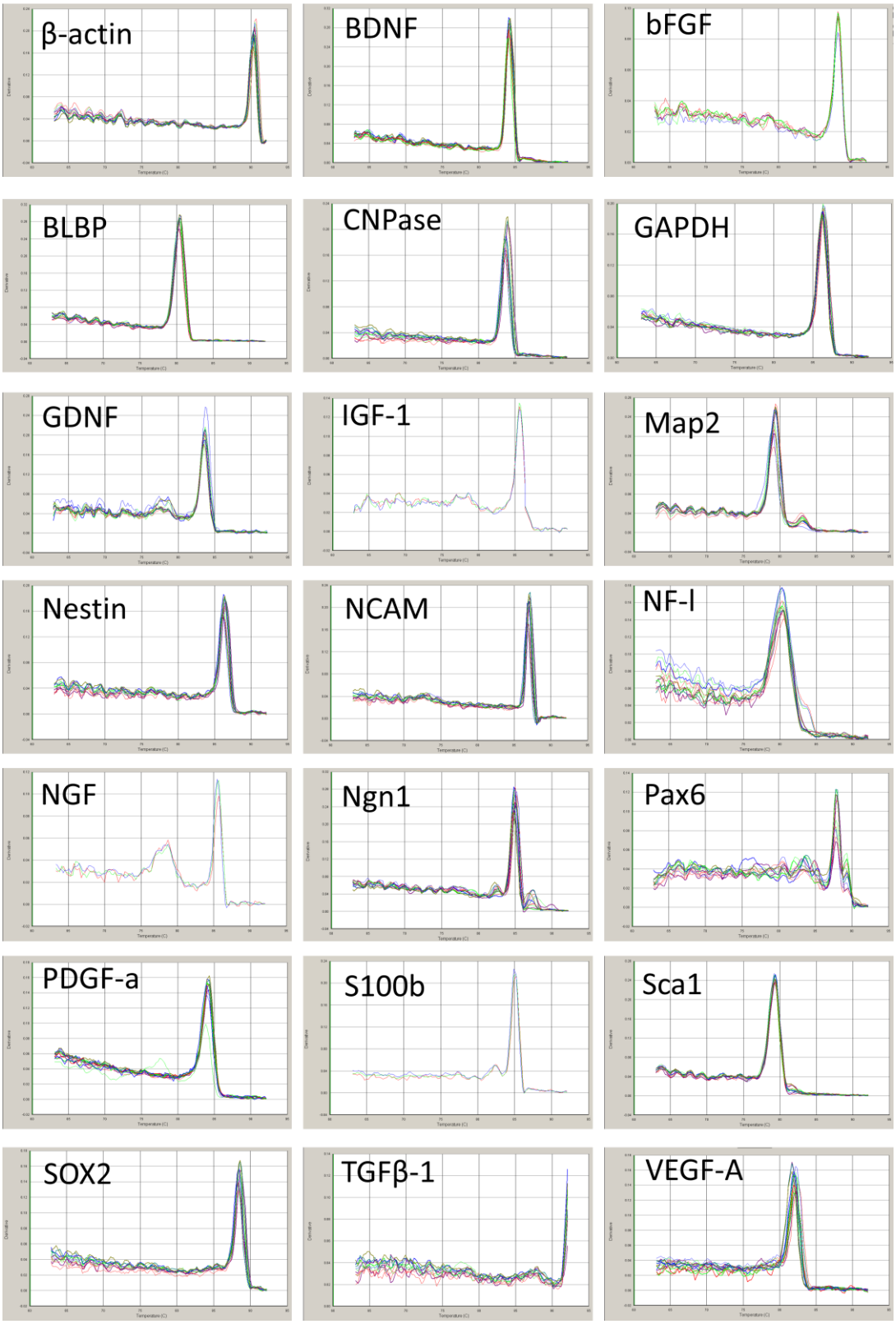

Appendix II: qPCR product sizes

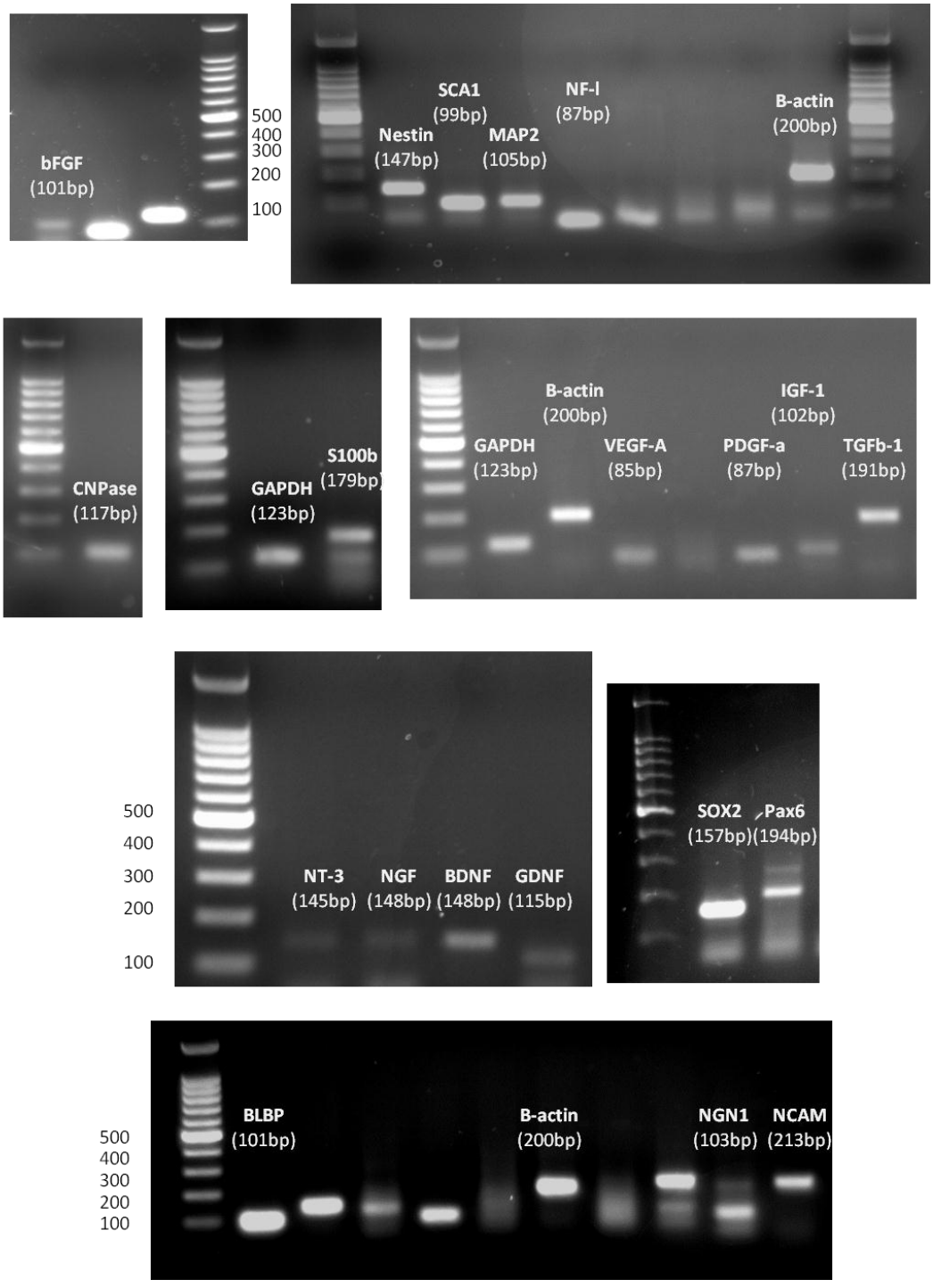

Appendix III: GFP mDPPC characterisation

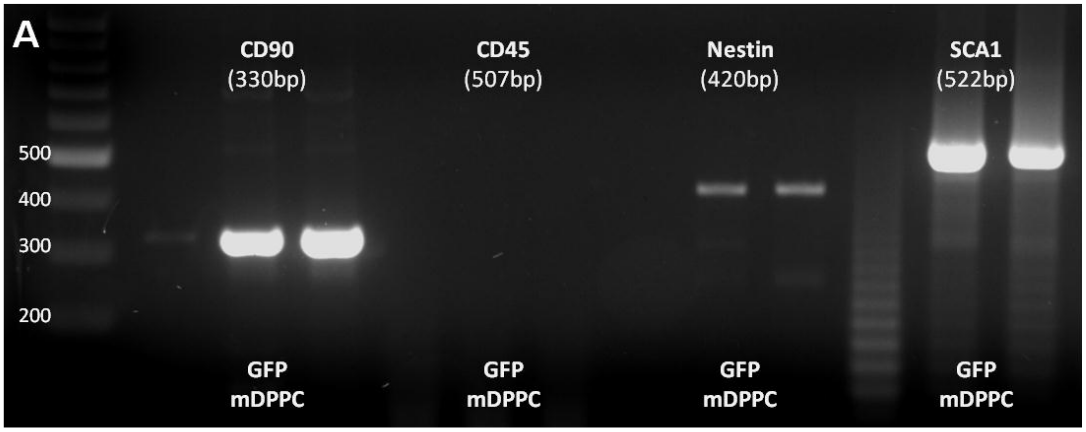

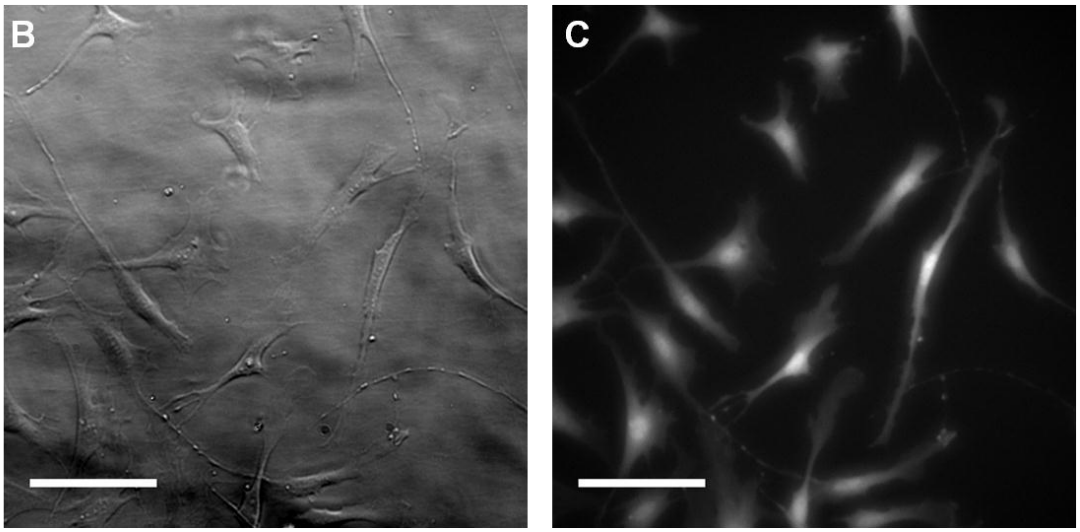

A) In DPPC culture medium, isolated GFP mDPPCs expressed the mesenchymal markers CD90 and SCA1 in addition to the early stage neural marker nestin, confirming their progenitor status. No expression of CD45 was identified confirming no contamination with haematopoetic cells. B) Phase contrast and (C) corresponding fluorescent image confirming ubiquitous expression of GFP. Scale bars = 100µm

Appendix IV: ex vivo isotype controls

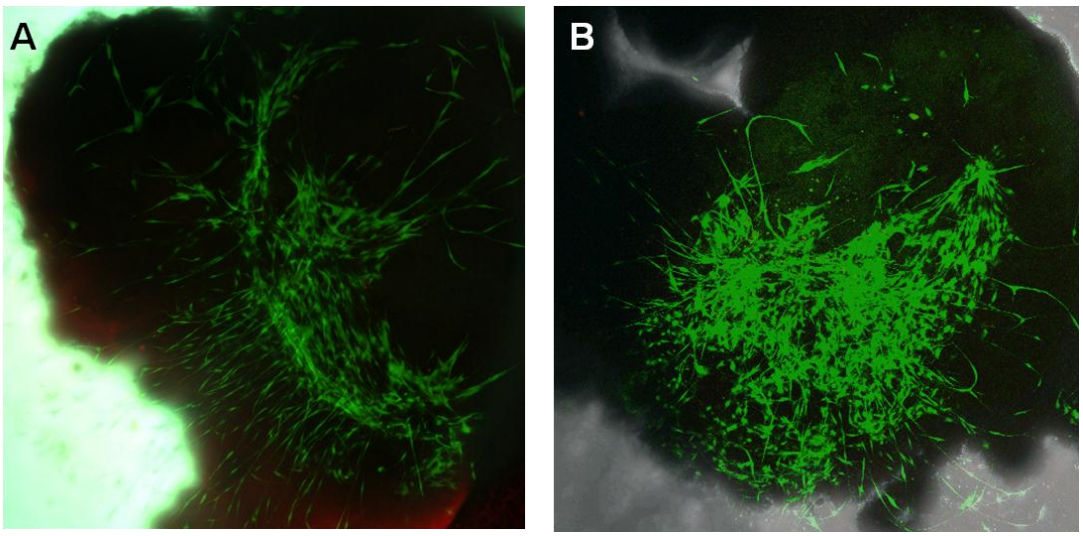

Merged images for (A) mouse IgG isotype control and (B) rabbit IgG isotype control stained *ex vivo* spinal cord slice cultures demonstrating the specificity of secondary antibody staining for synaptophysin & βIII-tubulin, respectively.

Appendix V: In vivo immunohistochemistry controls

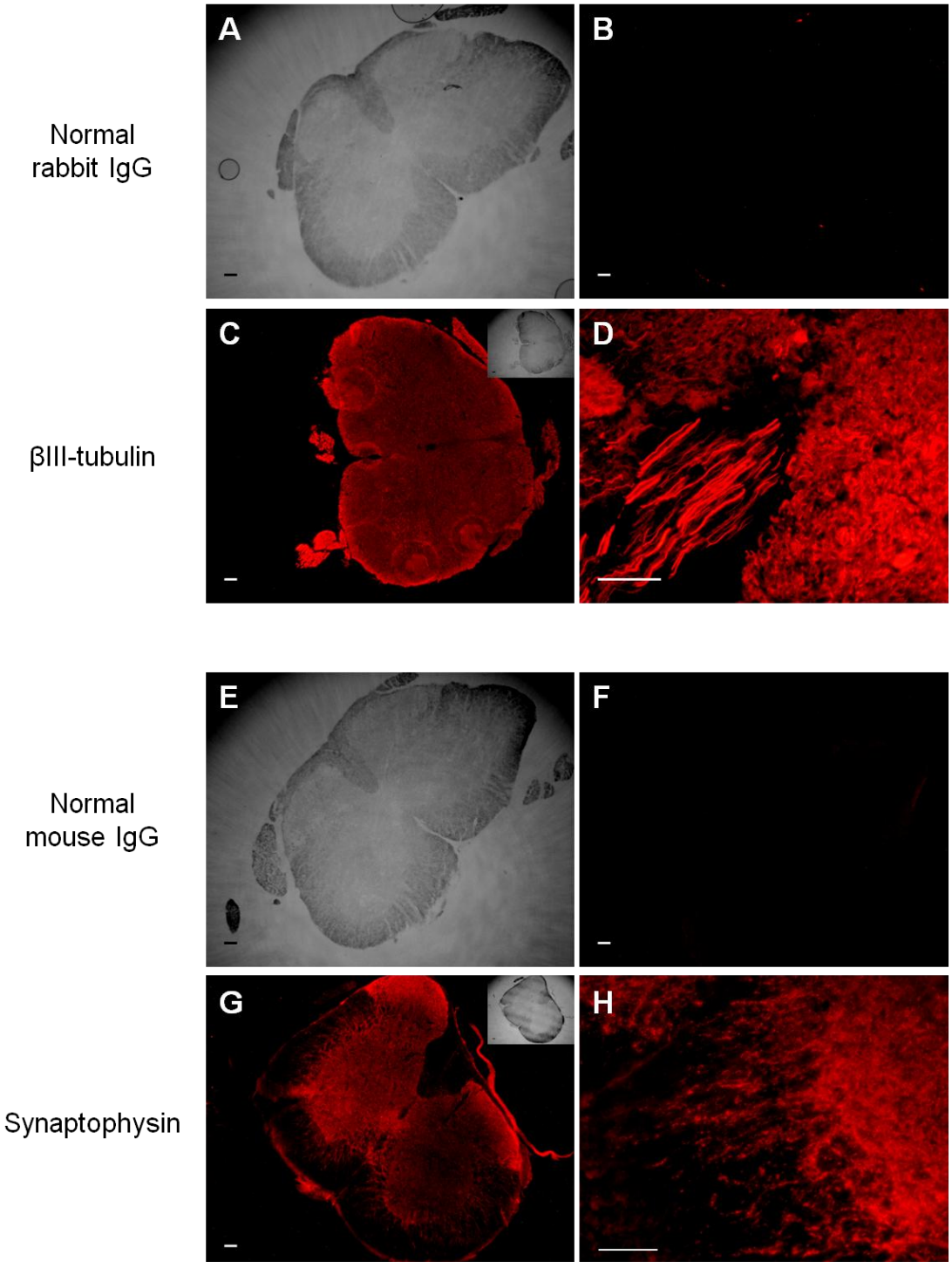

Bright field (A & E) and corresponding fluorescent images (B & F, respectively) for rabbit IgG (A & B) and mouse IgG (E & F) isotype control stains demonstrating specificity of secondary antibody stains. Low (C & G) and high (D & H) magnification images showing patterns of βIII-tubulin (C & D) and synaptophysin (G & H) staining in sham group tissue sections. Scale bars = 100µm